

**PHYSICO-CHEMICAL STUDIES ON DEGRADATION AND
STABILIZATION OF STYRENIC POLYMERS**

A thesis submitted to the
UNIVERSITY OF POONA
for the degree of
DOCTOR OF PHILOSOPHY

in
CHEMISTRY

by

AITHA VISHWA PRASAD
Division of Polymer Chemistry
National Chemical Laboratory
Pune – 411 008, India

November 1998

TH 1158

DEDICATED TO MY BELOVED PARENTS



राष्ट्रीय रासायनिक प्रयोगशाला (वैज्ञानिक तथा औद्योगिक अनुसंधान परिषद) पुणे - 411 008.

NATIONAL CHEMICAL LABORATORY (COUNCIL OF SCIENTIFIC & INDUSTRIAL RESEARCH) PUNE 411 008, (INDIA)

दूरभाष 91-212-336451-52 तार : केमेट्री केमल 0145-7266 फोन 91-212-330233 E-MAIL : pcs @ ems. ncl. res. in
TELEPHONE 91-212-331453 GRAM : CHEMISTRY IELEX 0145 - 7853 FAX 91-212-334761 rth @ ems. ncl. res. in
0212-337619

DECLARATION

Certified that the work incorporated in the thesis "**Physico-Chemical studies on degradation and stabilization of styrenic polymers**" submitted by Mr. Aitha Vishwa Prasad was carried out by the candidate under my supervision. Such material as has been obtained from other sources has been duly acknowledged in the thesis.

(R.P. Singh)

Research Guide

ACKNOWLEDGEMENT

I wish to place on record my deep sense of gratitude to my research supervisor, Dr. R.P. Singh who helped me immensely at this critical stage of my career. He taught, criticized, encouraged and advised me during all stages of my work. I will always be indebted to this patient and outstanding gentleman.

I owe a word of gratitude to Dr. S. Sivaram, Deputy Director and Head, Polymer Chemistry Division, National Chemical Laboratory, Pune, for his valuable suggestion, useful discussions and constant help during the course of this investigation. Without his critical evaluation and deep rooted knowledge, this thesis would not have become reality.

I am indebted to Dr. T.P. Mohandas, Dr. B.D. Sarwade, Dr. P.K. Saxena and Dr. S.Srinivas Reddy for their valuable suggestions and useful discussions during the course of the thesis work and Parag, Shailendra and Shrojal for the help in experimental work. I owe deeply to ever trustful Nabi, Raju, Pavan, Yenju, Gnaneshwar, Sainath and Subramanyam for always being with me.

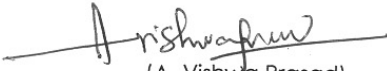
I am also thankful to Drs. N.N. Chavan, Dr. B.B. Idagae, C.V. Avadhani, D. Baskaran, C. Ramesh, P.P. Wadgaonkar, C. Bhasker, Menon, Mani, Arnab, Nikhil, Tushar, Binod, Radha, and Sarkar for their valuable suggestions and labmates Balu, Sreelatha, Rajesh, Sruti, nirmala, Raghu, Ramanathan, Jinu, Sandhya, Birajdar, Nitin, Mahuva, Neeta, Bindu, Anjana, Shinte, Bapat, Anjali, Subarno, Saptu, Sulatha and Soni for maintaining a friendly environment in the laboratory.

I am thankful to my friends Narshima Rao, Shivashankar, Tripura, Nagesh, Sahu, Patel, Bushan, Katti, Dash, Meena, Shivappa and Ramesh Babu for maintaining a friendly environment in the hostel.

I wish to thank Shaikh, Gracy, Suryavamshi and Kakade for the help in official matters.

I am extremely thankful beyond words for the patience, support and love given by my parents, brother, sister, and family members. I am thankful to my wife Shirisha for her strong support during these days.

Finally, I would like to thank the Director, National Chemical Laboratory, for allowing me to present the work in the form of a thesis and Council of Scientific and Industrial Research, New Delhi for the award of research fellowship for the last three years.


(A. Vishwa Prasad)

CONTENTS

◆	ABSTRACT	i
◆	GLOSSARY	iii
◆	LIST OF TABLES	iv
◆	LIST OF FIGURES	v

CHAPTER I

DEGRADATION AND STABILIZATION OF STYRENIC POLYMERS

1.0	Introduction	1
1.1	Methods of synthesis	2
	1.1.1 Free-radical polymerization	2
	1.1.2 Bulk-Suspension polymerization	5
	1.1.3 Emulsion polymerization	5
	1.1.4 Blending	5
1.2	Degradation of polymers	6
1.3	Types of Degradation	7
	1.3.1 Degradation in processing	7
	1.3.2 Photo-oxidative degradation	8
	1.3.3 Hydrolytic degradation	11
	1.3.4 Chemical degradation	11
	1.3.5 Mechano chemical degradation	13
	1.3.6 Radiation-induced degradation	14
	1.3.7 Metal-induced degradation	14
	1.3.8 Sensitized degradation	15
	1.3.9 Environmental degradation	15
	1.3.9.1 Biodegradation	15
	1.3.9.2 Weathering	16
	1.3.9.2.1 Chemicals	17
	1.3.9.2.2 Sunlight	17
	1.3.9.2.3 Humidity	17
	1.3.9.2.4 Wind	17
	1.3.9.2.5 Rain	17

1.4	General mechanism of degradation	18
1.4.1	Initiation	18
1.4.2	Propagation	18
1.4.2.1	Formation of polymer hydroperoxide	18
1.4.2.2	Formation of hydroxyl groups	19
1.4.2.3	Decomposition of polymer hydroperoxides	20
1.4.2.4	Decomposition of carbonyl groups	20
1.4.3	Termination	21
1.5	General mechanisms of photostabilization	22
1.5.1	Light screeners	23
1.5.2	UV absorbers	23
1.5.3	Antioxidants	26
1.5.4	Hydroperoxide decomposers	29
1.5.5	Excited-state quenchers	29
1.5.6	Hindered amine light stabilizers	30
1.6	Characterization of polymer degradation and stabilization	37
1.6.1	Spectroscopy	37
1.6.1.1	UV spectroscopy	37
1.6.1.2	Infrared spectroscopy	37
1.6.1.3	NMR spectroscopy	38
1.6.1.4	Chemiluminescence spectroscopy	38
1.6.1.5	Photoluminescence spectroscopy	38
1.6.1.6	X-ray photoelectron spectroscopy	38
1.6.2	Molecular weights	39
1.6.2.1	Viscosity	39
1.6.2.2	Gel permeation chromatography	39
1.6.3	Mechanical properties	39
1.6.4	Thermal analysis	39
1.6.5	Morphological analysis	40
1.6.6	GC-MS	40
1.6.7	X-ray analysis	40
1.7	Photo-oxidative degradation of styrenic polymers	42
1.7.1	Photo-oxidative degradation of polybutadiene	42
1.7.2	Photo-oxidative degradation of polystyrene	42
1.7.3	Photo-oxidative degradation of high impact polystyrene	44

1.8	Photostabilization of high impact polystyrene	51
1.9	References	56

CHAPTER II

OBJECTIVE AND SCOPE OF THE PRESENT INVESTIGATION

2.0	Introduction	65
2.1	Objectives of the present investigation	66
2.2	Approaches	67
2.3	References	69

CHAPTER III

POLYBUTADIENE CONTENT AND MICROSTRUCTURE IN HIGH IMPACT POLYSTYRENE

3.0	Introduction	70
3.1	Experimental procedures	70
	3.1.1 Materials	70
	3.1.2 Sample preparation	70
3.2	Analysis	70
	3.2.1 FT-IR Spectroscopy	70
	3.2.2 FT-Raman Spectroscopy	71
	3.2.3 ¹ H- and ¹³ C-NMR Spectroscopy	71
3.3	Results and Discussion	72
	3.3.1 Microstructure analysis of polybutadiene with FT-IR Spectroscopy	72
	3.3.2 Microstructure analysis of polybutadiene with FT-Raman spectroscopy	73
	3.3.3 Microstructure analysis of polybutadiene with ¹ H-NMR Spectroscopy	76
	3.3.4 Microstructure analysis of polybutadiene with ¹³ C-NMR Spectroscopy	79
3.4	Conclusions	82
3.5	References	85

CHAPTER IV

PHOTO AND THERMO-INITIATED OXIDATION OF HIGH IMPACT POLYSTYRENE

4.0	Introduction	87
4.1	Experimental procedures	87
4.1.1	Materials	87
4.1.2	Sample preparation	88
4.1.3	UV irradiation	88
4.1.4	Thermal irradiation	88
4.2	Analysis	88
4.2.1	¹³ C-NMR Spectroscopy	88
4.2.2	FT-IR analysis	89
4.2.3	Concentration profile analysis	89
4.2.4	Derivatization reactions	90
4.3	Results and Discussion	90
4.3.1	Characterization of the sample	90
4.3.2	Analytical aspects of photo-initiated oxidation at longer wavelengths	90
4.4	Kinetic aspects of the photodegradation	94
4.5	Derivatization reactions	94
4.5.1	SF ₄ treatment	94
4.5.2	NH ₃ treatment	98
4.6	Concentration profile analysis	98
4.7	Analytical aspects of thermal - initiated oxidation	100
4.8	Conclusions	100
4.9	References	103

CHAPTER V

CHAIN-SCISSION AND YELLOWING IN HIGH IMPACT POLYSTYRENE

5.0	Introduction	105
5.1	Experimental procedures	105
5.1.1	Materials	105
5.1.2	Sample preparation	105

5.1.3	UV irradiation	105
5.2	Analysis	106
5.2.1	FT-IR analysis	106
5.2.2	Viscosity measurement	106
5.2.3	Tensile/impact strength measurement	106
5.2.4	Yellowness/ Whiteness index measurement	106
5.3	Results and Discussion	107
5.3.1	Effects of irradiation on intrinsic viscosity	107
5.3.2	Changes in tensile/impact strength	111
5.3.3	Changes in yellowness/ whiteness index	112
5.4	Conclusions	113
5.5	References	116

CHAPTER VI

MORPHOLOGICAL CHANGES IN HIGH IMPACT POLYSTYRENE UPON PHOTO-OXIDATIVE DEGRADATION

6.0	Introduction	117
6.1	Experimental procedure	117
6.1.1	Materials	117
6.1.2	Sample preparation	117
6.1.3	Photo-irradiation	118
6.2	Analysis	118
6.2.1	¹³ C-NMR Spectroscopy	118
6.2.2	Scanning electron microscopy	118
6.3	Results and Discussion	118
6.3.1	Characterization by high resolution ¹³ C-NMR in solution	118
6.3.2	Morphological changes upon UV irradiation	125
6.3.2.1	High impact polystyrene	125
6.3.2.2	Styrene-Butadiene-Styrene copolymer	127
6.4	Conclusions	133
6.5	References	134

CHAPTER VII

NATURAL WEATHERING OF HIGH IMPACT POLYSTYRENE

7.0	Introduction	136
7.1	Experimental procedures	136
	7.1.1 Materials	136
	7.1.2 Sample preparation	137
	7.1.3 Natural weathering	137
7.2	Analysis	137
7.3	Results and Discussion	137
	7.3.1 Changes in carbonyl and hydroxyl region	137
	7.3.2 Kinetic aspects of the natural photo-oxidation of styrenic polymers	142
	7.3.3 Comparison of photo-products formation under natural and accelerated weathering exposure	143
7.4	Conclusions	143
7.5	References	153

CHAPTER VIII

PHOTOSTABILIZATION OF HIGH IMPACT POLYSTYRENE BY HINDERED AMINE LIGHT STABILIZERS (HALS)

8.0	Introduction	154
8.1	Experimental procedures	155
	8.1.1 Materials	155
	8.1.2 UV irradiation	156
	8.1.3 Scanning electron microscope	156
8.2	Analysis	157
8.3	Synthesis of 1,2,2,6,6-pentamethyl-4-piperidionol	157
8.4	Synthesis of styrene-maleic anhydrided (SMAN) copolymer	158
8.5	Synthesis of low and high mol.wt. polymeric SMAN-g-4-amino-2,2,6,6-tetramethyl piperidine	162
8.6	Synthesis of low and high mol.wt. polymeric SMAN-g-2,2,6,6-tetramethyl-4-piperidinol	165

8.7	Synthesis of polymeric SMAN-g-1,2,2,6,6-pentamethyl-4-piperidinol	166
8.8	Mixing of polymeric HALS	171
8.9	Diffusion measurement	172
8.10	Results and Discussion	173
8.10.1	Performance evaluation of polymeric HALS stabilizers in high impact polystyrene	173
8.10.2	Photostabilizing efficiency of polymeric HALS	175
8.10.3	Morphological changes upon UV irradiation	184
8.11	Conclusion	193
8.12	Reference	196
CHAPTER IX		
	Summary and Conclusions	200
	◆ SYNOPSIS	204
	◆ LIST OF PUBLICATIONS	210

ABSTRACT

This thesis presents the result on the degradation of heterophasic high impact polystyrene (HIPS) and stabilization by hindered amine light stabilizers (HALS). HIPS contains polystyrene as a continuous phase and polybutadiene as dispersed phase. The polybutadiene content varies from 5-20 wt-% in the copolymer. The polybutadiene phase microstructure exists in trans-1,4, cis-1,4 and vinyl-1,2 forms. The microstructure of polybutadiene in three different grades HIPS has been characterized with various spectroscopic techniques such as FT-IR spectroscopy, FT-Raman spectroscopy, ^1H and ^{13}C NMR spectroscopy.

The principal method employed for studying the extent of photo- and thermal oxidative degradation in HIPS was FT-IR spectroscopy. The photo-oxidation products were separated and analyzed with derivatization reactions with reactive gases such as sulfur tetrafluoride and ammonia. The extent of photo-products formation and stability of the polymer depends upon the composition of polybutadiene phase. The oxidative products profile in the photo-oxidized films was also carried out.

Intrinsic viscosity $[\eta]$, tensile impact strength and change in color (yellowness index) were studied in the photo-oxidized HIPS. These values were decreased with the exposure time. The photo-oxidized HIPS and SBS solutions were analyzed with ^{13}C NMR spectroscopic technique and their morphology was studied by SEM. The natural weathering and photo-oxidation of three different grades of HIPS showed the carbonyl and hydroxyl absorptions in FT-IR spectra. The rate of formation of the photo-products depends on the climatic condition in natural weathering while in accelerated weathering it is more than in natural weathering.

Styrene-maleic anhydride copolymer (different mol.wt.) was synthesized by free-radical copolymerization. 1,2,2,6,6-pentamethyl-4-piperidinol, 2,2,6,6-tetramethyl-4-piperidinol and 4-amino-2,2,6,6-tetramethyl piperidine were grafted on to styrene-maleic anhydride copolymer. These additives were incorporated by melt mixing. The solubility and diffusibility had been measured (in HIPS) with polymeric SMAN-g-1,2,2,6,6-pentamethyl-4-piperidinol, Tinuvin 770 and Tinuvin 144. The polymeric SMAN-g-1,2,2,6,6-pentamethyl-4-piperidinol is highly compatible with

the HIPS substrate. The low and high mol.wt. of 2,2,6,6-tetramethyl-4-piperidinol and 4-amino-2,2,6,6-tetramethyl piperidine were not compatible with the polymer matrix. These additives are forming intra and inter molecular hydrogen bonding in situ. The photostabilization efficiency of polymeric HALS was compared with conventional stabilizers (Tinuvin 770 and Tinuvin 144) also.

GLOSSARY

AIBN	2,2'-Azobisisobutyronitrile
4-DMAP	4-Dimethylaminopyridine
DMF	Dimethyl formamide
THF	Tetrahydrofuran
HIPS	High impact polystyrene
PS	Polystyrene
PB	Polybutadiene
SMAN	Styrene maleic anhydride
HALS	Hindered amine light stabilizer
DSC	Differential scanning calorimetry
TGA	Thermogravimetric analysis
FT-IR	Fourier transform infrared
SEM	Scanning electron microscope
WI	Whiteness index
YI	Yellowness index
ESR	Electron spin resonance
GPC	Gel permeation chromatography
HCl	Hydrochloric acid

List of Tables

1.1	Strength of chemical bonds	7
1.2	Degrading Agents and Types of Degradation	8
1.3	Spectral Sensitivity of Polymers	9
1.4	Enzymes and their reactions	16
3.1	Polystyrene content (mol %) in HIPS from FT-IR	73
3.2	^1H NMR chemical shifts from PB and PS homopolymers	78
3.3	Quantitative analysis of PB contents by ^1H and ^{13}C NMR	79
3.4	^{13}C NMR chemical shifts from PB and PS homopolymers	80
4.1	Composition of HIPS based on ^{13}C -NMR data	89
5.1	Yellowness index (YI) of irradiated HIPS upon irradiation	115
7.1	Natural weathering of styrenic copolymers	152
8.1	Synthesis of styrene-maleic anhydride copolymer	158
8.2	Molecular weight distribution of styrene-maleic anhydride copolymer	160
8.3	T_g values of polymeric light stabilizers	183

List of Figures

1.1	Effect of aging (85° C) on tensile properties of HIPS	47
1.2	Changes in carbonyl absorbance (1723 cm ⁻¹) in HIPS	49
1.3	Decay of polybutadiene unsaturation index (966 cm ⁻¹) of HIPS	50
3.1	Deformation region of HIPS/FTIR spectra. (A) pure polybutadiene (PB) and polystyrene (PS). (B) PB spectra obtained by subtraction (HIPS-PS)	74
3.2	Comparison of Raman spectra of PB, HIPS and PS	75
3.3	Proton NMR spectra of PB, HIPS, and PS (repetition time 3 s; scan number ca.300). (A) Complete spectra (0-8 ppm). (B) Expanded olefinic region (4-6 ppm)	77
3.4	Comparison of quantitative ¹³ C NMR spectra of PB, HIPS, and PS (delay time 30 s; scan number 300)	81
3.5	¹³ C NMR spectra of HIPS II . Comparison of quantitative (A) delay time 30 s, acquisition time 150 min and DEPT (B) delay time 5 s, $\theta = 45^\circ$, acquisition time 25 min.	83
4.1	Evolution of the IR spectra of HIPS (III) film (thickness = 106 μm) upon irradiation at $\lambda \geq 300$ nm, 60° C: (A) 0 h, (B) 9 h, (C) 19 h, (D) 29 h, (E) 39 h, (F) 49 h, (G) 64 h, (H) 74 h, (I) 84 h; a, c, and e represent the nonmodified spectra; b, d, and f represent the spectra from which the spectra (a) has been subtracted	91
4.2	Evolution of the IR spectra of a polystyrene film (thickness = 105 μm) upon irradiation at $\lambda \geq 300$ nm, 60° C (difference spectra): (A) 35 h, (B) 75 h, (C) 112 h, (D) 162 h, (E) 211 h	92
4.3	Effect of UV ageing on carbonyl, hydroxyl and unsaturation index of HIPS I (a), II (b), and III (c) (thickness 104, 104, and 114 μm)	95
4.4	Comparison of oxidation rates of HIPS I, II, and III with pure polystyrene by	96

	following the absorbance at 1723 cm ⁻¹	
4.5	Changes in FTIR spectra of a 25 h photo-oxidized HIPS (II) film after derivatization by (a) SF ₄ (24 h) and (b) NH ₃ (1 h) gases; before treatment, after treatment, and difference	97
4.6	Concentration profiles in HIPS II film; (a) photo-oxidized at $\lambda \geq 300$ nm, 60° C (thickness = 190 μ m, exposure time, 13 h), (b) thermo-oxidized at 120° C (thickness = 280 μ m, exposure time = 71 h)	99
4.7	Evolution of the IR spectra of HIPS (III) (thickness = 117 μ m) upon oven ageing at 120° C: (A) 41 h, (B) 64 h, (C) 86 h, (D) 153 h, (E) 276 h, (F) 428 h	101
4.8	Temperature dependence of thermo-oxidation rate of HIPS III: 80,100, 120° C.	102
5.1	Variation in $[\eta]$ of HIPS as a function of irradiation time	108
5.2	Variation in chain-scission (s) of HIPS with irradiation time	108
5.3	Effect of irradiation on unsaturation index (966 cm ⁻¹) of HIPS	110
5.4	Variation in tensile/impact strength of HIPS as a function of irradiation time	110
5.5	Variation in reflectance at 400 nm of HIPS samples with irradiation time	114
6.1	¹³ C NMR spectrum of HIPS 8350 neat in CDCl ₃ solution	119
6.2	¹³ C NMR spectrum of HIPS 8350 after 200 h UV exposure in CDCl ₃	121
6.3	¹³ C NMR spectrum of SBS neat in CDCl ₃ solution	122
6.4	¹³ C NMR spectrum of SBS after 100 h UV exposure in CDCl ₃ solution	123
6.5	¹³ C NMR spectrum of SBS after 300 h UV exposure in CDCl ₃ solution	124
6.6	SEM photographs of neat and photo-oxidized HIPS 8350 (a) neat film, (b) 100 h UV exposure, and (c) 250 h UV exposure	126
6.7	SEM photographs of SBS film cast from THF solvent: (a) neat film, (b) 50 h UV exposure, (c) 100 h UV exposure, and (d) 300 h UV exposure	128
6.8	SEM photographs of SBS film cast from CCl ₄ solvent: (a) neat film, (b) 50 h UV exposure, and (c) 200 h UV exposure	130

- 6.9 SEM photographs of SBS film cast from CHCl_3 solvent: (a) neat film, (b) 100 h UV exposure, and (c) 200 h UV exposure, and (d) 300 h UV exposure 131
- 7.1 FT-IR Spectral changes in carbonyl and hydroxyl region for various times of natural exposed HIPS III films during the months of April to August 138
- 7.2 Rate of carbonyl and hydroxyl group formation in HIPS (I to III) films in natural exposure during the months of April to August 139
- 7.3 FT-IR Spectral changes in carbonyl and hydroxyl region for various times of natural exposed HIPS III films during the months of September to March 140
- 7.4 Rate of carbonyl and hydroxyl group formation in HIPS (I to III) films in natural exposure during the months of September to March 141
- 7.5 FT-IR Spectral changes in carbonyl and hydroxyl region for various times of natural exposed PS films during the months of April to August 144
- 7.6 Rate of carbonyl and hydroxyl group formation in PS films in natural exposure during the months of April to August 145
- 7.7 FT-IR Spectral changes in carbonyl and hydroxyl region for various times of natural exposed PS films during the months of September to March 146
- 7.8 Rate of carbonyl and hydroxyl group formation in PS films in natural exposure during the months of September to March 147
- 7.9 FT-IR Spectral changes of HIPS III films in carbonyl and hydroxyl region for various time interval exposed in accelerated weathering 148
- 7.10 FT-IR Spectral changes of PS films in carbonyl and hydroxyl region for various time interval exposed in accelerated weathering 149
- 7.11 Rate of carbonyl and hydroxyl groups formation in HIPS III and PS films in accelerated weathering 150
- 7.12 FT-IR carbonyl group absorbance at 1725 cm^{-1} under accelerated and natural weathering of HIPS III films at various times (natural weathering (April to August) 151

8.1	IR spectra of styrene-maleic anhydride copolymer	159
8.2	¹³ C-NMR spectrum of styrene-maleic anhydride copolymer	159
8.3	IR spectra of (a) high mol.wt. polymeric SMAN-g-2,2,6,6-tetramethyl-4-piperidinol (AVP-49) and (b) polymeric SMAN-g-4-amino-2,2,6,6-tetramethyl piperidine (AVP-40)	163
8.4	Solid state CP/MAS ¹³ C-NMR spectra of high mol.wt. polymeric SMAN-g-4-amino-2,2,6,6-tetramethyl piperidine (AVP-40)	164
8.5	Solid state CP/MAS ¹³ C-NMR spectra of high mol.wt. polymeric SMAN-g-2,2,6,6-tetramethyl-4-piperidinol (AVP-49)	168
8.6	IR spectrum of polymeric SMAN-g-1,2,2,6,6-pentamethyl-4-piperidinol (AVP-59)	169
8.7	DSC thermogram of polymeric SMAN-g-1,2,2,6,6 pentamethyl-4-piperidinol (AVP-59)	169
8.8	¹³ C-NMR spectra of polymeric SMAN-g-1,2,2,6,6-pentamethyl-4-piperidinol (AVP-59)	170
8.9	Concentration distribution of polymeric SMAN-g-1,2,2,6,6-pentamethyl-4-piperidinol (AVP-59) in HIPS copolymer samples measured after diffusion time 120 h at 60° C.	174
8.10	Plot of carbonyl index vs irradiation time in HIPS films stabilized with various light stabilizers	176
8.11	Plot of hydroxyl index vs irradiation time in HIPS films stabilized with various light stabilizers	176
8.12	Plot of carbonyl index vs irradiation time in HIPS films stabilized with polymeric SMAN-g-1,2,2,6,6-pentamethyl-4-piperidinol (AVP-59)	177
8.13	Plot of hydroxyl index vs irradiation time in HIPS films stabilized with polymeric SMAN-g-1,2,2,6,6-pentamethyl-4-piperidinol (AVP-59)	177
8.14	Plot of carbonyl index vs irradiation time in HIPS films stabilized with Tinuvin 770 at different concentrations	179

8.15	Plot of hydroxyl index vs irradiation time in HIPS films stabilized with Tinuvin 770 at different concentrations	179
8.16	Plot of carbonyl index vs irradiation time in HIPS films stabilized with Tinuvin 144 at different concentrations	180
8.17	Plot of hydroxyl index vs irradiation time in HIPS films stabilized with Tinuvin 144 at different concentrations	180
8.18	TGA thermograms of polymeric SMAN-g-HALS stabilizers (AVP-40, 44, 49, 50 and 59)	182
8.19	DSC thermograms of polymeric SMAN-g-HALS stabilizers (AVP-40, 44, 49 and 50)	182
8.20	Plot of carbonyl index vs irradiation time in HIPS films stabilized with high mol. wt polymeric SMAN-g-4-amino-2,2,6,6-tetramethyl piperidine (AVP-40)	185
8.21	Plot of hydroxyl index vs irradiation time in HIPS films stabilized with high mol. wt polymeric SMAN-g-4-amino-2,2,6,6-tetramethyl piperidine (AVP-40)	185
8.22	Plot of carbonyl index vs irradiation time in HIPS films stabilized with low mol.wt polymeric SMAN-g-4-amino-2,2,6,6-tetramethyl piperidine (AVP-44)	186
8.23	Plot of hydroxyl index vs irradiation time in HIPS from stabilized with low mol.wt polymeric SMAN-g-4-amino-2,2,6,6-tetramethyl piperidine (AVP-44).	186
8.24	Plot of carbonyl index vs irradiation time in HIPS films stabilized with high mol. wt polymeric SMAN-g-2,2,6,6-tetramethyl-4-piperidinol (AVP-49)	187
8.25	Plot of hydroxyl index vs irradiation time in HIPS films stabilized with high mol. wt polymeric SMAN-g-2,2,6,6-tetramethyl-4-piperidinol (AVP-49)	187
8.26	Plot of carbonyl index vs irradiation time in HIPS films stabilized with low mol. wt polymeric SMAN-g-2,2,6,6-tetramethyl-4-piperidinol (AVP-50)	188
8.27	Plot of hydroxyl index vs irradiation time in HIPS films stabilized with low mol.wt polymeric SMAN-g-2,2,6,6-tetramethyl-4-piperidinol (AVP-50)	188
8.28	Plot of carbonyl index vs irradiation time (100 h) in comparison between HIPS and PS films stabilized with 1 wt-% various stabilizers	189

- 8.29 Plot of hydroxyl index vs irradiation time (100 h) in comparison between HIPS and PS films stabilized with 1 wt-% various stabilizers 189
- 8.30 SEM photographs of HIPS stabilized with polymeric SMAN-g-1,2,2,6,6-pentamethyl-4-piperidinol (AVP-59): (a) initial, (b) 75 h UV exposure, (c) 150 h UV exposure 190
- 8.31 SEM photographs of HIPS stabilized with polymeric SMAN-g-4-amino-2,2,6,6-tetramethyl piperidine (AVP-40): (a) initial, (b) 75 h UV exposure, (c) 150 h UV exposure 191
- 8.32 SEM photographs of HIPS stabilized with polymeric SMAN-g-2,2,6,6-tetramethyl-4-piperidinol (AVP-49): (a) initial, (b) 75 h UV exposure, (c) 150 h UV exposure 192
- 8.33 SEM photographs of HIPS stabilized with tinuvin 770: (a) initial, (b) 75 h UV exposure, (c) 150 h UV exposure 194
- 8.34 SEM photographs of HIPS stabilized with tinuvin 144: (a) initial, (b) 75 h UV exposure, (c) 150 h UV exposure 195

TH 1158

CHAPTER I

**DEGRADATION AND STABILIZATION OF STYRENIC
POLYMERS**

1.0 INTRODUCTION

Polymers are macromolecules built up by the linking together of large numbers of small molecules. The small molecules that combine with each other to form polymer molecules are termed monomers, and the reactions by which they combine are termed polymerizations. Polymerization processes in which two monomers are simultaneously polymerized is termed a copolymerization and the product is a copolymer. The copolymer is not an alloy of two homopolymers but contains units of both monomer incorporated into each copolymer molecule. The two monomers enter into the copolymer is determined by their relative concentrations and reactivities.

In the copolymer the two monomer units enter distributed randomly are called as random copolymers. There are three other types of copolymer structures alternating, block and graft. The alternating copolymer contains the two monomer units in equimolar amounts in a regular alternating distribution. Block and graft copolymers differ from the other copolymers in that there are long sequences of each monomer in the copolymer chain. A block copolymer is a linear copolymer with one or more long uninterrupted sequences of each polymeric species. A graft copolymer is a branched copolymer with a backbone of one monomer to which are attached one or more side chains of another monomer.

For many applications, the requirement is for a moderately priced polymer that can be molded easily and exhibits adequate stiffness and toughness over a wide range of temperatures. The basic and simplest solution to this problem is to modify existing polymers that already possess many of the desired properties, but are lacking in toughness and stiffness. High impact polystyrene (HIPS) consists of a glassy polystyrene phase (continuous phase) and polybutadiene as a dispersed phase. The PB phase is incorporated 5-20 wt-% during the synthesis of polystyrene. With the incorporation of PB, HIPS shows more impact strength (40 to 80 kJ m⁻²) as compared to pure PS (about 20 kJ m⁻²). Apart from these values, the elongation at break and fracture resistance are also increased several fold. With the addition of PB, there is an inevitable reduction in transparency, modulus and tensile strength, but these demerits are outweighed by the gains in fracture resistance.

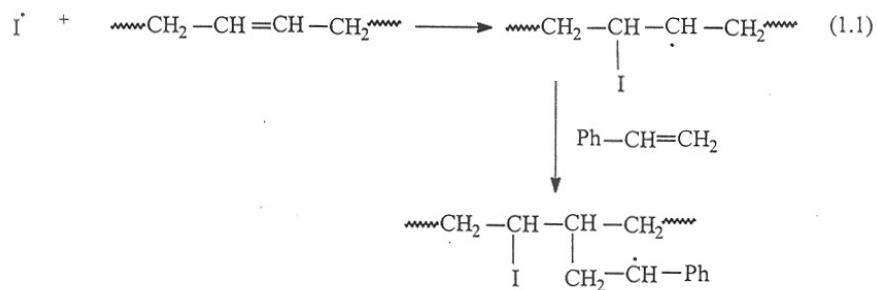
1.1 Methods of Synthesis

Ostromislensky¹ patented a process in 1927 for making toughened polystyrene by polymerizing a solution of rubber in styrene monomer. The process was not developed because the product was found to be cross-linked and therefore could not be molded. During the early years, HIPS materials were made by melt blending of PS and rubber, and their properties were generally inferior to those of the solution-grafted polymers. The new HIPS was made by dissolving styrene-butadiene rubber (SBR) in styrene monomer.² The subsequent commercial development of toughened polystyrene has been reviewed by Annos.³ The advantages of the solution-grafting process led to its general adoption by the industry, and by the early 1960s very little HIPS was being made by the blending route.⁴ Although there were numerous developments in HIPS production in the nature of modifications, the most significant was the replacement of SBR by polybutadiene as the standard toughening rubber. This development led to improvements in the fracture resistance of HIPS over a wide range of temperatures. HIPS is being manufactured by the following routes.

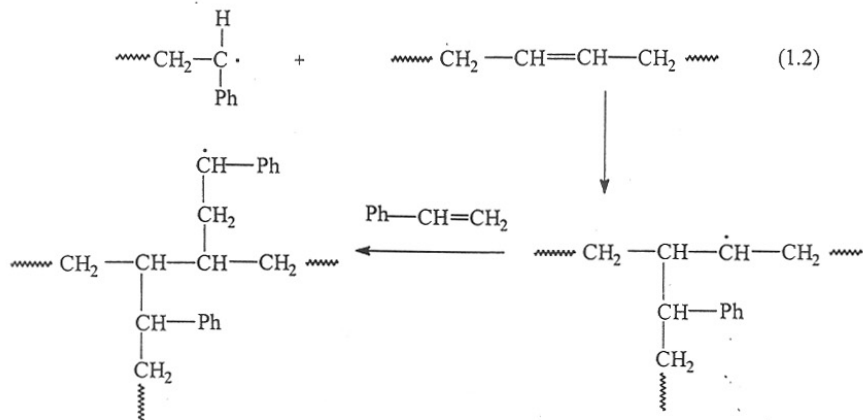
1.1.1 Free-Radical Polymerization

The improvement of impact resistance of PS is generally ensured by introducing PB before the free-radical polymerization of styrene. The PB nodules are then compatibilized by grafting of styrene units. Grafting is an important method for obtaining a strong bond between PB and the surrounding PS matrix. There are several possible mechanisms of grafting styrene onto PB. The active groups for grafting in PB are the double bond and the methylene hydrogen in the α -position. These places can be attacked by either initiator radical or by a growing polystyryl radical.^{5,6} The basic mechanisms are as follows: (Equations 1.1 - 1.4)

Reaction at a double bond with an initiator radical (I):



Reaction at a double bond with a polystyryl radical:



1.1.2 Bulk-Suspension Polymerization

Bulk-suspension polymerization is the standard process for the manufacture of HIPS. In this process, the partially polymerized rubber-incorporated styrene monomer is dispersed in droplets in water, and the finishing cycle consists of a suspension polymerization. It has not been successful by direct suspension polymerization to make rubber-toughened plastics by omitting the prepolymer isolation stage. Benzoyl peroxide is used as an initiator during prepolymerization, while the more stable dicumyl peroxide is active during the finishing cycle.

In this polymerization process the basic problem is the selection of suitable suspension stabilizers. These stabilizers will prevent the aggregation of the dispersed monomer-polymer phase. Apart from the stabilizers, its concentration, stirring intensity and the ratio of the aqueous and monomer-polymer phases are important for the size of the polymer beads and their size distribution.⁷⁻⁹

1.1.3 Emulsion Polymerization

Emulsion polymerization is the standard method of manufacturing toughened plastics.¹⁰ The process is comprised of two basic stages:

- a. Preparation of rubber latex: The water and soap are first charged to a pressure vessel and boiled to remove dissolved oxygen. The remaining ingredients (butadiene monomer, initiator, chain transfer agent) are added, and the reactor is sealed. Polymerization takes place at 50°C with stirring over two days, at the end of which the unreacted butadiene monomer is removed as vapor. The PB latex is then ready for the grafting stage.
- b. Grafting: In the second stage of the process, the styrene monomer is polymerized in the presence of PB latex to form a grafted polymer. This stage of the process requires additional water, soap, initiator, and chain transfer agent. The reaction is carried out at 50°C under nitrogen atmosphere.

1.1.4 Blending

The advances in bulk, bulk-suspension, and emulsion polymerization techniques have to some extent displaced blending as a method of manufacturing toughened plastics, but it is still used in commercial process. Several blending procedures are available.¹¹ The simplest and most commonly employed is melt blending in an extruder, Banbury mixer, or heated two-roll mill. More intimate mixing can be achieved by blending in solution, but the subsequent removal of solvent is inconvenient and expensive.

In these blending, the increase in the content of bound styrene in PB improves the compatibility with styrene. This will lead to an increase in the impact strength that can be attained for a constant content of the PB component in the blend. On the other hand, there is an increase in the T_g value for the PB and then a decrease in the impact strength at low temperatures.

1.2 Degradation of Polymers

All organic materials are susceptible to photo-oxidative degradation in varying degrees and appropriate conditions. Natural and synthetic polymers are sensitive to degradation in presence of oxygen and sunlight. The deteriorious effect of sunlight on polymeric materials having a complex set of reactions in which both the absorption of UV light and the presence of oxygen are participating.

When a molecule absorbs a quantum of light, it is activated into an electronically excited state. From this excited state many reactions takes place. The energy, which the molecule absorbs, depends on the wavelength of the light. The strength of chemical bonds shown in Table 1.1.

Sunlight is sufficient to break C-H bonds in polymers. Chemical reactions can also occur with the electronically excited states. The sunlight can initiate free-radicals, photoionizations, cyclizations, intramolecular rearrangements and chain-scissions in the polymer molecule. Apart from these reactions, the radiative and nonradiative photophysical process can also occur but with these reactions there is no net change in chemical nature.

Molecular weight of the polymer will decrease with the exposure to UV light due to chain scissions in the polymer backbone. Along with these results cross-linking

reactions can also occur in some cases and ultimately the polymer will become brittle.

Table 1.1: Strength of chemical bonds

Chemical Bond	Bond Energy (kcal/mole)	Wavelength of corresponding Energy (nm)
O-H	110.6	259
C-F	105.4	272
C-H	98.8	290
N-H	93.4	306
C=O	84.0	340
C-C	83.1	342
C-Cl	78.5	364
C≡N	69.5	410

1.3 Types of Degradation

There is a great interest at present in the degradation of polymeric materials. The initiating or degrading agent defines the type of degradation as shown in Table 1.2:

1.3.1 Degradation in processing

The processing of polymers in the temperature range of 100-300°C (pressures of 3-280 MPa) may cause result in their degradation. The resistance of plastics to degradation is affected by the conditions of processing.¹² Thermal processing operations, such as calendering, extrusion or injection molding, can cause chemical degradation, if not properly optimized. Prolonged melt processing of virgin polymers or repeated extrusion¹³ of recycled waste polymers causes chemical degradation and introduces oxygenated groups (chromophores) which accelerate their photodegradation. This degradation becomes particularly severe when air or oxygen are blown on the molten polymer during mixing. Some of the compounding additives incorporated into plastics may contain metal ions, which may promote degradation.¹⁴

Table 1.2: Degrading Agents and Types of Degradation

Degrading agents	Types of degradation
Light (ultraviolet, visible)	Photochemical degradation
X-, γ -rays, fast electrons, etc.	High-energy radiation-induced degradation
Laser light (pulsed mode)	Ablative photodegradation, involving photothermal and/or photochemical processes; laser flash photolysis
Electric field	Electric aging
Plasma	Corrosive degradation, etching
Microorganisms	Biodegradation or biological degradation
Enzymes in vivo, complex attack: hydrolysis ionization or dissolution	Bioerosion
Stress forces	Mechanical degradation, fatigue
Abrasive forces	Physical degradation, physical wear, environmental stress, cracking
Ultrasound	Ultrasonic degradation
Chemicals (acids, alkalis, salts, reactive gases, solvents, water)	Chemical degradation and/or decomposition, etching, solvolysis, hydrolysis
Heat	Thermal degradation and/or decomposition
Oxygen, ozone	Oxidation, oxidative degradation and/or decomposition; combustion
Light and oxygen	Photo-oxidation

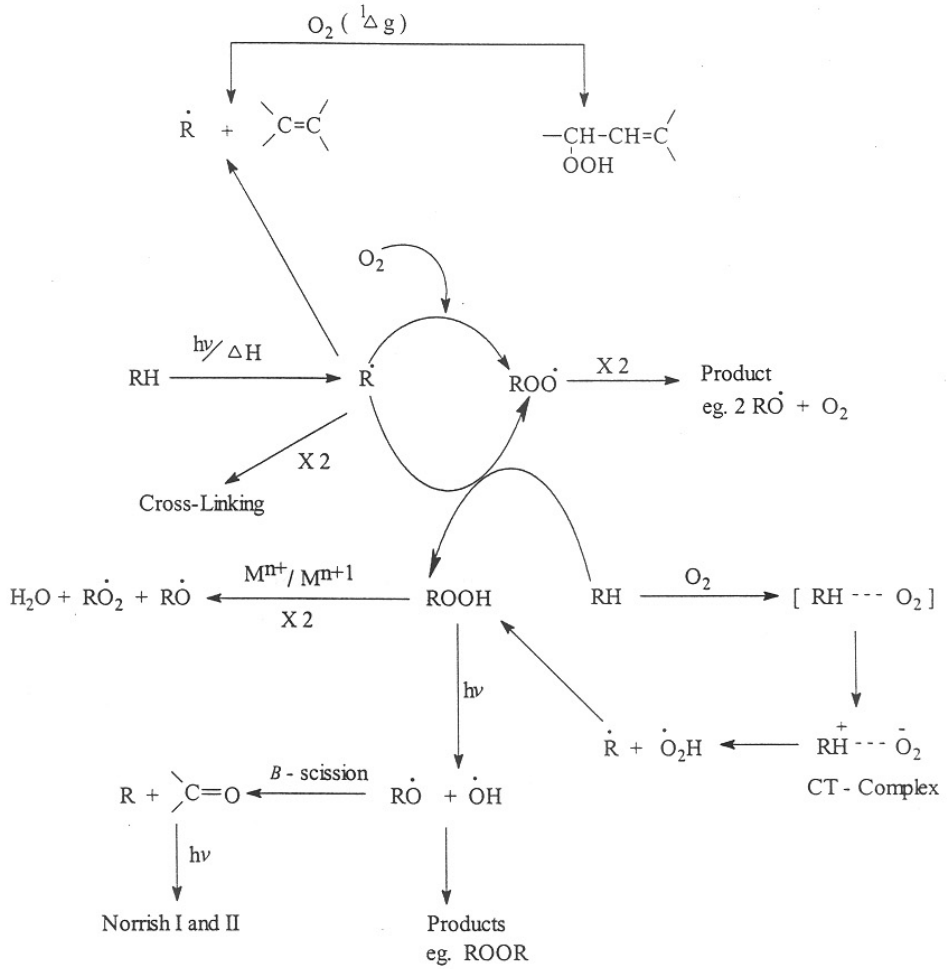
1.3.2 Photo-oxidative degradation

Chemical bonds can be broken by the ultraviolet (UV) radiation of the solar spectrum, leading to photodegradation.^{15,16} Generally UV light wavelength (λ) in the range of 280-400 nm is energetic enough to cleave the bonds. All polymers, when subjected to long-term exposure to weathering, degrade to different extents depending on their composition.^{17,18} UV light is sufficient to cleave the C-C bonds but the cleavage of C-C bond requires only 95-70 kcal/mole. The sensitivity of

polymers to degradation by UV light is shown in Table 1.3. This degradation is due to the absorption of energy in discrete units by specific functional groups (chromophores) that may be present in the chain. The main light-absorbing species may be carbonyl groups¹⁹, metallic impurities²⁰, dienes²¹, trienes²², hydroperoxides and O₂-polymer charge transfer complexes.²³ By the absorption of light, these species initiate and propagate the degradation of a polymer. The initiation leads to the formation of free-radicals that propagates the photo-oxidation of the polymers (scheme 1.1). Finally, it leads to chain-scissions or crosslinking in the polymer matrix. The chain-scission results into low molecular weight fragments whereas crosslinking causes the polymer insoluble and infusible. Weather encompasses the effects of all types of degradation.

Table 1.3: Spectral Sensitivity of Polymers

S.No	Polymer	Wavelength of greatest sensitivity (nm)
1	Polyacetals	300-320
2	Polybutadiene (ABS)	<380
3	Polycarbonate	295, 340
4	Polyethylene	<300
5	Polymethylmethacrylate	290-315
6	Polypropylene	310
7	Polystyrene	<430
8	Polysulfone	<320
9	PVC	310 & 370
10	Polyester	<315
11	PVA	<280
12	PPO	<370
13	Aromatic polyamide (Kevlar)	<450



Scheme 1.1 Photo-oxidation of Polymers

1.3.3 Hydrolytic degradation

In the hydrolytic degradation, the hydrolysis will take place in the polymer backbone. This is mainly occurring in natural polymers like proteins, cellulose and in synthetic polymers like polyamides, polyesters, lactam polymers, polyacrylates, polyurethanes and poly(vinyl acetal) etc.,. The hydrolytic degradation causes chain-scission and leads to a decrease in its physical properties.

Hydrolytic degradation can take place in neutral, acidic and alkaline conditions. This type of degradation is heterogeneous in nature, but in neutral and acidic medium within the polymer network it is homogenous in nature. This degradation will take place in bulk and will depend on humidity or in aqueous solutions over a wide range of pH.

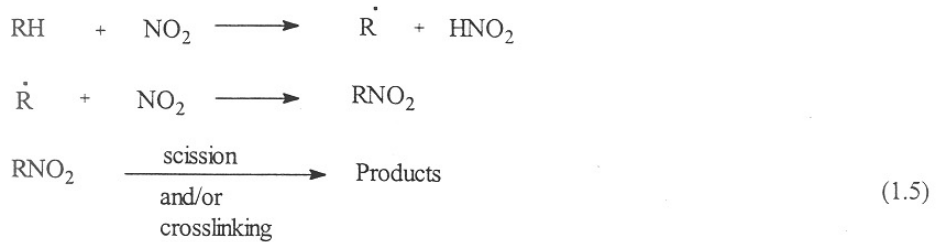
The rate of degradation in hydrolysis will be effected by a number of factors such as the film thickness, morphology (crystallinity, orientation) relative humidity, concentration of acid catalyst, dielectric constant of the polymer, auto catalysis by functional groups within the polymer, molecular orientation without formation of crystallinity type and ionizable or functional groups, electrostatic and steric effects, adsorption of water on the polymer and chain conformation.²⁴

1.3.4 Chemical degradation

In chemical degradation, a large number of atmospheric pollutants can attack the polymeric materials. In the atmospheric pollutants NO_2 , SO_2 are discussed. The other chemicals are mainly ozone, acids, alkalis, halogens and nitric acid.

Nitrogen dioxide (NO_2):

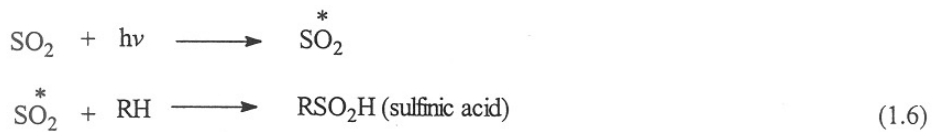
In the absence of oxygen, the NO_2 will react with hydrocarbons preferentially removing a tertiary hydrogen atom (Equation 1.5):



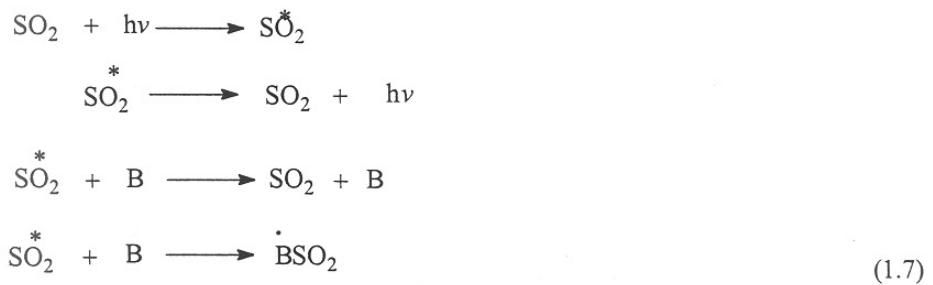
Sulfur dioxide (SO₂):

This is one of the most important air pollutants from the chemical industries. The SO₂ breaks down the bonds in the polymer network. The SO₂ will cause chain scission or crosslinking in the polymer backbone.

The possible mechanism²⁵ for the photoreaction of SO₂ with saturated (RH) (Equation 1.6): and unsaturated polymers (B) (Equation 1.7):



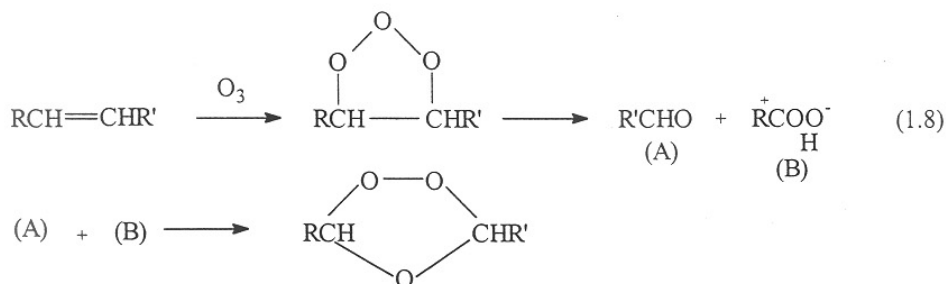
SO₂^{*} is excited SO₂ molecule without specifying whether it is in the singlet or triplet state



B = unsaturated polymer

Ozone (O₃):

Polymers are very sensitive to small concentration of ozone. The action of ozone on polymers leads to the chain scission and crosslinking within the polymer network. Finally polymers are turned to a change in surface properties (polarity, adhesion, surface tension). The reaction of ozone with olefins produces strained five membered rings²⁶ (Equation 1.8):



1.3.5 Mechano Chemical degradation

The mechanical forces also degrade the polymers.²⁷ The rubber solution did not give the desired properties when forced to pass through spiked rollers. Later, Staudinger observed that the polymer solutions while passing through fine jets resulted in a decrease of the molecular weight due to the mechanical degradation.^{28, 29} This can be divided into two parts, one is machining process and the other one is ultrasonic degradation. In the machining process, polymers will breakdown into low molecular weight fragments. This will depend on the machine-type operations. e.g. mastication, grinding, ball milling, roll milling etc. In ultrasonic degradation, the polymer solutions are subjected to ultrasonic vibrations.

a. Machine type:

In this process the formation of macro radicals occurs as a result of the applied mechanical forces. This radical generation will depend on the applied force direction. Non random chain scissions will occur in this degradation process. The rate of degradation will depend on the site of the scission in polymer chain. The rate of degradation will depend on a number of factors such as temperature, viscosity, chain configuration and type of mechanical equipment.

b. Ultrasonic degradation:

The polymers in solution are exposed to ultrasonic irradiation of high intensity. The ultrasonic waves will break the chemical bonds in the polymer matrix. The breaking of chemical bonds is called as “cavitation effects”. In the polymer solution the formation and violent collapse of small bubbles or voids will generate because of pressure changes which occur in a sound wave. These collapses can lead to the rupture of bonds.³⁰⁻³²

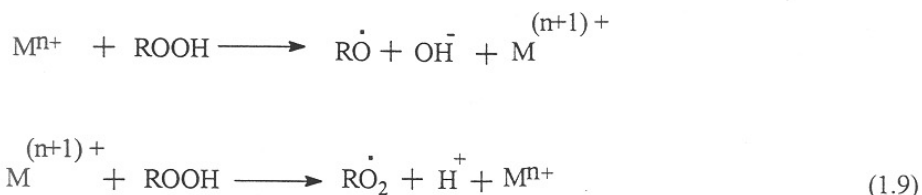
1.3.6 Radiation induced degradation

The high energy (X-rays, electron beams, γ -rays) are having wavelength (λ) in the range of 10 to 10^4 nm. They have imparting energy in the range of 10^5 to 10^{10} kcal/mole depending on the type of radiation. [X-rays (10^5 to 10^7 kcal/mole), electron beam (10^7 to 10^9 kcal/mole) and γ -rays (10^7 to 10^{10} kcal/mole).

For radiative degradations, specific groups (chromophores) are not needed for the absorption of high radiant energy. The degradation by gamma or electron radiation leads to severe degradation of the polymers, as manifested in post-irradiation embrittlement, discoloration and thermal instability.³³⁻³⁵ This problem is rather acute during the fabrication of disposable syringe barrels, in which embrittlement or lack of transparency cannot be tolerated. The primary events of high-energy radiation are ejection of a high-energy electron, which initiates a series of localized electron ejections, leading subsequently to excited states and finally to free-radicals. These free-radicals react readily with oxygen, giving rise to peroxy radicals, hydroperoxides, and other oxidation products. The absorption of energy from atomic radiation (γ -rays) is a function of electron density in the path of the radiation and is not affected in which atoms are linked.

1.3.7 Metal-induced degradation

Many commercial polymers contain metallic compounds as impurities. For example, the polymerization catalysts such as transition metals (Ti etc.) may remain in polyolefins at 2-10 ppm level. These residues can initiate the thermal and photodegradation.³⁶⁻³⁸ The traces of transition metals (catalytic residues) accelerate thermal oxidative degradation. They decompose hydroperoxides (Equation 1.9):



Many pigments are based on transition metals such as Zn, Fe, Cr, Cd etc., but they often enhance the thermal stability of stabilizer, neat-polyolefins, rather than accelerate degradation.^{39,40}

1.3.8 Sensitized degradation

The degradation of polymers can be induced and promoted by different inorganic and organic compounds. These compounds are excited by absorbed radiation/photons and subsequently decompose into free radicals that may initiate degradation and oxidation of a polymer. The excited compounds may transfer their excited energy to polymer molecules or oxygen molecules, forming singlet oxygen. Generally, these compounds behave either as a photoinitiator or as a photosensitizer. Careful investigation of sensitized photoreactions of polymers is important because most commercial polymeric materials contain different additives or metallic impurities that may act as a photosensitizer.^{14,41,42}

1.3.9 Environmental degradation

Environmental degradation is a combined effects of sunlight, heat, oxygen, water, chemical pollution in the environment, microorganisms, the mechanical effects of wind, rain and other similar forces.

1.3.9.1 Biodegradation

The biodegradation of polymers proceeds via hydrolysis and oxidation. This degradation is chemical in nature. The chemicals which initiate biodegradation come from fungi, bacteria and actinomycetes. In the biodegradation, the polymers are treated in different environments such as soil, aquatic, landfill, compost. Each environment contains different microorganisms and will follow the different degradation mechanism.

The soil contains fungi, bacteria and actinomycetes in the concentration of $5-900 \times 10^3$, $3-500 \times 10^6$ and $1-20 \times 10^6$ counts/g soil, respectively.⁴³ Besides soil, the fungi and bacteria are widely spread in water and air also. In the soil, fungi while in aquatic environment, the bacteria, are responsible for biodegradation. Bacterial concentration decreases in water with the increase in depth. In landfill, the degradation will take place with anaerobic (without oxygen) process, whereas in compost the degradation takes place in aerated process. The bacteria and fungi require H_2 , C, O_2 , N_2 as nutrients for growing.

Pure synthetic polymers are resistant to microbial attack because of hardness, limited water absorption and type of chemical structure. The susceptibility of a polymer to microbial attack depends on the enzyme availability. Enzymes are more complex proteins, which are able to catalyze specific reaction [each enzyme catalyzes one specific chemical reaction, (Table 1.4)]. Enzymes are very specific in their action, it will depend on the substrate concentration, specific site, temperature and pH. These are very specific about the stereoregularity of the polymers. The different enzymes are required for microbial degradation in different type of polymers. Around 2000 specific enzymes are known to cause biodegradation.⁴⁴

Table 1.4: Enzymes and their reactions

Enzyme	Reaction
Hydrolase or hydrolysis	: Esters, amides, acetals etc.,
Esterase or amidase	: Esterification or amidation
Isomerase or transferase	: Transferring atoms within one molecule
Reductase or oxidase	: Electron transfer reactions
Hydrogenase or dehydrogenase	: Proton addition or removal
Ligase	: Condensation reactions with formation of C-C, C-S, C-O or C-N bond

1.3.9.2 Weathering

In natural weathering sunlight, temperature, atmospheric pollutants, moisture, wind and rain play a significant role. Due to all these cumulative effects polymers will degrade.

1.3.9.2.1 Chemicals:

Mainly environmental pollutants such as nitrogen dioxide, sulfur dioxide, ozone and other gases will degrade the polymers. The pollution is mainly from the industries and other domestic activities.

1.3.9.2.2 Sunlight:

The sunlight is the main cause of polymer degradation in natural weathering. The earth's temperature depends on the sunlight duration. In general, temperature is less in passing from equatorial to polar regions. By absorbing the heat of the sun, polymer is activated and finally it will lead to degradation. The composition of solar radiation reaching the earth's surface is approximately 5% ultraviolet, 45% visible and 55% infrared.

TH 1158

1.3.9.2.3 Humidity:

The atmosphere contains an amount of water vapor which is measured in the form of humidity. The humidity is a ratio of quantity of water contained in a volume of air to that of the same volume which it would contain if the air is fully saturated at that temperature. This humidity catalyses the polymer degradation in natural weathering conditions.

1.3.9.2.4 Wind:

The atmosphere contains wind which generally carry dust particles, smoke and sand with it. Dust particles may also contain some chemicals which initiate the degradation in polymers. Dust can also have a protective effect on polymers. It can absorb a significant amount of solar radiation. It will show the dual nature of decreasing the temperature attained by polymer and decreases the extent of photo degradation.

1.3.9.2.5 Rain:

Rain also causes the degradation. The water droplets come forcefully from the clouds. These forceful droplets cause the degradation on the surface of polymers. The rain drops act like small bullets for high speed aircrafts due to relative velocity

effect. When a drop of water impinges on plastic materials at high velocity the stress developed, exerts a shear and the rapid radial wash of water acts with the shear stress to stack the material up due to plastic flow around the mouth of the crater produced. The process proceeds with the formation of lateral cracks and breaking of the material as the drops impinge into the crater already formed. As a result there occurs the rapid erosion of the plastic material.

1.4 General mechanism of degradation

The kinetic auto-oxidation reactions were invented by Bolland and Gee.⁴⁵ The photo-oxidation is a radical chain process initiated by photoactive functional groups present in the polymer chain. The degradation mechanism is divided mainly into three parts, (a) Initiation (b) Propagation (c) Termination.

1.4.1 Initiation

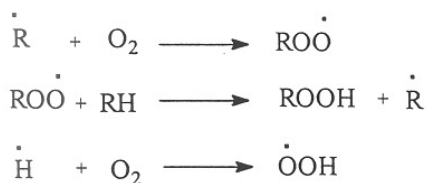
When polymers are exposed to UV radiation, ionizing radiation, heat etc., they generate a radical in the polymer backbone (Equation 1.10).



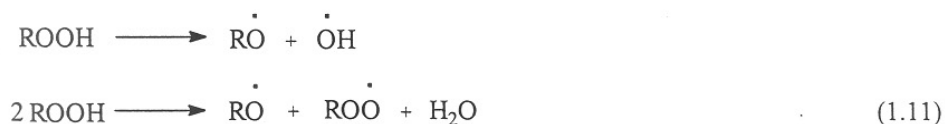
1.4.2 Propagation

In propagation, the degradative chain is prolonged by the following reactions.

1.4.2.1 Formation of polymer hydroperoxide



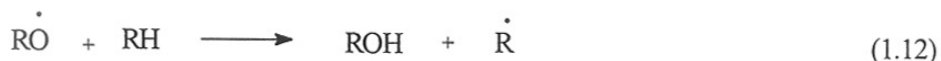
Chain branching:



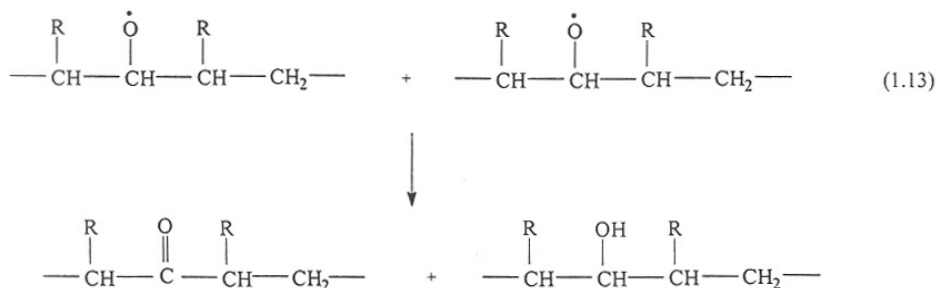
Polymer radical and oxygen react very fast, it leads to two unpaired electrons in the molecule of oxygen in the ground state ($\text{ROO}\cdot$) (Equation 1.11). This oxygen behaves as a biradical. In this process, the rate controlling step is the hydrogen abstraction. The rate constants for the hydrogen abstraction by peroxy radicals at primary, secondary and tertiary C-H bonds increase in the order $1^\circ < 2^\circ < 3^\circ$. The rate of the hydrogen abstraction at C-H bonds adjacent to the activating groups such as double bonds (allylic C-H bonds), aryl (benzylic C-H bonds), carbonyls, carboxyls, esters and amino groups is greatly enhanced by the combined effects of the decrease in the bond strength and the increase of the resonance stabilization energy of the radical formed.⁴⁶ Sometimes chain branching also takes place:

1.4.2.2 Formation of hydroxyl groups

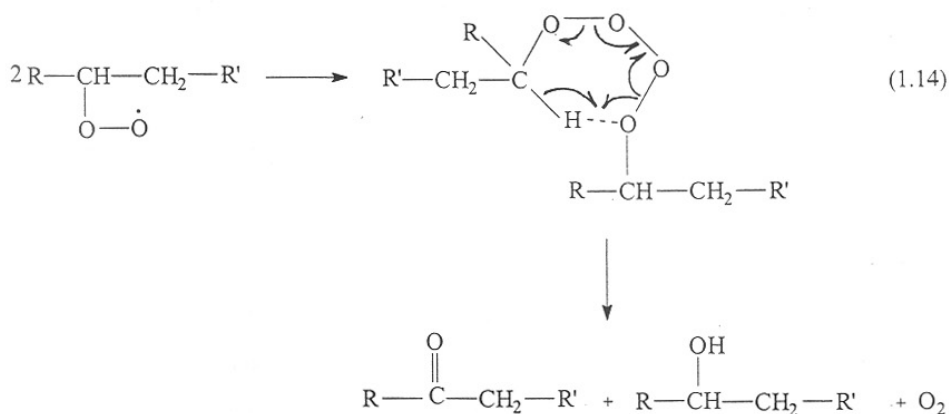
The hydroxyl groups are formed in the reaction between the alkoxy polymer radicals and other polymer molecule (Equation 1.12).



Reaction between two polymer alkoxy radicals by disproportionation method results in the carbonyl and hydroxyl groups formation^{47,48} (Equation 1.13).

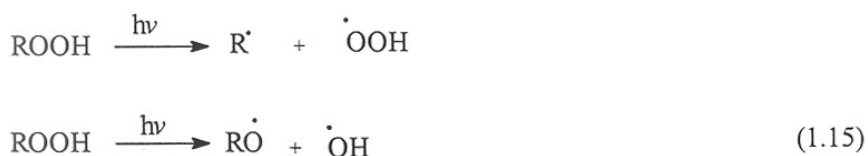


The bimolecular termination reaction for secondary and primary peroxy radicals undergoes a six member cyclic transition state (Russell mechanism).⁴⁹ This cyclic state is unstable and decomposes into a ketone, an alcohol and oxygen molecule (Equation 1.14).

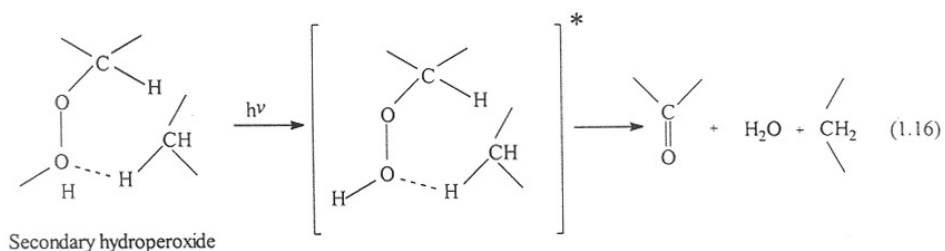


1.4.2.3 Decomposition of polymer hydroperoxides

Polymer hydroperoxides will decompose in photo-irradiation (Equation 1.15):



The free hydroperoxides will react with neighboring chains (from the same or another chain in polymer) leading to homolysis of the hydroperoxy bond. The primary and secondary hydroperoxides will decompose into aldehyde and ketone groups^{50,51} (Equation 1.16):



1.4.2.4 Decomposition of carbonyl groups

The carbonyl groups mainly decompose in two ways. The first one is Norrish type I and secondly is Norrish type II reactions.



When the oxygen pressure is high, the termination will take place by (Equation 1.19). In the solid state, sufficient oxygen concentration cannot be maintained, therefore, the termination will take place through (Equation 1.20). The polymer radicals may be coupled or crosslinked together (Equation 1.21). All these processes will depend on the chemical and physical structure of exposed polymers.

1.5 General mechanisms of photostabilization

At the time of heating, milling, or kneading, polymers may degrade or depolymerize. The plastic materials also deteriorate on exposure to natural and induced environmental conditions. A small amount of compounds called stabilizers are added into the polymer matrix to retard degradation and impart long-term outdoor stability to the polymer systems. Stabilizers are added to the polymers to improve their stability. Stabilizers will enhance the life-time of polymer and therefore its usefulness for longer time. Stabilizers will prevent, arrest or at least minimize the changes (which occur in degradation process) in the polymer matrix.

In general, a chemical reaction between an unstable ingredient of a polymer formulation and a stabilizer can be represented by this equation.



The equation describes a true stabilization process only if the "ingredient derivative" is less unstable than the "unstable ingredient" from which it is derived, and the "stabilizer residue" does not adversely affect the properties of the polymer formulation.

The stabilization does not occur through a single process, but by a combination of all the below proposed processes; their combined effect is known as synergism when

the cooperative action is greater than the sum of their individual effects taken independently.⁵²

1.5.1 Light screeners

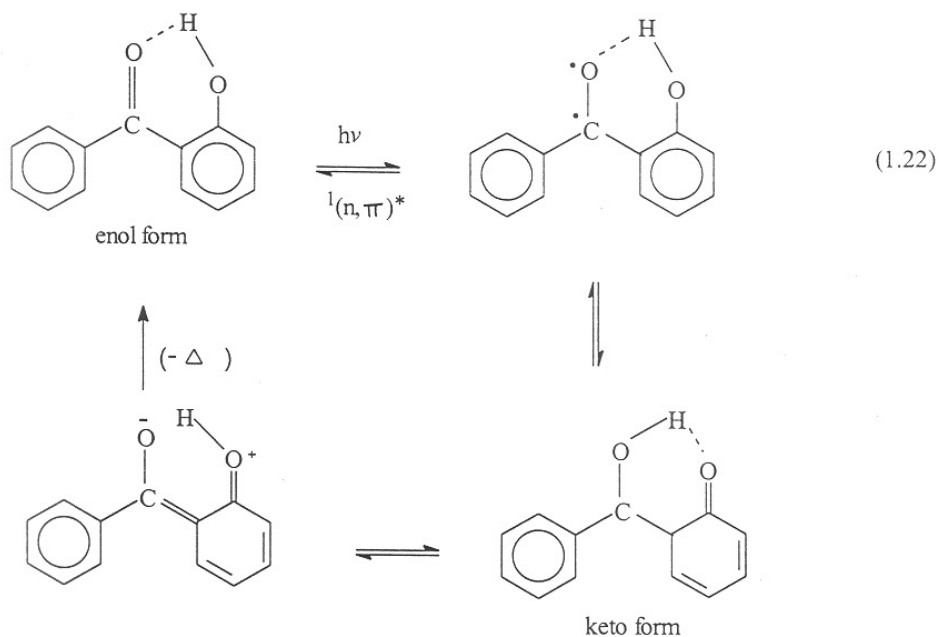
The light screeners are interposed as a shield between the radiation and polymer. They function either (a) by absorbing the damaging radiation before it reaches the photoactive chromophoric species in the polymer or (b) by limiting the damaging radiation penetration into the polymer matrix. The paints, coatings, and pigments show the screening activity and tend to stabilize the polymers.^{53, 54}

1.5.2 UV absorbers

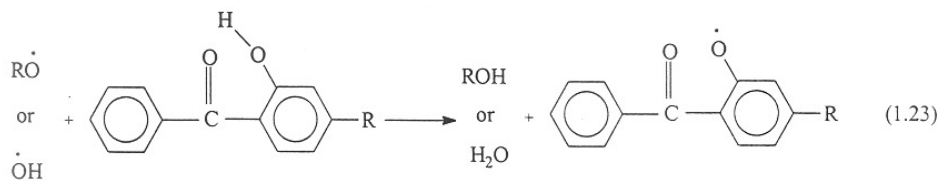
Generally, an ideal UV absorber will absorb the UV light in the 290-400 nm region.⁵⁵ In the photostabilization mechanism the UV absorber will absorb the harmful UV light and dissipate it as vibrational (thermal) energy, otherwise it will initiate the polymer degradation. UV absorbers follow the Lambert-Beer law. According to this principle the UV absorber should have a higher concentration, a longer light path and high extinction coefficient. The UV absorbers act through photophysical processes, intersystem crossing, internal conversion and molecular rearrangements. The hydroxybenzophenones, hydroxybenzotriazoles, p-hydroxybenzoates, 2-hydroxy phenyl-s-triazine and oxanilides are important groups of UV absorbers/ stabilizers in use since both groups absorb strongly in the UV region.^{56, 57}

Hydroxybenzophenones:

2-Hydroxybenzophenone on exposure to UV light forms a keto-enol tautomerism in the excited states. In this mechanism keto form will be transformed into enol form, this will return to keto form on losing thermal energy. This compound acts as a UV screeners and radical scavengers⁵⁸ (Equation 1.22):

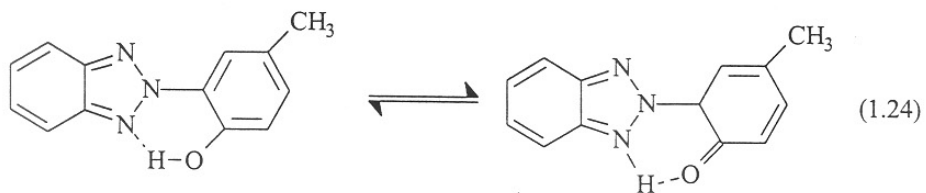


The keto-enol transformation is a reversible reaction, and it forms through a six member hydrogen bonding ring. The net result by the absorption and dissipation of light will not change the UV absorber (chemical nature). The UV absorber is able to undergo many activation-deactivation cycles. The o-hydroxybenzophenones act as a chain-breaking donors in photostabilization of polymers (Equation 1.23). This will also depend on the processing history.⁵⁹



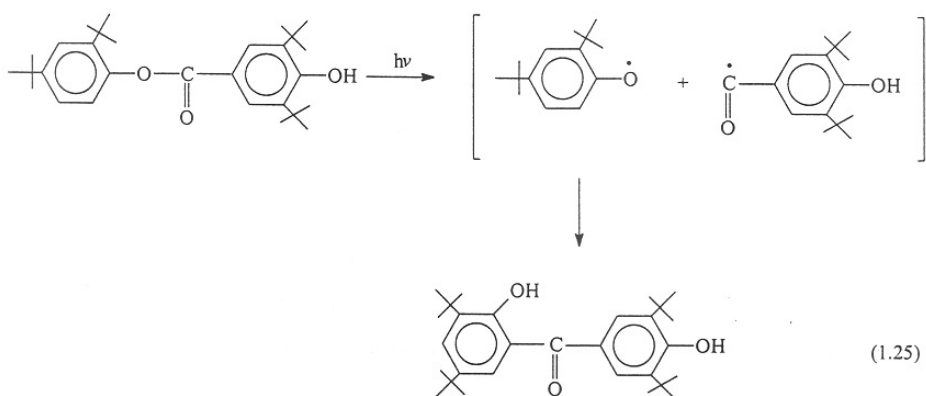
Hydroxybenzotriazoles:

This class of UV absorbers shows an intramolecular hydrogen bonding in the stabilization process (Equation 1.24). Werner had explained that the electron density shifts from the phenolic oxygen atom to the nitrogen atom of the triazole ring. In the excited singlet state, the proton shifts from the oxygen atom to the more basic nitrogen atom.⁶⁰



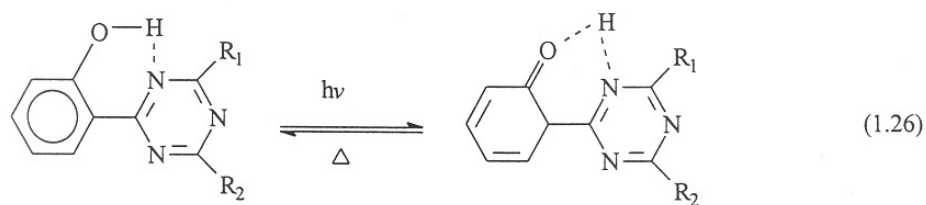
***p*-Hydroxybenzoates:**

p-Hydroxybenzoates stabilize the polymer through a Photo-Fries rearrangement (Equation 1.25). In the rearrangement process, *o*-hydroxybenzophenone is formed which acts as an UV absorber:



***2*-hydroxy phenyl-*s*-triazine:**

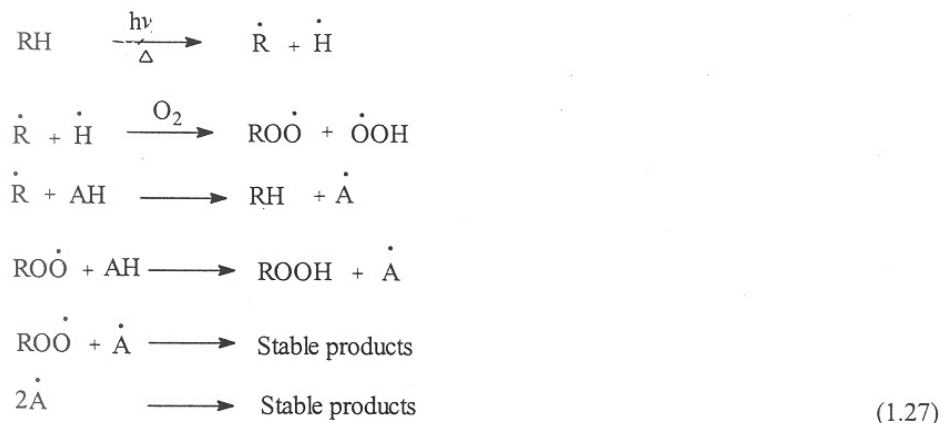
This class of stabilizers also stabilizes the polymers through intramolecular hydrogen bonding: (Equation 1.26)



The reverse reaction is exothermic. If there is a hydrogen bonding between the UV absorber and the polymer matrix, energy transfer becomes disrupted, and it may result in stabilizer degradation.

1.5.3 Antioxidants

The antioxidant (AH) may inhibit oxidation process by the following proposed mechanism (Equation 1.27):



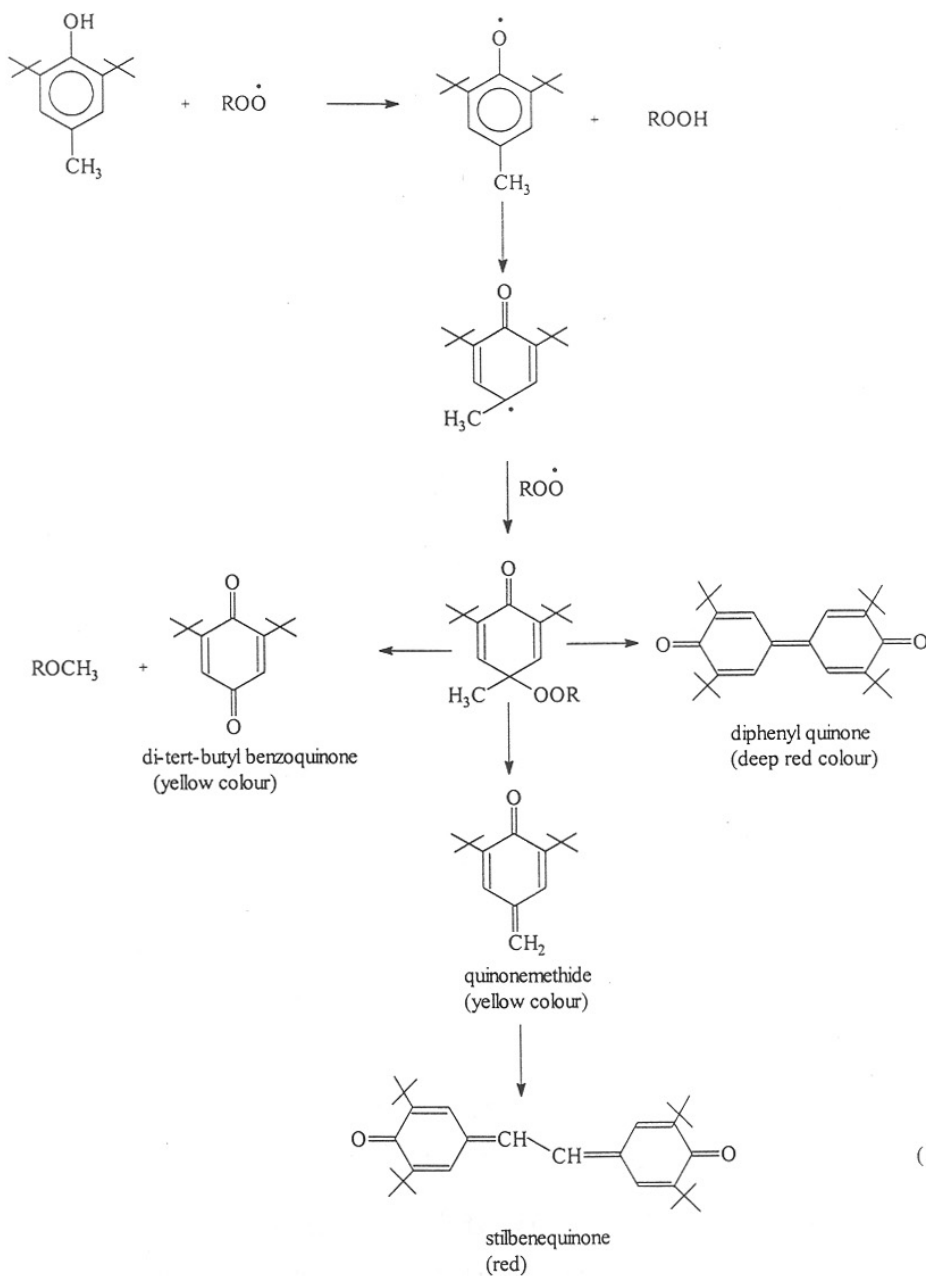
The antioxidant radical will stabilize through electron delocalization or resonance formation. Antioxidant radical does not react with the polymer to initiate a new radical.

Antioxidants act in two ways in the stabilization process. The first one is kinetic-chain breaking mechanism and secondly preventive mechanism. In chain-breaking mechanism, the antioxidants react with chain-propagating radicals to give inactive products. The preventive mechanism provides an alternative mechanism inhibiting the chain reaction by removing or deactivating radical generating species, which is responsible for its initiation. There are two kinds of antioxidants. The first one is primary antioxidants and the other one is secondary antioxidants.

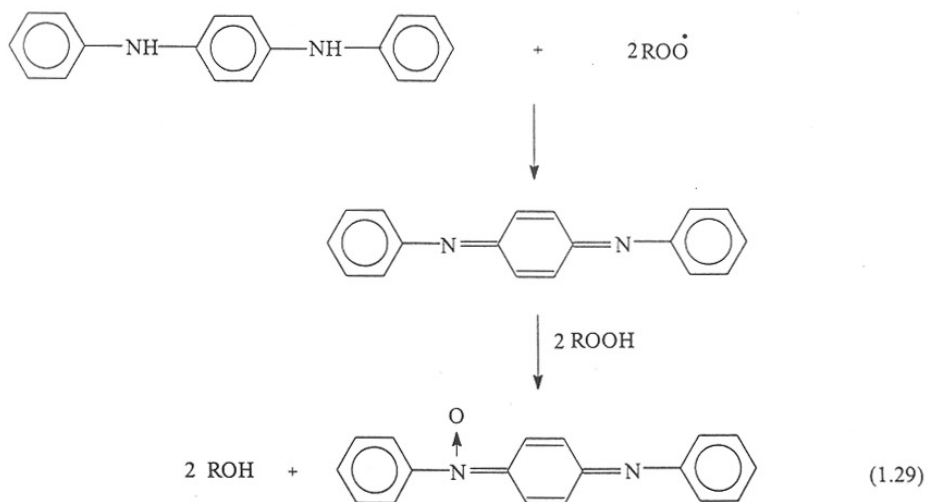
(a) Primary antioxidants:

Primary antioxidants act as a radical trapping or deactivating the radicals. Hindered phenols and secondary arylamines act as primary antioxidants. The hindered phenols donate their hydrogen to peroxy radicals.

Example: BHT (2,6-di tert.butyl-4-methyl-phenol)(Equation 1.28) oxidation products impart color to the polymer matrix. The color depends on the antioxidant structure. BHT is a highly volatile compound due to the CH_3 group which is easily replaced by the oxidation. Due to this reason it has highly volatile nature.



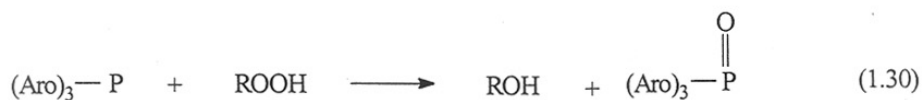
Secondary arylamine antioxidants are effective than phenolic antioxidants. These antioxidants act as chain terminators and peroxide decomposers (Equation 1.29):



(b) Secondary antioxidants:

Secondary antioxidants function in preventing the free-radicals formation, which is formed through decomposition of hydroperoxides in the polymer matrix. Generally, phosphorous and sulfur containing compounds are called as secondary antioxidants. These compounds will decompose the hydroperoxides, which are generated in oxidative process.

Example: (1) Phosphites function as the converts of hydroperoxides into alcohols and thus are converted themselves into phosphates⁶¹ (Equation 1.30) :

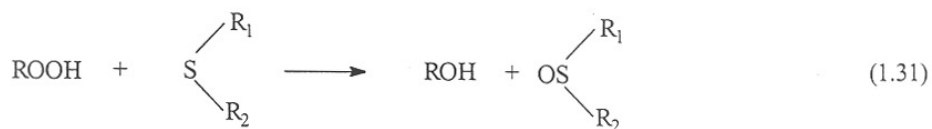


This reaction proceeds with a 1:1 stoichiometry by a non-radical mechanism, probably SN² mechanism at O-O bond with P as the nucleophile.

The reactivity of the phosphites towards hydroperoxides is depending on the polar and steric effects of the groups bound to phosphorous.

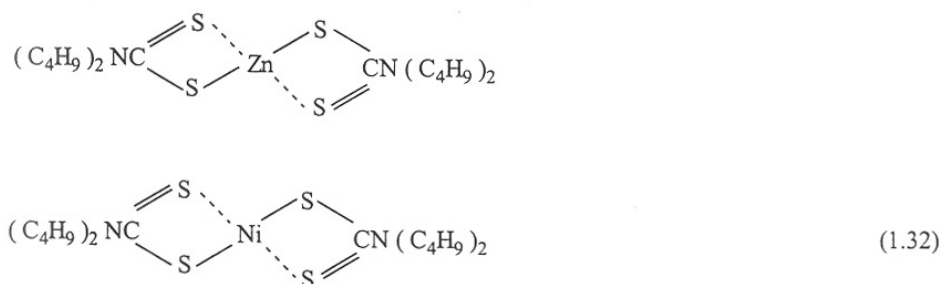
(2) Thio ethers:

Thio ethers react with hydroperoxides to form an alcohol and sulfoxide⁶² (Equation 1.31):



1.5.4 Hydroperoxide decomposers

The decomposition of hydroperoxides has a significant effect on the photostabilization of many polymers. Metal complexes of sulfur containing compounds such as dialkyldithiocarbamates are used as hydroperoxide decomposers in polypropylene⁵⁷ (Equation 1.32)

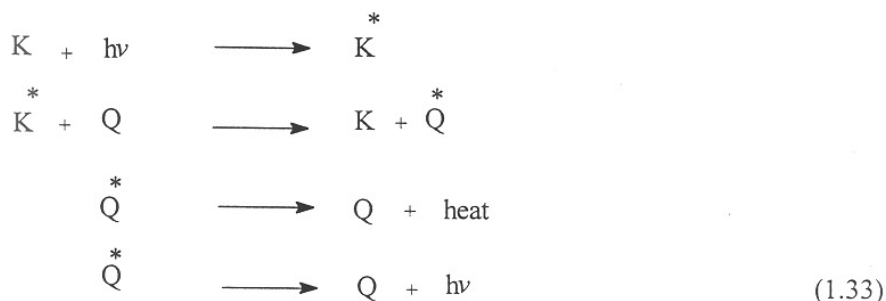


1.5.5 Excited-state quencher

The deactivation of the excited states of the chromophores in polymer is called as quenching (Equation 1.33). By absorbing photon/light, the chromophore is excited and initiates the photo-degradation in polymer. The energy can be dissipated either in the form of heat or as fluorescent or phosphorescent radiation. The excited-state quenchers are, generally, transition metal chelates with a variety of ligands.^{63,64}

The most reasonable explanation for the quenching is the exciplex formation between excited chromophore (carbonyl or ketone) and the ground state of the quencher. The mechanism involves energy transfer from both the singlet and triplet

excited states to the ground state of the quencher. In the solid state, transfer of energy occurs by resonance or dipole-dipole interactions.

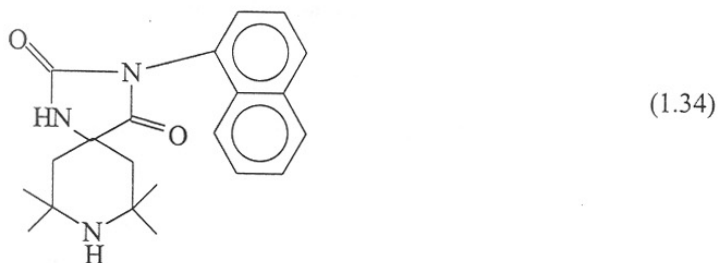


The energy transfer from excited chromophore to a quencher can proceed by two methods:

1. Long-range energy transfer (Forster mechanism): This method is based on dipole-dipole interaction and usually is observed in the quenching of excited states. In this process, the chromophore and quencher molecules are separated by a distance 5 to 10 nm even though quenching takes place through a strong overlapping between the emission spectrum of the chromophore and absorption spectrum of quencher.
2. Collisional (contact or exchange) energy transfer: This process requires the distance between quencher and chromophore <15 angstroms. Within this distance, energy transfer will take place.

1.5.6 Hindered amine light stabilizers

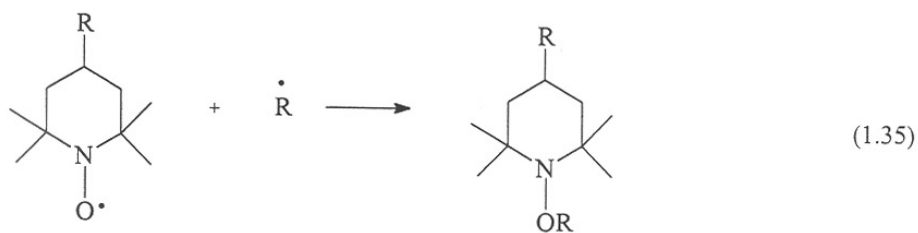
Tetramethyl piperidines are commonly called as hindered amines. The hindered amine light stabilizers (HALS) are multifunctional photostabilizers. The interest in this area was developed because of stable free-radical 2,2,6,6-tetramethyl-4-oxopiperidine-N-oxyl.⁶⁵ The nitroxyl radical was stable and showed an excellent radical scavenging property and showed slight yellowness in polymers as it is yellow in colour. Sanko Co., in Japan invented HALS for first time. (Equation 1.34).^{66, 67} This HALS showed UV stabilization in polypropylene, polystyrene and nylon. HALS have an excellent efficiency, due to their regenerative radical scavenging capability and oxidized derivatives.



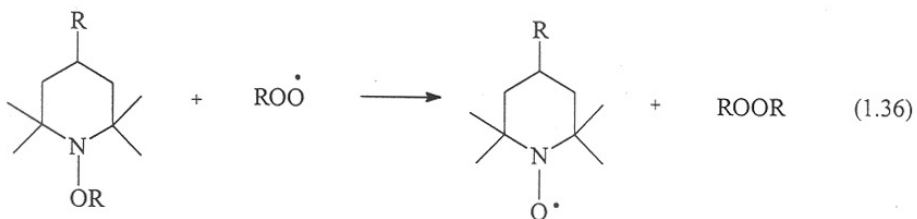
In the stabilization process HALS can function as:

- (a) Decomposer of the hydroperoxide groups.⁶⁸⁻⁷⁰
- (b) Decomposer of the peracids and trap acyl peroxy radicals.⁷¹⁻⁷⁴
- (c) Deactivators of the charge transfer complexes.^{75, 76}
- (d) Quenchers of the singlet oxygen and ketones.⁷⁷⁻⁷⁹
- (e) Decomposers of the ozone⁸⁰ and
- (f) Forms metal complexes⁸¹

The HALS is converted into corresponding nitroxyl radical under photo-oxidation. This was observed with E.S.R. spectroscopic method.⁸² The nitroxyl radical will react with polymer radical and results in hydroxylamine ether products (Equation 1.35):



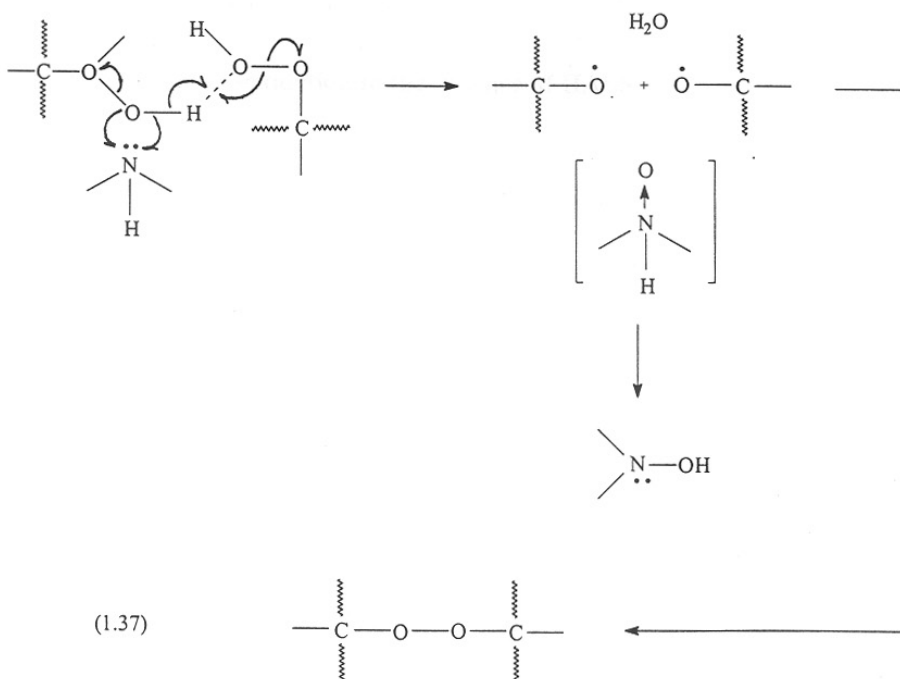
The peroxy radical can react with hydroxylamine ethers with regeneration of nitroxyl radicals (Equation 1.36):



(a) Decomposition of Hydroperoxides with HALS:

Carlsson et al.⁶⁹ studied HALS induced decomposition of polypropylene hydroperoxides in the solid state and in the presence of a liquid solvent. Amine-induced decomposition of polypropylene hydroperoxide is faster in the absence of a liquid solvent for the amine than in the presence of the solvent, probably because of the strong amine-hydroperoxide association that occurs in the solid state. The decomposition process in the solid state is a fast reaction to contribute to the effective stabilization. The HALS is converted to nitroxides in the reaction via hydroxylamine as intermediates.

The HALS induced decomposition of hydroperoxides in the preoxidized polypropylene in the solid state reaction is explained by equation 1.37. The concerted reaction between polypropylene hydroperoxides and HALS proceeds by the formation of water and nitrous oxide, which rapidly transform into hydroxylamine followed by the cage combination of two macro alkoxy radicals to yield peroxide:



(b) Decomposition of Peracids and scavenging acyl peroxy radicals:

The HALS reacts with peracids and forms the nitroxyl radicals, corresponding acids and water⁸³ (Equation 1.38).



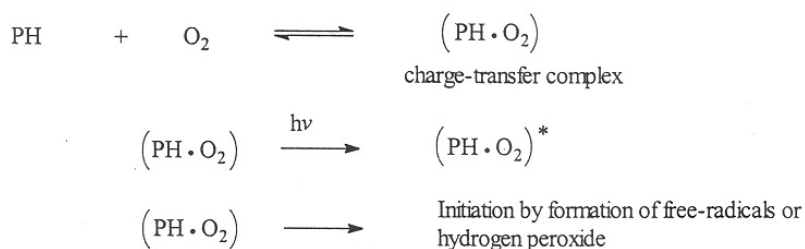
HALS is an effective scavenger for acyl peroxy radicals⁷² (Eq. 1.39):



(c) Deactivation of oxygen charge transfer complexes:

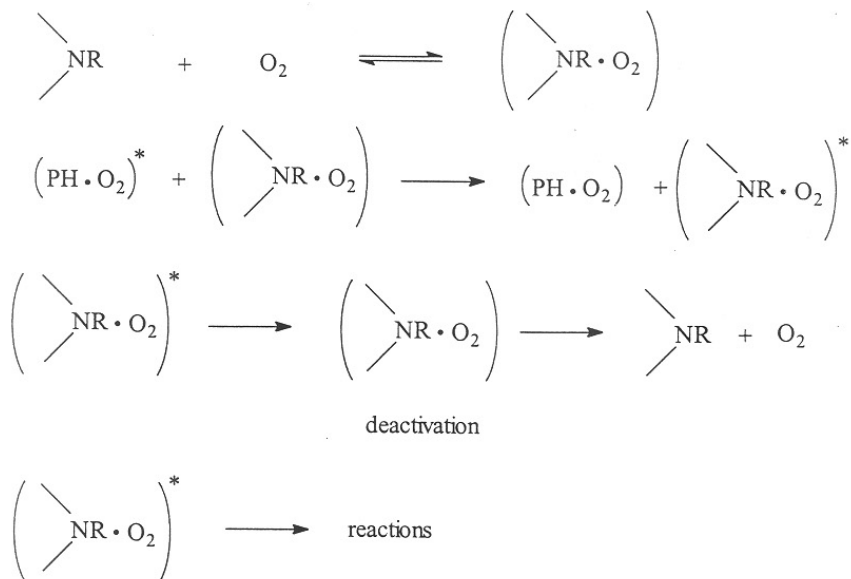
Gugumus⁷⁵ proposed a new mechanism of polymer stabilization with charge-transfer complexes (CTC) in polyethylene. According to him the new initiation and stabilization mechanism by HALS is: (Equations 1.40 and 1.40a):

1. Initiation of photo-oxidation in the absence of HALS (1.40)



2. Stabilization by HALS:

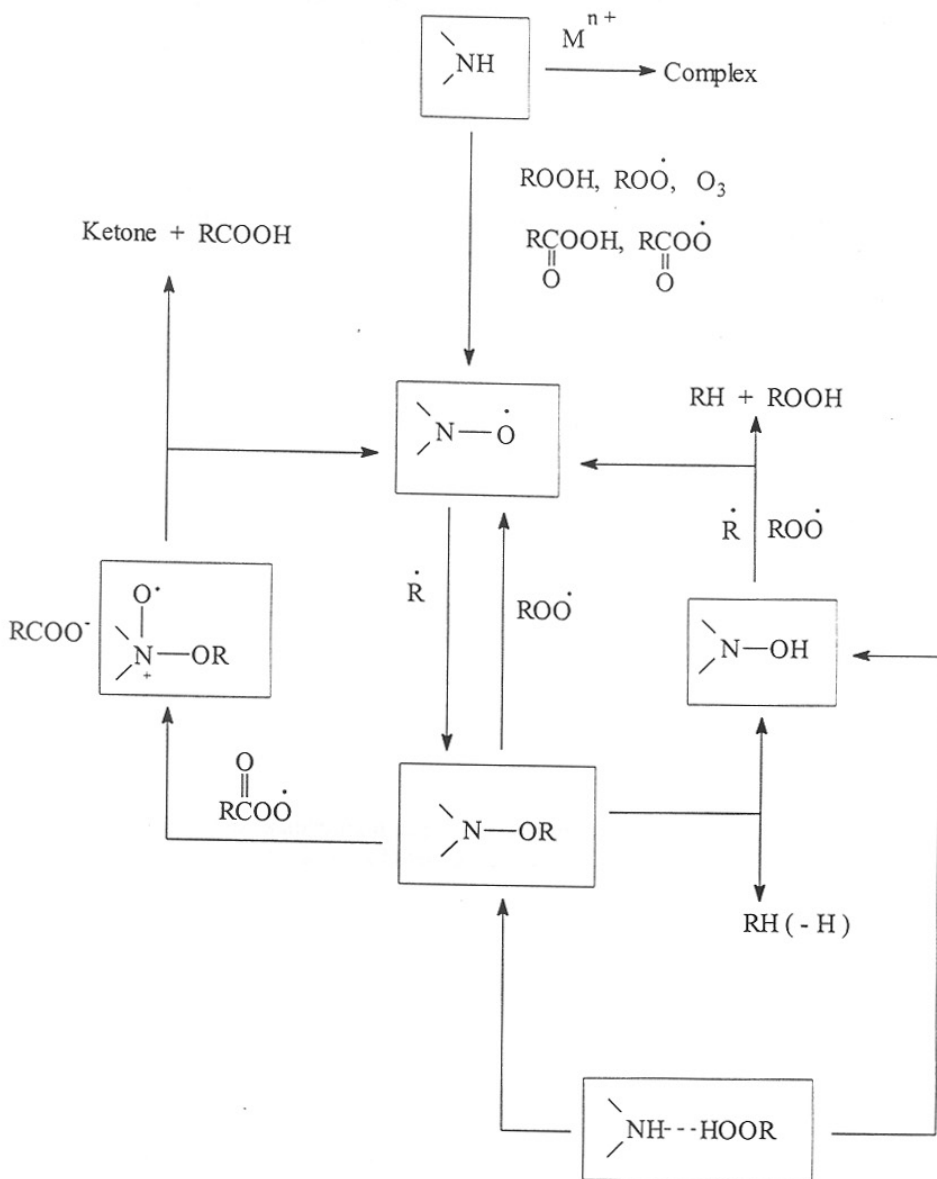
(1.40a)



(d) HALS as singlet quenchers:

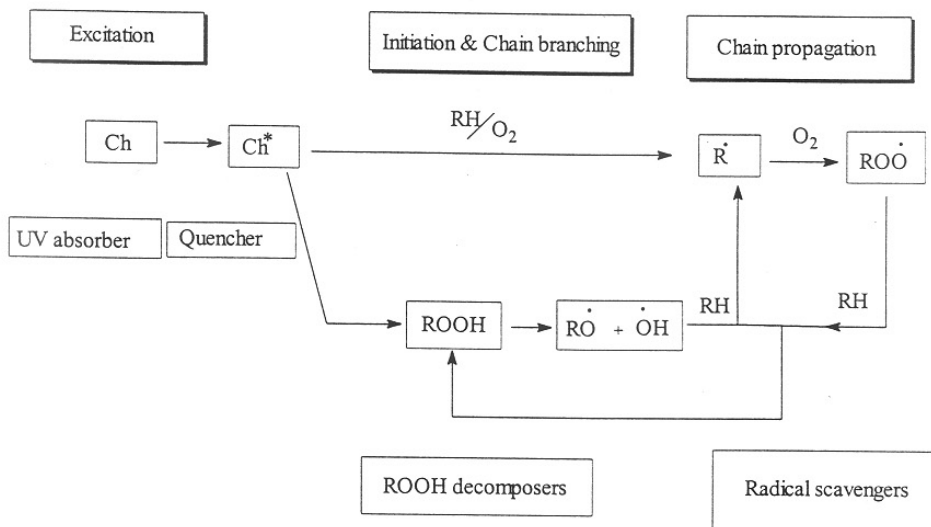
The quenching efficiency depends on the steric hindrance at the nitrogen atom and on the ionization potential of the amine. Bortolus et al.⁷⁹ have explained that the quenching efficiency of Piperidinyl-N-oxyl free radicals is more than the parent HALS. The HALS compounds effectively deactivate the singlet and triplet excited states of carbonyl groups also. The classical Norrish I and II reactions occurring in the first $^3(n-\pi)^*$ state of ketones are efficiently quenched by HALS.

The overall photostabilization mechanism with HALS is the formation of a stable nitroxyl radical, which scavenges the alkyl radicals giving hydroxylamine derivatives. The hydroxylamine derivative scavenges the alkoxy, peroxy radicals and regenerates the nitroxyl radicals. The mechanism has been shown in scheme 1.2.



Scheme 1.2: Stabilization mechanism of HALS

The photostabilization of polymers at different stages of auto-oxidation by various classes of stabilizers has been shown in scheme 1.3.



Scheme 1.3: Photostabilization of polymers at different stages of auto-oxidation by Various classes of stabilizers

In conclusion we can say that a good stabilizer should have the following qualities:

- (i) Stabilizer should be compatible with the polymer matrix.
- (ii) It should show stability to light.
- (iii) It should be stable at processing temperature.
- (iv) Stabilizer should not react in an unfavorable manner with the polymer.
- (v) Stabilizer should not be toxic.
- (vi) It should not discolor the polymer
- (vii) Cost should be lower and consistent with stabilizer performance.

1.6 Characterization of polymer degradation and stabilization

A number of methods are available for measuring the deterioration of weathered polymers (Scheme 1.4). Their validity depends on the nature of material and the mode of deterioration. The known destructive characterization techniques are often preferred since they limit the number of specimens and the same specimen can be reexamined.

1.6.1 Spectroscopy

Degradation of polymers is usually related to chain-scission, crosslinking, crystallization, phase separation and pyrolysis etc. A number of following spectroscopic methods have been used to characterize the degradation of polymers.

1.6.1.1 *UV spectroscopy*

This technique affords a simple, sensitive and non-destructive means of detecting degradation. UV spectroscopy is widely used to determine the unsaturation and chromophoric groups in photo-oxidative degradation studies. In the degradation process new chromophoric groups are generated which can be identify with this technique.⁸⁴

1.6.1.2 *Infrared Spectroscopy*

Since long infrared (IR) spectroscopy is one of the most widely used technique identifying changes in the chemical structure of the degraded polymers.⁸⁵ FT-IR spectroscopy is frequently used with photoacoustical, attenuated total reflectance (ATR), and microscopical attachments. The surface changes in the solid films can be easily observed with ATR. The photo-oxidized polymers showed the functional groups and unsaturation in the polymers. In the photo-oxidation, the hydroxyl and the carbonyl group formation is the main indication of the photo-degradation. The degradation profile of the photo-oxidized samples as a function of depth has been also determined by the microscopic attachment in FT-IR of microtomed sections from an exposed polymer films.

1.6.1.3 NMR Spectroscopy

The NMR spectroscopy is an useful technique to find the changes in the photo-oxidized polymer.^{86, 87} This method is very sensitive as compared to IR. ¹³C NMR spectra shows the carbonyl group formation, unsaturation, quiniods structure and alcohol functional groups in the photo-oxidized polymers. The epoxide groups formed in elastomers/rubbers during photo-oxidation are easily detected by ¹³C NMR spectra.

1.6.1.4 Chemiluminescence Spectroscopy

The oxidative degradation of most polymers is accompanied by emission of very low levels of light [chemiluminescence (CL)].⁸⁸ This method gives better results in the early stage of degradation. CL is very sensitive technique to detect low level of photo-oxidation. If an oxidized polymer heated in the N₂, it will emit an amount of light which is proportional to the peroxide content.⁸⁹

1.6.1.5 Photoluminescence Spectroscopy

The photoluminescent study of polymeric materials had been used as a means of revealing their structural identification.⁹⁰ The intensity of emission depends on the extent of the oxidation of the polymer. The fluorescence excitation spectrum can identify the absorbing species during photo-oxidation of polymers.⁹¹ Allen et al.⁹² emphasized the role of phosphorescence species in the thermal and photo-oxidation. The carbonyl impurities are responsible for the phosphorescence. The hydroperoxide decomposition is the source for photoluminescence and the intensity depends on the concentration of hydroperoxide.

1.6.1.6 X-ray Photoelectron Spectroscopy

X-ray photoelectron spectroscopy (XPS) is also useful in the determining the degradative products. XPS is a sensitive tool to determine an increase in the amount of oxygen during the photo-oxidation process. With this technique we can measure quantitatively the oxygen, nitrogen and carbon on the surface. The changes in structure, bonding and reactivity of the degraded polymer surfaces can be measured by XPS.⁹³ The O_{1s}/C_{1s} ratio can measure the degree of oxidation.

1.6.2 Molecular weight

1.6.2.1 Viscosity

The viscosity measurement is a technique to measure the molecular weight of polymers. During the degradation process, the viscosity may increase or decrease. If there is an increase in viscosity value, it indicates that crosslinking is taking place during the degradation process. The reduction in viscosity means the chain-scission in the polymer backbone. Gilray⁹⁴ used the melt flow index method to follow the degradation of polyolefins.

1.6.2.2 Gel permeation chromatography

GPC measurements have replaced viscosity technique to a great extent and are generally used in estimating molecular weight distribution, number average mol.wt. and weight average mol.wt of polymers.⁹⁵ Weathering process mostly effects the molecular weight of the polymer. During the degradation process, crosslinking and chain scission occur in the polymer chains. Changes in mol.wt can be observed from the surface area under the GPC peak and from the change in the elution volume. To interpret the results, a standard calibration curve will be used (i.e. PS, PMMA). GPC analysis can indicate simultaneous occurrence of scission in branching which is not possible to measure in viscosity measurements.

1.6.3 Mechanical properties

Much emphasis has been given on the mechanical properties upon exposure. The changes in tensile strength, elongation and modulus are the basic assessment techniques for weathering trials.^{96, 97} During the degradation process tensile strength may increase or decrease. The increase and decrease in tensile strength in polymers is due to crosslinking and chain-scission upon longer irradiation times, respectively. A major drop in the tensile strength is observed in the severely degraded sample. The major changes are also found in the modulus of rubbers as a result of weathering.⁹⁸

1.6.4 Thermal analysis

The thermal analysis of polymers can give the following properties:

- (i) phase changes can be studied via heats of transition
- (ii) temperature effects the rate of reaction in chemical processes.
- (iii) complex molecules can be studied from fragments produced by pyrolysis.

Thermogravimetry technique provides the kinetic informations on the degradation, oxidation, evaporation or sublimation of polymers in any condensed form. Activation energies, rate constants and decomposition temperatures can determine with this technique.⁹⁹ The oxidized polymer shows lower glass transition temperature (T_g). Crystallinity changes can be determined with this technique.

1.6.5 Morphological Analysis

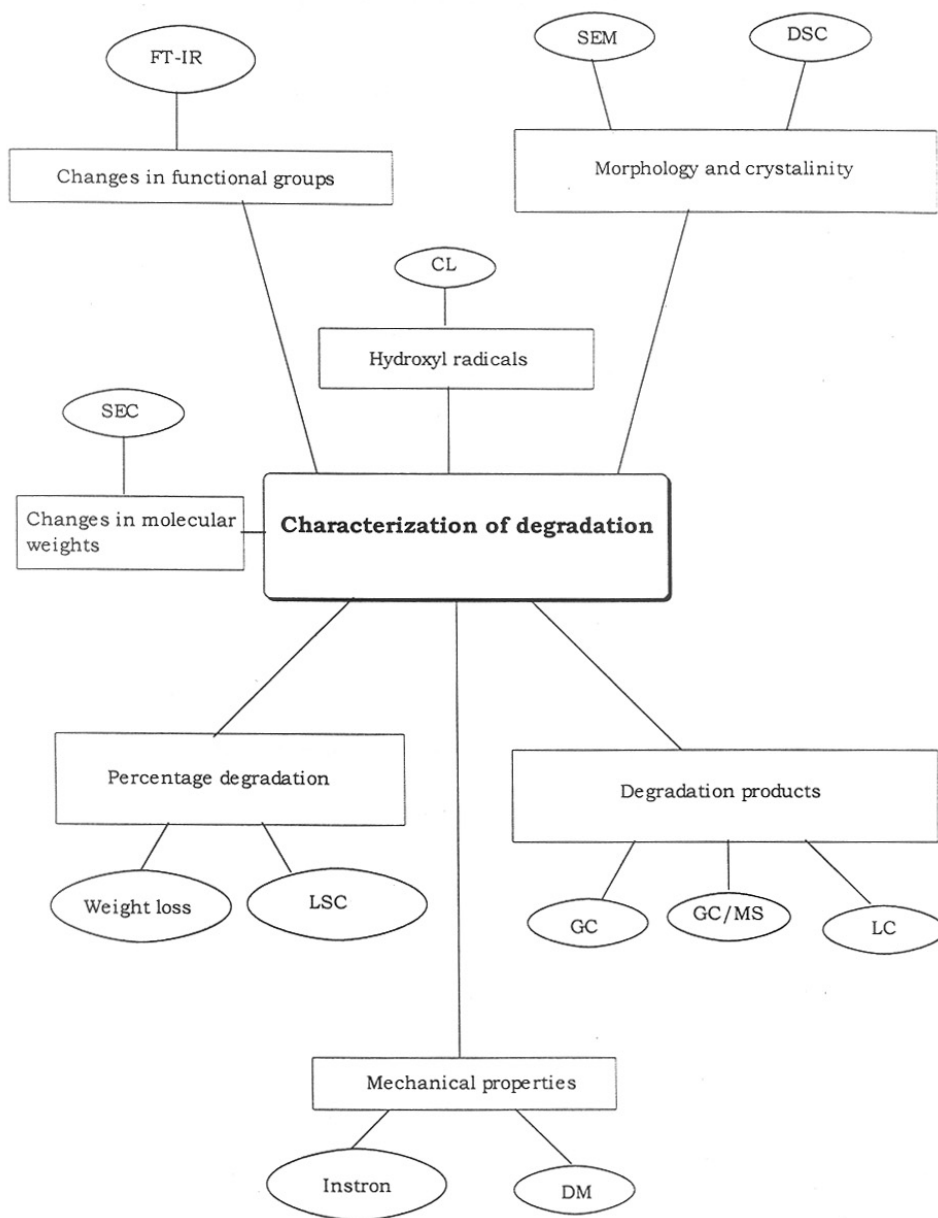
Scanning electron microscope is a powerful tool for analyzing the polymer morphology in homopolymers, heterophasic polymers and polymer blends. The oxidation mainly occurs on the surface of the polymer and results in surface damage. The degraded samples showed micro-cavities on the surface, which are developed into micro-cracks on longer irradiation.^{100, 101}

1.6.6 GC-MS

During the degradation process several different low mol.wt compounds are generated in the polymer system. These products can be analyzed by GC, LC and GC-MS. Using highly efficient capillary columns, complex mixtures of volatile polymer degradation products can be completely separated and identified. A specific advantage of this technique is that pyrolysis is accompanied online under high vacuum.^{102, 103}

1.6.7 X-ray analysis

Wide angle X-ray scattering and small angle X-ray scattering were used to study the crystallinity changes in the polymers during the degradation process. Polychromatic irradiations or thermal aging significantly change the X-ray diffraction pattern. The increase in crystallinity may be due to regularity in polymer chain upon irradiation or aging.

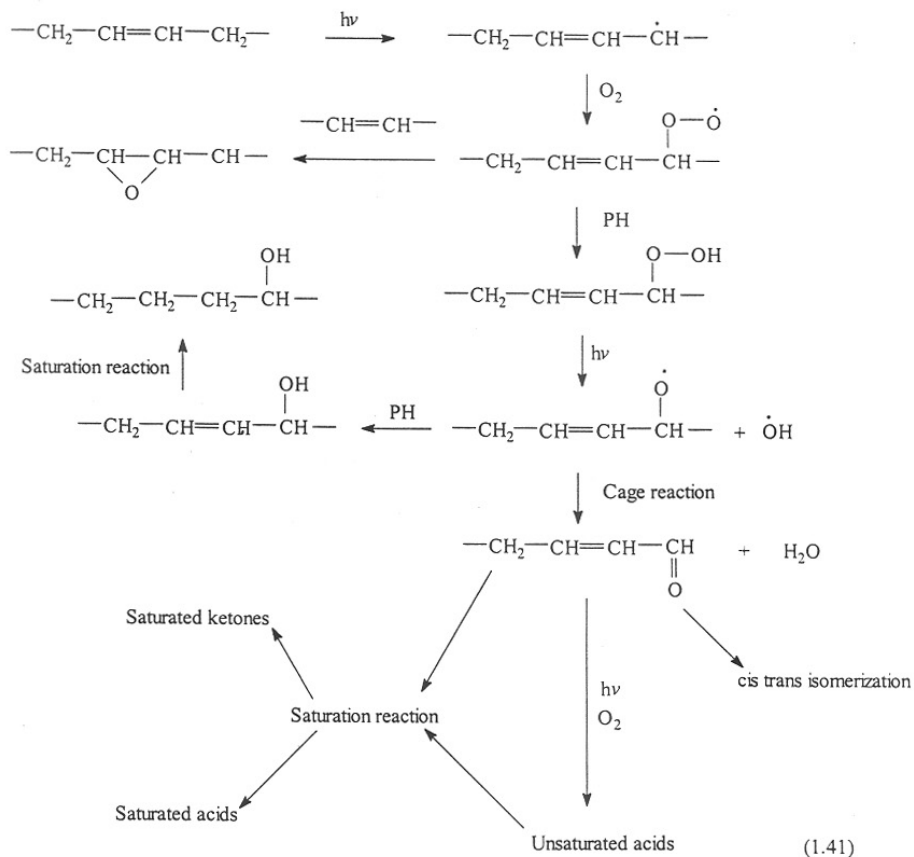


Scheme 1.4: Characterization techniques for polymer degradation

1.7 Photo-oxidative degradation of Styrenic polymers

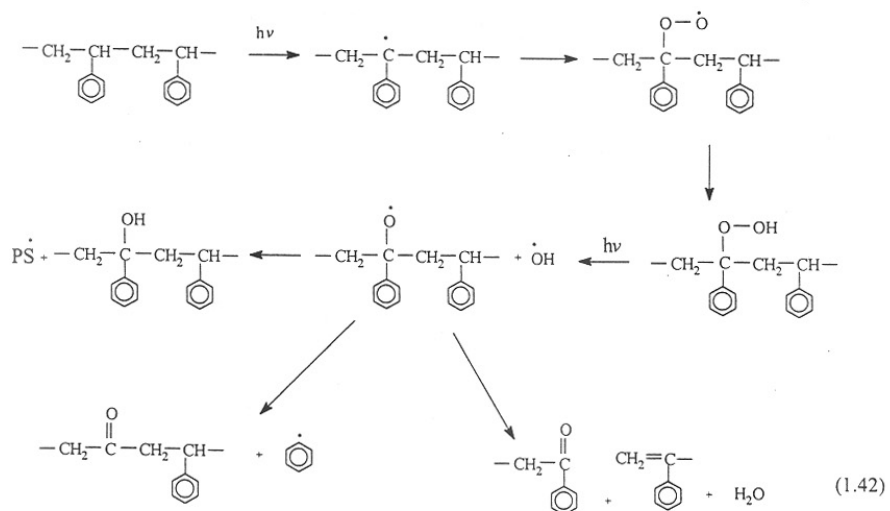
1.7.1 Photo-oxidative degradation of polybutadiene

Polybutadiene photo-oxidation can occur (hydrogen abstraction) in the α - position to the double bond. This abstraction mechanism usually compete with the addition mechanism (Equation 1.41):



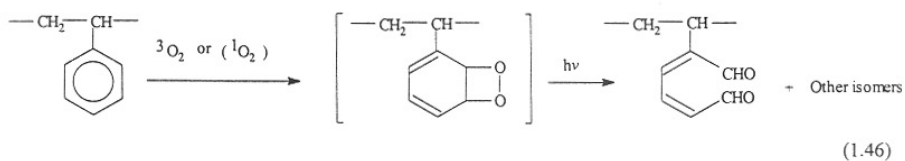
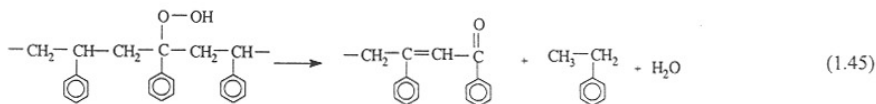
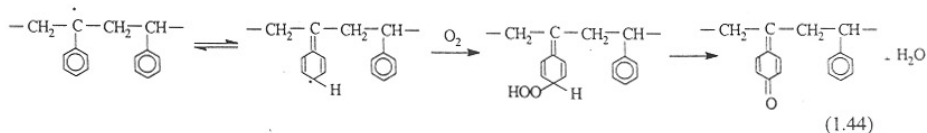
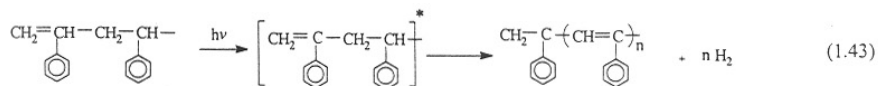
1.7.2 Photo-oxidative degradation of polystyrene

Upon exposure to UV light, polystyrene becomes brittle and shows yellowness. The photo-oxidation mechanism of polystyrene is given (Equation 1.42):



The yellowness is because of the oxidized products. The following products are identified:

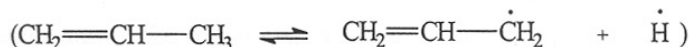
- (i) Polyenes (Equation 1.43)
- (ii) Quinomethanes (Equation 1.44)
- (iii) Benzalacetophenones (Equation 1.45)
- (iv) Carbonyl compounds (Equation 1.46)



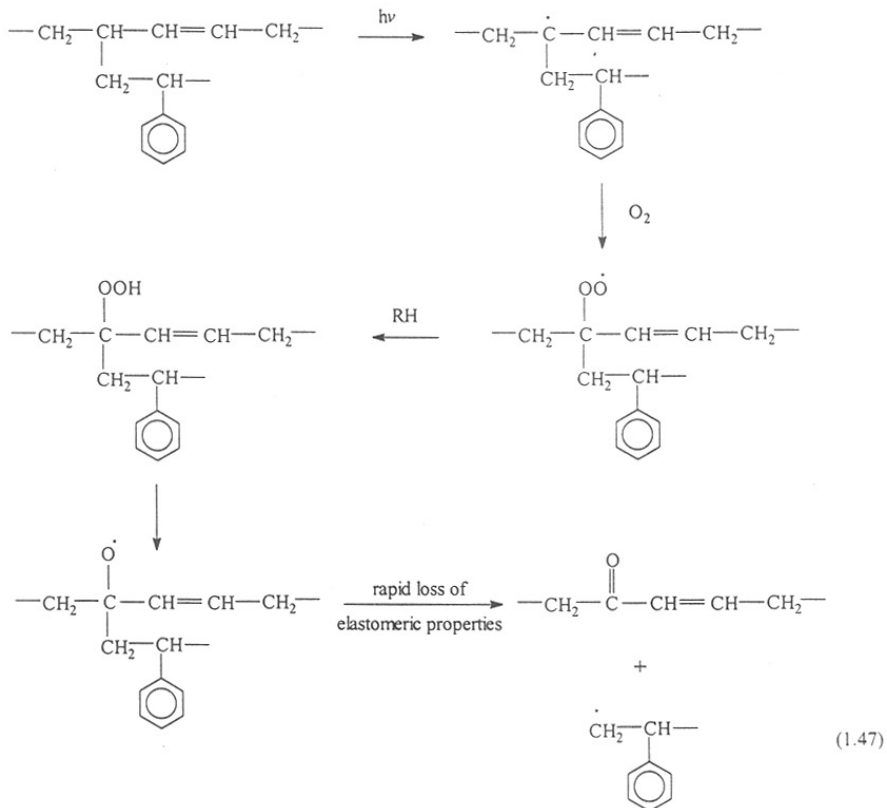
1.7.3 Photo-oxidative degradation of High impact polystyrene

High impact polystyrene (HIPS) exhibits diverse behavior on the composition of polybutadiene under the influence of light, heat and radiation.^{104, 105} The photo-oxidation of polystyrene¹⁰⁶ and polybutadiene¹⁰⁷ has been studied individually, and the mechanism of photo-oxidation is well documented. The yellowing in polystyrene has been studied by several researchers.^{15, 108, 109}

The mechanism of degradation and stabilization of HIPS broadly resembles that of polystyrene and polybutadiene, yet there are major differences that arise mainly from their distinct chemical compositions and structures. Scott^{109a} postulated that the C–H bond of polystyrene is more stable than the C–H bond of the allyl group of the polybutadiene due to the induction effect and steric hindrance of the phenyl group and delocalization of radicals by the allyl group:



Therefore, oxidation naturally begins in the rubbery phase (allyl group) of polybutadiene. Although voluminous literature has been accumulated in the area but there is no concise compilation and organization of the literature.^{104-106, 110-114} The photo-oxidative degradation mechanism of HIPS is (Equation 1.47):



Gaffer et al.^{105, 111, 112} studied the chemical and physical changes of HIPS during artificial weathering. During the viscoelastomeric technique, the damping peak at -80°C (corresponding to the β -transition temperature of the polybutadiene phase) disappeared completely within 14 h of irradiation, but a sharp increase in the complex modulus at 20°C was observed, along with the increase of carbonyl/hydroxyl groups. The polybutadiene phase is selectively degraded by UV light during the initial stages of the oxidation process. The allylic hydroperoxides were responsible for both the thermal and UV-initiated oxidations rather than

carbonyl groups. The same authors observed the gel formation¹⁰⁵ within 6h irradiation, which was followed by an equally rapid fall corresponding to the onset of carbonyl formation, suggesting that the initially formed gel is photocatalytically unstable and breaks down to give stable oxygen-containing end products in the polymer.

The surface hardness of HIPS decreased and swelling degree increased significantly on exposing the film to HCl at 40°C and then UV radiation.¹¹⁵ Chaing¹¹³ investigated that the yellowing in HIPS is the result of degradation in the allyl group of the polybutadiene phase. The degradation proceeds via peroxy radicals. A broad hydroxyl and carbonyl band in the infrared (IR) absorption spectra is observed in the yellow-colored HIPS samples. GPC results also indicated that the processed and/or UV-irradiated samples yielded low molecular weight fractions. Gupta and Dhandole¹¹⁶ proposed that during γ -radiolysis in air, HIPS oxidize randomly with a loss in the molecular weight. Irradiation of HIPS with ⁶⁰Co γ -rays in the absence of oxygen resulted in a steady increase in tensile strength, up to a dose of 300 Mrad.¹¹⁷ Due to cross-linking in the PB, phase elongation at break decreased to half of its initial value at a dose of 190 Mrad, and the impact strength decreased by 50% at 230 Mrad. In air, at a dose rate of 0.372 Mrad/sec, the tensile strength, elongation and impact strength decreased to half of their initial values at doses of 90, 40, and 30 Mrad, respectively. This is because of radiochemical oxidation of the rubber phase. Tosi et al.¹¹⁸ studied the γ -rays and UV light degradation of HIPS in the presence of pigment. The γ -rays and UV irradiation and pigmentation led to the formation and redistribution of defects in HIPS.

Soloveva et al.¹¹⁹ inhibited the oxidative thermal degradation of HIPS by the addition of antioxidants such as Irganox 1010, NG 2246 and Ionol during polymerization in which the polymerization of styrene proceeds due to antioxidant. The physico-mechanical properties of HIPS were not adversely affected by the addition of antioxidants during polymerization. The effects of aging on HIPS have been studied as a function of aging time in both, air and nitrogen.¹²⁰ (Figure. 1.1) Aging in a nitrogen atmosphere is largely a physical process and results in higher modulus, higher tensile strength, and greater decrease in elongation. The aging in air involves both chemical and physical aging. The initial upward trend in tensile

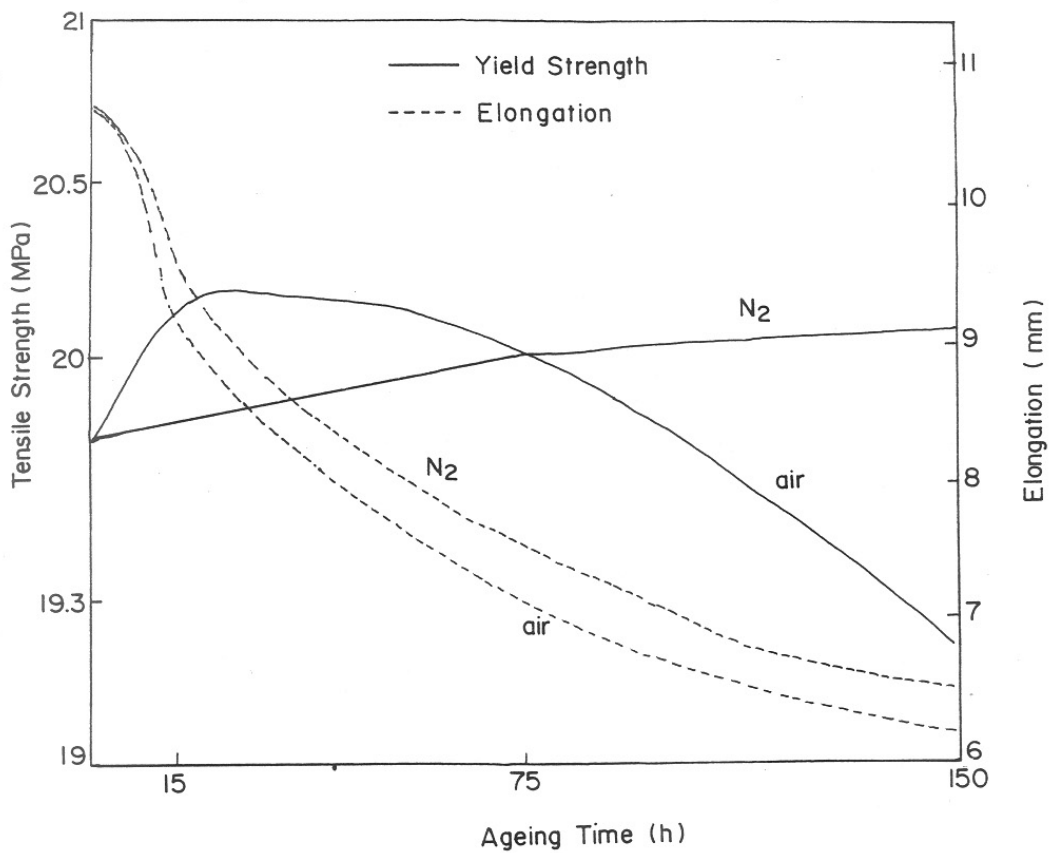


FIG.1.1 EFFECT OF AGING (85°C) ON TENSILE PROPERTIES OF HIPS

strength on annealing in air is attributed to the oxidatively induced cross-linking through interaction of atmospheric oxygen with double bonds present in polybutadiene. The decrease in tensile strength on longer exposure is indicative of oxidative embrittlement. The aging in nitrogen significantly reduces the thermal oxidative effects, thus causing an increase in tensile strength, and the results obtained are essentially indicative of physical aging. Gupta et al.¹²¹ studied the effect of γ -irradiation on HIPS and found a decrease in intrinsic viscosity and molecular weight with irradiation. The atmospheric oxygen leads to enhanced chain scission over cross-linking and causes oxidation during γ -irradiation.

Salman¹²² studied the photo-oxidative aging of virgin and recycled HIPS. The optical properties of exposed samples exhibited changes as a result of discoloration. The transmittance and reflection decrease, whereas absorbance increases with increasing recycling of HIPS. The photo and thermo-oxidative degradation of different grades of HIPS have been studied by Israeli and coworkers.¹²³ The carbonyl absorbance increases with irradiation time. The kinetic curves of the photo- and thermo-oxidation of HIPS are given in Figure 1.2. For all the samples, a fast rate of photo-oxidation was observed for the first 50 h of exposure. After this period, which probably corresponds to the complete oxidation of polybutadiene, a slow oxidation rate was observed that is finite. In thermal-oxidation, the changes are very similar to those observed that are finite. In thermal oxidation, the changes are very similar to those observed in photo-oxidation, but the kinetics curves are characterized by an induction period followed by the fast oxidation of polybutadiene. The carbonyl group formation increases with increasing temperature. All the samples gave similar oxidation products, but in varying quantities, which have been identified and quantified by derivatization reactions by treating the samples with ammonia and sulfur-tetrafluoride gas.

Figure 1.3 shows that polybutadiene unsaturation decreases with exposure time and disappears completely after 23, 45, and 55 h irradiation, respectively, for samples A, B, and C.¹²⁴ The decay of unsaturation in previously heated HIPS films (PB 8.2 mole-%) in air during irradiation is fast. Figure 1.3 shows that polybutadiene unsaturation was also destroyed during thermal oxidation, and the unsaturation of an oxidized sample decayed within 10 h of UV irradiation only¹¹². These observations

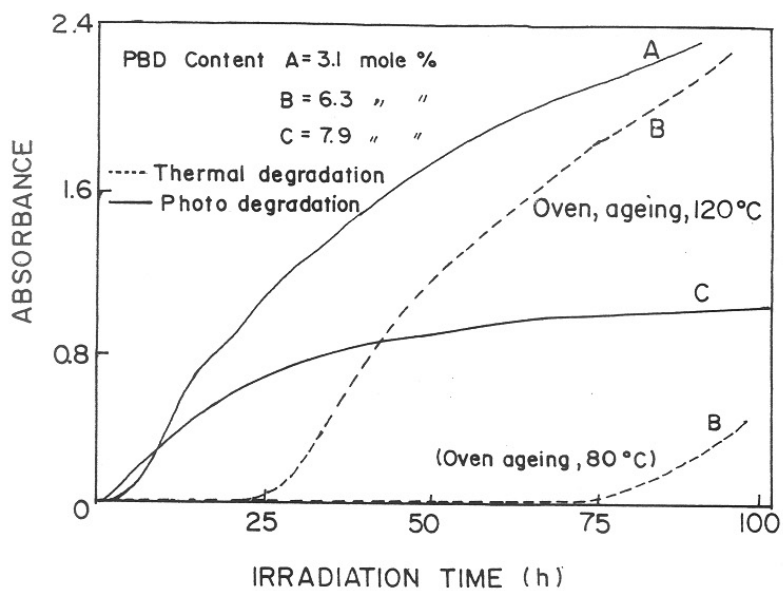


FIG.1.2 CHANGES IN CARBONYL ABSORBANCE (1723 cm^{-1})
IN HIPS

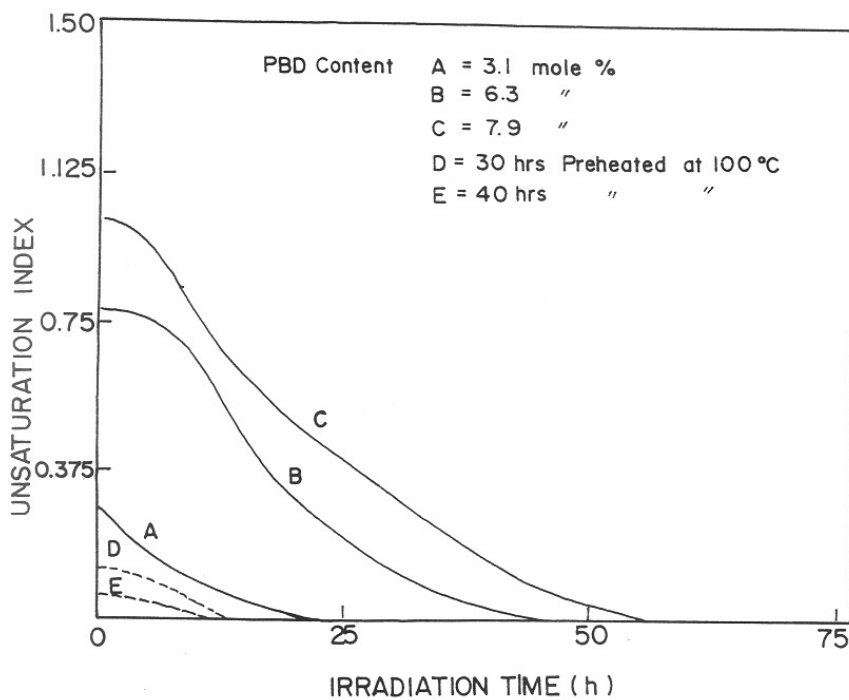


FIG. I.3 DECAY OF POLYBUTADIENE UNSATURATION INDEX (966 cm^{-1}) OF HIPS

suggest that the polybutadiene phase is completely degraded on irradiation and the sample underwent rapid photo-yellowing, yielding a measurable increase within 50h that became more severe at longer periods.

1.8 Photostabilization of High impact polystyrene

Stabilization is the most important aspect of the toughened polymers. A simple toughening model based on the crack-opening displacement of craze breakdown between adjacent rubber particles is suggested, with interparticle distance as the most important variable.

Dremin et al.¹²⁵ have studied the effect of a number of antioxidants on the thermal stability of HIPS. The trinonyl phosphate stabilized HIPS gave superior color stability and mechanical properties even at 180-250°C. Dremin and Andreev¹²⁶ have compounded the thermal stability of various hindered phenol-and phosphate-based antioxidants in HIPS. The stabilizer effectiveness was measured in terms of carbonyl absorption (1690 cm^{-1}) by infrared spectroscopy. A synergistic mixture of 6-hydroxy dibenz-oxaborin derivatives and dialuryl-3,3'-thiodipropionate or *tris*-2-hexadecyl hydroquinone improves the melt index¹²⁷ of a HIPS sample from 1.79 to 1.18, respectively, for samples without and with the synergistic mixture at 230°C. The visual observation of color of the oxidized resin also indicated that the stabilized sample was less degraded. The HIPS samples stabilized by 2,2',2'',2'''-(ethylene dinitro) tetraethanol tetrakis [3-(3,5-di-*tert*-butyl-4-hydroxy phenyl) propionate] and related compounds resisted oxidative deterioration for 1200h, while a neat sheet deteriorated after 3h of accelerated aging in an oven at 149°C.¹²⁸ Kirillova and Fratkina¹²⁹ have stabilized HIPS with organic additives against UV light. HIPS with improved color, thermal and light degradation¹³⁰ was made by treating it with the phenolic antioxidants i.e. bis [*p*-(arylamino)phenoxides].¹³¹

The *w,w'*-thiobis [N-(3-*tert*-butyl-4-hydroxyphenyl) alkane carboxamide] stabilized HIPS sample had an 860 h lifetime in a pressure furnace at 150°C, compared to 3 h for unstabilized sample¹³². The light stability was improved by incorporating aromatic isophthalate into the matrix of HIPS¹³³. The synergistic system of zinc oxide with secondary organic additives showed promising UV stabilization for impact polystyrene and other polymers.¹³⁴ The HIPS stabilized with 2,9-di(1-

naphthoxy)-3,8-dioxadecane and 1-butoxy-1-(1-naphthoxy) ethane had better oxidative degradation resistance¹³⁵ than the sample containing BHT and other conventional antioxidants. The derivatives of hexahydrotriazine also stabilized HIPS.¹³⁶

A high-impact polystyrene resin¹³⁷ containing methyl-3-*n*-dodecyl thiopropionate had better retention of elongation than an unstabilized resin after aging 6 h at 75°C. The initial impact and tensile strength of HIPS during accelerated and natural weathering were improved by incorporating α -cyano- β , β -diphenylacrylates into its matrix.¹³⁸ Richard et al.^{139, 140} improved the color of HIPS containing halogenated fireproofing agent by the addition of benzotriazole derivative light stabilizers and hydroxy phenyl ester antioxidants. The later acts as an acid acceptors. The best color stability was obtained with a mixture of 2-(3', 5'-di-*tert*-butyl-2'-hydroxy phenyl)-5'-chlorobenzotriazole and octadecyl 3-(3',5'-ditert-butyl-4'-hydroxyphenyl) propionate. Further improvement is obtained by adding an epoxy cresol novolac resin and zinc stearate or tin maleate. Bradley et al.¹⁴¹ prevented discoloration and made HIPS flame retardant by incorporating chlorinated benzotriazoles into the matrix of HIPS.

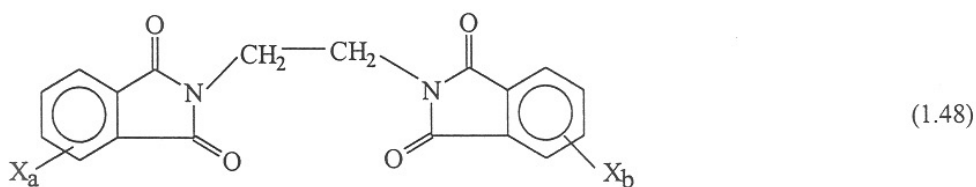
Scott¹⁴² investigated that the photo-oxidative degradation of the polybutadiene phase of rubber-modified styrene can be prevented by a synergistic combination of conventional phenolic antioxidants and benzophenone derivatives. Pierotti and Deannin¹⁴³ compared the effectiveness of conventional UV absorbers, carbon black, ZnO, and surface coatings against UV degradation of HIPS. Fine particle size ZnO in combination with phenolic antioxidants was more effective than UV absorbers. The carbon black filled phenolic antioxidant composition was extremely effective in stabilizing against embrittlement; however, color was limited to opaque black. Lamination with acrylic and/or poly(vinyl fluoride) film provided high photostability with the complete color range. The well-known antioxidant 2,6-di-*tert*-butyl-4-methylphenol and its important transformed oxidation products, that is, 3,5,3',5'-tetra-*tert*-butylstilbenequinone and 2,6-di-*tert*-butyl-1,4-benzoquinone, also show a stabilizing effect in HIPS against thermal and photodegradation.¹⁴⁴ Tris(2,4-di-*tert*-butyl phenyl) phosphite has been used as a food antioxidant in HIPS.¹⁴⁵

The *o,o*-diisopropyl-1-hydroxy-1-methyl-2-phenyl-2-nitroethyl phosphonate is a good stabilizer against photo-oxidation of HIPS.¹⁴⁶ The melt blending of octadecyl-3(3',5'-di-*tert*-butyl-4-hydroxy phenyl) propionate and 2,2'-methylene bis(6-*tert*-butyl-4-ethyl phenol) with HIPS at 85°C showed no color change compared to light yellow, brown, and dark brown in the absence of these ingredients.¹⁴⁷ The photochemical degradation of HIPS during weathering was substantially reduced by incorporating 0.5% bis(2,2,6,6-tetramethyl-4-piperidienyl)sebacate and/or 2-(2-hydroxy-5-methyl phenyl) benzotriazole.¹⁴⁸ HIPS stabilized with 0.1% 3-[(3-*tert*-butyl-4-hydroxy-5-methyl benzyl) thio]propionamide had improved elongation and yellowness index.¹⁴⁹ The migration of *n*-octadecyl-3-(3,5-di-*tert*-butyl-4-hydroxyphenyl) propionate from HIPS is a significant practical problem.¹⁵⁰ This antioxidant stabilizes the product under natural weathering and migration of the additives into the foodstuff at the contact surface is found due to diffusion from the dispersed rubber phase.

The *N*-(2,2,6,6,-tetramethyl piperidinyl)amides of saturated carboxylic acids have been used as light and heat stabilizers of HIPS.¹⁵¹ The heat and light-resistant composition was obtained by adding 0.5% alkyl hydroxyphenyl propionate derivatives into the HIPS matrix.¹⁵² The HIPS samples blended with ethylene bis(stearimide) and stearyl-3-*tert*-butyl-4-hydroxy-5-methyl phenyl propionate gave an impact strength and yellowness index, respectively, of 7.4 kg-cm/cm and 1.8 initially and 6.5kg-cm/cm and 38.1 after 14 days exposure at 120°C versus 7.2 kg-cm/cm and 19 initially and 2.8 kg-cm/cm and 52.3 after 14 days, respectively, using stearyl-3,5-di-*tert*-butyl-4-hydroxy phenyl propionate. The 2,4-di-*tert*-amyl-phenol, 2,2'-methylene bis[4-methyl-6-(1-methyl cyclohexyl)phenol] and tris(nonyl phenyl) phosphite act as antioxidants and heat stabilizers for styrenic polymers.¹⁵³ HIPS samples containing a mixture of these stabilizers after exposure to light in an industrial atmosphere for 6 months had impact flexural strength of 73.0kJ/m², notched impact strength of 8.8 kJ/m², flexural strength of 51 N/mm² and tensile strength of 29 N/mm², while it had the same properties at 60 kJ/m², 5 kJ/m², 22 N/m², and 23 N/mm², respectively, under similar conditions with no stabilizers. Triethylene glycol bis[3-(3-*tert*-butyl-4-hydroxy-5-methyl phenyl)]propionate also

shows synergism with amyl phenol derivative.¹⁵⁴ Gilg and Evans¹⁵⁵ found phenolic antioxidants and metal deactivators suitable for stabilization of HIPS.

The heat stability of HIPS was improved by melt blending a mixture of ethylene bis(stearamide)phosphite derivatives and 4,4'-butylidene bis(6-tert-butyl-m-cresol) with HIPS.¹⁵⁶ The injection-molded test piece showed izod impact strengths of 7.3 and 6.5 kg cm/cm and color differences of 11.8 and 15.6 initially and after 14 days at 110°C, respectively, versus izod impact strengths of 6.8 and 5.2 kg cm/cm and color differences of 12.3 and 20.8 initially and after 14 days at 110°C, respectively, for a similar composition without stabilizer. A composition with good resistance to fire, heat and UV light was made by incorporating bis(pentabromophenyl) succinate and Sb₂O₃ into the HIPS matrix.¹⁵⁷ Nishibori et al.¹⁵⁸ made HIPS heat, light, and fire resistant by mixing it with hexabromocyclododecane and bis(2,6-di-tert-butyl-4-methylphenyl) pentaerythritol diphosphate. The composition had a color change of 21 after 60 min at 210°C and 1.6 after 24 h fado-o-meter exposure. Tsunoda and Yamauchi¹⁵⁹ made a high-impact-strength and good heat/light resistance composition that consists of HIPS, halogen containing compounds of the general formula (1.48):



(Where X = Br, Cl, and a, b = 1-4), TiO₂, Sb₂O₃, benzotriazole, ethylene bis-steramide and HALS. The title compound shows a color change of 2.8 in 300 h weather-o-meter exposure. The composition of HIPS with improved light resistance and an excellent balance of gloss, impact resistance and rigidity is composed of 96 parts of HIPS, 2 parts hindered amine and 2 parts benzotriazole.¹⁶⁰ The light, heat and flame-retardant and impact resistant composition is composed of HIPS, 2,4,6-tris(2,4,6-tribromophenoxy)-1,3,5-triazine, alkylene bis(tetrabromo phthalimide), brominated epoxy resin and Sb₂O₃.¹⁶¹ The title compound had a UL-94 flame retardance V-O, a heat distortion temperature of 83.4°C and impact strength of 8.4

kg cm/cm versus a UL-94 flame retardance V-O, a heat distortion temperature of 80.2°C and impact strength of 6.1 kg cm/cm without tetrabromophthalimide derivatives.

1.9 References:

1. I.I. Ostromislensky, *U.S. Pat.* 1,613,673 (1927)
2. H. Keskkula, A.E. Platt, R.F. Boyer, in 'Encyclopedia of Chemical Technology', 2nd ed., Vol. 19, Wiley-Interscience, New York, 1969, p.85
3. J.L. Annos, *Polym.Eng. Sci.*, **14**, 1 (1974)
4. U.S. Court of Appeals (9 th Circuit), cases 71-1371 and 71-1372 (1971)
5. H. Willersinn, *Makromol. Chem.*, **101**, 296 (1967)
6. K. Dinges, H. Schuster, *Makromol. Chem.*, **101**, 200 (1967)
7. R.B. Bishop, '*Practical Polymerization for Polystyrene*', Catiners Publishers, Boston, 1971
8. N. Platzer, *Ind. Eng. Chem.*, **62**, 1-7 (1970)
9. J. Zach, *Synt. Kauc.*, **22**, 1 (1971)
10. C. Placek, Chemical Process, Review No. 46, Noyes Data Corp., Park Ridge, NJ, 1970
11. C.D. Han, Y.M. Kim S.J. Chen, *J. Appl. Polym. Sci.*, **19**, 2831 (1975)
12. F.P. La Mantia, *Polym. Degradn. Stab.*, **15**, 283(1986)
13. Z. Zamorsky, J. Muras, *Polym. Degradn. Stab.*, **14**, 41 (1986)
14. Z. Osawa, *Polym. Degradn. Stab.*, **20**, 203 (1983)
15. A. Davis, D. Sims (Eds.), '*Weathering of Polymers*', Applied Science Publishers, London, 1983, Chaps. 5 and 6
16. R.W. Kuchkuda, *Plast. Eng.*, **33**, 32 (1977)]
17. J.D. Cooney, *Polym. Eng. Sci.*, **22**, 492 (1982)
18. A. Davis, '*Weathering of Polymers, in Developments in Polymer Degradation-I*' (N. Grassie, Ed.), Applied Science Publishers, London, 1977, p.249
19. A. Charlesby, R.H. Partridge, *Prog. Roy. Soc.*, **A283**, 312 (1965)

20. N. Uri, *Israel J. Chem.*, **8**, 125 (1970)
21. M.U. Amin, G. Scott, L.M.K. Tillakeratne, *Eur. Polym. J.*, **11**, 85 (1975)
22. J.F. Mealock, F.B. Mallory, F.P. Gay, *J. Polym. Sci. A1, Polym...*, **6**, 2921 (1968)
23. D.G.M. Wood, T.M. Kallman, *Chem. Ind.*, 423 (1972)
24. D.A.S. Ravens, J.E. Sisley, in E.M. Fettes (Ed.), " *Chemical reactions of polymers*", Interscience publishers, John Wiley & Sons, Inc., New York (1964)
25. H.H.G. Jellinek, F.F. Flajsman, F.J. Kryman, *J. Appl. Polym. Sci.*, **13**, 107 (1969)
26. S.W. Bonson, *Adv. Chem.Ser.*, **77**, 74 (1968)
27. T. Hancock, " *Personal Narrative of the origin and progress of the Caoutchouc or India-Rubber manufacture in England*", Longmans Green & Co. Ltd., London, 1857
28. H. Staudinger, W. Heuer, *Ber.*, **67**, 1159 (1934))
29. H. Staudinger, E. Dreher, *Ber.*, **69**, 1091 (1936)
30. A. Weissler, *J. Appl. Phys.*, **21**, 171 (1950)
31. D.W. Ovenall, G.W. Hastings, P.E.M. Allen, *J. Polym. Sci.*, **33**, 207 (1958)
32. P.E.M. Allen, G.M. Burnett, G.W. Hastings, H.W. Melville, D.W. Ovenall, *J. Polym. Sci.*, **33**, 213 (1958).
33. J.L. Williams, T.S. Dunn, V.T. Stannet, *Radia. Phys. Chem.*, **19**, 291 (1982)
34. T.S. Dunn, J.L. Williams, *J. Indus, Irrad. Technol.*, **1**, 33 (1983)
35. F. Yoshii, K. Makuuchi, I. Ishigaki, *Polym. Commun.*, **29**, 146 (1989)
36. N.S. Allen, K.O. Fatinikum, T.J. Henman, *Eur. Polym. J.*, **19**, 551 (1983).
37. D.J. Carlsson, A. Garon, D.M. Wiles, *Macromolecules*, **9**, 695 (1976)
38. O. Cicchetti, F. Gratini, *Eur. Polym. J.*, **8**, 561 (1972).
39. P.P. Klemchuk, *Polym. Photochem.*, **3**, 1 (1983)

40. N.S. Allen, ed., '*Degradation and stabilization of polyolefins*', Applied Science Publishers Ltd., London, 1983, p.337
41. D.J. Harper, J.F. McKeller, *J. Appl. Polym. Sci.*, **17**, 3503 (1973)
42. P.P. Klemchuk, *Ullman's Ency. Indus. Chem.*, **A3**, 95 (1985)
43. A.L. Andrady, *J. Macromol. Sci. Rev. Macromol. Chem. Phys.*, **C34**, 25 (1994).
44. George Wypych, '*Hand book of material weathering*', 2nd edition, ChemTec Publishers, Canada, Chapter 19, 1995, p.523
45. J.L. Bolland, G. Gee, *Trans. Faraday. Soc.*, **42**, 236 (1946)
46. F. Faucitano, A. Buttafaia, G. Camino, L. Greci, *Trends in polymer Sci.*, **4**, 92 (1996)
47. J.H. Adams, J.E. Goodrich, *J. Polym. Sci. C A-1*, 1269 (1970)
48. L. Balaban, J. Majer, K. Veely, *J. Polym. Sci.*, **C-22**, 1059 (1969)
49. G.A. Russell, *J. Am. Chem. Soc.*, **79**, 3871 (1957)
50. F. Gugumus, Paper presented at the 18th colloquium of Danubian countries for Natural and Artificial ageing of plastics, Villach, Austria, 22-26 June 1987.
51. F. Gugumus, Paper presented at the European symposium on polymeric materials, Lyon, France, 14-18 September 1987
52. M.S. Olcott, H.A. Matill, *Chem. Rev.*, **29**, 25 (1941)
53. H. Schonhorn, P.L. Luongo, *Macromolecules*, **2**, 364 (1969)
54. H. Heskins, J.E. Guillet, *Macromolecules*, **1**, 97 (1968)
55. O. Cicchetti, *Adv. Polym. Sci.*, **7**, 70 (1970)
56. H.J. Hiller, *Eur. Polym. J. Suppl.*, 105 (1969)
57. D.J. Carlson, D.M. Wiles, *J. Polym. Sci. Polym. Chem. Ed.*, **12**, 2217 (1970)
58. P. Vink, Th. J. Van Veen, *Eur. Polym. J.* **14**, 533 (1978)
59. N.S. Allen, M. Edge, '*Fundamental of polymer degradation and stabilization*', Elsevier Applied Science, London, 1992, chap. 5, p. 109

60. T. Werner, *J. Phys. Chem.*, **83**, 320 (1979)
61. D.G. Pobedimskii, N.A. Mukmeneva, P.A. Kirpichnikov, '*Developments in polymer stabilization*', G. Scott (Ed.) vol. **2**, Applied Science Publishers, 1979, p.125
62. K. Schwarzenbach, '*Plastic Hand book*', R. Gachter, H. Muller (Eds.), Hanser Publishers, New York, Chap. 1, 1984, p. 7
63. R.P. Fros, D.O. Cowan, G.S. Hammond, *J. Phys. Chem.*, **68**, 3747 (1964).
64. J.P. Guillony, C.F. Cook, *J. Polym. Sci. A1, Polym. Chem.*, **11**, 1927 (1973)
65. M.B. Neiman, E.G. Rozantsev, Y.G. Mamedora, *Nature*, **196**, 472 (1962)
66. K. Murayama, S. Morimura, T. Kuramada, I. Watanabe, *British Pat.* 1196224
67. K. Murayama, S. Morimura, T. Kuramada, I. Watanabe *US. Pat.* 3,542,729 (1970)
68. K. Murayama, S. Morimura, J. Yoshioka, *J. Bull. Chem. Soc. Jpn.*, **42**, 1640 (1969)
69. D.J. Carlsson, K.H. Chan, J. Durmis, D.M. Wiles, *J. Polym. Sci. Polym. Chem. Ed.*, **20**, 575 (1982)
70. X. Yang, Y. Chan, L.C. Dickinson, J.C.W. Chien *Polym. Degrad. Stab.*, **20**, 1 (1988)
71. B.N. Felder, R. Schumacher, F. Sitek, '*Hindered amine light stabilizers-A mechanistic study in photodegradation and photostabilization of coatings*', in P.S. Pappas and F.H. Winslow (Eds.): ACS Symposium series **151**, Washington D.C., 1981
72. B.N. Felder, '*Mechanistic studies of sterically hindered amines in photooxidation of liquid polypropylene model substances*', In P.P. Klemchuk (Ed.): Polymer stabilization and degradation: ACS Symposium Series **280**, Washington D.C., 1985.
73. P.P. Klemchuk, M.E. Gande, *Polym. Degrad. Stab.*, **22**, 241 (1988)

74. P.P. Klemchuk, M.E. Gande, E. Cordola, *Polym. Degrad. Stab.*, **27**, 65 (1990)
75. F. Gugumus, 'Developments in polymer stabilization - 1', G. Scott (Ed.), Applied Science Publishers, London, p.261
76. F. Gugumus, *Angew. Makro. Chem.*, **176/177**, 241 & 3070 (1990)
77. D. Bellus, H. Lind, J.F. Wyatt, *J. Chem. Soc., Chem. Commun.*, 1199 (1972)
78. R. Ballardini, G. Beggiato, P. Bortolus, .A. Faucitano, A. Buttafava, F. Gratani, *Polym. Degrad. Stab.*, **7**, 41 (1984)
79. P. Bortolus, S. Dellonte, A. Faucitano, F. Gratani, *Macromolecules*, **19**, 2916 (1986)
80. J. Lucki, J.F. Rabek, B. Ranby, *J. Appl. Polym. Sci.*, **36**, 1067 (1988)
81. S.P. Fairgrieve, J.R. Mac Callum, *Polym. Degrad. Stab.*, **8**, 107 (1984)
82. D.J. Carlsson, D.W. Gratton, T. Suprunchuk, D.M. Wiles, *J. Appl. Polym. Sci.*, **22**, 2217 (1978)
83. T. Toda, E. Mori, C. Murayama, *Bull. Chem. Soc. Jpn.*, **45**, 1904 (1972)
84. N.Z. Searle, 'Analytical Photochemistry and Photochemical Analysis', (J.M. Fitzgerald, Ed.), Marcel Dekker, New York, 1971
85. Y. Israeli, J. Lacoste, J. Lemaire, R.P. Singh, S. Sivaram, *J. Polym. Sci. Part A. Polym. Chem.*, **32**, 485 (1994)
86. V. Reinohl, J. Sedlar, M. Navratil, *Polym. Photochem.*, **1**, 165 (1981)
87. L. Banks, E.Ellis, *Polym. Bull.*, **1**, 377 (1979)
88. N.C. Billingham, J.W. Burdan, I.W. Kaluske, E.S.O. Keefe, *Polym. Mater. Sci. Eng.*, **58**, 43 (1988)
89. R.L. Matisova, Zr. Foder, J. Rychly, *Polym. Degradn. Stab.*, **3**, 371 (1980-81)
90. N.S. Allen, J. Horner, J.F. Mc Keller, *The Analyst*, **101**, 260 (1976)
91. D.J. Carlsson, D.M. Wilis, *Polym. Lett.*, **8**, 419 (1970)
92. N.S. Allen, J.F. Mc Keller, G.O. Philips, *J. Polym. Sci. Polym. Lett. Ed.*, **12**, 253 (1974)

93. D.T. Clarke, A. Dilks, *'Developments in polymer degradation-1*, (N. Grassie, Ed.), Applied Science Publishers, London, 1977
94. H.M. Gilray, *ACS Symp. Ser.* **95**, 5 (1979)
95. A. Holmstrom, *ACS Symp. Ser.*, **95**, 45 (1979)
96. G.M. Ruhnke, L.F. Biritz, *Kunststoffe*, **62**, 250 (1972)
97. W.W. Wright, *Composites*, **12**, 201 (1981)
98. J. Wright, *Eur. Rubber. J.*, **159**, 13 & 34 (1977)
99. A. Vishwa Prasad, R.P. Singh, *Materials. Res. Bull.*, **30**, 1407 (1995)
100. H. Kaczmarek, *Polymer*, **37**, 189 (1996)
101. A. Vishwa Prasad, R.P. Singh, *J. Appl. Polym. Sci.*, (**inpress**)
102. G. Montaudo, C. Puglisi, M. Blazro, K. Kishore, K. Ganesh, *J. Anal. Appl. Pyrolysis*, **29**, 207 (1994)
103. B. Plage, H.R. Schutten, *J. Anal. Appl. Pyrolysis*, **15**, 197 (1989)
104. C. Adam, J. Lacoste, J. Lemaire, *Polym. Degrad. Stab.*, **29**, 185 (1989)
105. A. Ghaffar, A. Scott, G. Scott, *Eur. Polym. J.*, **13**, 83, 89 & 989 (1977)
106. B. Mailhot, J.L. Gardette, *Macromolecules*, **25**, 4127&4129 (1992)
107. C. Adam, J. Lacoste, J. Lemaire, *Polym. Degrad. Stab.*, **24**, 185 (1989)
108. C. Sawidas, J.A. Stretanski, L.R. Castello, *'Stabilization of Polymers and Stabilizer Process'*, in Advance in Chemistry Series, No. **85** (R.F. Gould, Ed.), ACS, Washington, DC, 1968, P.187
109. J.F. Rabek, *Mechanisms of Photophysical Processes and Photochemical Reactions in Polymers*, Wiley, New York, 1987, p.510
- 109a G. Scott, *Atmospheric Oxidation and Antioxidants*, Elsevier, London, 1965, p.25
110. C. Adam, J. Lacoste, J. Lemaire, *Polym. Degrad. Stab.*, **29**, 305 (1990)
111. A. Gaffar, A. Scott, G. Scott, *Eur. Polym. J.*, **11**, 271 (1975)

112. A. Gaffar, A. Scott, G. Scott, *Eur. Polym. J.*, **12**, 615 (1976)
113. W.Y. Chiang, *Ta Tung Hsuech Pao*, **9**, 129 (1979)
114. J.F. Rabek and B. Ranby, '*Photo-degradation, Photo-oxidation and Photo Stabilization of Polymers*', Interscience, New York, 1975
115. N. Piperov, *Plast. Massy.*, **9**, 51 (1978)
116. M.C. Gupta, A.D. Dhandole, *Proc. Nucl. Chem. Radio. Chem. Symp.*, 493 (1980)
117. H. Wilski, E. Gaube, S. Roesinger, *Colloid Polym. Sci.*, **260**, 559 (1982)
118. B. Tosi, S.V. Karimov, Kh. M. Aslanova, *VINITI*, 6278 (1982)
119. I.V. Soloveva, V.M. Buiatova, E.I. Egorova, E.I. Kirillova, S.V. Kuznetrova, *Plast. Massy.*, **9**, 13 (1983)
120. C.C. Chen, M. Habibullah, J.A. Saver, *J. Appl. Polym. Sci.*, **28**, 3911 (1983)
121. M.C. Gupta, B.S. Srirao, B.P. Kanphande, V.P. Bansod, *Polym. Commun.*, **25**, 334 (1984)
122. S.R. Salman, *Polym. Plast. Technol. Eng.*, **32**, 115 (1993)
123. Y. Israeli, J. Lacoste, J. Lemaire, R.P. Singh, S. Sivaram, *J. Polym. Sci. Pt. A., Polym. Chem.*, **32**, 485 (1994)
124. R.P. Singh, R.A. Raj, A. Vishwa Prasad, S. Sivaram, J. Lacoste, J. Lemaire, *Polym. Int.*, **36**, 309 (1995)
125. V.D. Dremin, N.V. Galeisko, A.P. Andreev, V.B. Zovina, V.M. Reznik, *Plast. Massy.*, **2**, 15 (1967)
126. V.D. Dremin, A.P. Andreev, *Plast. Massy.*, **5**, 20 (1967)
127. L.J. McCabe, H.J. Address, F.M. Seser, *U.S. Pat.* 3,404,123 (1968)
128. M. Dexter, J.D. Spivack, D.H. Steinberg, *U.S. Pat.* 3,435,065 (1969)
129. E.I. Kirillova, G.P. Fratkina, *Plast. Massy.*, **11**, 58 (1969)
130. D.E. Miller, *Fr.* 1,572,579 (1969)

131. L.A. Skriplko, E.G. Rozantsev, P.I. Levin, *Sin. Issled. Eff. Khim. Dobavok. Polim. Mater.*, **2**, 72 (1969)
132. M. Knell, M. Dexter, *Ger. Offen.*, 2,014,165 (1970)
133. A.Y. Coran, C.G. Anagnostopoulos, *Ger.* 1,494, 195 (1970)
134. D.S. Carr, B. Baum, S. Margosiak, A. Llompert, *Mod. Plast.*, **48**, 160 (1971)
135. M. Braid, *U.S. Pat.* 3,683,032 (1972)
136. M. Knell, D.H. Steinberg, *U.S. Pat.*, 3,694,440 (1972)
137. M. Dexter, D. Steinberg, *U.S. Pat.*, 3,758,549 (1973)
138. G.V. Kutimova, A.A. Ebimov, R.S. Burmistrova, Z.G. Popova, *Plast. Massy.*, **2**, 14 (1975)
139. B. Richard, F. Joseph, T. Lowrence, *Fire Retard. Proc. Int., Symp. Flammability, Fire Retard.*, 14 (1976)
140. B. Richard, F. Joseph, T. Lowrence, *Polym. Eng. Sci.*, **14**, 782 (1977)
141. R. Bradelgy, J. Farber, L. Testa, *Polym. Eng. Sci.*, **17**, 782 (1977)
142. G. Scott, 'Toughening Plastics', Int. Corp. Paper No. 5, p13 (1978)
143. R.J. Pierotti, R.D. Deanin, *Addit. Plast.*, **2**, 103 (1978)
144. J. Virt, L. Rosik, J. Pospisel, *Eur. Polym. J.*, **16**, 247 (1980)
145. U.S. Food and Drug Administration, Fed. Regist. 2 Jan (1981)
146. L.A. Zhidkova, G.M. Baranov, G.V. Kutimova, A.A. Etimov, A.F. Tyutereva, *Plast. Massy.*, **10**, 42 (1980)
147. Japan Synthetic Rubber Co., Ltd., *Jpn. Kokai Tokkyo Koho JP* 58,33,924 (1983)
148. P.D. Gabriele, J.R. Geib, R.M. Iannucc, W.J. Reid, *ACS Symp. Ser.*, **229**, 317 (1983)
149. J. John, F.P. Cortolano, *Eur. Pat. Appl. EP.*, 145,658 (1985)
150. J. Klahin, K. Figge, F. Meiez, *Angew. Makromol. Chem.*, **131**, 73 (1985)

151. V.I. Paramonov, Z.G. Popova, R.D. Fibina, T.A. Pankova, G.V. Kutimova, A.A. Efimov, E.I. Kirillova, *USSR, SU* 871,487 (1987)
152. M. Yagi, K. Tajima, M. Takahashi, K. Iaochi, T. Takeuchi, *Jpn. Kokai Tokkyo Koho JP* 63,122,750 (1988)
153. J. Runge, H. Marschner, W. Fischer, *Ger. (East) DD* 264, 935 (1989)
154. J. Runge, B. Hamann, D. Frenzel, H. Marschner, W. Fischer, R. Hentel, *Ger. (East) DD* 264,931 (1989)
155. B. Gilg, S. Evans, *Eur. Pat. Appl. EP.*, 333,643 (1989)
156. T. Haruna, M. Takahashi, T. Kano, *Jpn. Kokai Tokkyo Koho JP* 03,28,257 (1991)
157. T. Matsuba, K. Kubo, K. Kawahata, *Jpn. Kokai Tokkyo Koho JP* 03,56,550 (1991)
158. S. Nishibori, M. Konor, T. Nabeshina, *Jpn. Kokai Tokkyo Koho JP* 03,234,747 (1991)
159. R. Tsunoda, T. Yamauchi, *Jpn. Kokai Tokkyo Koho JP* 04,15,248 (1992)
160. A. Yamazalev, Y. Tsubakura, Y. Suetsugu, *Jpn. Kokai Tokkyo Koho JP* 03,220,256 (1992)
161. S. Nishibori, H. Kondo, T. Nabeshima, *Jpn. Kokai Tokkyo Koho JP* 04,335,048 (1992)

CHAPTER II

OBJECTIVE AND SCOPE OF THE PRESENT INVESTIGATION

2.0 INTRODUCTION

Degradation of polymers is an important phenomenon specially in heterophasic polymers. Many polymer based products are used in daily life. The causes for degradation of polymers are heat, light, ozone, atmospheric pollutants, microorganism and polymer processing.

Among all these, ultra violet light which is a part of sunlight, plays a major role in the photo-degradation. UV radiation is known to affect most polymer materials, creating excited states and free-radicals, which are capable of initiating a large number of reactions such as chain-scission, crosslinking and oxidation. The exposure of polymers to the UV light over a period of time leads to deterioration in physical properties. During the degradation, polymer loses its molecular weight and mechanical properties, changes in morphology, embrittlement and impairment of transparency. All these changes occur randomly in the polymers due to the chain-scissions. The degree of deterioration will depend on the extent of the degradation and nature of the degradation. The polymeric impurities such as chromophores, trienes and dienes will absorb the UV light. The photodegradation of polymers is a serious issue and has economic and environmental implication. The outdoor use of polymeric materials is severely limited by their poor stability in sunlight, resulting in considerable consumption of energy and resources due to the necessity of frequent replacement of the materials. The photo-oxidation mechanism is a complex reaction. Plastic manufacturers recognized that by increasing the resistance of polymers to the sunlight, the applications of these materials could be extended. This provided a strong incentive for the development of additives to protect polymers from the degradation.

Styrenic polymers have valuable properties and are continuously finding new applications in the daily life. The photo-oxidation of polystyrene¹⁻⁴ and polybutadiene⁵ were studied individually. The high impact polystyrene (HIPS) is a heterophasic copolymer. It has polystyrene as a continuous and polybutadiene as a dispersed phase. The photo-oxidation is mainly occurring at the polybutadiene phase. At the molecular level, the effect of photo-oxidation on HIPS is chain-scissions resulting in the formation of free-radicals which migrate along the chain. The free-

radicals will react with atmospheric oxygen and result in the formation of aldehydes, ketones, free acids and their esters.⁶ Apart from these properties, crosslinking is also occurring in the polybutadiene phase.^{7, 8} The photo-oxidative degradation can be partially prevented by incorporating the stabilizers like antioxidants, UV absorbers, excited state quenchers and hindered amine light stabilizers into the polymer matrix. The stabilizers are incorporated during the polymer processing. The additive should have better compatibility with the polymer substrate. The low molecular weight stabilizers will leach out from the polymer through evaporation, migration or extraction. A good compatible stabilizer will give better protection to the polymer. In the photostabilization process, hindered amine light stabilizers (HALS) are new and most effective stabilizers. They are multifunctional stabilizers as their action is not limited to a single step. In the photo-oxidation process their transformation products also act as stabilizers and undergo multiple regeneration.⁹⁻¹¹ The low molecular weight HALS is easily leached out from the polymer, therefore, there is a trend to synthesize a high molecular weight HALS.¹²

2.1 Objectives of the present investigation

The objective of the present investigation is to understand the degradation mechanism of heterophasic HIPS upon thermal and photo-oxidation. This will provide a clear idea of the photostabilization of this polymer. The objectives of the present investigations are:

1. To determine the polybutadiene content and its microstructure in heterophasic high impact polystyrene.
2. To examine the thermal and photo-oxidative degradation in the heterophasic HIPS (different grades) and comparison of the results with the glassy polystyrene homopolymer.
3. Evaluation of chain scission, changes in mechanical properties, color (yellowness) and surface morphology upon UV irradiation in HIPS.
4. To study the natural weathering of heterophasic HIPS and the comparison of photoproducts formation under natural and accelerated exposure condition.

5. To design, synthesize and property evaluation of specific polymeric stabilizers in HIPS.

2.2 Approaches

Photo-oxidation of HIPS

- 1 The polybutadiene content and its microstructure will be determined with various spectroscopic methods.
- 2 The thermal and photo-oxidized products will be analyzed by FT-IR and ^{13}C NMR spectroscopy.
- 3 The photo-oxidized films will be treated with gaseous NH_3 and SF_4 for the rapid identification and better resolution of the various carbonyl species, alcohols and hydroperoxides.
- 4 The heterogeneity in the thermal and photo-oxidized film will be determined with micro-FT-IR spectroscopy.
- 5 The changes in intrinsic viscosity, tensile impact strength and yellowness index upon photo-irradiation will be studied and compared with their respective irradiated and unirradiated samples.
- 6 The morphology of photo-oxidized film will be analyzed with scanning electron microscopy and compared with their unirradiated sample.
- 7 Natural weathering behavior of various HIPS copolymers will be examined and the photo product formation under natural weathering will be compared with their respective accelerated photo-irradiated samples.

Stabilization of HIPS

- 1 The stabilizing effect of conventional stabilizers (Tinuvin 770 and Tinuvin 144) will be estimated.
- 2 Styrene-maleic anhydride copolymer will be synthesized by free-radical copolymerization.

- 3 Styrene-maleic anhydride copolymer with HALS functionality in the chain will be prepared by grafting.
- 4 The photostabilizing efficiency of polymeric HALS will be compared with conventional HALS (Tinuvin 770 and Tinuvin 144) at different concentrations.

2.3 References

1. B.G. Achhammer, M.J. Reiney, F.W. Reinhart, *J. Res.Nat.Bur.stand.*, **47**, 116 (1951)
2. N.A. Weir, P. Kutok, K. Whiting, *Polym. Degradn. Stab.*, **24**, 247 (1989)
3. B. Ranaby, J.F. Rabek, Photodegradation, photooxidation and photostabilization of polymers: Principles and applications, Wiley Publishers, London (1975)
4. B. Mailhot, J.L. Gardette, *Macromolecules*, **25**, 4127 (1992)
5. C. Adam, J. Lacoste, J. Lemaire, *Polym. Degradn. Stab.*, **24**, 185 (1989)
6. J. Sedlacek, J. Rosik, *Chem. Zvesti.*, **26**, 412 (1972)
7. G. Scott, 'Developments in polymer stabilization', Applied Publishers, London, Vol. 1, 309 (1979)
8. A. Ghaffar, A. Scott, G. Scott, *Eur. Polym. J.*, **13**, 89 (1977)
9. P.D. Garbiele, J.R. Geib, R.M. Iannule, W.J. Reid, ACS Symp. Ser. 229, 317 (1983)
10. R. Tsunoda, T. Yamauch, *Jpn. Kokai Tokkyo Koho JP* 04,15,248 (1992)
11. A. Yamazalev, Y. Tsubakera, Y. Suetsugu, *Jpn. Kokai Tokkyo Koho JP* 03,220,256 (1982).
12. [M. Minagawa, K. Kittawa, *Macromol. Chem. Macromol. Symp.*, **70-71**, 433 (1993)

CHAPTER III
**POLYBUTADIENE CONTENT AND MICROSTRUCTURE
IN HIGH IMPACT POLYSTYRENE**

3.0 INTRODUCTION

The improvement of impact resistance of polystyrene (PS) is generally ensured by polybutadiene (PB) introduced before the free radical polymerization of styrene. The PB nodules are then compatibilized by grafting of styrene units. This blend of PS and PB is termed as high impact PS [HIPS] where the PB content is in the range of 3-8 mol %. The property improvement¹ is due to the chemical interaction between the growing PS chain and the rubber, chemical crosslinking of the rubber and occlusion of the cocontinuous polymer phase inside the rubber particles, which increases the effective volume of the rubber phase.

Many methods²⁻⁴ are in use for the characterization of PB. However, because of its low content and microstructure distribution (*cis*-1,4, *trans*-1,4, and *vinyl*-1,2) in the blends (HIPS), several complementary techniques are required for its analysis. This chapter describes the advantages and limitations of ¹H- and ¹³C NMR, IR and Fourier transform (FT)-Raman spectroscopies for the determination of both the content and microstructure of PB present in commercially available HIPS.

3.1 EXPERIMENTAL PROCEDURES

3.1.1 Materials

Commercial samples of HIPS from Polychem, India (HIPS I and III) and Elf-Atochem, France (HIPS II and HIPS IV) were compared with a commercial PS from Elf-Atochem, France and with a PB containing all of the three microstructures (PB) from Aldrich-Europe. A few samples were extracted with methanol to ensure that additives were not interfering with the analysis.

3.1.2 Sample preparation

All the materials were pressed in an electrically heated laboratory press at 180°C for 2 min to get 100- μ m films suitable for the IR analysis

3.2 ANALYSIS

3.2.1 FT-IR Spectroscopy

Films are characterized by FT-IR spectroscopy (Nicolet instruments impact 400), 100 scans, with DTGS detection.

3.2.2 FT-Raman Spectroscopy

Films are characterized with FT-Raman spectroscopy (Nicolet instruments impact 910), 100 scans; laser, 1064 nm, 10 Å, respectively. In these analysis heat accumulation was observed in 100 μm thick samples, a continuous IR emission was perturbing the spectral baseline. To avoid this problem, analysis were performed on thicker samples (>200 μm)

3.2.3 ¹H and ¹³C NMR Spectroscopy

NMR spectra were obtained on polymer samples dissolved or swollen (concentration ca. 40 mg/ mL) in CDCl₃ (25° and 50°C), C₆D₆ (25°C), and o-dichlorobenzene-D₄ (25° and 110°C), with a Bruker AC 400 instrument at 400 MHz with trimethylsilane (TMS) or solvent as internal reference. The best resolution was obtained with CDCl₃ sampling at 25°C. The conditions were as follows:

1. ¹H NMR: repetition time 3 s, 90° pulse, accumulation of ca. 300 scans.
2. ¹³C NMR:
 - (a) Quantitative: delay time 30 s, 300 scans.
 - (b) J-mod: this technique,⁵ based on the modulation of the coupling constant, allows the differentiation of primary and tertiary carbons from secondary and quaternary ones; delay time 1.5 s, 8000 scans.
 - (c) Distortionless enhancement by polarization transfer (DEPT) pulse sequence is an improvement of insensitive nuclei enhancement by polarization transfer (INEPT). The sequence is as follows:

¹ H (delay time)	$(\pi/2) x \tau$			
	$(\pi) x \tau$	$(\theta) y$	τ	Decouple
¹³ C				
	$(\pi) x \tau$	$(\pi/2) x$	τ	acquire

Where $\tau = \frac{1}{2} J$, J being an average ^1H - ^{13}C coupling constant setting to 135 Hz (we checked that the sequence is rather insensitive to this value if $120 < J < 200$ Hz). θ is the proton pulse of variable length ($\theta_1 = gB_1t_1$); in our experiments, $t_1 = 4.25 \mu\text{s}$ ($\theta = 45^\circ$). (Some experiments were performed with $\theta = 135^\circ$ to differentiate secondary carbons). The delay time of 5 s was longer as usual.⁶ The x, y referred to the rotating frame of the spectrometer. This technique usually allows the shortening of the delay time between two pulses and, consequently, reduces the acquisition time necessary to get quantitative data. The quaternary carbon atom of PS and the residual CH of CDCl_3 are not detected by this technique. In all ^{13}C experiments, sequences were obtained using a gate decoupling to avoid possible intensity distortions arising from Nuclear Overhauser Effect (NOE) factors.

3.3 RESULTS AND DISCUSSION

3.3.1 Microstructure analysis of PB with FT-IR Spectroscopy

The main advantage of FTIR spectroscopy for polymer analysis is that it is nondestructive and is usable in the solid state. From the comparison of IR spectra of both PS and PB, it is obvious that PS can be identified by its medium band at 542 cm^{-1} and/or by its weak absorption bands at 1943, 1870, and 1803 cm^{-1} according to the sample thickness. PB is characterized^{7, 8} by the deformation bands present at 994 (*vinyl*-1,2), 967 (*trans*-1,4), 912 (*vinyl*-1,2), and 729 cm^{-1} (*cis*-1,4). A number of earlier articles emphasize the difficulty in quantifying the contribution of each structure because of the overlapping of the bands⁹ and poor resolution of the *cis*-1,4 band¹⁰. To obviate this difficulty, Silas et al.⁹ considered that each band resulted from the contribution of the three microstructures. Richardson and Sacher¹⁰ proposed that the *cis*-1,4 content can be determined by subtracting the contribution of (*trans*-1,4 + *vinyl*-1,2) from the total concentration in PB.

The comparison of PS and PB spectra in the $1100\text{-}600 \text{ cm}^{-1}$ region is shown in Figure 3.1(A); it can be seen that the band at 728.7 cm^{-1} overlaps with the strong bands of PS at 700 and 760 cm^{-1} and renders the quantification of the PB content by IR spectroscopy all the more difficult. However, the 542 cm^{-1} band (not shown) is typical of PS and it is possible to measure its absorption coefficient via a careful measurement of the sample thickness. The value obtained ($\epsilon_{542 \text{ cm}^{-1}} = 19.8 \text{ mol, l}$

cm) can be used via the Beer-Lambert law for the determination of PS content in HIPS (see Table 3.1), but the accuracy of this method decreases for very low PB contents.

However, a precise subtraction of the PS contribution in HIPS is now possible with modern FTIR instruments. Figure 3.1 (B) shows the PB spectra obtained by Omnic software (Nicolet) from subtraction of HIPS I, II, III, and IV, PS.

Microstructure of *trans*-1,4 and 1-2 are clearly revealed at 966.0, 912.7, and 995.2 cm^{-1} , respectively, but the *cis*-1,4 contribution cannot be evaluated; this fact is particularly dramatic for sample III for which, as we will see later, the *cis*-1,4 contribution is very high.

Table 3.1: Polystyrene Content (mol %) in HIPS from FT-IR

HIPS I	HIPS II	HIPS III	HIPS IV
94	91	87	84

3.3.2 Microstructure analysis of PB with FT-Raman spectroscopy

Since the discovery of Raman effect in 1928, there have been a lot of improvements in all aspects of the instrumentation (source, collector, and detector). Upto 1986, the developments were mainly the source (laser) and the detector (photomultiplier), but the polymer analysis was often limited by fluorescence emission from impurities that made it difficult or even impossible to measure the Raman spectrum.¹¹ One typical advantage of FT-Raman developed in 1986 by Hirschfeld and Chase¹² is to reduce or to eliminate the fluorescence by the use of a near-IR excitation source [in our case, 1064 nm (9394 cm^{-1})]; other advantages are the same as for FTIR (high constant resolution over the range of wave numbers, accurate wave number calibration, etc.). Raman spectroscopy in this spectral region is virtually free from fluorescence interference and photochemical sample damage.

As shown in Figure 3.2, the PS and PB present in HIPS I, II, III, and IV can be differentiated by their 1600 and 1660 cm^{-1} band, respectively. The wide band around 1660 cm^{-1} for PB results in fact from the contribution of *trans*-1,4 (1666 cm^{-1}), *cis*-

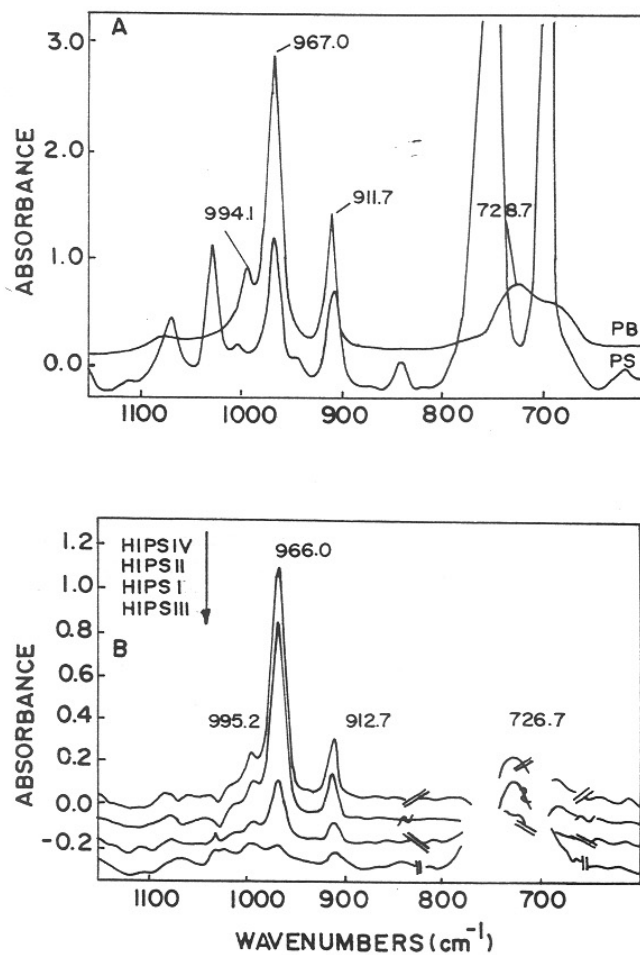


FIG.3.1: DEFORMATION REGION OF HIPS/FTIR SPECTRA. (A) PURE POLYBUTADIENE (PB) & POLYSTYRENE (PS). (B) PB SPECTRA OBTAINED BY SUBTRACTION (HIPS - PS).

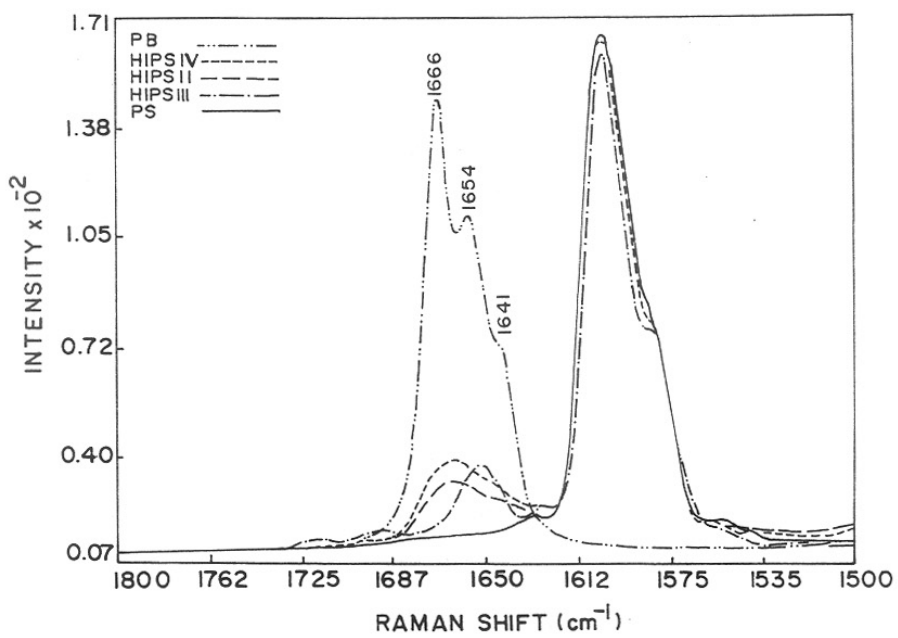


FIG.3.2:COMPARISON OF RAMAN SPECTRA OF PB,HIPS,& PS

1,4 (1654 cm^{-1}), and *vinyl* (1641 cm^{-1}) microstructures; and some authors¹³ claim that the relative content of each microstructure can be directly derived from the deconvolution of this band. The band shapes observed ensure that HIPS III is mainly *cis*-1,4 and that HIPS I, II, and IV contain appreciable quantities of *cis*- and *trans*-1,4 structures and a lower content in vinyl.

3.3.3 Microstructure analysis of PB ^1H NMR spectroscopy

^1H -NMR spectroscopy of PB has been extensively developed for the determination of microstructures,¹⁴⁻¹⁷ tacticity (vinyl structures),¹⁸ or for the determination of PB content in copolymers and consequently for the determination of reactivity ratios (r_1 , r_2).¹⁹⁻²² In the case of polymer blends, we can generally expect some simplifications compared to simple copolymers because of the absence of comonomer chemical linkages. In the particular case of HIPS, because of the synthetic method based on the polymerization of styrene in which PB is dissolved, we can expect to have some copolymerization between the residual double bonds of PB and styrene.

These PB/PS linkages ensure compatibilization of the blend, but their content is too low to be detected by ^1H -NMR. So we can assume that the ^1H -NMR spectrum is just a superposition of PB and PS homopolymers.

As shown in Figure 3.3 and Table 3.2, PS and PB moieties can be differentiated from the aromatic (6.3-7.5 ppm) and the olefinic (4.8-5.6 ppm) regions, respectively.²³⁻²⁸

In addition, we can see that ^1H -NMR at 400 MHz (CDCl_3) has the potential to separate the olefinic resonance peaks of *vinyl*, *cis*- and *trans*-1,4 protons. Attempts to further resolve the *cis* and *trans* protons by increasing the temperature (50°C in CDCl_3 , 110°C in *o*-dichlorobenzene D_4) were not successful. This result is quite significant because the literature²⁶⁻²⁸ recommends the evaluation of the *cis* and *trans* content only by ^{13}C -NMR because of the poor resolution of ^1H -NMR at lower magnetic fields.

The expanded 4-6 ppm region reported in Figure 3.3 (B) for PB, PS, and HIPS I, III and IV clearly shows that a full determination of PB (content and microstructure)

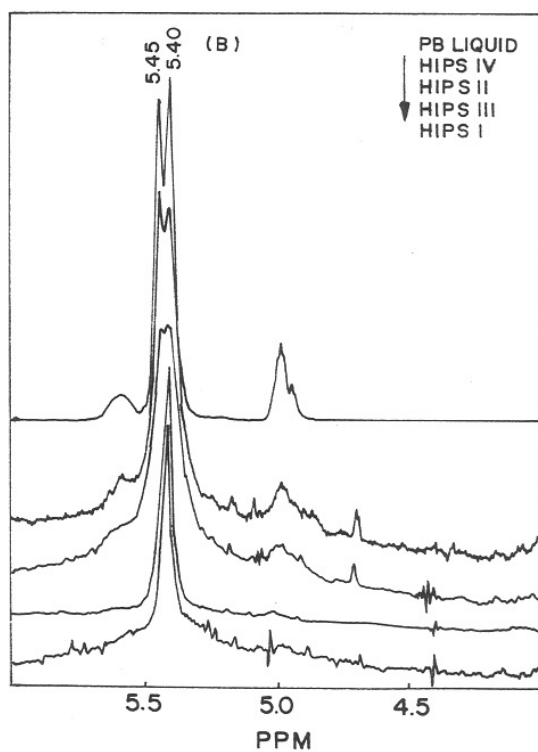


FIG.3.3: PROTON NMR SPECTRA OF PB, HIPS, AND PS (REPETITION TIME 3 s; SCAN NUMBER ca. 300). (A) COMPLETE SPECTRA (0-8 ppm). (B) EXPANDED OLEFINIC REGION (4-6 ppm)

can be done by proton NMR. However, the determination of the *cis/trans* content is not too accurate by this method.

We can consider that the area of aromatic peaks corresponds to five protons of PS (the contribution of residual CHCl_3 at 7.27 ppm is negligible). The peak area at 5.0 and 5.6 ppm corresponds to one ($=\text{CH}$) or two ($\text{CH}_2=$) protons of vinyl; and the contribution of two protons ($\text{CH}=\text{CH}$) of both *cis* and *trans* microstructures can be deduced from the deconvolution of peaks at 5.40 and 5.45 ppm, respectively. Table 3.3 reports the results obtained from both ^1H - and ^{13}C NMR.

Table 3.2: ^1H NMR Chemical shifts from PB and PS homopolymers

Chemical shifts (ppm) ^a	PB ²⁵⁻²⁸	PS ²³⁻²⁵
1.35	CH_2 (1-2)	
1.50		CH_2
1.92		CH (aliphatics)
2.05	CH_2 (t1-4)	
2.10	CH_2 (c1-4)	
5.00	$\text{CH}_2 = \text{CH}$ (1-2)	
5.40	$\text{CH} = \text{CH}$ (c1-4)	
5.45	$\text{CH} = \text{CH}$ (t1-4)	
5.60	$\text{CH}_2 = \text{CH}$ (1-2)	
6.55		CH (arom, m, m', p)
7.10		CH (arom.o, o')

^aThis work

Table 3.3: Quantitative Analysis of PB Contents by ^1H - and ^{13}C NMR

		vinyl-1,2	cis-(1,4)	trans-(1,4)	c + t	PS
PB	^{13}C	14	38	48	86	-
	DEPT	14	35	51	86	-
	^1H	15	43 ^a	42 ^a	85	-
HIPS I	^{13}C	-	4	1.5	5.5	94.5
	DEPT	-	2.3	<1	<3.3	>96.7
	^1H	<0.5	3	-	3	>96.5
HIPS II	^{13}C	-	3	3	6	94
	DEPT	-	2.1	2.3	4.4	95.6
	^1H	-	4.5 ^a	4.5 ^a	9	91
HIPS III	^{13}C	-	11	-	11	89
	DEPT	-	9.5	-	9.5	90.5
	^1H	<1	8	-	8	>91
HIPS IV ^b	^{13}C	-	11	8	19	81
	DEPT	-	3.2	3.2	6.4	93.6
	^1H	-	5 ^a	5 ^a	10	90

^aApproximate values

^bResults are slightly sample dependent

3.3.4 Microstructure analysis of PB with ^{13}C NMR Spectroscopy

^{13}C NMR spectroscopy is known to be more suitable than ^1H NMR for the determination of *cis* and *trans* contents of PB²⁶⁻²⁸ because the resonances of methylene protons at 1.98 and 2.03 ppm or olefinic protons at 5.40 and 5.45 ppm are difficult to resolve even at high magnetic fields. Despite a lower sensitivity, the large range of ^{13}C chemical shifts enables a complete characterization of the resonances of all the carbons of PS and PB (Table 3.4); nevertheless, quantitative analysis is more difficult because of variations in relaxation times and Overhauser effects.²⁹

Table 3.4: ^{13}C NMR Chemical shifts from PB and PS Homopolymers

Chemical shifts (ppm) ^a	PB ²⁵⁻²⁸	PS ²³⁻²⁵
25.0	CH ₂ (1-2)	
27.4	<u>C</u> H ₂ -CH = (c1-4)	
32.7	<u>C</u> H ₂ -CH = (t1-4)	
40.4		CH (aliphatic)
44.0		CH ₂ (aliphatic)
43.5	CH (1-2)	
114.0	<u>C</u> H ₂ -CH (1-2)	
127.7		C (arom.p)
127.7-128		C (arom.o, o',m, m')
129.2	CH = CH (c1-4)	
129.7	CH = CH (t1-4)	
142.7	CH ₂ = <u>C</u> H (1-2)	
145.4		C1 (aromatic)

^aThis work

As we can see in Figure 3.4, *cis* and *trans* PB microstructure can be identified in HIPS both in the aliphatic (27.4 and 32.8 ppm) and in the olefinic region (129.2 and 129.3 ppm). Vinyl microstructures are not present in any of the HIPS spectra. The unexpected peak at 29.7 ppm is also present in pure PS: it can be tentatively attributed to a head-head methylene linkage in pure PS. The J-mod and DEPT (135°) spectra performed on HIPS IV were consistent with this assignment.

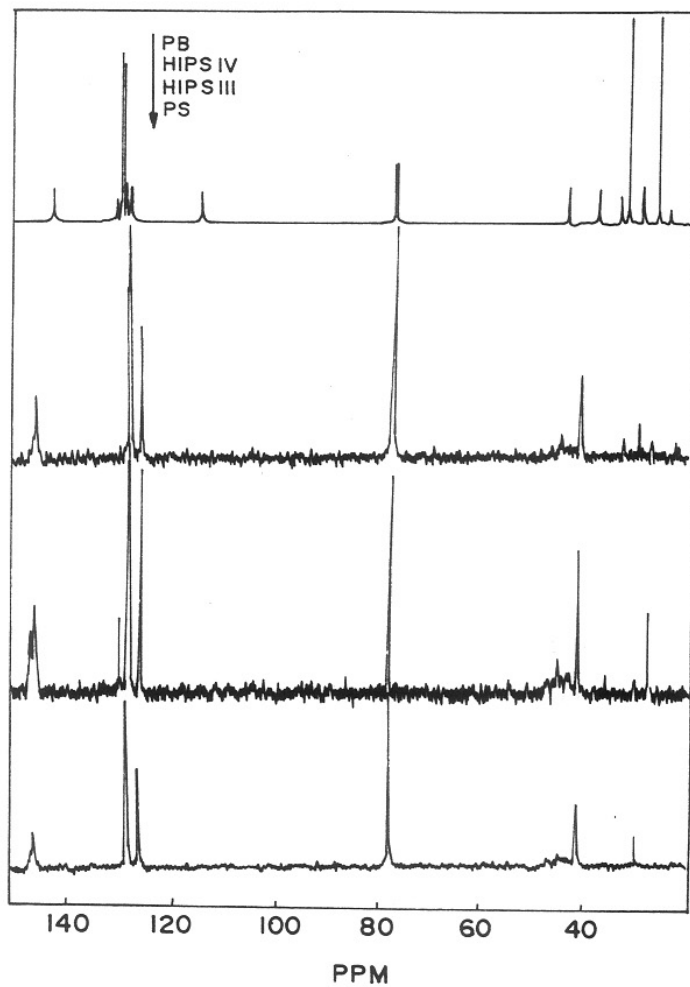


FIG.3.4: COMPARISON OF QUANTITATIVE ^{13}C -NMR SPECTRA OF PB, HIPS, AND PS (DELAY TIME 30 s; SCAN NUMBER 300)

Sato et al.²⁸ showed that ¹³C NMR quantitative determination of PB microstructures was possible because of similar values of NOE and relaxation times for aliphatic carbons; but the quantitative determination of PB content in HIPS needs to assume that at least one of the PS carbons (presumably the methine carbon) has similar NOE values and relaxation times to PB. The best accuracy can be obtained by using quantitative programs available in modern NMR instruments (see Experimental); but these sequences need long delay time to ensure the complete relaxation of the carbon nucleus and results in very long analysis times. An elegant alternative consists of the use of DEPT sequences^{6, 30, 31} that provide complete quantitative ¹³C spectra for all except quaternary carbon atoms. Mathematical treatment of the sequence leads to the conclusion that for CH₃, CH₂, and CH carbon atoms, the signal intensities have to be multiplied by the ratio $(3\sqrt{2}) / 4, 1,$ and $\sqrt{2}$, respectively.

Figure 3.5 shows the spectra obtained by the two quantitative methods. The scan numbers (300), were identical but, because of the shorter delay time, the analysis duration was six times lower for DEPT. As we can see, DEPT sequences lead to a drastic increase of the signal to noise ratio; we can also observe the disappearance of both quaternary carbon of PS and solvent peaks.

For both methods, the PB contents and microstructures can be determined (i) from the aliphatic region by considering the peaks area at 25.4 (*vinyl*-1,2), 27.4 (*cis*-1,4), 32.7 (*trans*-1,4), and 40 ppm (PS) and / or (ii) from the olefinic region by using the peaks at 114.0 (*vinyl*-1,2), 129.2 (*cis*-1,4), and 129.7 ppm (*trans*-1,4) vs. aromatic carbon of PS (127.7 ppm). Results from ¹³C-, quantitative, and DEPT (PB aliphatic region), and ¹H NMR analysis are reported in Table 3.3.

3.4 CONCLUSIONS

All five methods give essentially the same trend with respect to PB content and microstructure: PB content in HIPS IV > III > II > I, with I and III mainly *cis*, II and IV essentially *cis* and *trans*.

The vinyl (1,2) structures are well characterized by FTIR because relatively higher values for absorption coefficient, but Raman and ¹H-NMR confirm their low content, and no detection was possible by ¹³C-NMR. Some important differences appear in the values for absolute concentration (Table 3.3) probably because the

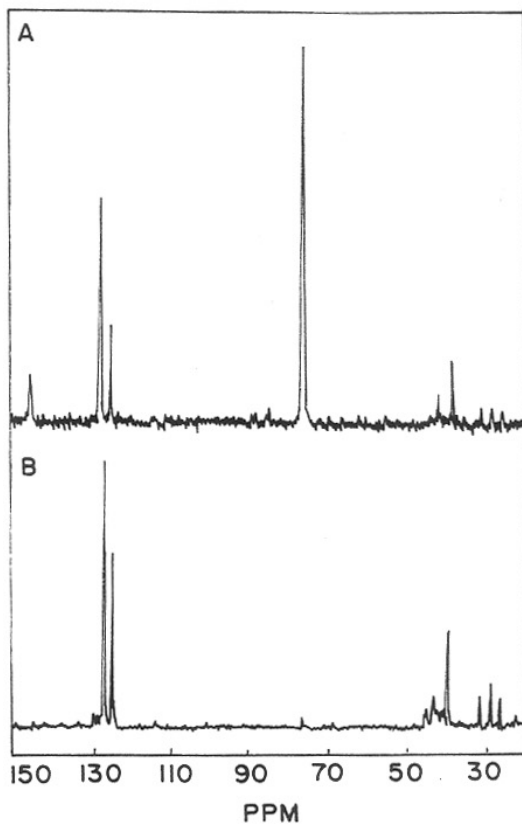


FIG.3.5.¹³C-NMR SPECTRA OF HIPS II.
COMPARISON OF QUANTITATIVE (A)
DELAY TIME 30s, AQUISITION TIME 150
min. AND DEPT (B) DELAY TIME 5s ,
 $\theta = 45^\circ$, AQUISITION TIME 25 min.

measurement accuracy was not sufficient for such low PB contents (the relative experimental uncertainties were assumed to be 15% for FTIR and ^{13}C -NMR and 10% for proton and ^{13}C DEPT NMR).

Except for HIPS IV, DEPT and quantitative ^{13}C NMR give similar results proving that DEPT is a very good technique for polymer characterization allowing fast analysis and good signal to noise ratio.

^1H NMR could be a universal technique for determining both the rubber content and microstructure. However, even at 400 MHz, the resolution of *cis* and *trans* olefinic protons is still insufficient to ensure a quantitative estimation.

3.5 References

1. H.F. Mark, N.M. Bikales, C.G. Overberger, G. Manges, J.I. Kroschwitz, *Encyc. Polym. Sci. Eng.*, **16**, 88 (1989)
2. V.D. Mochel, *J. Polym. Sci. A-1*, **10**, 1009 (1972)
3. A.D.H. Von Clague, J.A.M. Brockhoven, J.W. De Haan, *J. Polym. Sci. B.*, **11**, 299 (1973)
4. Y. Tanaka, K. Hatada, *J. Polym. Sci. B.*, **11**, 569 (1973)
5. C. Le Coq, J.Y. Lallemand, *JCS Chem. Commun.*, 150 (1981)
6. A.E. Derome, 'Modern NMR Techniques for Chemistry Research', 2nd ed., Pergamon Press, Oxford, UK, 1987
7. J.L. Binder, *J. Polym. Sci. A1*, **1**, 47 (1963)
8. J. Morero, *Chem. Ind. (Milano)*, **41**, 758 (1959); C.A.: **54**, 4269 (1960)
9. R.S. Silas, J. Yates, V. Thornton, **31**, 529 (1959)
10. W.S. Richardson, A. Sacher, *J. Polym. Sci.*, **13**, 229 (1954)
11. J.L. Cornell, *Rubber Chem. Technol.*, **43**, 322 (1970)
12. T. Hirschfeld, B. Chase, *Appl. Spectrosc.*, **40**, 133 (1986)
13. H.G.M. Edwards, D.W. Farewell, A.F. Johnson, L.R. Lewis, N.J. Ward, N. Webb, *Macromolecules*, **25**, 525 (1992)
14. K.F. Elgert, B. Stutzel, P. Frenzel, H.J. Cantaw, R. Streck, *Makromol. Chem.*, **170**, 257 (1973)
15. F. Conti, A. Segre, P. Pini, L. Porri, *Polymer*, **15**, 5 (1974)
16. Y. Tanaka, H. Sato, M. Ogawa, K. Hatada, Y. Terawaki, *J. Polym. Sci., Polym. Lett. Ed.*, **12**, 369 (1974)
17. J.L. Gerry, *Rev. Gen. Caoutch. Plast.*, **54**, 103 (1977)
18. F. Conti, M. Delfini, A.L. Segre, D. Pini, L. Porri, *Polymer*, **15**, 816 (1974)

19. I. Ya. Slonin, A.N. Lynbinou, 'The NMR of Polymers', Plenum, New York, 1970
20. F.A. Bovey, G.D.V. Thiers, *J. Polym. Sci.*, **38**, 73 (1959)
21. R.J. Angelo, R.M. Ikeda, M.L. Wallach, *Polymer*, **6**, 141 (1965)
22. W.L. Senn, Jr., *Anal. Chim. Acta.*, **29**, 505 (1963)
23. E.R. Santee, R. Chang, M. Morton, *J. Polym. Sci., Polym. Lett. Ed.*, **11**, 449 (1973)
24. Q.T. Pham, R. Petiaud, H. Waton, M.F. Llauro-Darricades, '*Proton and Carbon NMR Spectra of Polymers*', Penton Press, London, 1991
25. F.A. Bovey, '*High Resolution NMR of Macromolecules*', Academic Press, New York, 1972
26. S. Bywater, Y. Firat, P.E. Black, *J. Polym. Sci.*, **22**, 669 (1984)
27. S. Bywater, *Polymer Commun.*, **24**, 203 (1983)
28. H. Sato, K. Takebayashi, Y. Tanaka, *Macromolecules*, **20**, 2418 (1987)
29. J.C. Randall, *ACS Symp. Ser.*, **247**, 131 (1986)
30. H. Gunther, *La Spectroscopie de RMN*, Masson, Paris, 1993.
31. S. Ramakrishnan, *Macromolecules*, **24**, 3753 (1991)

CHAPTER IV

**PHOTO AND THERMO-INITIATED OXIDATION OF
HIGH IMPACT POLYSTYRENE**

4.0 INTRODUCTION

Most of the organic polymers undergo irreversible chemical changes and gradually loss of properties with the UV exposure. When polymers are exposed to UV light, it causes changes in color and embrittlement. In crystalline polymers, the chemical changes are accompanied by changes in morphology also which will contribute to the overall changes in the properties.

The improvement in the impact resistance of polystyrene is generally ensured with polybutadiene introduced before the free-radical polymerization of styrene. The polybutadiene nodules are then compatibilized by grafting onto styrene units. This blend of polystyrene and polybutadiene is termed as high impact polystyrene (HIPS), where the polybutadiene is in low content (3-8 mole-%) in the matrix. The high impact polystyrene contains polystyrene as a continuous phase and polybutadiene as a dispersed phase. It behaves as two distinct phases. The polybutadiene phase will exist in the three forms, i.e. cis-1,4, trans-1,4 and vinyl-1,2. The polybutadiene phase is susceptible to photo-oxidation in high impact polystyrene. Apart from this in all the nonabsorbing polymer, the light is absorbed by uncontrolled chromophores (probably impurities). The photo-oxidation is generally heterogeneous and occurs only in the surface layers after short exposures.

The present chapter deals with the chemical changes occurring during the photo- and the thermal initiated oxidation of several HIPS containing various amount of polybutadiene. The influence of microstructure will also be examined.

4.1 EXPERIMENTAL PROCEDURES

4.1.1 Materials

Commercial samples of high impact polystyrene sample I was supplied by Polychem, India, whereas sample II and III were supplied by ELF-Atochem, France. For comparison, pure polystyrene which is used in this study, was supplied by ELF-Atochem, France.

4.1.2 Sample preparation

Thin polymer films (thickness $\sim 100 \mu\text{m}$) were prepared by pressing the polymer pellets in a preheated carver press at 180°C at 150 kg/cm^2 platen pressure for 2 min. The films quenched cooled rapidly in the press.

4.1.3 UV irradiation

Films were irradiated in SEPAP 12/24 (From M/s Material Physico Chimique, Neuilly/Marne, France) at 60°C . The unit consists of four 400W 'medium pressure' mercury sources filtered by a pyrex envelope supplying radiation of wavelengths longer than 300 nm. These sources are located at the four corners of a square chamber ($50 \times 50 \text{ cm}$). The inside walls of the chamber are made up of high reflection aluminum. Twenty-four samples are irradiated on a rotating support located at center of the chamber. The surface temperature of each sample can be measured by a thermocouple in close contact with the sample. Two fans on the walls of the chamber are monitored by an Eurotherm device and afford a regulation of the temperature of the sample ($\pm 2^\circ\text{C}$ between $40\text{-}80^\circ\text{C}$).

4.1.4 Thermal irradiation

Films were thermally treated in a forced air circulation oven at 80, 100 and 120°C for various periods.

4.2 ANALYSIS

4.2.1 ^{13}C NMR Spectroscopy

^{13}C NMR spectra recorded on a Bruker MSL 300 NMR Spectrometer operating at 75.47 MHz with pulse 3.5 μs , pulse repetition 20s, scan number 800-200, J.MOD. Spectra were recorded at room temperature using CDCl_3 as a solvent. The distribution of polybutadiene microstructure and its content in the HIPS sample were determined with NMR. The composition is given in Table 4.1. Peak resonances at 27.7, 32.9 and 40.7 ppm were attributed to CH_2 (cis-1,4), CH_2 (trans-1,4) and CH (PS) respectively. The content in vinyl-1,2 microstructure was negligible as estimated by ^{13}C NMR [resonance peaks at 34.7 (CH_2) and 44.1 (CH) ppm].

Table 4.1: Composition of HIPS based on ^{13}C NMR data

Sample	Cis-1,4 PB (wt-%)	Trans-1,4 PB (wt-%)	Vinyl-1,2 PB (wt-%)	PS (wt-%)
I	3.3	0.9	-	95.8
II	5.6	5.5	-	88.9
III	12.6	13.8	-	73.6

4.2.2 FT-IR analysis

The microstructure of photo and thermal oxidized products were identified with good resolution by Fourier transform infrared (FT-IR) (Nicolet 20 SX) Spectrometer equipped with a TGS detector. Spectra were recorded using 32 scans summations at a normal resolution of 2 cm^{-1} .

A weak band detected at 911 cm^{-1} is for vinyl. In fact the absorption coefficient of vinyl group is high enough at 911 cm^{-1} ($\epsilon = 184$) and other microstructures are expected to absorb also at this frequency¹ with very low absorption coefficients ($\epsilon_{\text{cis-1,4}} = 1.9$; $\epsilon_{\text{trans-1,4}} = 2.4$). The vinyl content can be thus assumed to be only a few percent of the total unsaturation in polybutadiene.

4.2.3 Concentration profile analysis

Gardette et al.^{2,3} described the measurements of oxidation product profiles in thermal and photo-oxidized films. Measurements were performed on Nicolet 800 equipped with a Nicplan microscope (liquid nitrogen cooled MCT detector, 128 summations). The oxidized films were maintained between the two polypropylene sheets (2mm thick) and then sliced with a Reichert and Jung microtome. Slices of a thickness of ca. $25\text{ }\mu\text{m}$ were obtained and then examined through the FT-IR microscope.

4.2.4 Derivatization reactions

The photo-oxidized (25 h, HIPS II) films were exposed to NH_3 and SF_4 reactive gases at room temperature in a simple flow system which could be sealed off by valves to allow reaction to proceed. Since SF_4 attacks glass, this reaction was carried out in a teflon bottle. From changes in FT-IR, it was inferred that the reactions were virtually completed in 24 h for SF_4 and 1 h for NH_3 .

4.3 RESULTS AND DISCUSSION

4.3.1 Characterization of the sample

The polybutadiene content in high impact polystyrene was determined by ^{13}C NMR spectroscopy and also with IR spectroscopy. The polybutadiene portion exists in three forms: cis-1,4, trans-1,4 and vinyl-1,2. Vinyl-1,2 has assumed as a low content with IR spectroscopy. The detailed composition is given in Table 4.1. The photo-oxidation and thermal oxidation in the presence of air was affected in the molecular structure of the chains.

4.3.2 Analytical aspects of the photo-initiated oxidation at longer wave lengths

In high impact polystyrene, the polybutadiene phase is susceptible to photo-oxidation. The photo-oxidation of high impact polystyrene at longer or shorter wavelengths leads to the formation of radicals generated in the unsaturated alkene (which is present in butadiene). This radical is involved in the hydrogen abstraction in the α -position to the double bond. The abstraction of hydrogen atom usually competes with the addition mechanism. Those generated radicals react with oxygen and subsequently forms the hydroperoxides. These hydroperoxides are the primary photoproducts. The hydroperoxidation occurs prior to saturation of double bond and subsequently, the photolysis of hydroperoxides leads to hydroxylated and carboxylated groups. The IR spectral changes along with exposure time in SEPAP 12/24 is shown in Figure 4.1. A very fast oxidation leading to the evolution of hydroxyl group (band centered at 3450 cm^{-1}) and carbonyl group (band centered at 1717 cm^{-1} and shifting to 1725 cm^{-1} for longer exposure) is also evident in the figure. The polybutadiene portion is decreasing with the increasing of the irradiation

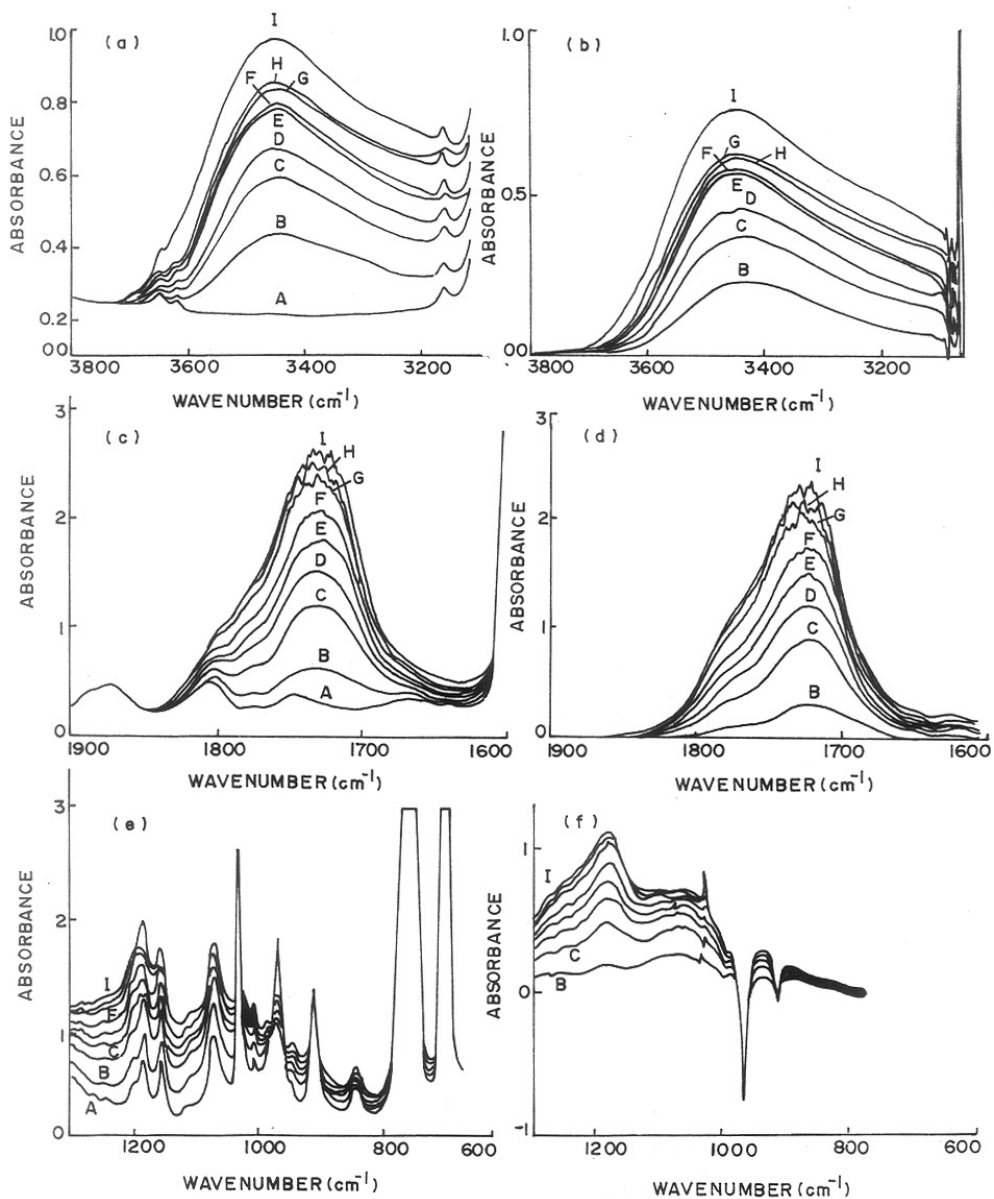
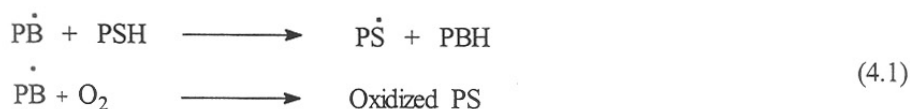


FIG.4.1: EVOLUTION OF IR SPECTRA OF HIPS (III) FILM (THICKNESS = $106\ \mu\text{m}$) UPON IRRADIATION AT $\lambda \geq 300\text{nm}$, 60°C : (A) 0h, (B) 9h, (C) 19h, (D) 29h, (E) 39h, (F) 49h, (G) 64h, (H) 74h, (I) 84h; a, c, AND e REPRESENT THE NONMODIFIED SPECTRA; b, d AND f REPRESENT THE SPECTRA FROM WHICH THE SPECTRA (A) HAS BEEN SUBTRACTED.

time, at bands 966 cm^{-1} (trans-1,4), 911 cm^{-1} (vinyl-1,2) and 727 cm^{-1} (cis-1,4). These results show that the polybutadiene phase is preferentially oxidized in the photo-oxidation. Figure 4.2 shows that the photo-oxidation of pure polystyrene was relatively slow process and that the shape of both hydroxyl and carbonyl regions are very different in comparison of high impact polystyrene. The oxidative attack occurs at the allylic position in the butadiene phase during thermal process and photo-oxidation. The photo-oxidation led to the photolysis of the hydroperoxides which are formed at the initiation of oxidation reaction and competes with crosslinking and chain scission.⁴ Scott et al.⁵ have observed in the photo-oxidized HIPS films, the disappearance of the damping peak at -80°C after 14 h irradiation of the sample. This was accompanied by a sharp increase in the complex modulus at 20° .

Lemaire et al.⁶ explained the degradation mechanism of pure polybutadiene under thermal and photo-oxidation conditions. The radical oxidation of unsaturated alkenes involved in hydrogen abstraction in the α -position to the double bond.⁷ In these both mechanisms, the formation of unstable alkyl and peroxy radicals are the main products. These radicals will react with oxygen and will be converted into secondary hydroperoxides or α,β -unsaturated ketones. All these products represent an important source of radicals able to initiate the oxidation of polystyrene by a hydrogen atom abstraction (Equation 4.1).



Some authors⁸⁻¹³ have studied these phenomena and estimated the oxidation of polybutadiene and the associated loss of mechanical properties. Gardette et al.³ explained the photo-oxidation of pure polystyrene and have measured the rate of its photo-oxidation also. They found that the rate of photo-oxidation of PS is very low in comparison to PB and nature of the photoproducts were also different. From these results, we can conclude that the fragile site of oxidation^{4, 14, 15} in HIPS is PB phase in spite of its low content.

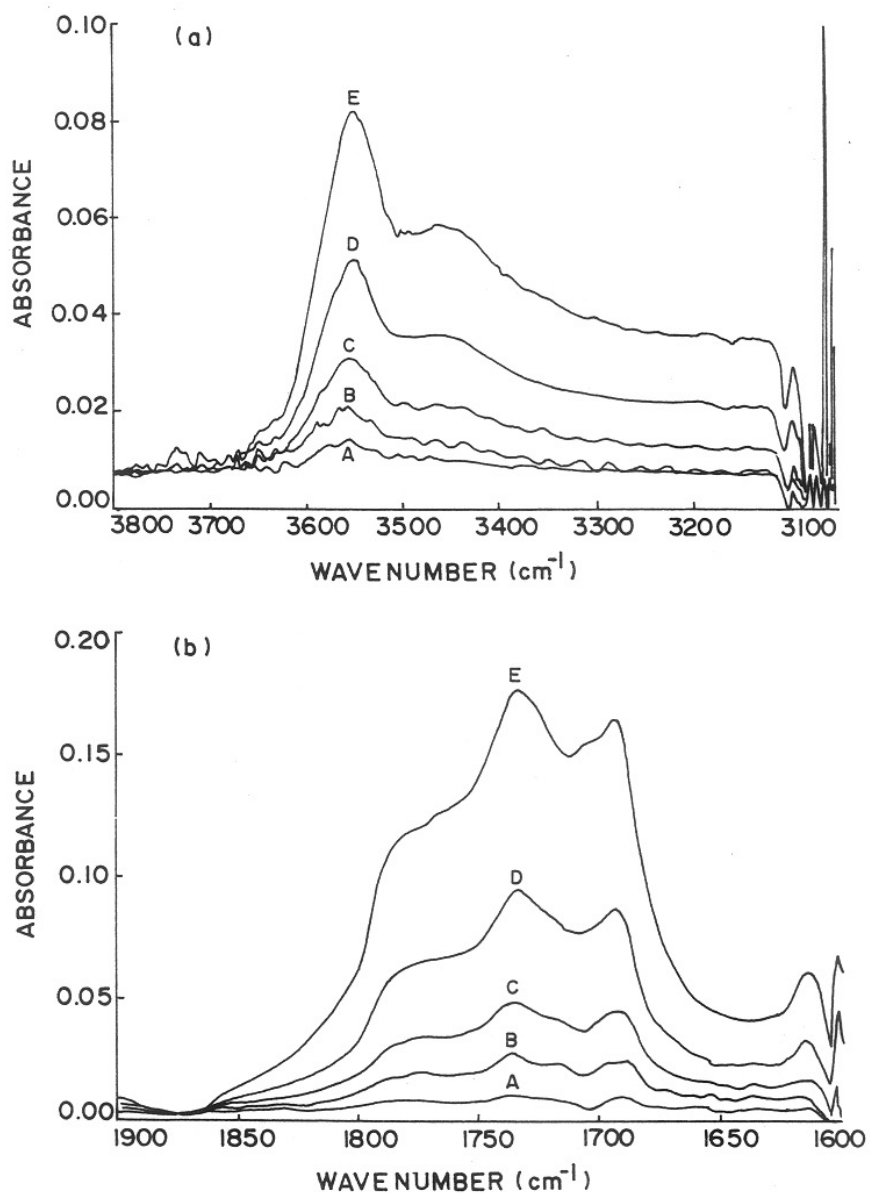


FIG.4.2: EVOLUTION OF THE IR SPECTRA OF A POLYSTYRENE FILM (THICKNESS = $105 \mu\text{m}$) UPON IRRADIATION AT $\lambda \geq 300 \text{ nm}$, 60°C (DIFFERENCE SPECTRA): (A) 35 h, (B) 75 h, (C) 112 h, (D) 162 h, (E) 211 h.

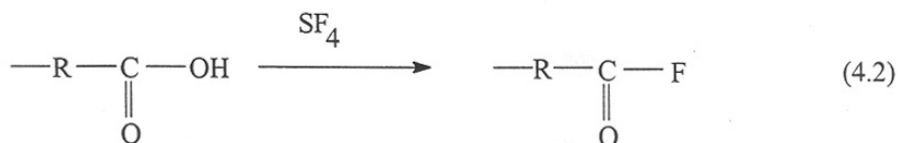
4.4 Kinetic aspects of the photodegradation

The kinetic curves of the photo-oxidation of HIPS I, II and III are given in Figure 4.3. In all the HIPS copolymers, the fast rate of oxidation occurred in the initial 50 h of exposure. The formation of carbonyl and hydroxyl groups increase with the increasing butadiene content in the copolymer. The formation of photoproducts and disappearance of unsaturation will depend on the polybutadiene content. After 50 h, a very slow rate of oxidation was observed. This second step probably corresponds to the photo-oxidation of styrene moieties, but this will be induced by the presence of polybutadiene as it is evident from the photo-oxidation of pure polystyrene. The comparison of the photo-oxidation of pure polystyrene and high impact polystyrene is compared in Figure 4.4. In our studies the photo-oxidation is mainly occurring in the polybutadiene phase and it also depends on the composition of the polybutadiene. Polystyrene oxidation will start after 50 h, but the pure polystyrene does not show any oxidation before 110 h, it means that polybutadiene phase acts as initiator for polystyrene phase in high impact polystyrene. Based on this observation we can say that the three types of high impact polystyrene copolymers behave similarly.

4.5 Derivatization reactions

4.5.1 SF₄ treatment

The SF₄ reacts with aldehydes and ketones and converted them into gem-difluoro compounds. The carboxylic acids also react with SF₄ to give 1,1,1-trifluorides.¹⁶ But the main product is acyl fluoride only. Generally, the SF₄ exposure of the films causes complete loss of all the hydroxyl absorption and generates acyl fluorides at 1810-1850 cm⁻¹ (Equation 4.2):



The 25 h photo-oxidized HIPS II film shows absorption at 1840 cm⁻¹ (Figure 4.5a) and this was observed in aliphatic polymers also.^{17, 18} The pure polystyrene shows

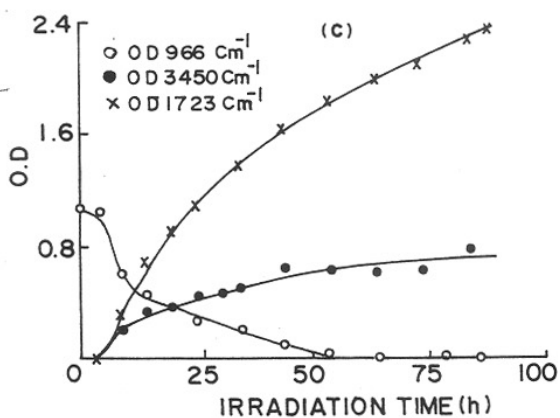
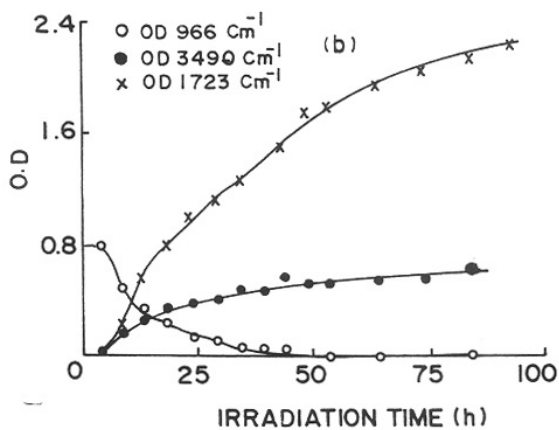
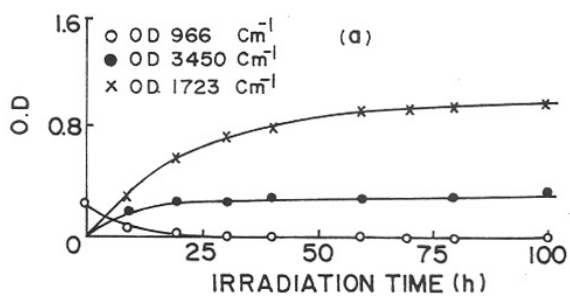


FIG.4.3: EFFECT OF UV AGEING ON CARBONYL, HYDROXYL AND UNSATURATION INDEX OF HIPS I (a), II (b) AND III (c) (THICKNESS 104, 104 AND 114 μm)

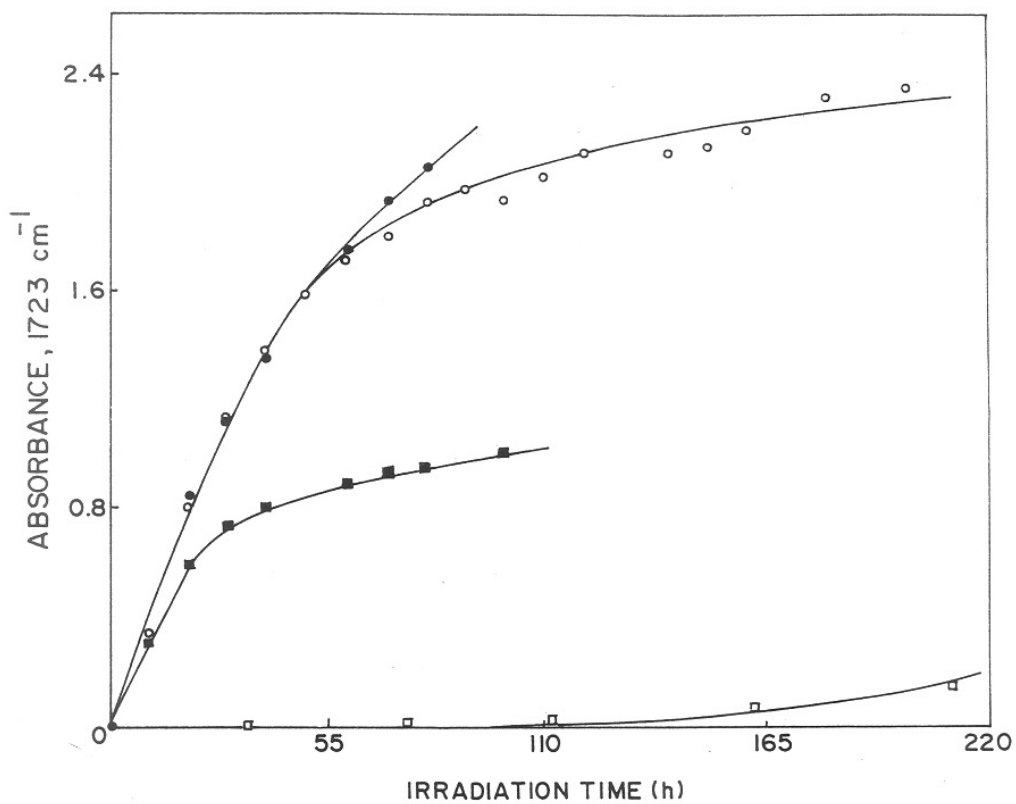


FIG. 4.4: COMPARISON OF OXIDATION RATES OF HIPS I (—■—) HIPS II (—○—), AND HIPS III (—●—) WITH PURE POLYSTYRENE (—□—) BY FOLLOWING THE ABSORBANCE AT 1723 cm⁻¹.

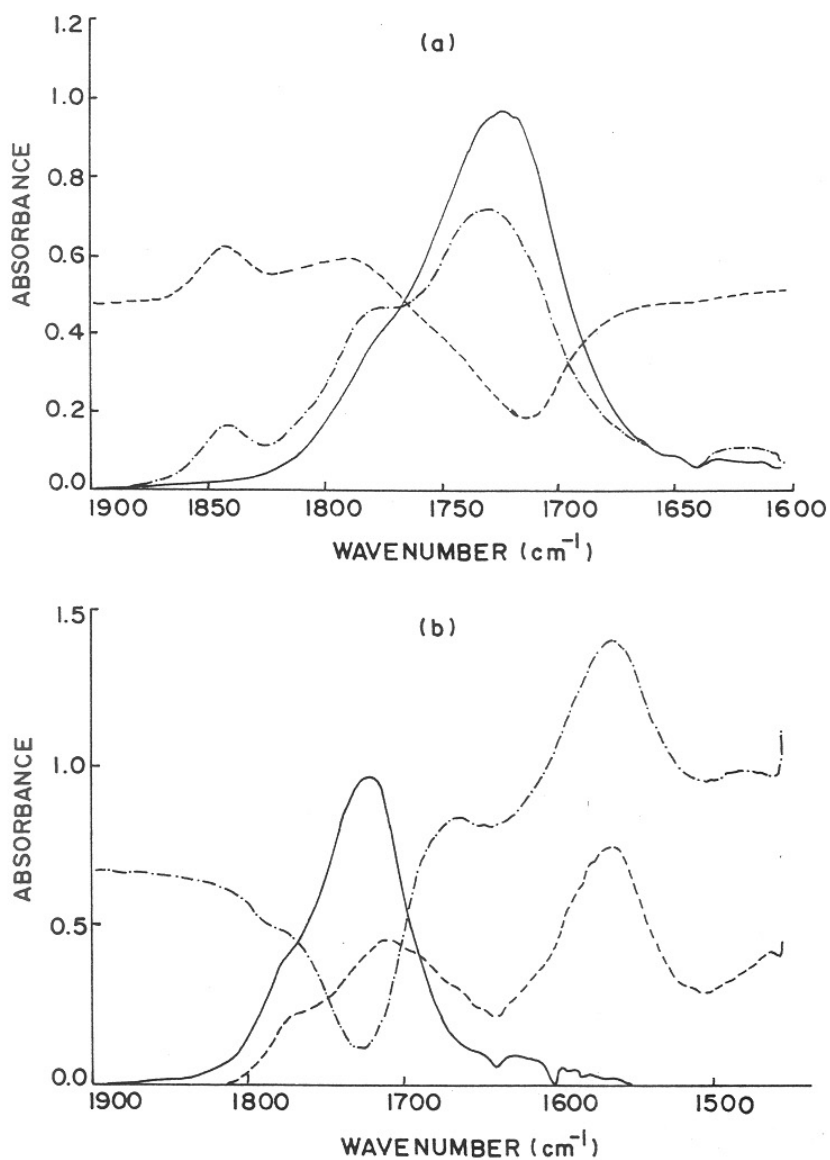
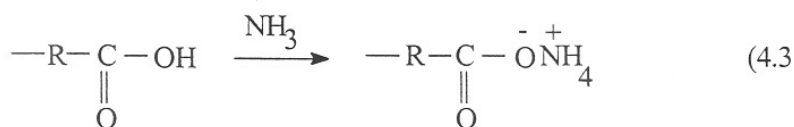


FIG.4.5: CHANGES IN FTIR SPECTRA OF A 25h PHOTO-OXIDIZED HIPS(II) FILM AFTER DERIVATIZATION BY (a) SF₄ (24h) AND (b) NH₃ (1h) GASES: (—) BEFORE TREATMENT, (-----) AFTER TREATMENT, (-·-·-·-) DIFFERENCE [(-----)-(—)].

aromatic acid fluorides³ at 1813 cm⁻¹. SF₄ reaction was used to measure quantitatively the carboxylic acid groups.¹⁷ The SF₄ derivatization reaction also establishes that the photo-oxidation initiates in the polybutadiene phase.

4.5.2 NH₃ treatment

The overlapping of carbonyl region was separated and identified by derivatization reactions of polymeric acids. The 25h photo-oxidized HIPS II film after treatment with NH₃ led to the formation of ammonium carboxylate (Equation 4.3):



The ammonium carboxylate shows its appearance at 1565 cm⁻¹ in HIPS^{18, 19} (Figure 4.5b) while in PS this band³ was observed at 1553 cm⁻¹.

4.6 Concentration profile analysis

The photoproduct distribution through the matrix of HIPS II has been measured in a plane perpendicular to the axis of irradiation by using the micro FT-IR technique. The concentration profiles measured at OD_{966 cm⁻¹}, OD_{3450 cm⁻¹} and OD_{1723cm⁻¹} as a function of the depth (Figure 4.6a). Generally butadiene based polymers show a very sharp profile in oxidation products and unsaturated groups. The concentration profile depends upon irradiation wavelength and the thickness of the film. In HIPS the photo-oxidation was localized within 10 μm which implies that the oxidation leads to formation of crosslinking reactions in the presence of oxygen. This result explains that the oxidation stops after a short irradiation time as the crosslinking of the sample makes the polymer impermeable to oxygen. The pure polystyrene³ oxidized at long wavelengths does not show any photoproduct distribution profile because the permeability to oxygen is quite high and crosslinking are not sufficient to decrease the oxygen permeability. The photo and thermal oxidation (Figure 4.6a & b) shows the distribution of carbonyl, hydroxyl and polybutadiene unsaturated groups in the HIPS. The sharp profiles observed are again consistent with a process involving selective oxidation of polybutadiene phase in the first stage of the reaction.

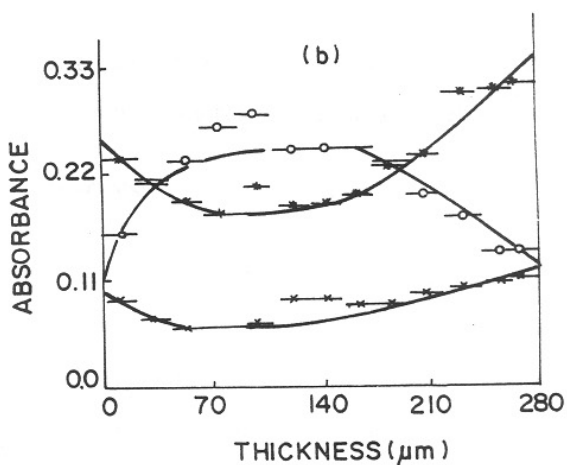
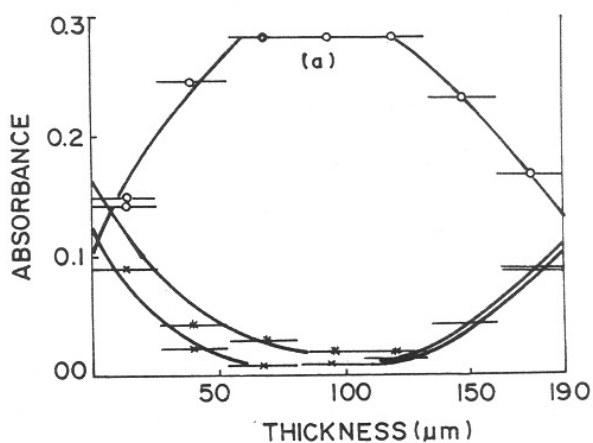


FIG.4.6: CONCENTRATION PROFILES IN HIPS II FILM: (o) $OD_{966\text{ cm}^{-1}}$, (x) $OD_{3450\text{ cm}^{-1}}$ (*) $OD_{1723\text{ cm}^{-1}}$, (a) PHOTOOXIDIZED AT $\lambda \geq 300\text{ nm}$, 60°C (THICKNESS = $190\ \mu\text{m}$, EXPOSURE TIME, 13h), (b) THERMOOXIDIZED AT 120°C (THICKNESS = $280\ \mu\text{m}$, EXPOSURE TIME = 71h)

4.7 Analytical aspects of thermal-initiated oxidation

HIPS I, II and III films have been exposed in an aerated oven at 80, 100 and 120°C. The changes are very similar to those in photo-oxidation. A broad band for hydroxyl group is appearing in the range 3200-3700 cm^{-1} and a carbonyl group from at 1550-1850 cm^{-1} (Figure 4.7). There is an increase in the peak area with the exposure time. The band appearing at 1696 cm^{-1} is typical for polybutadiene oxidation and has been attributed to α,β -unsaturated ketones, which can accumulate in the thermal oxidation. But this is very unstable in even $\lambda \geq 300$ nm in photo-oxidation. The kinetic curves showed (Figure 4.8) by an induction period, followed by a fast oxidation of polybutadiene and then by a slow oxidation of polystyrene. Figure 4.8 shows the kinetics of carbonyl groups formation at three temperatures showing an increase in the rate with increasing temperature. The thermal degradation of pure polystyrene and high impact polystyrene had been studied by Gupta et al.²⁰⁻²² It was observed that in the presence of air the random chain scissions are occurring in the weak links in polymer backbone (polybutadiene phase) which is undergoing through the oxidative degradation via peroxide formation. The thermally oxidized films showed yellowing, which increases with ageing time.²³

4.8 CONCLUSIONS

The high impact polystyrene films were changed significantly by thermal and photo-oxidation. The result of photo-oxidation at longer wavelengths and of thermal oxidation of HIPS is compared with pure polybutadiene and pure polystyrene with IR spectroscopy. The polybutadiene phase is main site for oxidation in thermal and photo-oxidation. The first step of oxidation in HIPS can be explained with pure polybutadiene. Thermal oxidation is characterized by accumulation of α,β -unsaturated ketones. The oxidation of unsaturated polybutadiene (in HIPS) and saturation of double bonds occur simultaneously which lead that polybutadiene phase is highly oxidized and crosslinked at the surface. Some of the radicals formed in degradation of polybutadiene can act as initiators of the oxidation of the polystyrene matrix which became less stable than pure polystyrene. These results imply that stabilization of HIPS will have to be concentrated mainly in the polybutadiene part.

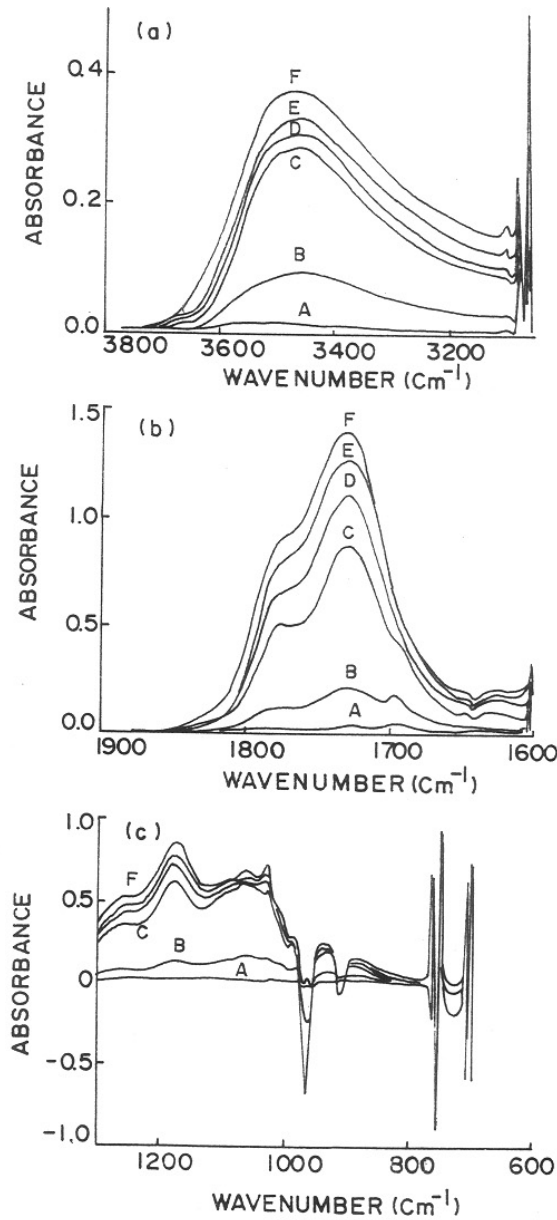


FIG.4.7: EVOLUTION OF THE IR SPECTRA OF HIPS (III) (THICKNESS = $117 \mu\text{m}$) UPON OVEN AGEING AT 120°C : (A) 41h (B) 64h, (C) 86h, (D) 153h, (E) 276h, (F) 428h

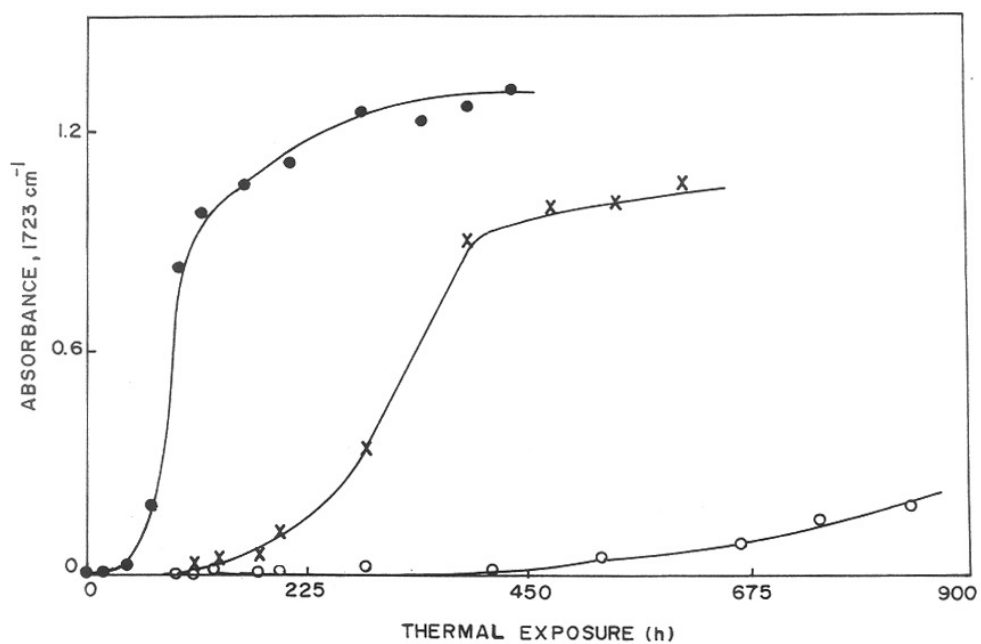


FIG. 4.8: TEMPERATURE DEPENDENCE OF THERMOOXIDATION RATE OF HIPS III (○) 80°C, (x) 100°C, (●) 120°C.

4.9 References

1. R.S. Silas, J. Yates, V. Thornton, *Anal. Chem.*, **31**, 529 (1959)
2. X. Jouan, J.L Gardette, *Polymer. Commun.*, **28**, 329 (1987)
3. B. Mailhot, J.L Gardotte, *Macromolecules*, **25**, 4119 & 4127 (1992)]
4. A. Ghaffar, A. Scott, G. Scott, *Eur. Polym. J.*, **12**, 615 (1976)
5. A. Ghaffar, A. Scott, G. Scott, *Eur. Polym.J.*, **11**, 271 (1975)
6. C. Adam, J. Lacoste, J. Lemaire, *Polym. Degradn. Stab.*, **24**, 185 (1989)
7. D.E. Vansickle, F.R. Mayo, R.M. Arluck, M.G. Syz, *J. Am. Chem. Soc.*, **89**, 967 (1967)
8. M. Mlinac-Misak, J. Jelencic, M. Bravar, *Die. Angew. Makromol. Chem.*, **173**, 153 (1989)
9. W.L. Hawkins, (Ed.,) '*Polymer Stabilization*', Wiley Inter. Sci., New York, 1972
10. A. Ghaffar, A. Scott, G. Scott, *Eur. Polym. J.*, **13**, 83 & 89 (1977)
11. G. Scott, M. Tahan, *Eur. Polym. J.*, **13**, 981 (1977)
12. W.Y. Chiang, *Ta Tung Hsuech Pao*, **9**, 129 (1979)
13. C. Adam, J. Lacoste, J. Lemaire, *Polym. Degrad. Stab.*, **29**, 305 (1990)
14. L.R. Schmidt, *J. Appl. Polym. Sci.*, **23**, 2463 (1979)
15. J. Virt, L. Rosik, J. Kovarove, J. Pospil, *Eur. Polym. J.*, **16**, 247 (1980)
16. J. March, '*Advanced Organic chemistry*', Mc Graw-Hill Kogaksusha, Tokyo, 1977.
17. D.J. Carlsson, R. Brousseau, C. Zhang, D.M. Wiles, *ACS. Symp. Ser.*, **364**, 376 (1988)
18. J. Lacoste, D.J. Carlsson, *J. Polym. Sci. Chem. Ed.*, **30**, 493 (1992)

19. D.J. Carlsson, R. Brousseau, C. Zhang, D.M. Wiles, *Polym. Degr. Stab.*, **17**, 303 (1987)
20. M.C. Gupta, J.D. Nath, *J. Appl. Polym. Sci.*, **25**, 1017 (1980)
21. M.C. Gupta, J. Nambiar, *Colloid. Polym. Sci.*, **261**,709 (1983)
22. M.C. Gupta, J. Nambiar, *Colloid. Polym. Sci.*, **259**, 1081 (1981)
23. M.F.Al-Jarrah, Salman R. Salman, Saud A. Hammo, *Polym. Degr. Stab.*, **23**, 75 (1988)

CHAPTER V

**CHAIN-SCISSION AND YELLOWING IN HIGH
IMPACT POLYSTYRENE**

5.0 INTRODUCTION

The effect of UV irradiation on polymers induces crosslinking, chain-scission and changes in molecular structure. All polymers are oxidized and their properties are deteriorated to certain extent by molecular oxygen and other oxidizing species present in the atmosphere. Molecular oxygen is the most abundant oxidizing species in the atmosphere and oxidizes polymers by a free-radical chain mechanism. The photolysis of the high impact polystyrene in the solid phase has been postulated to depend upon the mobility of free-radicals within the polymer matrix and their bimolecular recombination.

The present chapter deals with the photo-oxidative degradation behaviour of HIPS in which the polybutadiene phase constitutes the weak site for photo-oxidative degradation. This chapter reports the results of the study.

5.1 EXPERIMENTAL PROCEDURES

5.1.1 Materials

Commercial samples of high impact polystyrene (HIPS I) obtained from Polychem India. Sample II (HIPS-7240) and Sample III (HIPS-8350) were obtained from Elf-Atochem, France. Pure polystyrene was supplied by Polychem, India and used for comparison in this study. Prepared samples were used without further purification to avoid any change in the polymer composition. The composition of these samples are already given in Table 4.1 of chapter IV.

5.1.2 Sample preparation

Films of thickness about 100 μm were prepared by pressing the polymer in a preheated Carver press at 200°C by applying 150 kg/cm^2 platen pressure for 2 min. The films quenched cooled rapidly in the press.

5.1.3 UV irradiation

All samples were photo-irradiated in SEPAP 12/24 for different periods at 60°C. (SEPAP12/24 is described in chapter IV)

5.2 ANALYSIS

5.2.1 FT-IR analysis

FT-IR spectroscopy was used to monitor the photoproduct formation and loss of unsaturation during the photo-oxidation.

5.2.2 Viscosity measurement

The intrinsic viscosity $[\eta]$ was measured in toluene (concn = 0.12 wt%) at $30 \pm 0.5^\circ\text{C}$ by Ubbelohded viscometer. Solution was centrifuged to eliminate the gel content. The viscosity average molecular weight (\bar{M}_v) was determined with Mark-Houwink equation¹ (Equation 5.1):

$$[\eta] = K \bar{M}_v^a \quad (5.1)$$

where $[\eta]$ = intrinsic viscosity, \bar{M}_v = viscosity average molecular weight, 'K', and 'a' are Mark-Houwink constants and values depends on the solvent and temperature. The constant 'a' is related to the solvent power and to the expansion factor (α). It depends on the thermodynamic interactions between polymer segments and solvent molecules.

$$[\eta] = 1.10 \times 10^{-5} \bar{M}_v^{0.725}$$

5.2.3 Tensile/impact strength measurement

The tensile/impact strength test specimens were prepared by Minimax molded at 200°C . The diameter of the tab of the bar was 4.5 mm and of the neck 1.5 mm. Tensile strength was determined by an impact tester model CS-183 TI-085 (CSI, Cedar Knolls, New Jersey, USA) using the ASTM D-1822 method.²

5.2.4 Yellowness/Whiteness index measurement

Yellowness index (YI) and whiteness index (WI) were determined in accordance with ASTM D 1925³ by reflectance measurements using a Color Mate HDS colorimeter (Milton Ray, USA) with integrating sphere. Samples were placed in the reflectance part of the sphere using a standard white ceramic tile as reference. The

instrument is designated to give YI values on the basis of CIE standard illumination C (CIE 1931 2° standard) observer viewing.⁴ YI was obtained from the tristimulus values X_{CIE} , Y_{CIE} and Z_{CIE} relative to source C using the below expression (Equation 5.2):

$$YI = [100(1.28 X_{CIE} - 1.06 Z_{CIE})] Y_{CIE} \quad (5.2)$$

Several values of YI obtained from different parts of the samples were used to obtain an average value of the yellowness index.

5.3 RESULTS AND DISCUSSION

5.3.1 Effects of irradiation on intrinsic viscosity

The measurement of molecular weights of high polymers gives important information on the progress of degradative process. Viscosity measurement has been proved to be a valuable method of following polymer degradation due to its simplicity in operation. The values of both 'K' and 'a' depend on the solvent. The intrinsic viscosity $[\eta]$ of a polymer is a measure of the relative size of the polymer in the solvent used. Upon UV irradiation at $\lambda \geq 290$ nm, high impact polystyrene films result in a rapid decrease of intrinsic viscosity $[\eta]$ with irradiation time. This is because of random chain-scission in the polymer backbone. Figure 5.1 shows that the intrinsic viscosity initially decreases rapidly on exposure and tends to increase at 45 h. This is due to the chain-scissioning in polybutadiene at initial hours of exposure and at 45 h, the crosslinking was observed. The chain scissions and crosslinking are taking place simultaneously. After 45 h, there is a further rapid decrease in intrinsic viscosity which slows down later indicating crosslinking again at longer irradiation hours. The decrease in intrinsic viscosity after 45 h exposure is due to chain-scissions in polystyrene phase also. These results are clearly showing a two-phase oxidation behavior of HIPS. Intrinsic viscosity, chain-scissions and crosslinking depend on exposure time. The chain-scissions and crosslinking ratios increase in air as compared in vacuum. Figure 5.2 clearly shows increase in chain-scissions with exposure time. This phenomena has been explained by Gueskins et al.⁵ for polystyrene. The chain-scission causes formation of macroradicals on polymer backbone. These macroradicals further react with oxygen to form peroxide

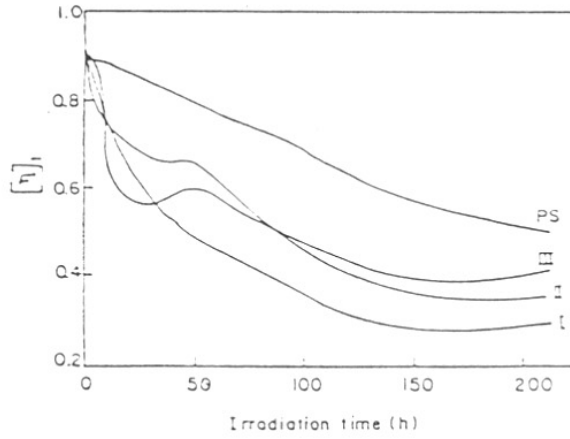


FIG. 5.1: VARIATION IN $[\eta]$ OF HIPS³ AS A FUNCTION OF IRRADIATION TIME

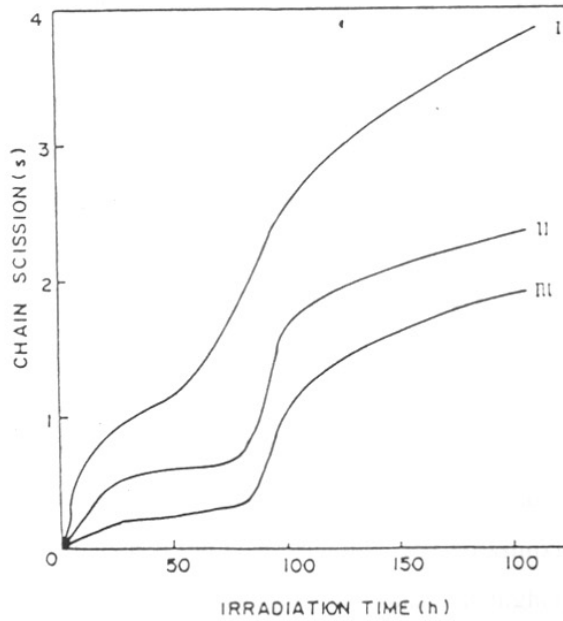


FIG. 5.2 VARIATION IN CHAIN-SCISSION (S) OF HIPS WITH IRRADIATION TIME

intermediates. These peroxide intermediates dissociate spontaneously to cause oxidative degradation. In high impact polystyrene, the polystyrene phase oxidizes in a single stage. Polystyrene oxidation starts when all the polybutadiene phase was oxidized. The polystyrene homopolymer showed a steady and very slow decrease in intrinsic viscosity with increasing exposure time. This result showed that the polybutadiene phase sensitizes the photo-oxidation of polystyrene in high impact polystyrene. This is measured with FT-IR spectroscopy by measuring the carbonyl group formation and decrease in unsaturation at 966 cm^{-1} (Figure 5.3). The rate of photo-oxidation depends on the polybutadiene in HIPS. The polybutadiene phase is oxidized completely within 20h for sample I, 45h for sample II and 50h for sample III. The viscosity, chain-scission and unsaturation measurement index clearly showed that the oxidation of polystyrene is hastened in the presence of polybutadiene.

Upon higher energy radiation (γ -irradiation) the high impact polystyrene showed the intrinsic viscosity decrease initially and then increase at longer irradiation.⁶ Gupta et al.⁶ also explained the two types of crosslinking in the polymer: (I) intermolecular between two macro radicals and (II) intramolecular between two monomer units of the same macromolecule. The intermolecular crosslinking between two macro radicals leads to an increase in the molecular weight of the polymer. But Davis et al.⁷ have pointed out that in the case where the dominant process is mainly chain-scission and although the molecular weight distribution may change, the ratio of the weight average molecular weight (\bar{M}_w) to number average molecular weight (\bar{M}_n) will remain the same throughout the degradation.

The polystyrene homopolymer exposed to γ -rays, resulted in chain-scissions and crosslinking. The chain-scission and crosslinking are decreasing with the increasing dose rate. The ratio between the chain-scission and crosslinking⁸ is greater than 4. This value is consistent with Saito's calculations.⁹ At higher irradiation dose, the chain-scission and crosslinking decrease because of the crosslinking and main chain-scission are due to the combination and dissociation of the macroradicals. At low irradiation dose the chain-scission is occurring than crosslinking.

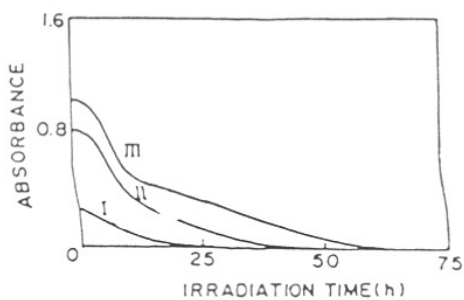


FIG. 5.3 EFFECT OF IRRADIATION ON UNSATURATION INDEX (966 cm^{-1}) OF HIPS

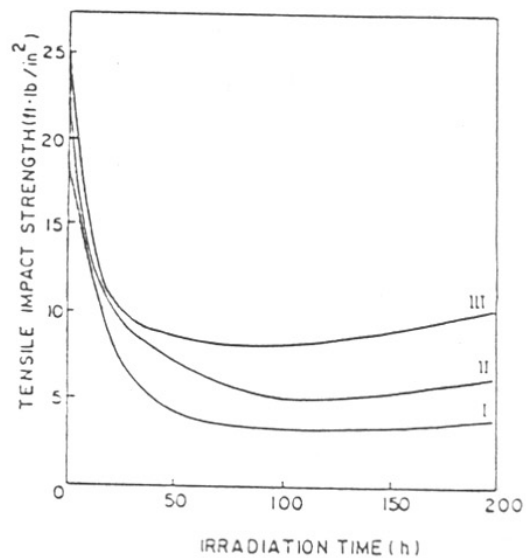


FIG. 5.4 VARIATION IN TENSILE/IMPACT STRENGTH OF HIPS AS A FUNCTION OF IRRADIATION TIME. $1\text{ ft-lb/in}^2 = 2.103\text{ kJm}^{-2}$

Chain-scission

The average number of scissions (s) per single chain length is evaluated using the equation (Equation 5.3).¹⁰

$$\frac{P_{v,0}}{P_{v,t}} = \left(\frac{2}{S} \right) (\bar{e}^{-s} + S - 1) \quad (5.3)$$

where $p_{v,0}$ and $p_{v,t}$ represent the viscosity-average chain length initially and at any time t during the degradation process. Figure 5.2 shows plots of chain-scission as a function of irradiation time. Equation 5.4 is valid only for those cases where $p_{v,0}$ is small and for larger values of $p_{v,0}$:

$$\frac{S}{P_{v,0}^{-1}} \cong \frac{S}{P_{v,0}} = \alpha \quad (5.4)$$

where α is the degree of oxidative degradation.

5.3.2 Changes in tensile/impact strength

The tensile impact strength depends on the polybutadiene content in high impact polystyrene. The tensile impact strength of the polymer decreases as a function of irradiation time. (Figure 5.4). The tensile impact strength initially decreases rapidly with the exposure time and then the curve becomes almost parallel to the X-axis after 40, 70 and 100 h irradiation, respectively, for sample I, II and III. Slight increase in impact strength was observed at longer periods, which is due to crosslinking. As irradiation time increases, the polybutadiene phase gets vanished and the impact strength of HIPS approached equal to that of polystyrene homopolymer value (16.8 KJ/m²). These observations suggested that the polybutadiene phase was oxidized initially. Apart from this the unsaturation (polybutadiene phase) was observed to decrease with increasing irradiation time in the FT-IR spectra (Figure 5.3) also. Thus, the loss in tensile impact strength is due to loss in polybutadiene phase. The shape of the tensile impact strength curves with

irradiation time (Figure 5.4) is very similar to intrinsic viscosity curves (Figure 5.1). These observations indicate that the polybutadiene phase selectively oxidizes initially.

Wilski et al.¹¹ have studied the effects of γ -rays on high impact polystyrene. They observed that the irradiation of high impact polystyrene with ^{60}Co - γ -rays in the absence of oxygen showed a steady increase in tensile strength and decrease in elongation at break upto a dose of 300 Mrad. This is due to crosslinking of the polybutadiene phase. But contrary to this in the long term irradiation in air, the tensile strength, elongation and impact strength decreased to half of their initial values at doses of 90, 40 and 30 Mrad., respectively. This is because of radiochemical oxidation in the polybutadiene phase. The mechanical properties did not changed for the sample which was stored in dark place for 14 year also.

5.3.3 Changes in yellowness/whiteness index

The HIPS sample turned opaque (translucent) and developed yellowness shortly after irradiation. Scott¹² postulated that the C-H bond of polystyrene is more stable than the C-H bond of the allyl group of PBD due to the induction effect and steric hindrance of the phenyl group and delocalization of radicals by the allyl group:



Therefore, oxidation naturally begins in the rubbery phase (allyl group) of PBD. The yellowing of polystyrene is well documented¹³⁻¹⁵ but scanty information is available in the literature¹⁶ for yellowing of HIPS.

The X, Y, Z tristimulus values of samples I and III are given in Table 5.1. The samples underwent rapid photoyellowing upon irradiation yielding a measurable increase within 50 h which became more severe at longer periods. A study of the tristimulus values indicates that the observed changes in yellowing are due to variations in lightness as well as chromaticity. The parameters calculated ($L = 10 Y^{1/2}$) from tristimulus values are the direct measure of lightness of the surface colour varying between zero (black) and 100 (white).

The colorimetric datas show a relatively small change in L but significant changes in a and b values, indicating that discoloration is not a mere change in lightness. The positive value of b indicates red/yellowness while the negative a value corresponds to greenish/blueness. The starting material itself (Sample III) with $L = 88.84$, $a = -0.32$ and $b = 3.24$ may be described as having a very light yellow-green surface. The value of a decreases while that of b increases with YI (Table 5.1). This indicates an increase of yellow-green colour with irradiation.

Table 5.1 shows the variations of yellowness index (YI) of HIPS samples with irradiation time. The YI of the irradiated sample I increased approximately linearly with time (upto 100 h) but the rate of increase fell thereafter. The decrease is probably a result of the slow loss of yellow brittle surface layer due to handling or leaching reactions at longer periods. In fact the thickness decreases with irradiation. The slower yellowing of sample I compared with that of sample III is expected on account of its lower elastomer content. The reflectance curves for irradiated samples (I and III) at 400 nm are shown in Figure. 5.5. The reflectance at a given wavelength (400 nm) decreases as a function of irradiation time. This observation also clearly indicates that yellowing is accompanied by a decrease in reflectance in the visible range.

5.4 CONCLUSIONS

Studies of solution viscosity of HIPS show that irradiation causes random chain-scission and produces smaller molecular weight fractions. In spite of weak links in polystyrene, the oxidation initiates in the PBD phase. After ~ 50 h of irradiation, the HIPS samples behave purely as polystyrene. All the samples suffer yellowing as a result of photo-oxidative degradation.

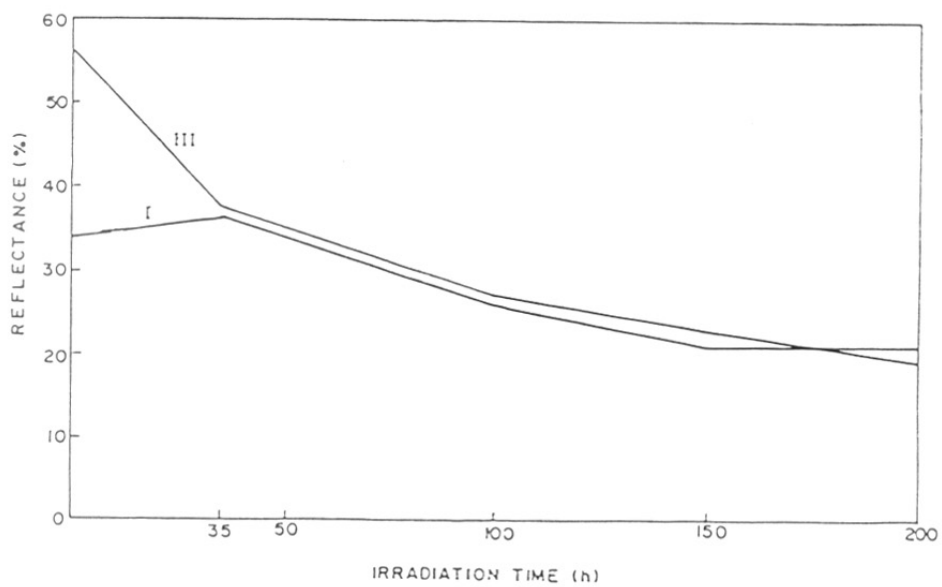


FIG. 5.5 VARIATION IN REFLECTANCE AT 400 nm OF HIPS SAMPLES WITH IRRADIATION TIME

Table 5.1. Yellowness index (YI) of irradiated HIPS upon irradiation

Sample	Irradiation time (h)	Tristimulus values			YI	WI ^a
		L^*	a^*	b^*		
I	0	86.40	-1.37	8.46	12.73	26.88
	35	86.99	-1.45	9.46	18.62	23.76
	100	85.81	-1.93	15.25	28.88	-0.39
	150	85.00	-2.00	19.0	35.58	-14.86
	200	85.00	-2.08	19.10	35.60	-14.86
III	0	88.84	-0.32	3.24	7.52	53.85
	35	87.48	-2.01	11.16	21.22	17.09
	100	86.38	-2.31	17.60	32.47	-9.07
	150	85.78	-2.38	19.95	36.51	-17.88
	200	84.88	-2.25	22.89	41.66	-28.19

5.5 References

1. F. Danusso, C. Moraglio, *J. Polym. Sci.*, **24**, 161 (1957)
2. Annual Book of ASTM standards, American Society for Testing and Materials, Philadelphia, Vol. 1979, part 35, (1981)
3. Annual book of ASTM Standards, American Society for Testing and Marterials, Philadelphia, Vol. 8, 02 (1988)
4. F.W. Billmeyer, M. Sultzman, '*Principles of Colour Technology*', Interscience, New York, 1966, p.38.
5. G. Gueskins, D. Baeyeans-volant, G. Detauneoss, Q. Lu-Vinh, C. David, *Eur. Polym. J.*, **14**, 291 (1978)
6. M.C. Gupta, B.S. Srirao, B.P. Kanphade, V.P. Bansod, *Polymer Commn.*, **25**, 334 (1984)
7. A. Davis, D. Sims, '*Weathering of Polymers*', Applied Science Publishers, London, 1983, p.208.
8. S. Egusa, K. Ishigure, Y. Tabala, *Macromolecules*, **13**, 171 (1990).
9. O. Saito, in '*Radiation Chemistry of Macromolecules*', Vol. I (M. Dole Ed.), Academic Press, New York, 1972, chapter.11.
10. I. Sakurada, S. Qkamura, *Z. Phys. Chem. A.*, **187**, 289 (1940)
11. H. Wilski, E. Gaube, S. Rosinger, *Colloid. Polym. Sci.*, **260**, 559 (1982)
12. G. Scott, '*Atomspheric oxidation and antioxidants*', Elsevier, London, 1965, p.25.
13. B.G. Achhammer, M.J. Reiney, L.A. Wall, F.W. Reinhart, *Nat. Bur. Stand. (US) Circ.*, **525**, 205 (1953).
14. L.A. Wall, D.W. Brown, *J. Phys. Chem.*, **61**, 129 (1957).
15. N. Grassie, N.A. Weir, *J. Appl. Polym. Sci.*, **9**, 999 (1965).
16. W.Y. Chiang, *Ta Tung Hsuech Pao*, **9**, 129 (1979).

CHAPTER VI

**MORPHOLOGICAL CHANGES IN HIGH IMPACT POLYSTYRENE
UPON PHOTO-OXIDATIVE DEGRADATION**

6.0 INTRODUCTION

In recent years there has been a lot of interest in the area of thermoplastic elastomers.^{1, 2} High impact polystyrene (HIPS) consists of a continuous glassy polystyrene (PS) matrix and an elastomeric dispersed polybutadiene (PB) phase.³⁻⁵ In Styrene-Butadiene-Styrene (SBS) tri-block copolymer, the central domain is PB and end domains are PS. These two phases behave as two distinct phases, where the PS block acts as crosslink, as well as a filler, in the network system.⁶

In both these polymers, the PB phase is more susceptible to photo-oxidation.⁷ The photo-oxidized polymer loses its weight and mechanical properties and shows discoloration and surface embrittlement. The photo-oxidation of HIPS and SBS has been studied by IR technique^{8, 9}, but less attention has been paid to the mechanism of photo-oxidation by ¹³C NMR and morphological changes upon photo-irradiation in HIPS and SBS. The ¹³C NMR spectroscopy provides a very useful and sensitive method for detection of photoproducts in the photo-oxidized polymers. Scanning Electron Microscopy (SEM) is a powerful tool for morphology characterization. The morphology can be defined as the sum of the fluctuations of characteristic quantities (such as the density, chemical composition etc.,) along a positional coordinate and the interface associated with them, having a size from several units to several hundred nanometers. It means that a material heterogeneity can be studied by microscopic methods. In the present investigation we have studied ¹³C NMR and morphological changes upon photo-oxidation of HIPS and SBS.

6.1 EXPERIMENTAL PROCEDURES

6.1.1 Materials

HIPS [HIPS 8350] sample obtained from M/s. Elf-Atochem, France and SBS was received through the courtesy of M/s. Shell Company, USA.

6.1.2 Sample preparation

HIPS films were prepared by solution casting. The material was dissolved in toluene (2.00 wt-%), and cast over mercury surface. The solvent was evaporated at room temperature and then dried in a vacuum oven for 24 h at 50°C. SBS films were also

prepared by solution casting with various solvents like (CCl₄, THF, and CHCl₃). The material was dissolved in the solvent (2.00 wt-%) and cast over mercury surface, evaporated at room temperature and dried in a vacuum oven for 24 h at 50°C. Thin films (~ 0.2 mm thickness) were obtained.

6.1.3 Photo-Irradiation

Films were irradiated in SEPAP 12/24 (Material Physico Chimique, Neuilly/Marne, France) at 60°C. The unit consists of four 400W 'medium pressure' mercury sources filtered by a pyrex envelope supplying radiation of wavelengths longer than 300 nm. The equipment is described elsewhere.¹⁰

6.2 ANALYSIS

6.2.1 ¹³C NMR Spectroscopy

Neat and photooxidized films were dissolved and swollen in CDCl₃. ¹³C NMR spectra were recorded on a Bruker MSL 300 spectrometer in 10-mm tube at 25°C, TMS as the internal standard.

6.2.2 Scanning electron microscopy

The films were examined by scanning electron microscope (Leica Cambridge Stereoscan 440 model) for morphological changes. The neat and oxidized films were placed in stoppered bottles containing Osmium tetroxide (2 % aqueous) and allowed to stand for 48 h. The films were washed with water and dry ethanol. The stained samples dried under vacuum for 24 h at 50°C. The gold coated samples were examined under electron microscope.

6.3 RESULTS AND DISCUSSION

6.3.1 Characterization by high resolution ¹³C NMR in solution

¹³C NMR spectroscopy is known to be more suitable for the determination of *cis*, *trans* and vinyl contents of PB in HIPS⁵. Figure 6.1 shows the *cis*-1,4, *trans*-1,4 and *vinyl*-1,2 in both the aliphatic (27.3 and 32.6 ppm) and olefinic region (114.2 ppm). The resonance peaks at δ 27.3, 32.6, 114.2 ppm are *cis*-1,4, *trans*-1,4 and *vinyl*-1,2,

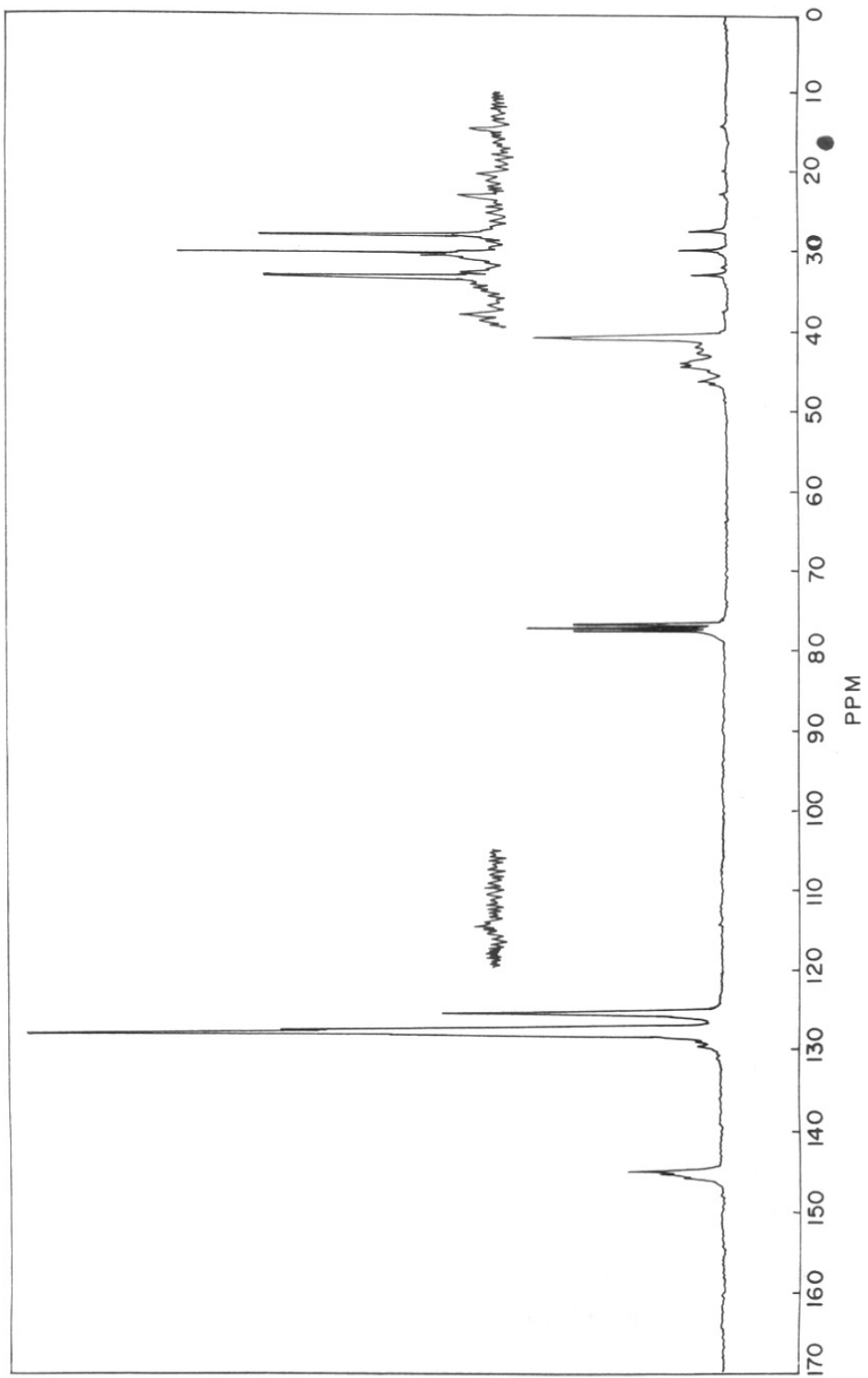


FIG. 6.1: HIPS 8350 NEAT IN CDCl_3 SOLUTION

respectively. These units have σ and π orbitals. The lowest energy state in these orbitals is a (π - π^*) nature. The intensity of these peaks decrease with the increasing the exposure time (Figure 6.2), meaning that initial photo-oxidation occurs at the PB phase only. The photo-oxidized films showed hydroxyl and carbonyl bands at 3450 and 1717 cm^{-1} , respectively. We observed a decrease of unsaturation (997 cm^{-1}) in the PB portion⁷ which is in agreement of our ^{13}C NMR results. The neat sample dissolved very well in CDCl_3 , but the photo-oxidized films were phase separated in CDCl_3 . We were unable to detect the peaks for epoxides and alcohols due to the low content of PB. Scott¹¹ postulated that the C-H bond of PS is more stable than the C-H bond of the allyl group of PB due to the induction effect, the steric hindrance of the phenyl group, and delocalization of radicals by the allyl group:



therefore, oxidation naturally begins in the rubbery phase (allyl group) of PB. The yellowing in HIPS is due to PS, which is well documented.^{12, 13} Due to crosslinking, the phase separation was observed in photo-oxidized films (200 h) in CDCl_3 solvent.

In SBS triblock copolymer also, the PB block is susceptible for photo-oxidation. The *cis*-1,4, *trans*-1,4 and *vinyl*-1,2 PB phases (Figure 6.3) were present in the SBS copolymer also. The photo-oxidized (100 h irradiation) SBS films showed appearance of *cis*-epoxides (δ 56.4 ppm), *trans*-epoxides (δ 58.3 ppm) and alcohol (δ 71.2 ppm) in Figure 6.4, but on longer hours of irradiation there is a decrease in epoxides and alcohol peaks (Figure 6.5). This decrease with longer irradiation is due to the decomposition of epoxides and alcohols to carbonyls end products. The generation of these groups and then their decomposition confirms that oxidation primarily initiates in the PB phase of SBS. Adam et al.¹⁴ also observed a weak resonance in PB. The weak signals are responsible for alcohols (65-77 ppm) and peroxides (78-88 ppm). The peaks at δ 56.4, 58.3 ppm are identified¹⁴ as a *cis* epoxide and *trans* epoxide, respectively. The very weak crosslinking peaks were also observed at δ 29.5, 40.3, 41.6 and 42.4 ppm. The following mechanism is proposed for epoxide formation: (Equation 6.1)

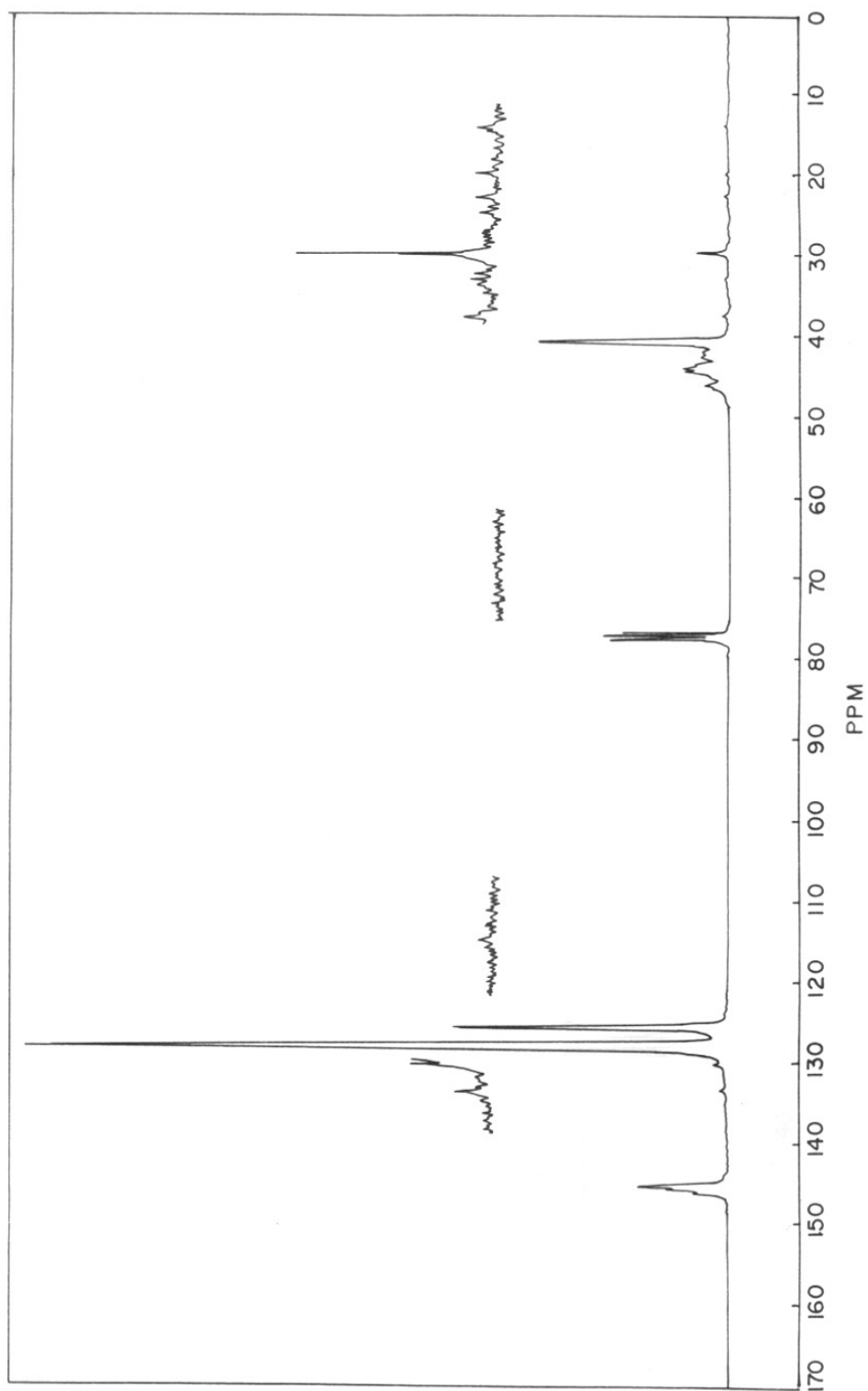
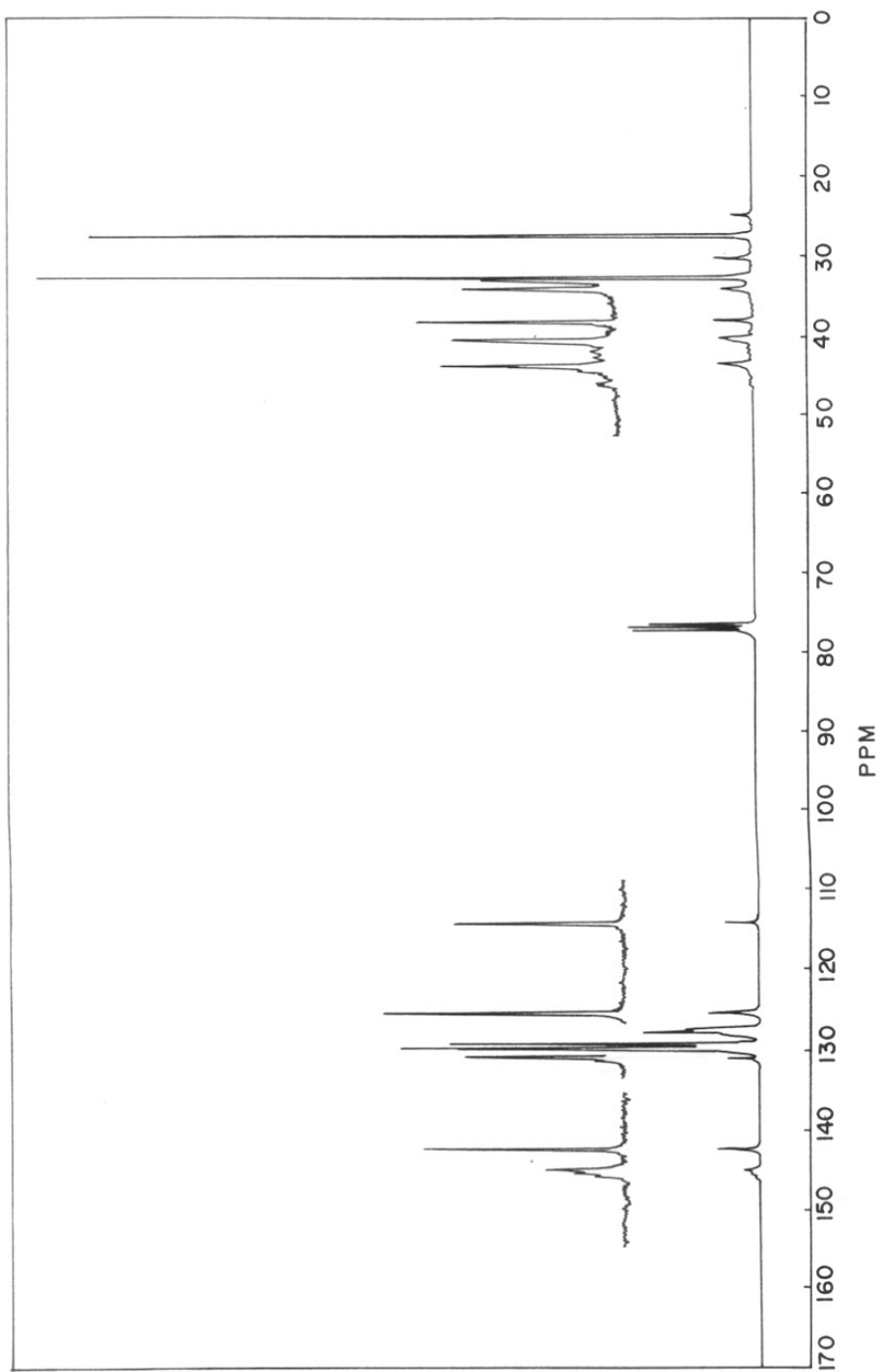
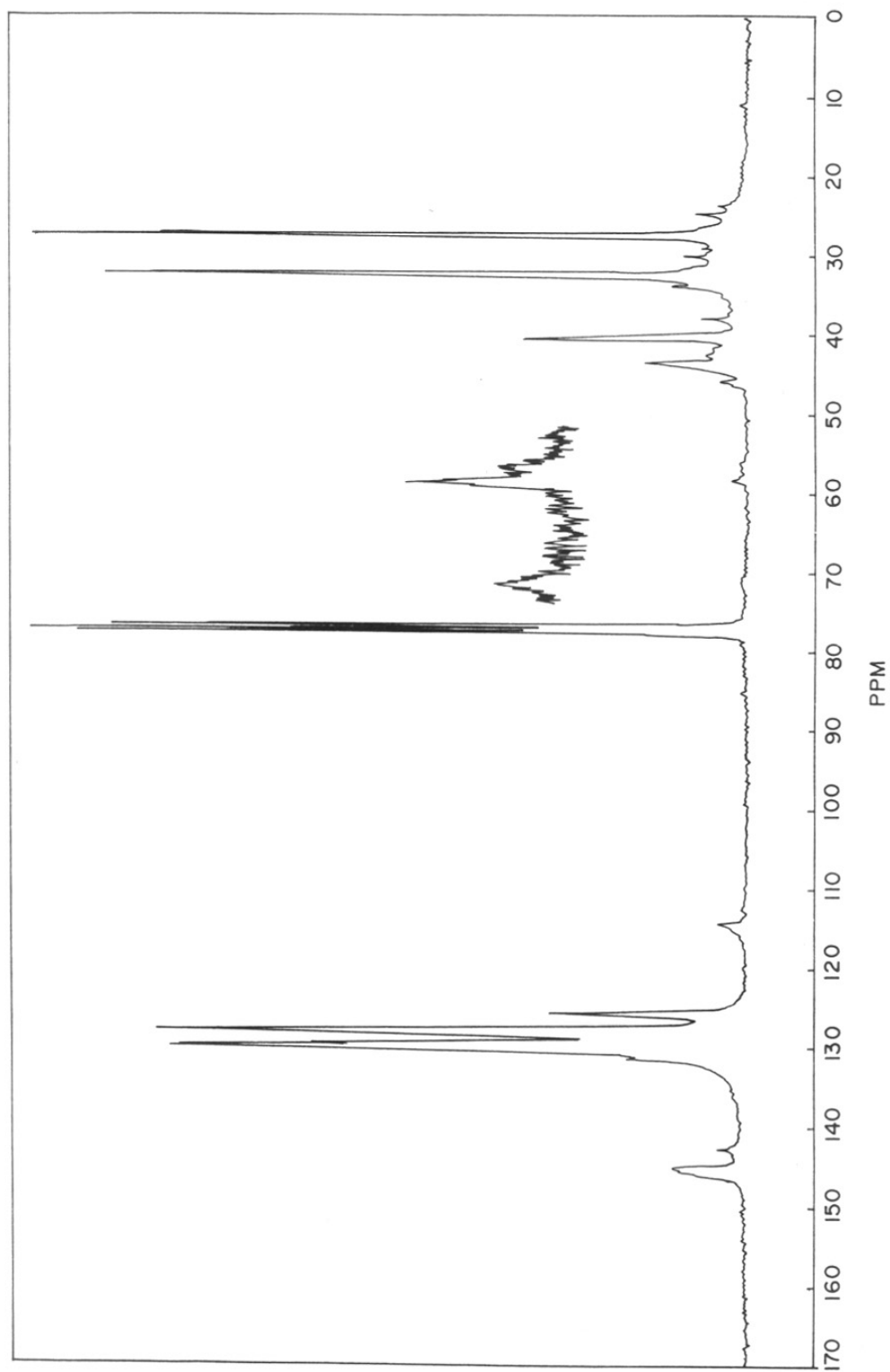


FIG. 6.2: HIPS8350 AFTER 200h UV EXPOSURE IN CDCl_3 SOL.

FIG.63:SBS NEAT IN CDCl_3 SOLUTION

FIG.6.4:SBS AFTER 100h UV EXPOSURE IN CDCl_3 SOLUTION

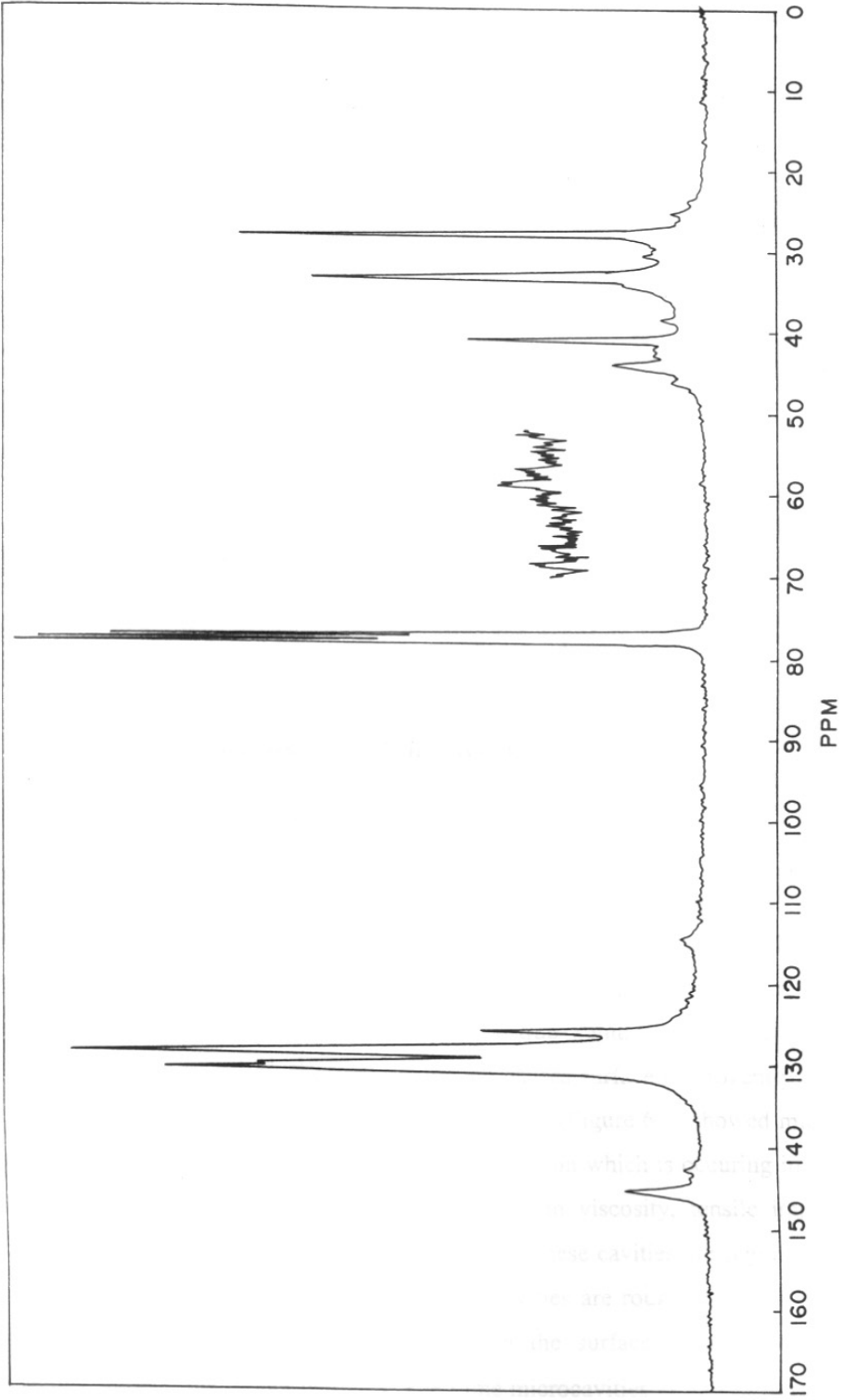
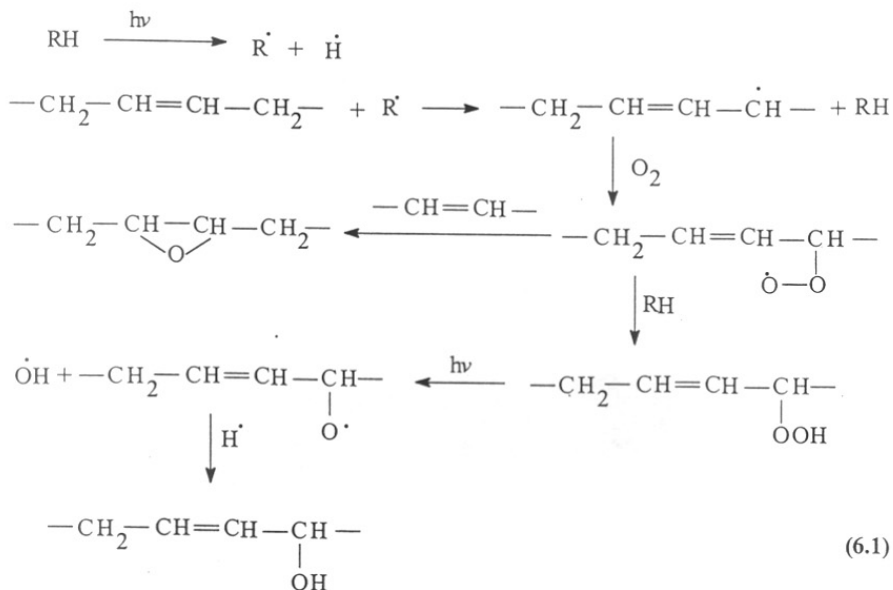


FIG.6.5:SBS AFTER 300h UV EXPOSURE , IN CDCl₃ SOLUTION

1,1-dimethyl-1



The PB peak intensities decrease with increasing the exposure time, meaning that photo-oxidation initiation occurs in the PB phase in SBS copolymer also.

6.3.2 Morphological changes upon UV irradiation

6.3.2.1 High Impact polystyrene

The micrographs of HIPS sample in Figure 6.6 illustrate the phase separation. The spherical PB phase is dispersed in continuous PS phase. In toluene solvent the PS matrix is soluble and the rubber particles can swell to such an extent that the resulting system appears to the naked eye as a true solution, particularly on sufficiently high dilution.^{15, 16} The photo-oxidation causes surface heterogeneity and generates degradation products. The 100 h exposed film (Figure 6.6) showed micro cavities on the surface. This was because of chain scission which is occurring in the PB phase initially. We have explained the changes in viscosity, tensile impact strength and yellowing upon exposure to UV light.¹⁷ These cavities are regular and spherically in nature. The internal surface of the cavities are rough in nature. The film irradiated (250 h) showed micro cracks on the surface. The cracks are propagating through the rubber particles. The same microcavities (150-250 μm) are observed in combustion treatment in the poly(2,6-dimethyl-1,4-phenylene ether)-



Fig. 6.6: SEM photographs of neat and photo-oxidized HIPS 8350 (a) neat film, (b) 100 h UV exposure, and (c) 250 h UV exposure

HIPS blends.¹⁸ In thermal degradation, the material forms gases that create a cellular structure in the whole specimen. The cellular structure is the precursor of the char that is formed on the outer surface of the burning material. The char contains large voids whose walls (5 μm thick) show the presence of numerous 'secondary' closed cells. The secondary cells might derive from the degradation of rubber domains.

6.3.2.2 Styrene-Butadiene-Styrene Copolymer

The morphology in the SBS triblock copolymer changes with the solvent system. Photo-oxidized films showed surface embrittlement and yellowness. This was because of the chain scission in the PB portion. Photo-oxidized SBS films showed microcracks and microcavities on the polymer surface. The breaking of polymer bonds under UV irradiation produces fragments that occupy more volume than the original macromolecules, causing strains and stress that can be responsible for the formation of microcracks.¹⁹

Tetrahydrofuran [THF, solubility parameter 9.1 ($\text{cal}\cdot\text{cm}^{-3}$)^{1/2}] is a good solvent for PS compared to PB²⁰, therefore, the THF solvent system showed the phase separation very well.²¹ The swollen endblocks aggregated into a spherical form (Figure 6.7). Photo-oxidized films showed the aggregation of PS block very well (50 h). The 100 h exposed film showed the microcavities on the polymer surface. This was due to the initial degradation of the PB portion. The 300 h irradiated film showed microcracks on the surface.

Carbon tetrachloride [CCl_4 , solubility parameter 8.6 ($\text{cal}\cdot\text{cm}^{-3}$)^{1/2}] is a good solvent for both the PB and PS.²⁰ In SBS- CCl_4 solution, an interface exists between the PS and PB portions. This was observed with dynamic mechanical testing.²² At 50 h exposure, the PB portion started to degrade and phase separation is very clearly observed in Figure 6.8. At longer hours (200 h) the PS phase also started to degrade as is evidenced by the cracks on the white portion.

In chloroform [CHCl_3 , solubility parameter is 9.3 ($\text{cal}\cdot\text{cm}^{-3}$)^{1/2}] solvent the PS and PB phase separated very well.²³ The microcracks are observed (Figure 6.9) on the film surface upon UV exposure. At 100 h UV exposure, the microcavities are

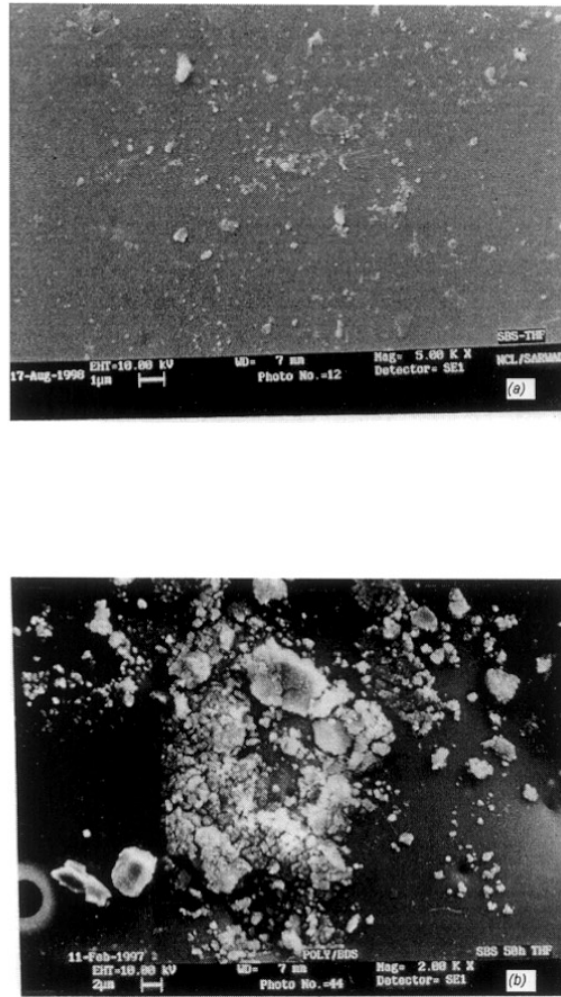


Fig. 6.7: SEM photographs of SBS film cast from THF solvent: (a) neat film and (b) 50 h UV exposure

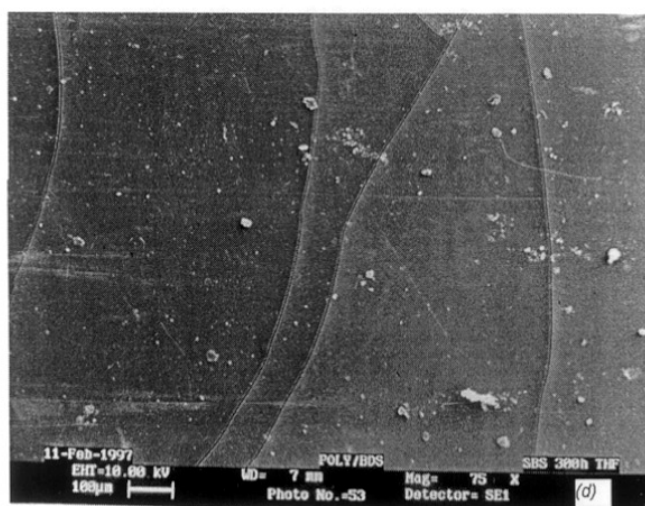
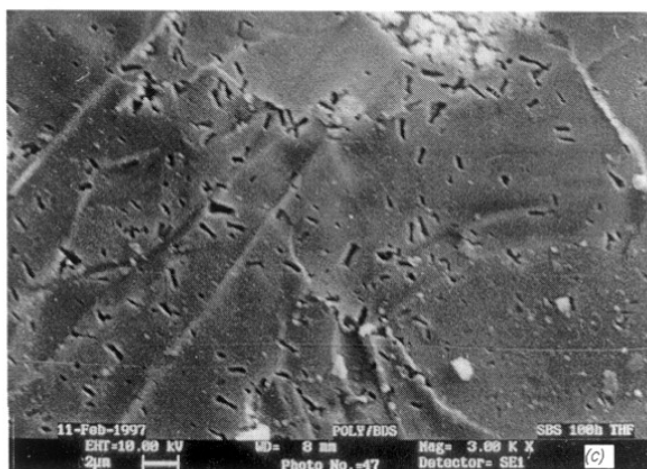


Fig. 6.7: SEM photographs of SBS film cast from THF solvent : (c) 100 h UV exposure, and (d) 300 h UV exposure

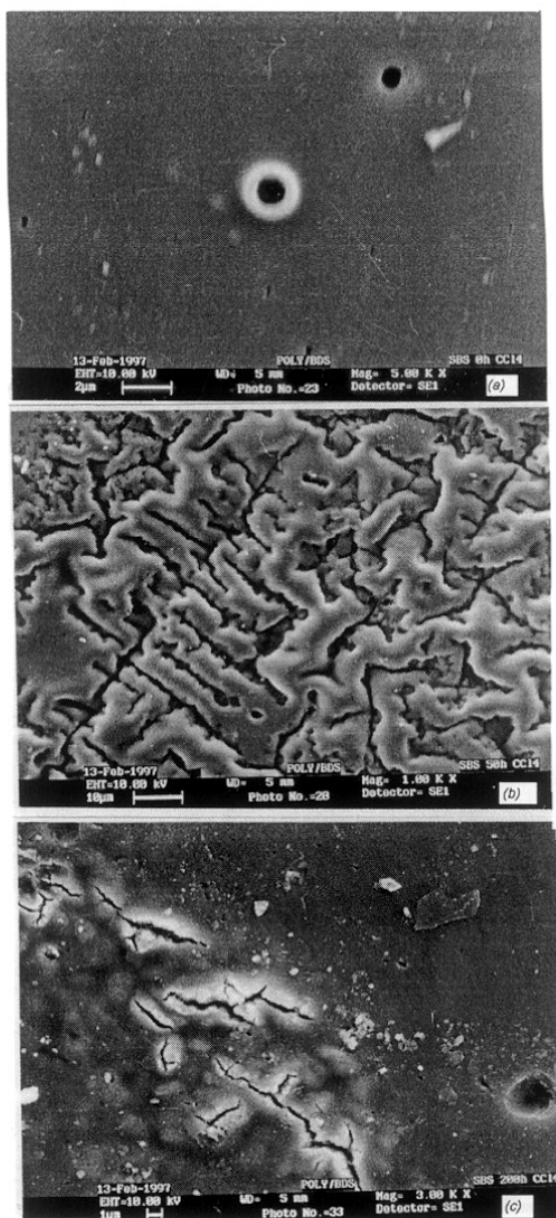


Fig. 6.8: SEM photographs of SBS film cast from CCl_4 solvent: (a) neat film, (b) 50 h UV exposure, and (c) 200 h UV exposure

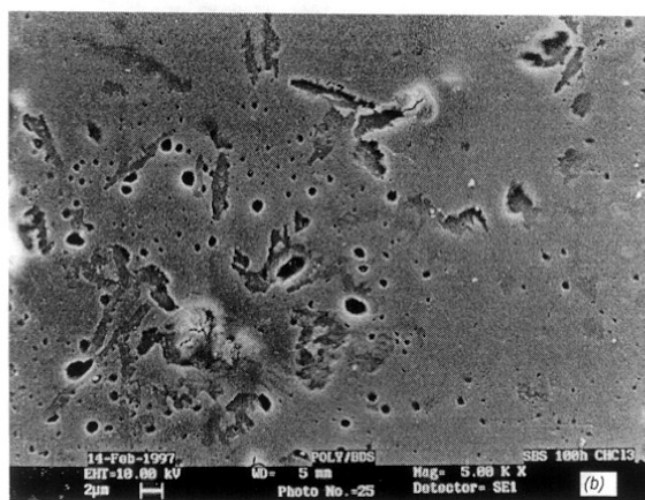
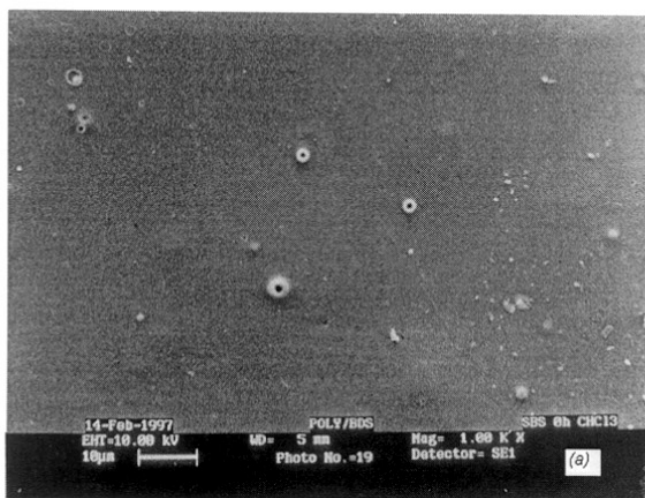


Fig. 6.9: SEM photographs of SBS film cast from CHCl₃ solvent: (a) neat film, and (b) 100 h UV exposure

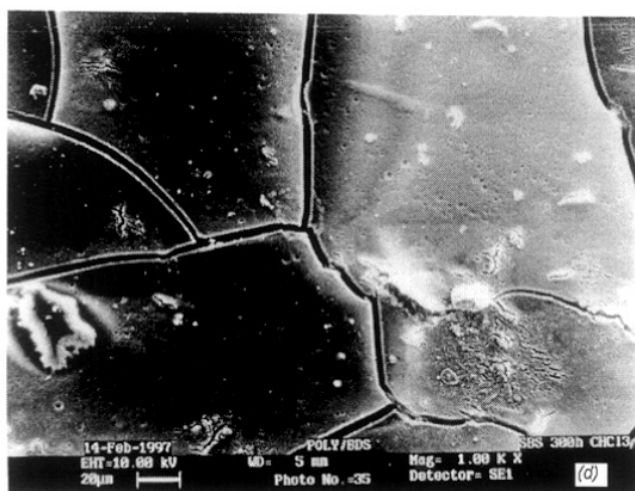
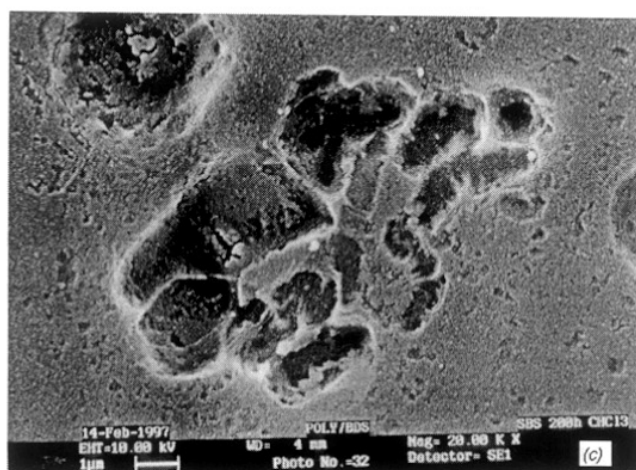


Fig. 6.9: SEM photographs of SBS film cast from CHCl_3 solvent: (c) 200 h UV exposure, and (d) 300 h UV exposure

formed and the PS phase also started degradation. The microcavities are irregular in shape and the internal surface of the cavities are rough in nature. At a longer exposure the macrocracks and macrocavities were observed on surface.

6.4 CONCLUSIONS

The characterization and assignment of a particular signal in a glassy insoluble polymer network are the major analytical applications of the NMR technique. The best results are expected in solution, but on photo-irradiation, the samples are slightly crosslinked. The samples of HIPS and SBS subjected to polychromatic irradiations underwent cracks on the surface that led to the serious loss of impact strength in the former and elastomeric properties in the later. The microcracks were developed due to the formation of photoproducts during irradiation. Both the polymers also displayed distinct microphase separation.

6.5 References:

1. C. Adam, J. Lacoste, J. Lemair, *Polym. Degrad. Stab.*, **24**, 185 (1989)
2. S. Sivaram, R.P. Singh, *Adv. Polym. Sci.*, **101**, 169 (1991)
3. G.E. Molau, H. Keskkula, *J. Polym. Sci., Part A-1*, **4**, 1595 (1966)
4. A. Vishwa Prasad, R.P. Singh, *J. Macromol. Sci., Rev. Macromol. Chem. Phys.*, **C37**, 581 (1997)
5. J. Lacoste, F. Delor, J.F. Pilichowski, R.P. Singh, A. Vishwa Prasad, S. Sivaram, *J. Appl. Polym. Sci.*, **59**, 953 (1996)
6. J.F. Beecher, L. Marker, R.D. Bradford, *J. Polym. Sci, Part C.*, **26**, 117 (1969)
7. Y. Israeli, J. Lacoste, J. Lemaire, R.P. Singh, S. Sivaram, *J. Polym. Sci. Part A. Polym. Chem.*, **32**, 485 (1994)
8. A. Ghaffar, A. Scott, G. Scott, *Eur. Polym. J.*, **13**, 89 (1977)
9. R.P. Singh, Vijayanand, P.N. Thanki, S. Sivaram, FRPM' 97 Sept.24-26, 1997, Lille, France.
10. R.P. Singh, R. Mani, S. Sivaram, J. Lacoste, D. Vaillant, *J. Appl. Polym. Sci.*, **50**, 1871 (1993)
11. G. Scott, '*Atmospheric Oxidation and Antioxidants*', Elsevier, London, 1965, p.25
12. B.G. Achhammer, M.J. Reiney, L.A. Wall, F.W. Reinhart, *Nat. Bur. Stand. (US) Circ.* **525**, 205 (1953).
13. N. Grassie, N.A. Weir, *J. Appl. Polym. Sci.*, **9**, 999 (1965)
14. C. Adam, J. Lacoste, G. Dauphin, *Polymer. Commn.*, **32**, 317 (1991)
15. G.E. Molau, H. Keskkula, *J. Polym. Sci. Part A-1*, **4**, 1595 (1966)
16. D. Hace, V. Kovacevic, D. Pajc-Liplin, *Polym. Eng. Sci.*, **36**, 1140 (1996)
17. R.P. Singh, R.A. Raj, A. Vishwa Prasad, S. Sivaram, J. Lacoste, J. Lemaire, *Polym. Inter.*, **36**, 309 (1995)

18. A.B. Boscoletto, M. Checchin, M. Tavan, G. Camino, L. Costa, M.P. Luda, *J. Appl. Polym. Sci.*, **53**, 121 (1994)
19. Halina Kaczmarek, *Polymer*, **37**, 189 (1996)
20. Ging-Ho Hsiue, Mu-Yuan M. Ma, *Polymer*, **25**, 882 (1984)
21. J.F. Beecher, L. Marker, R.D. Bradford, *J. Polym. Sci. Part C.*, **26**, 117 (1969)
22. G.H. Hsiue, D.J. Chen, Y. King, *J. Appl. Polym. Sci.*, **35**, 995 (1988)
23. J. Bandrup, E.H. Immergul, "*Polymer Handbook*", 3rd edition, John Willey & Sons, New York, Pvii/528 (1989)

CHAPTER VII

NATURAL WEATHERING OF HIGH IMPACT POLYSTYRENE

7.0 INTRODUCTION

Upon exposure of polymers to environmental condition, the physical and chemical attack leads to their degradation. The UV light and heating effects of solar radiation play major role and the polymer leads to chain-scission. The solar UV light (295-400 nm) irradiation reaching to earth surface is generally $\leq 5\%$, but it is sufficient energy to break the bonds of polymers. As a consequence of degradative reactions, the polymer losses its properties like mechanical, rheological, thermal, electrical, changes in color and finally leads to embrittlement. Thus the service life becomes limited, due to weathering¹ of polymers. Weathering implies the action of individual or a combination of various environmental factors on polymers, i.e. heat, light, ionizing radiation, oxygen, ozone, humidity, rain, wind, dust, bacteria and chemical pollutants. Apart from structural and morphological changes, the natural aging also depends on geographic locations (latitude, longitude, mountain, sea, desert, etc.), seasons, environmental and atmospheric conditions. In India, Pakistan or Saudi Arabia, where the sun falling is greater (250 kW cm^{-2}), the weathering life is only 2-5 years.

The natural weathering and artificial weathering of polymers like LDPE², PP³, LDPE-LLDPE blends⁴ and E-P copolymers⁵ had been discussed earlier but the terrestrial degradation of styrenic copolymers has not been studied. In this chapter, the natural weathering behavior of styrenic copolymers with different polybutadiene content and its comparison with polystyrene is discussed. The carbonyl groups formation in natural exposure is compared with corresponding accelerated weathering.

7.1 EXPERIMENTAL PROCEDURES

7.1.1 Materials

The materials investigated were high impact polystyrene (HIPS) (sample I) obtained from Polychem, India. HIPS 7240 (sample II) and HIPS 8350 (sample III) samples obtained from Elf-Atochem, France. A commercial sample of polystyrene (Polychem, India) was also examined for comparison. The samples which contained processing antioxidants, were used without purification to avoid any change in the

polymer composition. The content of polybutadiene in HIPS was determined⁶ by ¹³C-NMR and FTIR spectroscopy and was found to be 3.1, 6.3 and 7.9 mol%, respectively, for HIPS I, HIPS II and HIPS III.

7.1.2 Sample preparation

Thin transparent films (~100 μm) were made in an hydraulic press at 200°C by applying 150 kg cm⁻² pressure.

7.1.3 Natural weathering

The polymer films were mounted without stress on wooden frames inclined at 45° to the horizon and was exposed facing south-west at the terrace about 20m above ground at NCL, Pune, India located at 73°51' E longitude and 18°32' N latitude. The weathering test was carried out in two different climate conditions, September to March and April to August. During this periods the average values of sunshine temperature was ranged from 25 to 30°C and 35 to 43°C, respectively. The daily average sunshine time was around 10h. Accelerated weathering has been carried out in a SEPAP 12/24. The details of SEPAP 12/24 have been described in chapter IV, section 4.2.3.^{7, 8}

7.2 ANALYSIS

The natural and accelerated films have been characterized by FT-IR spectroscopy with Perkin Elmer 16PC

7.3 RESULTS AND DISCUSSION

7.3.1 Changes in carbonyl and hydroxyl region

The natural photo-oxidation of HIPS I, HIPS II, HIPS III and PS films showed in FTIR spectra, the carbonyl absorption (1850-1550 cm⁻¹) band centered at 1725 cm⁻¹ which shows the formation of carboxylic acids. The hydroxyl region (3700-3200 cm⁻¹) absorption band centered from 3320 to 3550 cm⁻¹ is due to the intramolecular hydrogen bonded hydroperoxides and alcohols (Figures.7.1 to 7.4). The rate of photo-oxidation depends on the content of the polybutadiene.^{6, 9} The mechanism of the photo-oxidation is as follows (Equation 7.1):

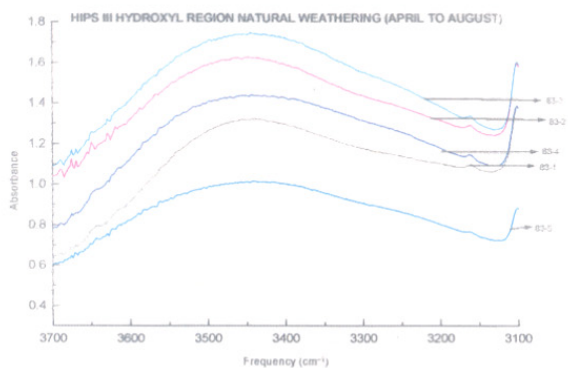
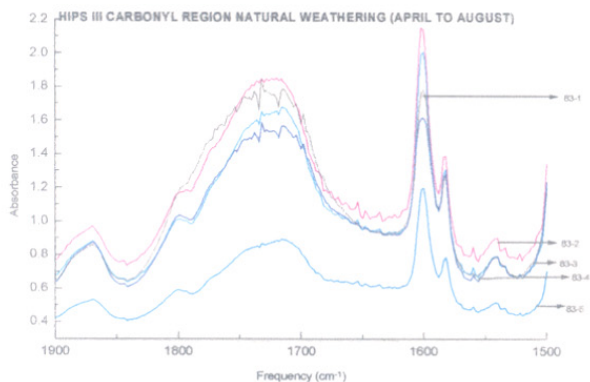


Figure 7.1 FT-IR Spectral changes in carbonyl and hydroxyl region for various times of natural exposed HIPS III films during the months of April to August

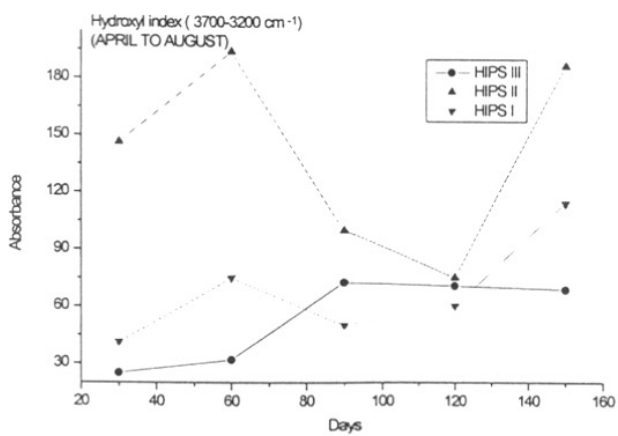
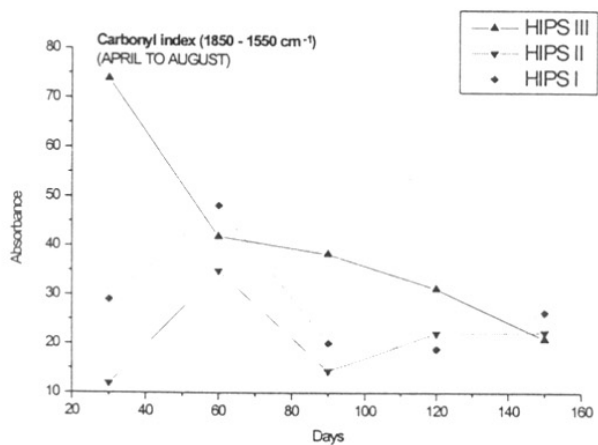


Figure 7.2 Rate of carbonyl and hydroxyl group formation in HIPS (I to III) films in natural exposure during the months of April to August

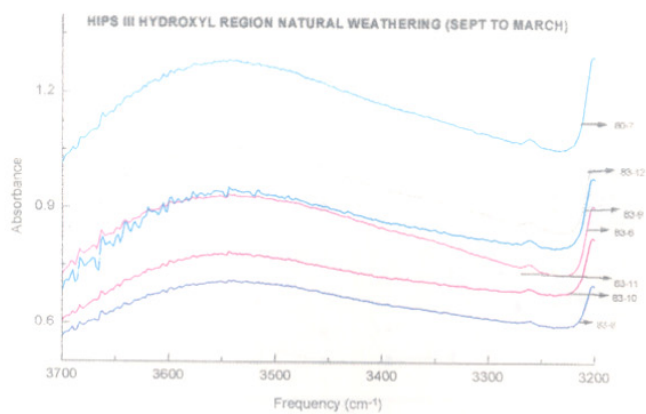
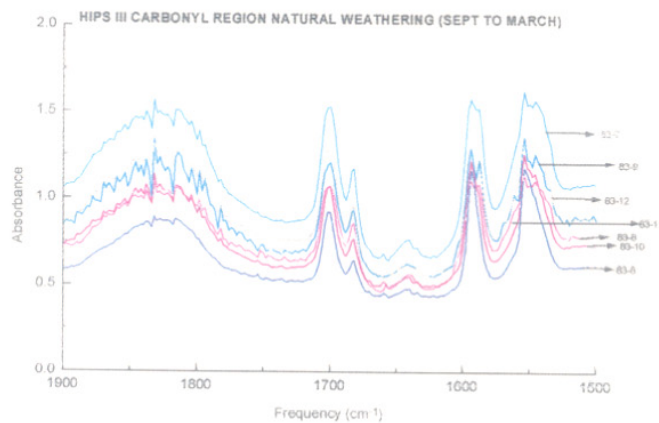


Figure 7.3 FT-IR Spectral changes in carbonyl and hydroxyl region for various times of natural exposed HIPS III films during the months of September to March

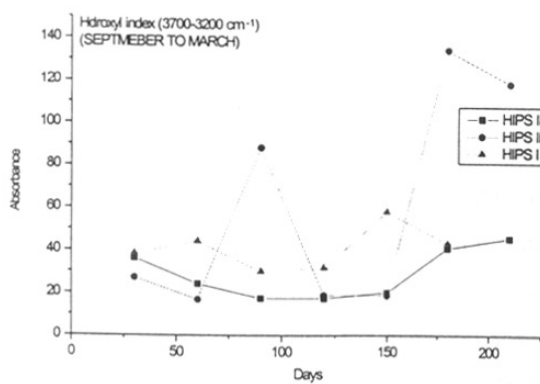
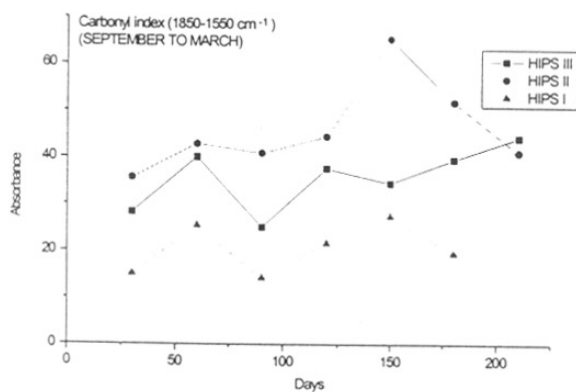
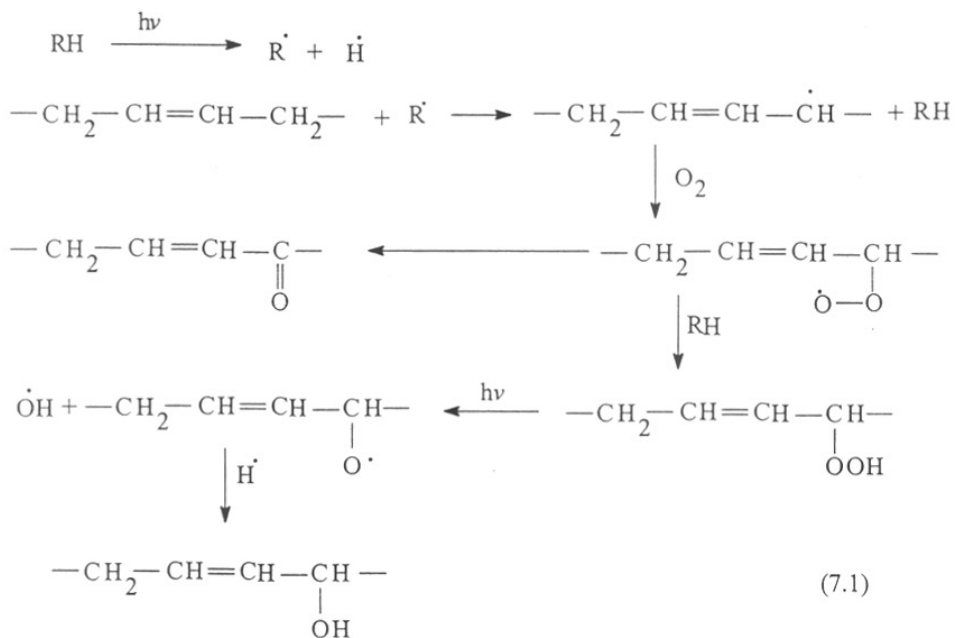


Figure 7.4 Rate of carbonyl and hydroxyl group formation in HIPS (I to III) films in natural exposure during the months of September to March



It clearly shows that the polybutadiene is oxidized initially. Mailhot et al.¹⁰ have explained detailed analysis of IR spectra combined with physical and chemical treatment of photo-oxidized PS.

7.3.2 Kinetic aspects of the natural photo-oxidation of styrenic polymers

The rate of photo-oxidation of HIPS I, HIPS II, HIPS III and PS films in natural weathering, increases as is evident from Figure 7.2, with the increase of carbonyl and hydroxyl groups formation from April to August. In the month of April, the formation of carbonyl groups is more as compared to the hydroxyl region in HIPS III (Figure 7.1 & 7.2). During this time the temperature was 40-44°C and the humidity in the environment was very less. The rainy session starts in India from the month of June which shows that the hydroxyl absorption is more in this period. In Figure 7.2 the same behavior is observed in HIPS I and HIPS II. The rate of photo-oxidation in natural weathering also depends on the polybutadiene content. The rate of photo-oxidation in natural weathering HIPS III is minimum from October to January (Figure 7.3 & 7.4) and maximum in March. During this period the temperature is 30-35°C. HIPS I and HIPS II also showed the same behavior (Figure

7.4). In the photo-oxidation process, the polybutadiene oxidizes via formation of unstable alkyl, peroxy radicals and the unstable intermediate hydroperoxides lead to the formation of carbonyl groups. The photo-oxidation of PS is minimum and that of HIPS (I to III) films is maximum. (Figures 7.5 to 7.8). These result shows that the polybutadiene phase is oxidized initially in high impact polystyrene films. The nomenclature of samples is given in Table 7.1

7.3.3 Comparison of photo products formation under natural and accelerated weathering exposure

The natural and accelerated weathering of HIPS III and PS showed the carbonyl absorptions in the region of $1850-1550\text{ cm}^{-1}$ where the band centered at 1720 cm^{-1} . The hydroxyl group absorptions in the region of $3700-3200\text{ cm}^{-1}$, centered at 3450 cm^{-1} . The rate of photo product formation is more in accelerated weathering (Figure 7.9 & 7.10). Figure 7.11 shows that with the irradiation time there is an increase in the carbonyl and hydroxyl groups formation. The carbonyl group formation is compared in Figure 7.12.

7.4 CONCLUSIONS

The natural and photo-oxidation of styrenic copolymers showed the carbonyl and hydroxyl absorptions. The rate of formation of photoproducts in accelerated weathering is more than natural weathering.

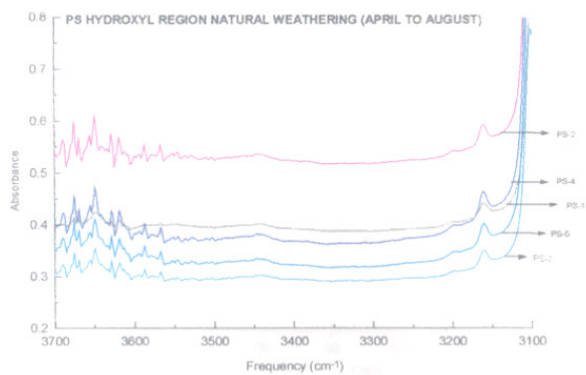
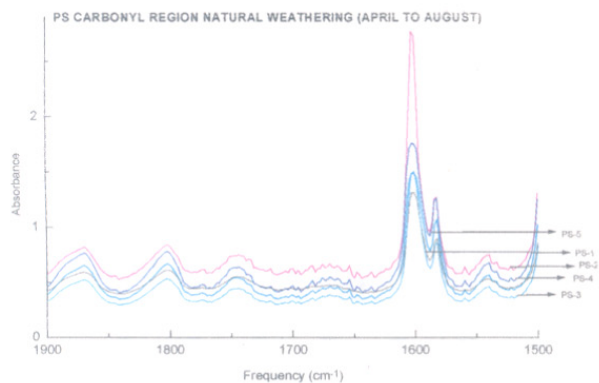


Figure 7.5 FT-IR Spectral changes in carbonyl and hydroxyl region for various times of natural exposed PS films during the months of April to August

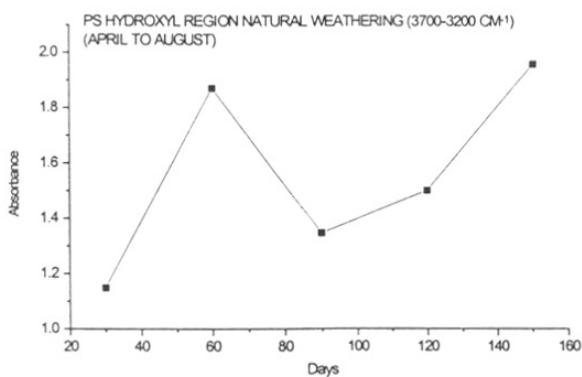
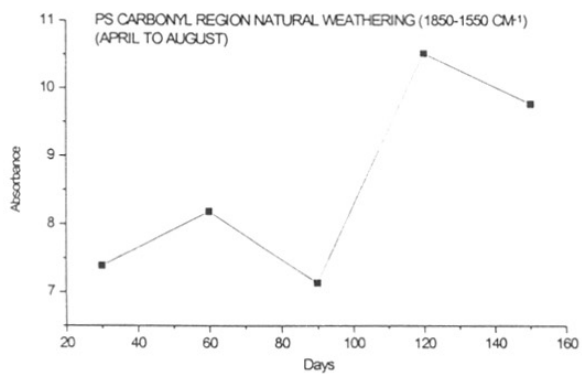


Figure 7.6 Rate of carbonyl and hydroxyl group formation in PS films in natural exposure during the months of April to August

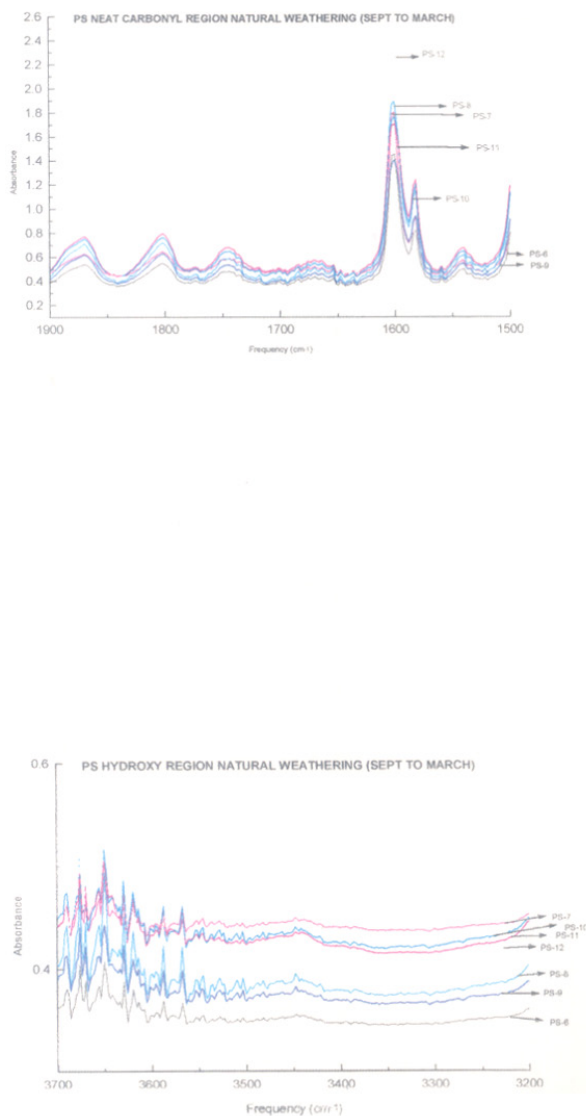


Figure 7.7 FT-IR Spectral changes in carbonyl and hydroxyl region for various times of natural exposed PS films during the months of September to March

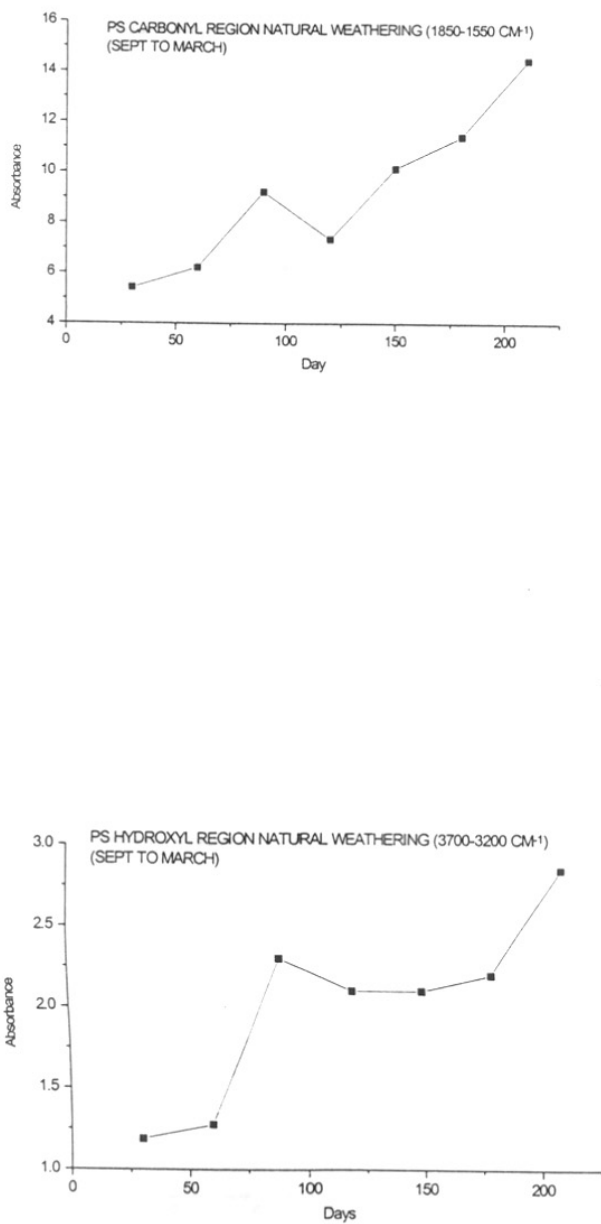


Figure 7.8 Rate of carbonyl and hydroxyl group formation in PS films in natural exposure during the months of September to March

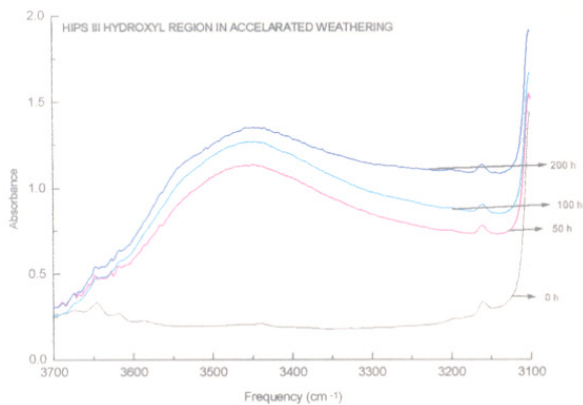
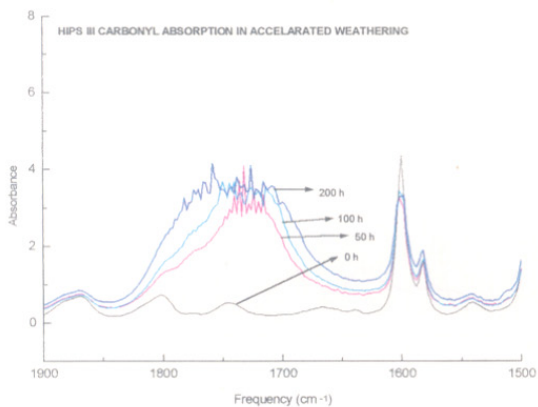


Figure 7.9 FT-IR Spectral changes of HIPS III films in carbonyl and hydroxyl region for various time interval exposed in accelerated weathering

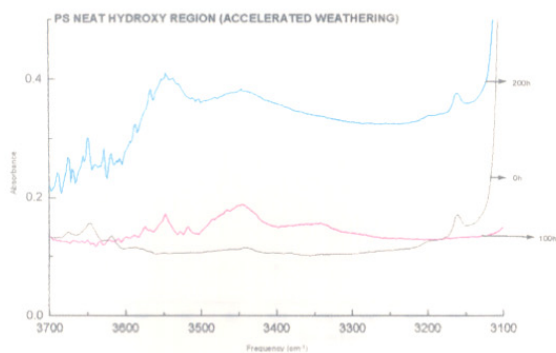
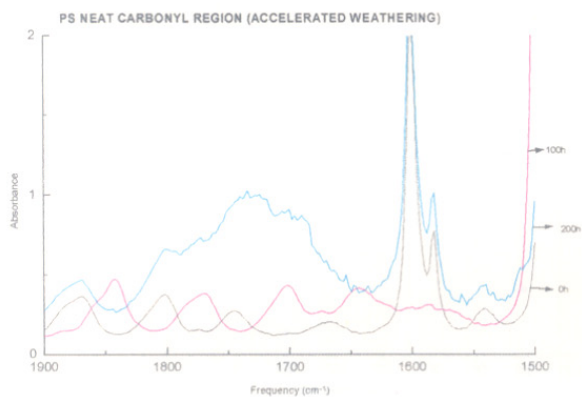


Figure 7.10 FT-IR Spectral changes of PS films in carbonyl and hydroxyl region for various time interval exposed in accelerated weathering

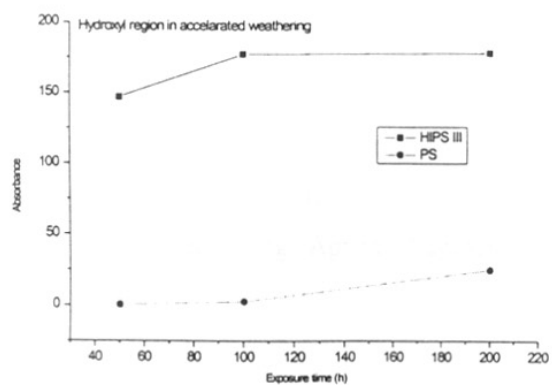
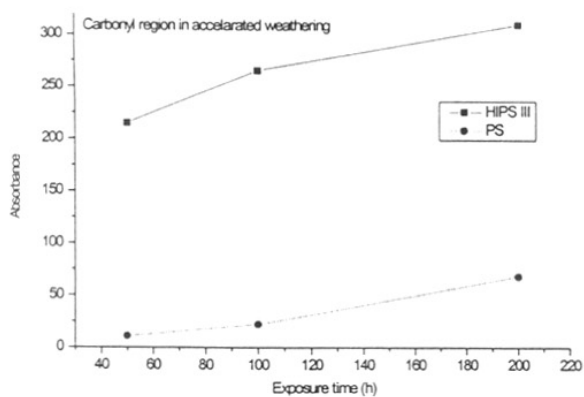


Figure 7.11 Rate of carbonyl and hydroxyl groups formation in HIPS III and PS films in accelerated weathering

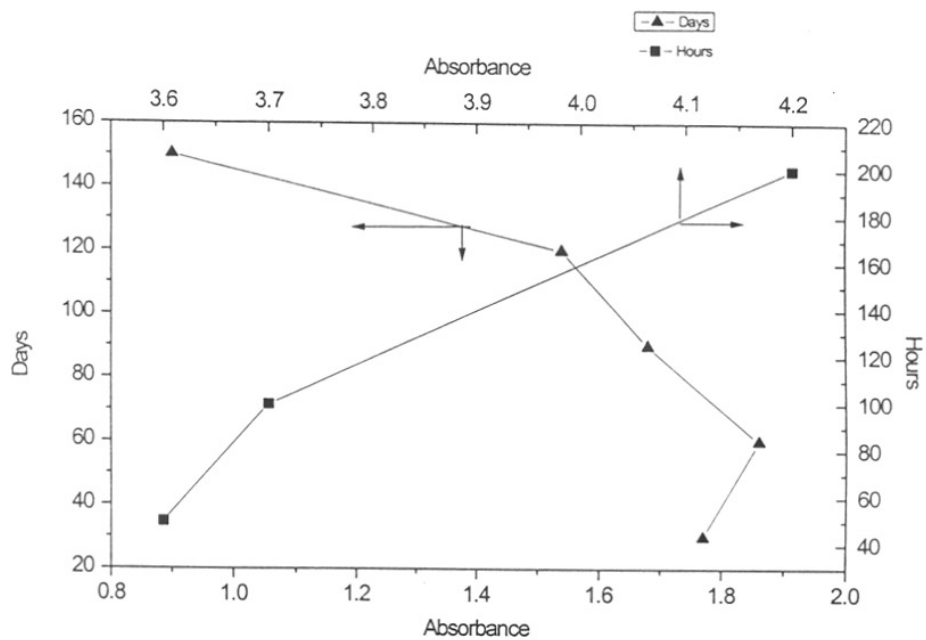


Figure 7.12 FT-IR carbonyl group absorbance at 1725 cm^{-1} under accelerated and natural weathering of HIPS III films at various times (natural weathering (April to August))

Table 7.1 Natural weathering of styrenic copolymers

Month	HIPS 8350	HIPS 7240	HIPS	PS
	CODE	CODE	CODE	CODE
April	83-1	72-1	HI-1	PS-1
May	83-2	72-2	HI-2	PS-2
June	83-3	72-3	HI-3	PS-3
July	83-4	72-4	HI-4	PS-4
August	83-5	72-5	HI-5	PS-5
September	83-6	72-6	HI-6	PS-6
October	83-7	72-7	HI-7	PS-7
November	83-8	72-8	HI-8	PS-8
December	83-9	72-9	HI-9	PS-9
January	83-10	72-10	HI-10	PS-10
February	83-11	72-11	HI-11	PS-11
March	83-12	72-12	HI-12	PS-12

7.5 References

1. A. Davis, "*The weathering of polymers*", in *Developments in polymer degradation-I* (N. Grassie. Ed.), Applied Science Publisher, London, 1977
2. N. Khraishi, Amin Al- Robaidi, *Polym. Degrd and Stab.*, **32**, 105 (1991)
3. Alfonso J. Chirinos-Padron, *Polym. Degrd and Stab.*, **29**, 49 (1990)
4. M. Trojan, A. Daro, R. Jacobs, C. David, *Polym. Degrd and Stab.*, **28**, 275 (1990)
5. R. Mani, R.P. Singh, S. Sivaram, *Polymer Intern.*, **44**, 137 (1997)
6. Y. Israeli, J. Lacoste, J. Lemaire, R.P. Singh, S. Sivaram, *J. Polym. Sci., Polym. Chem. Ed.*, **32**, 485 (1994)
7. J. Lemaire, R. Arnaud, J.L. Gardette, *Rev. Gen. Cautch. Plast.*, **87**, 613 (1981)
8. Ly Tang, D. Sallet, J. Lemaire, *Macromolecules*, **15**, 1437 (1981)
9. R.P. Singh, R.A. Raj, A. Vishwa Prasad, S. Sivaram, J. Lacoste, J. Lemaire, *Polym. Inter.*, **36**, 309 (1995)
10. B. Mailhot, J.L. Gardette, *Macromolecules*, **25**, 4127 & 4129 (1992)

CHAPTER VIII

**PHOTOSTABILIZATION OF HIGH IMPACT POLYSTYRENE BY
HINDERED AMINE LIGHT STABILIZERS (HALS)**

8.0 INTRODUCTION

Most commercially available polymers are stabilized against thermal and photo-oxidative degradation with small molecules. This is achieved by blending the polymer with appropriate stabilizers, which ensure that the desirable polymer properties are maintained throughout its service life. For stabilization, Hindered Amine Light Stabilizers [HALS], UV absorbers, antioxidants, radical scavengers and pigments are used. For proper functioning of any additive, its chemical structure is also important. For longer stability of polymer, the stabilizer must remain in its matrix in the active form. The effectiveness of long time stabilization depends not only on the chemical nature of the additive but also on their physical loss. The rate of the additive loss depends on the compatibility of the additive with the polymer and is controlled by its volatility, extractability, solubility and diffusion coefficient.¹⁻⁷ To improve all these properties, the additives should have higher molecular weight or it should be bounded to the polymer substrate. To achieve the high molecular weight, the additive should be able to polymerize, copolymerize or graft onto the polymer substrate.

HALS are one of the most effective stabilizers for polymers which are attracting world wide scientific and industrial interest. Low molecular weight HALS vaporize easily and have poor extraction resistance, and decrease their effectiveness.^{8, 9} Therefore, there has been a trend towards the use of polymeric HALS.^{10, 11} The stabilization of HIPS with various additives had been studied by several workers.¹²⁻¹⁷

Kulich and Wokowicz¹⁸ explained stabilization of HIPS for the additives like thiodipropionate, phosphite and phenolic antioxidants with SEM and X-ray energy-dispersive spectrometry (XEDS). Lee et al.¹⁹ have studied the polystyrene (PS) stabilization with polymeric styrene-2,2,6,6-tetramethyl piperidiny methacrylate stabilizer. They have studied the ABS/SBS stabilization also. The high efficiency of HALS as inhibitors of polymer photo-oxidation is considered to be determined primarily by a complex set of reactions involving the scavenging of active alkyl and peroxy radicals formed during the oxidation.²⁰⁻³¹

The stabilization mechanism of HALS has been studied in both the solid state as well as in the solution of the polymer. The bimolecular rate constants of the reactions of alkyl radicals with nitroxides to form amino ethers in solvents are generally high. (ca. 10^7 - 10^9 $M^{-1}S^{-1}$).³²⁻³⁴ In the solid polymers the rate of scavenging of alkyl radicals associated with the polymer is probably controlled only by molecular diffusion of the nitroxide. The peroxy radicals are known to be much less reactive than alkyl radicals in the reaction with nitroxides, therefore, nitroxide scavenging of peroxy radicals is not considered as an important reaction in the stabilization of polymers by HALS.

At the given external conditions, the volatility of a stabilizer is determined mainly by its molecular characteristics, but the rate of evaporation from a polymer matrix is strongly influenced by diffusion process.³⁵ The rate of diffusion of small molecules in polymers is governed by the mobility of both the penetrant and the polymer chains. The size and shape of the diffusing material is determined by the magnitude and distribution of free volume in the polymer.³⁶⁻⁴¹ The small molecules transport in polymers takes place in the amorphous phase only. Therefore, the behavior of small molecules can be described by a two-phase model assuming an impermeable crystalline and a permeable amorphous phase. Thus the penetration rate of small molecules depends on the amount of the free volume in the polymer. The structure of the polymer also determines the diffusion of long-chain molecules (longer than 30 CH_2 units) in amorphous region.

The solubility of small molecules in polymers is determined by the free volume of the polymer, the size and shape of the penetrant and the polymer-polymer as well as polymer-additive interaction.^{42, 43, 44}

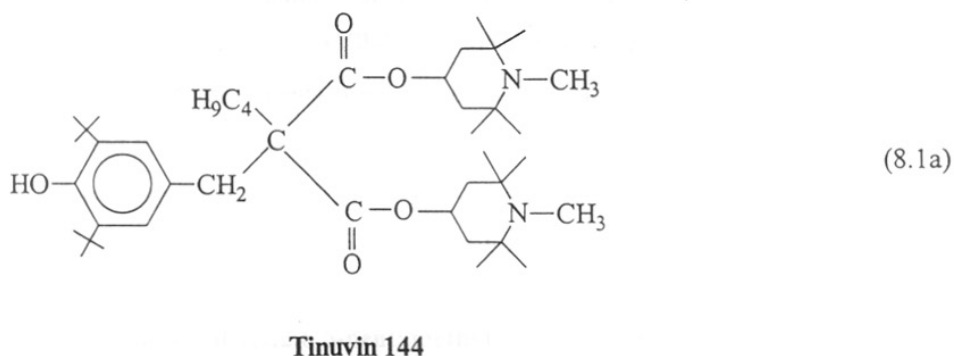
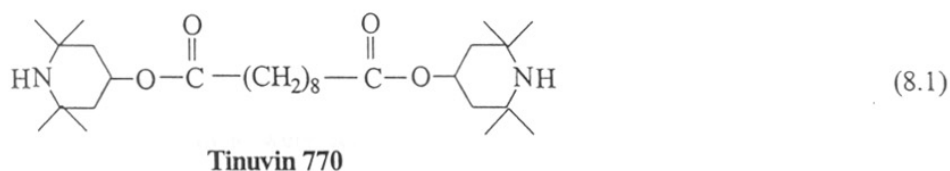
The present chapter deals with the stabilization of HIPS with polymeric HALS. The diffusibility and solubility of polymeric HALS in HIPS matrix were also studied.

8.1 EXPERIMENTAL PROCEDURE

8.1.1 Materials

Styrene was washed with 10% aqueous sodium hydroxide to remove t-butyl catechol, then washed with water and dried over CaH_2 for overnight and distilled

before use. Maleic anhydride was purified by recrystallization from chloroform and dried under vacuum. AIBN was recrystallized from methanol and dried under vacuum. DMF was dried over CaH_2 and distilled. 2,2,6,6-tetramethyl-4-piperidinol, 4-amino-2,2,6,6-tetramethyl piperidine, 4-dimethyl amino pyridine (4-DMAP) and Montmorillonite K10 clay was obtained from Aldrich Chemicals, USA and used as received. HIPS 8350 and PS were obtained from Elf-Atochem, France and used as received. The conventional HALS, namely bis(2,2,6,6-tetramethyl-4-piperidinyl)sebacate (Tinuvin 770) (white crystals) and 2-tert-butyl-2-(4-hydroxy 3,5-di-tert-butyl benzyl) [bis(methyl-2,2,6,6-tetramethyl-4-piperidinyl)]dipropionate (Tinuvin 144) (white powder) obtained from M/s Ciba-Geigy were used as received (structures 8.1 and 8.1a).



8.1.2 UV irradiation

All samples were photo-irradiated in SEPAP 12/24 as described in section 4.2.3 in chapter IV.

8.1.3 Scanning electron microscope

The films were examined by scanning electron microscope (Leica Cambridge Stereoscan 440 model) for morphological changes. 1 wt-% of light stabilizers such

as polymeric SMAN-g-1,2,2,6,6-pentamethyl-4-piperidinol (AVP-59), high mol. wt. polymeric SMAN-g-4-amino-2,2,6,6-tetramethyl piperidine (AVP-40), high mol. wt. polymeric SMAN-g-2,2,6,6-tetramethyl-4-piperidinol (AVP-49), Tinuvin 144 and Tinuvin 770 were melt blended in HIPS matrix. The UV exposed films were placed in stoppered bottles containing osmium tetroxide (2 % aqueous) and allowed to stand for 48 h. The films were washed with water and dry ethanol. The stained samples dried under vacuum for 24 h at 50°C. The gold coated samples were examined under electron microscope.

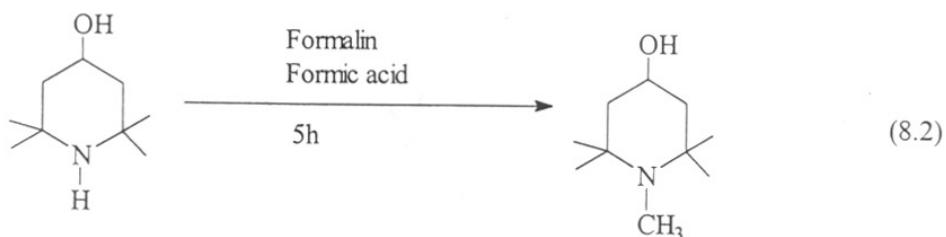
8.2 ANALYSIS

Styrene-maleic anhydride copolymer and polymeric light stabilizers were characterized by IR Shimadzu 180 model and FT-IR analysis was carried out with Perkin - Elmer 16 PC FT-IR instrument. UV analysis was performed by Hewlet Packard Model 5911 – Diode array UV spectrometer. Solid state CP/MAS ^{13}C -NMR spectra and ^1H -NMR were recorded with Bruker MSL-300 spectrometer using TMS as the internal standard. The molecular weight and molecular weight distribution of styrene-maleic anhydride copolymer was determined by Waters GPC-150 and GPC-II (AVP-37, AVP-43 and AVP-57) equipped with a refractive index detector. The measurements were carried out using μ -styrigel columns (10^3 , 500, 100 Å) and Pl gel columns of (10^4 , 10^3 , 500, 100 Å) pore size columns respectively, at ambient temperature (27°C) and THF as an eluent at a flow rate of 1.0 mL/min. The GPC curves were analyzed with the calibration curve obtained by PS standards.

8.3 Synthesis of 1,2,2,6,6-pentamethyl-4-piperidinol

2,2,6,6-tetramethyl-4-piperidinol (3.55 g, 0.02 mol), 37 % formalin (3.3 mL) and 1 mL formic acid were taken in a 250 mL round bottom flask fixed with a reflux condenser. The contents were heated over a steam bath for 5h. The reaction mixture was made basic using 10M potassium hydroxide and the product was extracted with ether (3×100 mL), and dried over anhydrous potassium carbonate. The ether extract was evaporated to get the product, which was purified by sublimation at 88°C under reduced pressure (0.05 mm). The white sublimate weighed 3.5 g. (Equation 8.2) (Yield 92 %, m.p. 72-74°C, Lit: m.p. 73-74°C⁴⁵) The ^1H -NMR spectra recorded in

CDCl_3 [δ (ppm) 1.00 (s, a, 6H), 1.1 (s, e, 6H), 1.25-1.4 (t, a, 2H), 1.75-1.85 (dd, e, 2H), 2.45 (s, 3H(N-CH₃))].



8.4 Synthesis of styrene-maleic anhydride (SMAN) copolymer

In a 500 mL round bottom flask styrene, maleic anhydride, and AIBN were dissolved in dry DMF. Polymerization was carried out at 60°C for different intervals (Table 8.1) under argon atmosphere.

Table 8.1

<i>Expt. No.</i>	<i>AIBN</i> (g)	<i>DMF</i> (mL)	<i>Time</i> (h)
AVP-37	3.33	125	15.0
AVP-43	3.00	200	2.0
AVP-57	2.60	200	1.5

Styrene 10.4 g (0.1 mol), Maleic anhydride 9.806 g (0.1 mol), Temp = 60° C

The reaction mixture was precipitated from methanol, filtered and redissolved in methyl ethyl ketone and precipitated with methanol, filtered and then dried under reduced pressure at 60°C for 24h (Equation 8.3). IR spectra and ¹³C NMR spectra are shown in Figure 8.1 to 8.2. The number average mol.wt., weight average mol.wt and molecular weight distribution of styrene-maleic anhydride copolymers are given in Table. 8.2

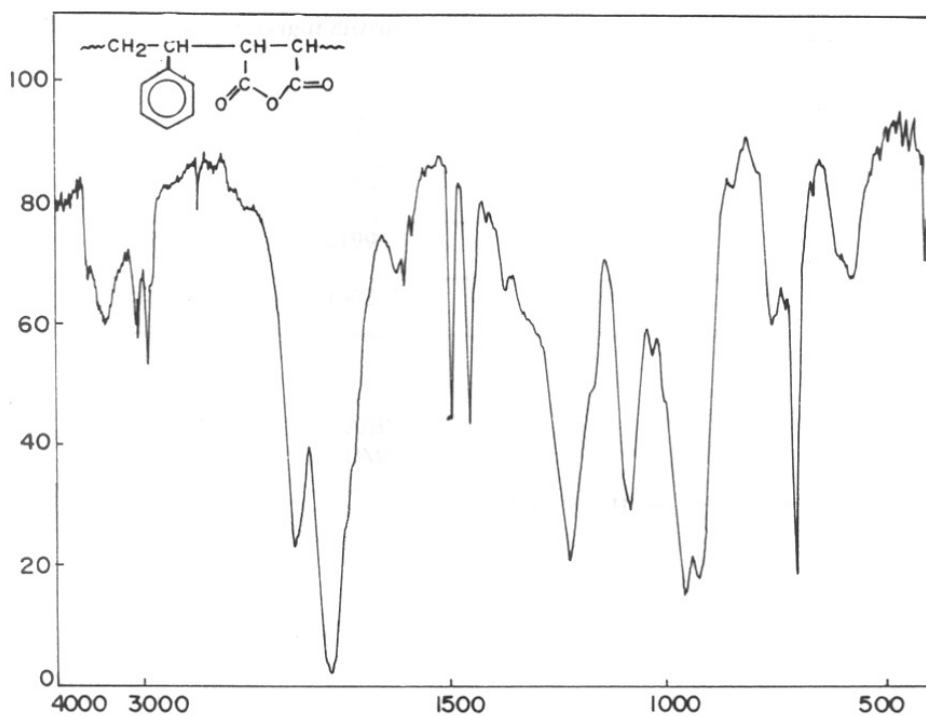


FIG.8.1:IR SPECTRA OF STYRENE MALEIC ANHYDRIDE COPOLYMER

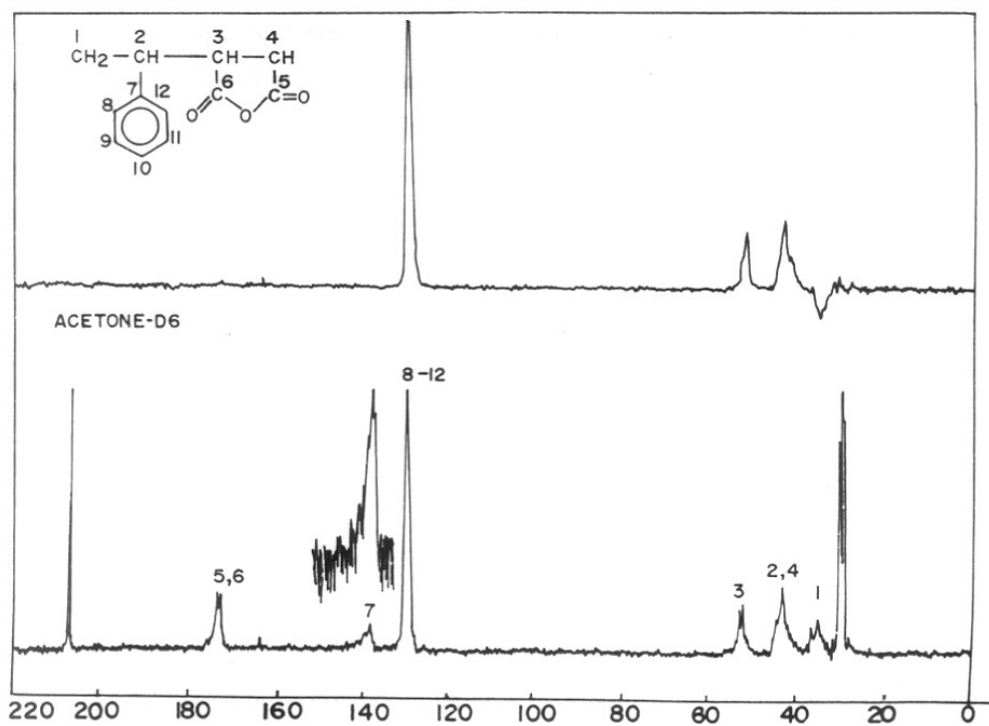
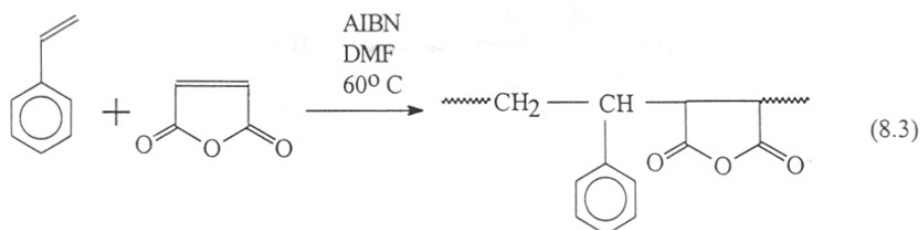
FIG.8.2: ^{13}C -NMR SPECTRUM OF STYRENE MALEIC ANHYDRIDE COPOLYMER

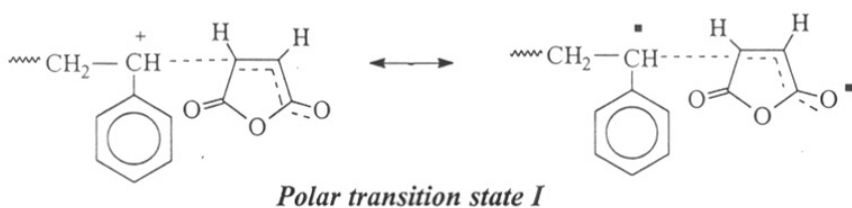
Table 8.2: Molecular weight distribution of styrene-maleic anhydride copolymer

<i>Expt. No.</i>	\bar{M}_n	\bar{M}_w	<i>MWD</i>
AVP-37	3654	7370	2.01
AVP-43	2199	5698	2.59
AVP-57	1662	2437	1.46

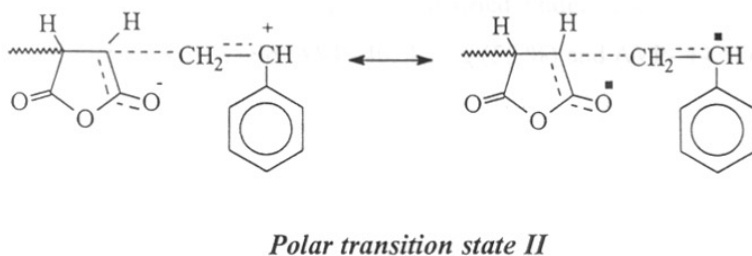


Mechanism:

Styrene and maleic anhydride forms alternating copolymers over all ranges of monomer feed ratios at moderate temperatures.^{46, 47} The alternating tendency in the copolymerization has been explained by two different mechanistic ways.⁴⁸ The first one assumes the presence of a transition state in which the electron poor maleic anhydride accepts charge from the electron rich styrene donor.^{49, 50} This can occur when either monomer is present at the growing end of the macro radical thereby leading to either polar transition state I or II (Equation 8.4):



(8.4)



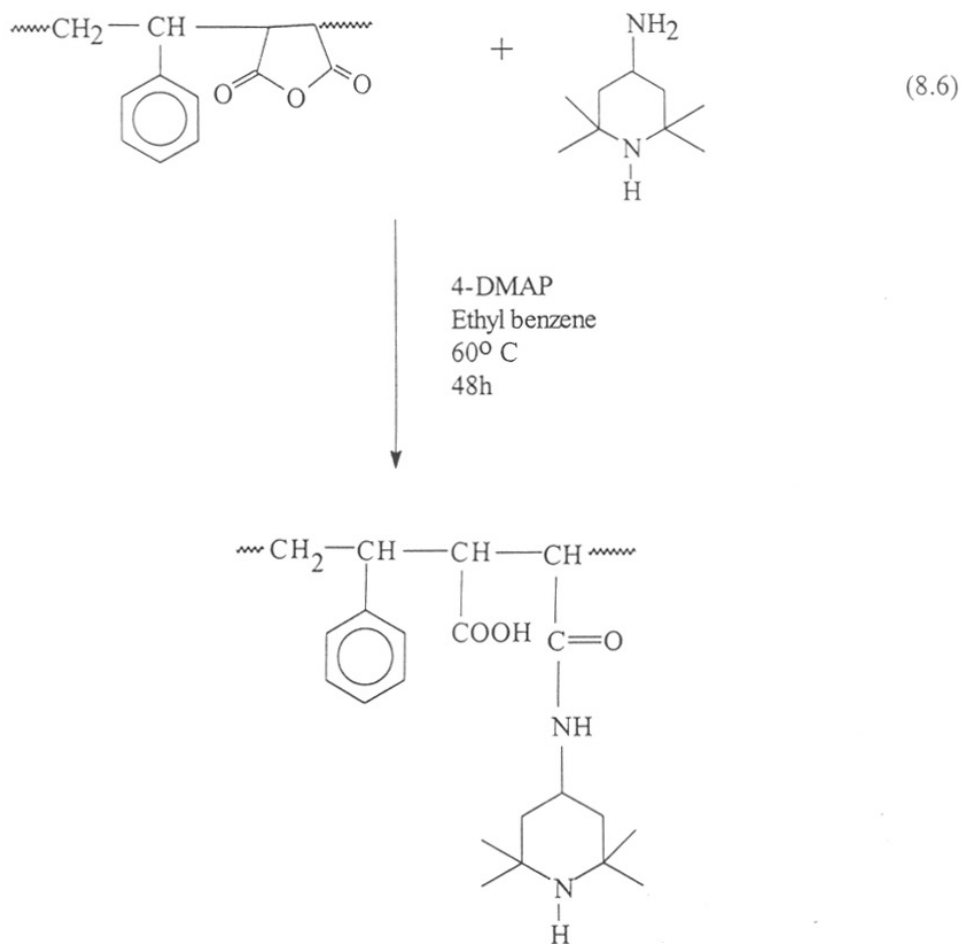
The second explanation observed for these alternating copolymers attributes this phenomenon to the addition of the growing chain radical to a styrene-maleic anhydride charge-transfer complex.^{51, 52} In this an equilibrium exists between styrene, an electron donor (D) and maleic anhydride, an electron acceptor (A) to form styrene-maleic anhydride charge transfer complex (Equation 8.5):



Brown and Fujimori^{53, 54} described that the styrene-maleic anhydride radical copolymerization by the polar transition states model via a strong penultimate effect.

8.5 Synthesis of low & high mol.wt. polymeric SMAN-g-4-amino-2,2,6,6-tetramethyl piperidine

In a 500 mL round bottom flask 150 mL of ethylbenzene was taken in which 3g (0.01 mol) styrene-maleic anhydride copolymer, 4.6 mL (0.02 mol) of 4-amino-2,2,6,6-tetramethyl piperidine and 190 mg of 4-DMAP were added. To this reaction mixture 1 mL of glacial acetic acid was added dropwise for 5 min and the reaction was carried out for 48h at 60°C under argon atmosphere. The reaction mixture was precipitated from methanol, filtered and dried under reduced pressure for 24h at 60°C (Equation 8.6). Yield: AVP-40: 4.15 g (55 %) and AVP- 44: 4.62 g (61.4 %)



The high mol.wt. polymeric SMAN-g-4-amino-2,2,6,6-tetramethyl piperidine (AVP-40) had been characterized by IR spectra and solid state CP/MAS ^{13}C -NMR spectra are showed in.Figure. 8.3b and 8.4.

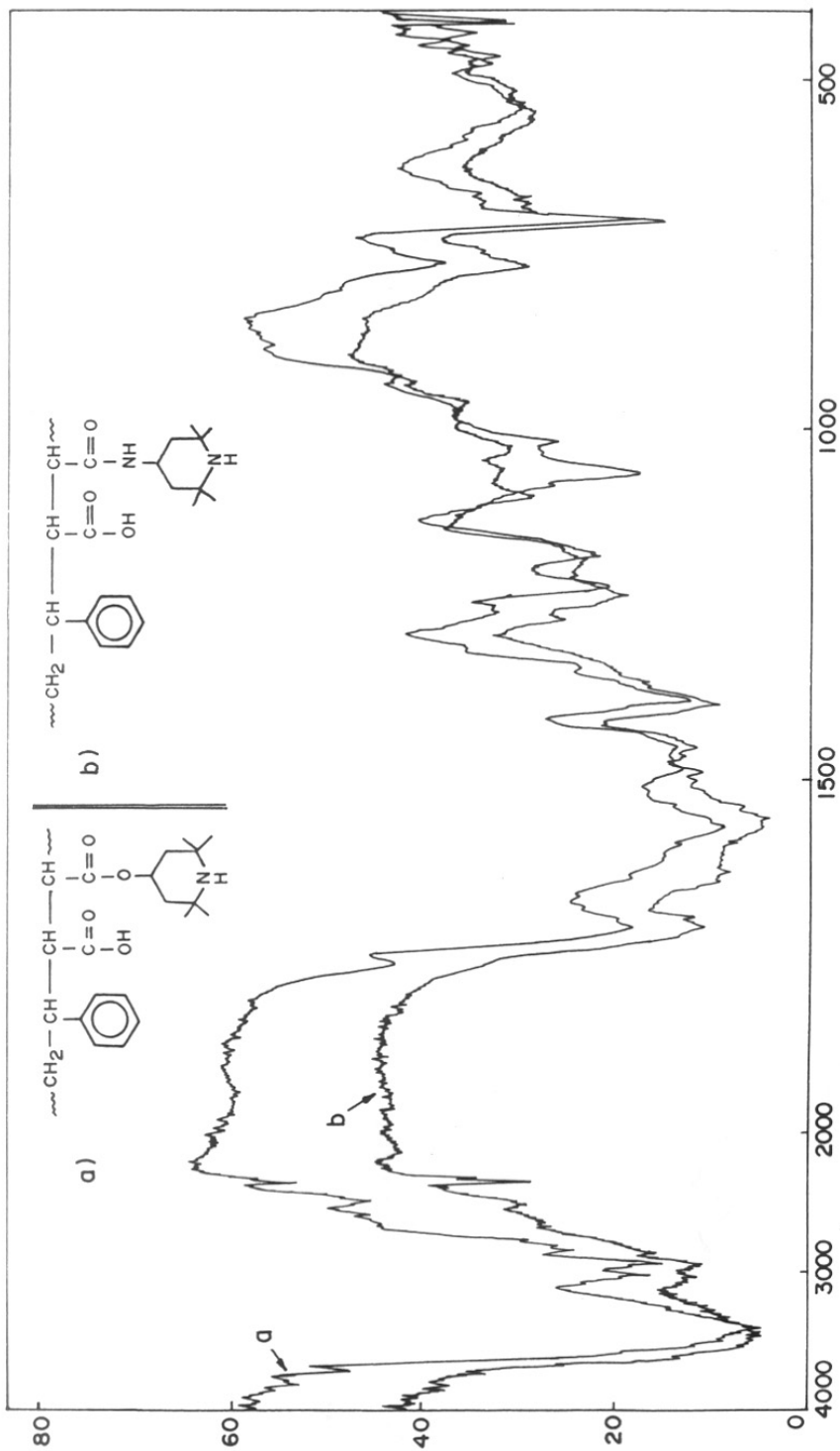


FIG.8.3:IR SPECTRA OF HIGH MOL. WT. POLYMERIC SMAN-g-2,2,6,6-TETRAMETHYL-4-PIPERIDINOL (AVP-49) AND^bSMAN-g-4-AMINO 2,2,6,6-TETRAMETHYL PIPERIDINE (AVP-40).

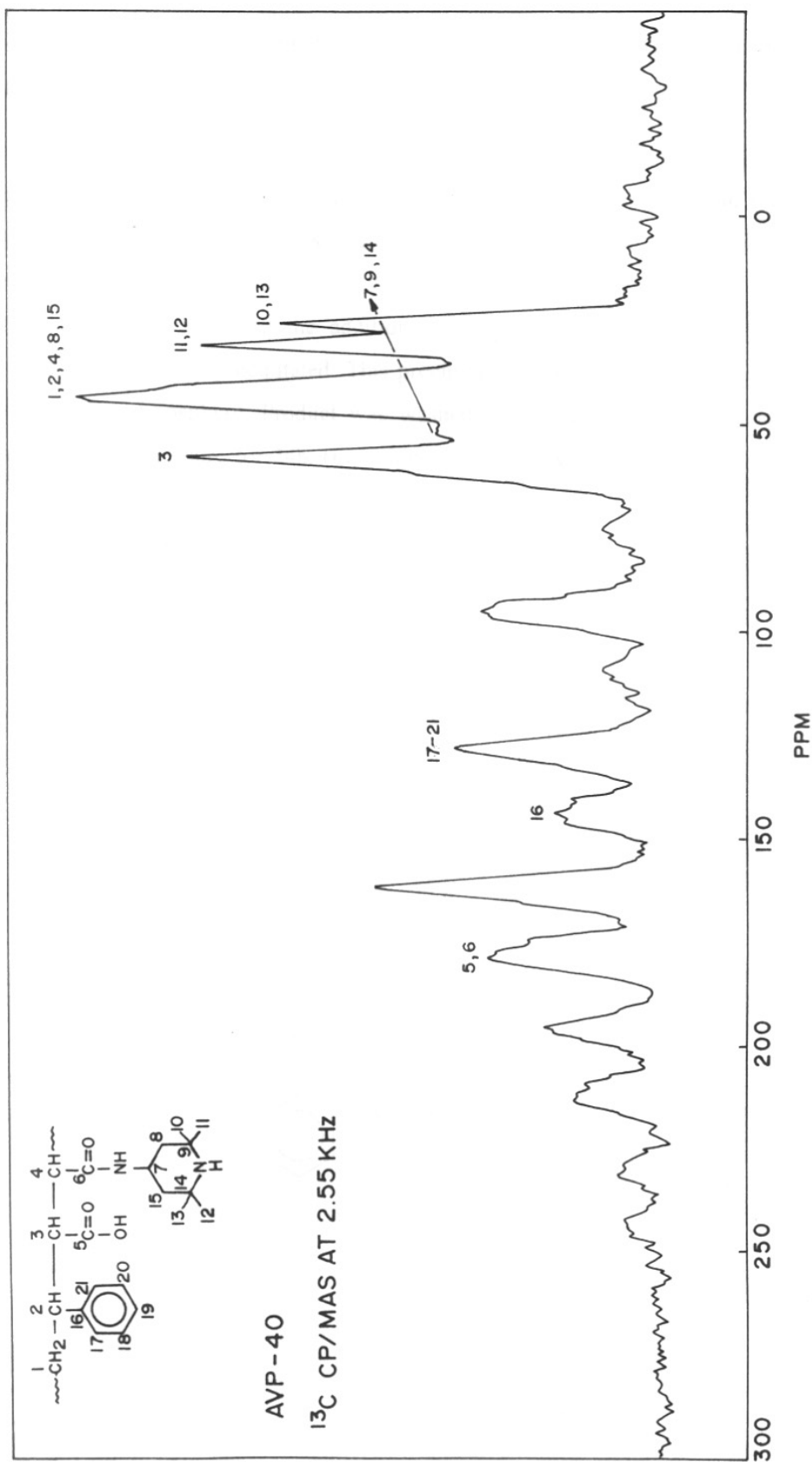
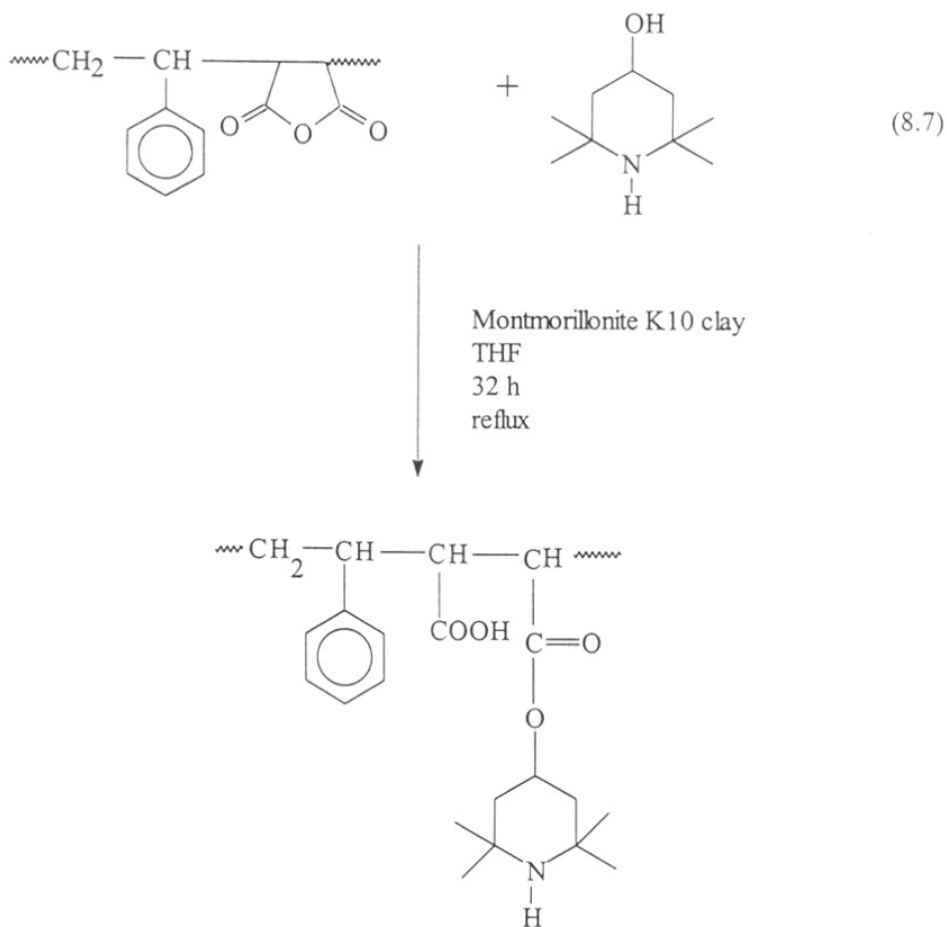


FIG.8.4: SOLID STATE CP / MAS ^{13}C -NMR SPECTRA OF HIGH MOL. WT. POLYMERIC SMAN - g - 4 - AMINO - 2,2,6,6 -
 TETRAMETHYL PIPERIDINE (AVP - 40)

8.6 Synthesis of low & high mol.wt polymeric SMAN-g-2,2,6,6-tetramethyl-4-piperidinol

In a 500 mL round bottom flask, 2.5 g (0.01 mol) of styrene-maleic anhydride copolymer was dissolved in 200 mL THF and 150 mg of montmorillonite K10 clay was added as catalyst. To this reaction mixture 3.89 g (0.02 mol) of 2,2,6,6-tetramethyl-4-piperidinol (dissolved in 50 mL THF) was added dropwise to the solution for 15 min. With the addition of 2,2,6,6-tetramethyl-4-piperidinol, the reaction mixture was precipitated. This precipitated mixture was refluxed for 32 h under argon atmosphere. Product was washed with n-hexane, filtered and dried under reduced pressure for 24h. (Equation 8.7) Yield: AVP – 49: 3.85 g (60.3 %), AVP – 50: 3.67 g (60 %)

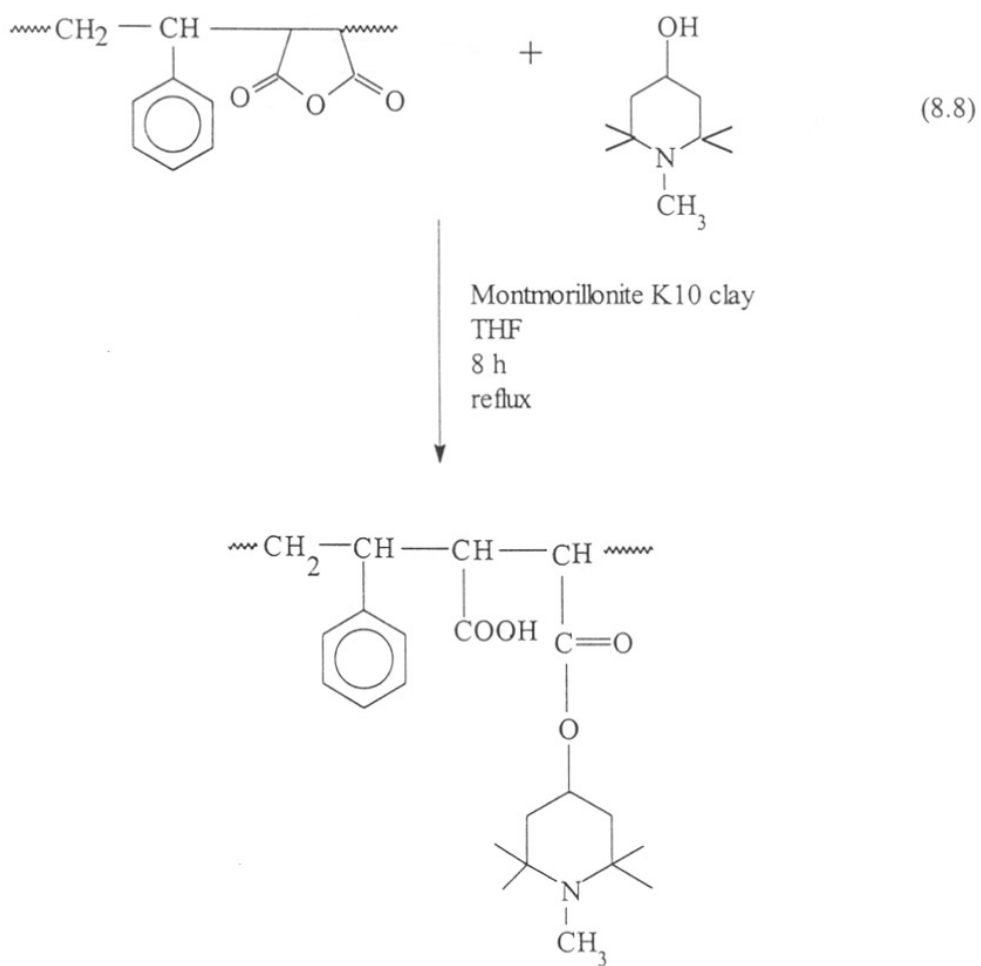


The high mol.wt. polymeric SMAN-g-2,2,6,6-tetramethyl-4-piperidinol (AVP-49) was characterized by IR spectra and solid state CP/MAS ^{13}C -NMR spectra are shown in Figures. 8.3a and 8.5, respectively.

8.7 Synthesis of polymeric SMAN-g-1,2,2,6,6-pentamethyl-4-piperidinol (AVP-59)

In a 500 mL round bottom flask, 2.5 g (0.01 mol) styrene-maleic anhydride copolymer was dissolved in 200 mL THF in which 150 mg of montmorillonite K10 clay was added as catalyst. To this reaction mixture, 4.104 g (0.02 mol) 1,2,2,6,6-pentamethyl-4-piperidinol (dissolved in 50 mL of THF) was added dropwise for 15 min. With the addition of 1,2,2,6,6-pentamethyl-4-piperidinol the reaction solution was precipitated. The precipitated mixture was refluxed for 8 h under argon atmosphere. Product was washed with n-hexane, filtered and dried under vacuum for 24 h (Equation 8.8). Yield: 4.15 g, (69 %)

This additive was characterized by FT-IR spectra, DSC thermograms and ^{13}C -NMR spectra are shown in Figures. 8.6 to 8.8.



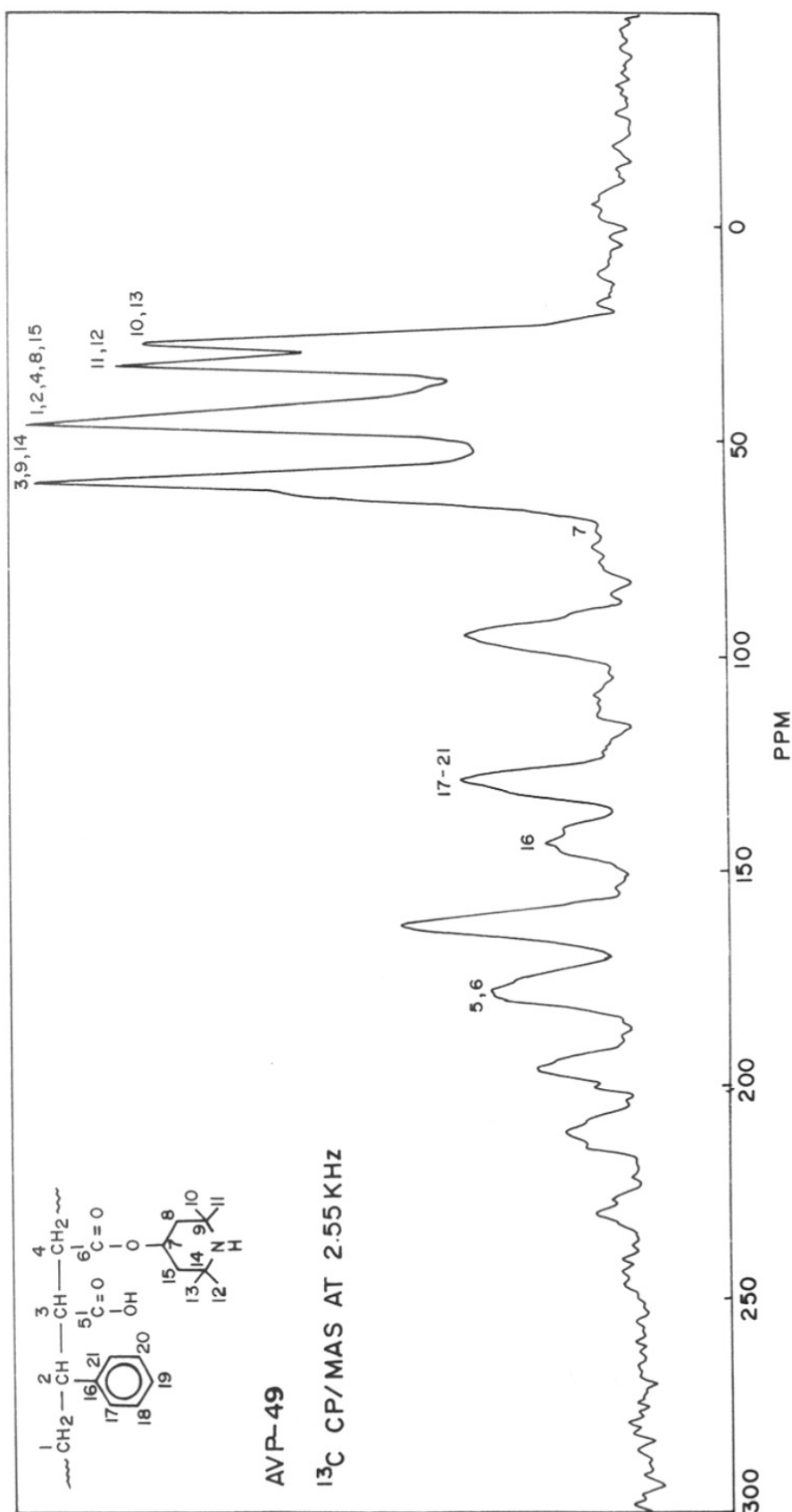


FIG. 8.5: SOLID STATE CP/MAS ^{13}C -NMR SPECTRA OF HIGH MOL. WT. SMAN-g-2,2,6,6-TETRAMETHYL-PIPERIDINOL - (AVP-49)

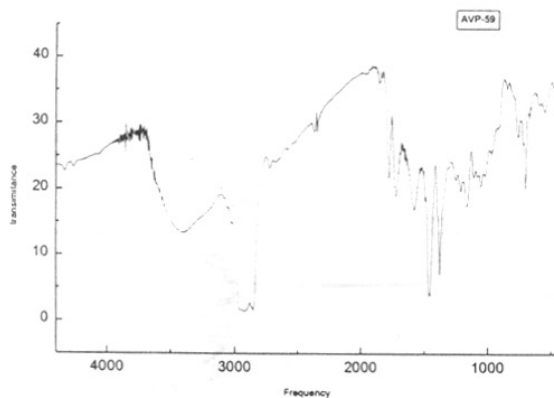


Fig. 8.6 IR spectrum of polymeric SMAN-g-1,2,2,6,6-penta methyl-4-piperidinol (AVP-59)

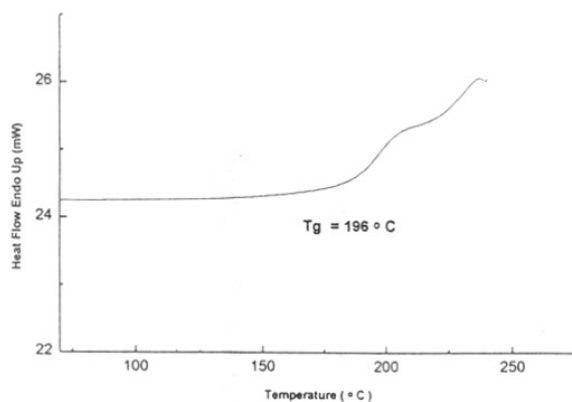


Fig. 8.7: DSC thermogram of polymeric SMAN-g-1,2,2,6,6 penta methyl-4-piperidinol (AVP-59)

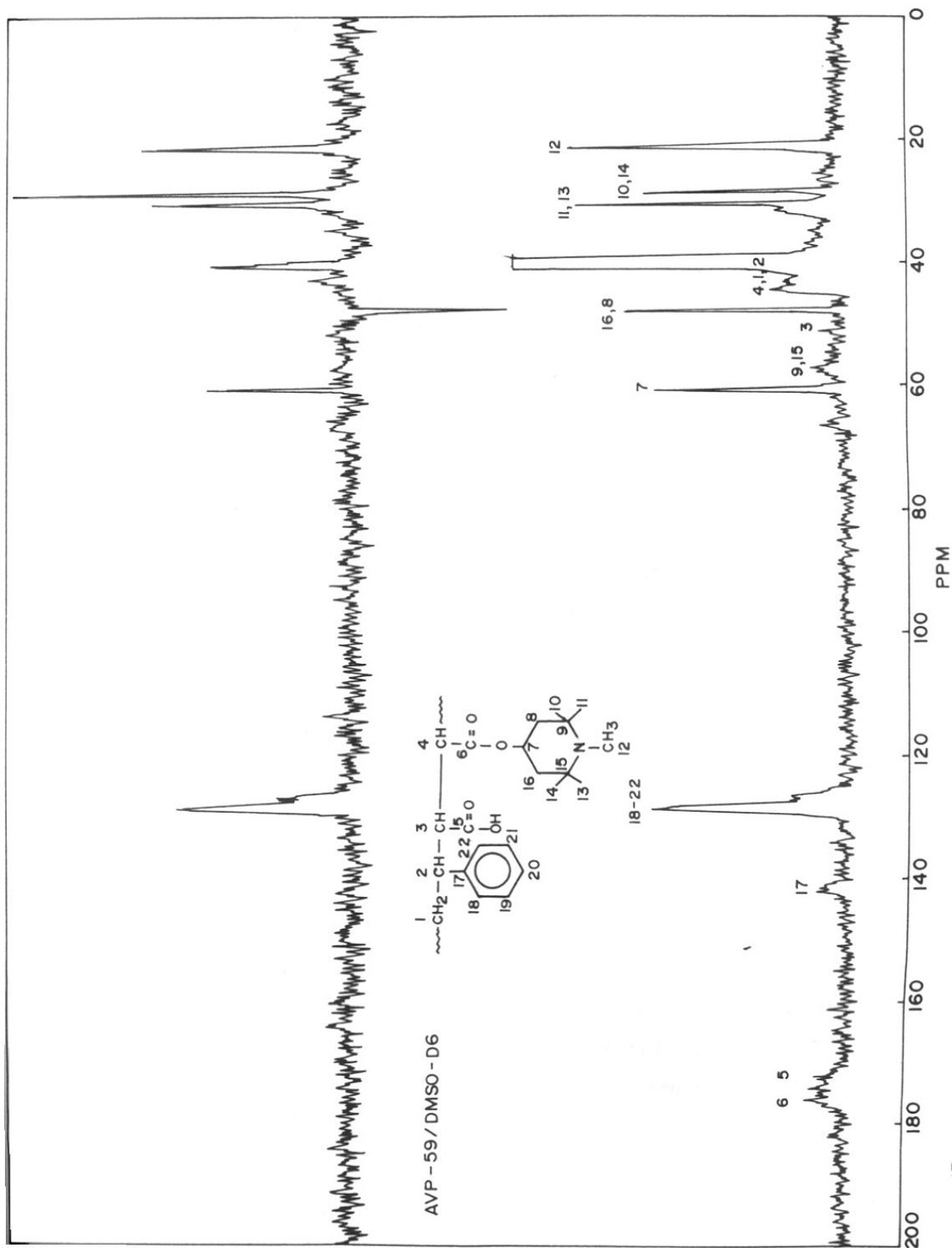
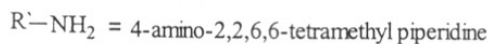
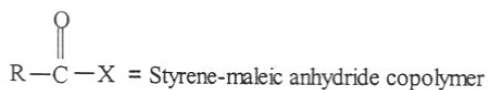
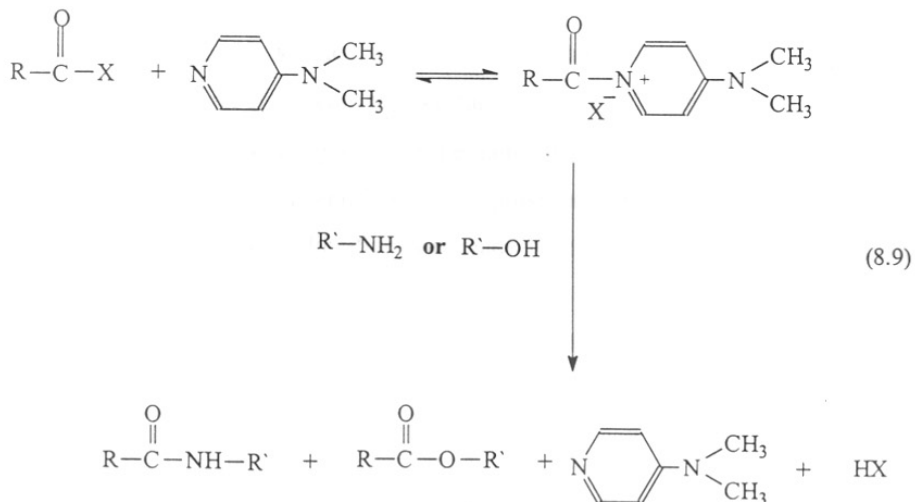


FIG.8.8: ¹³C-NMR SPECTRA OF POLYMERIC SMAN-g-1,2,2,6,6- PENTA METHYL - 4- PIPERIDINOL (AVP - 59)

Mechanism:

Since 4-DMAP is a strong nucleophile⁵⁵ it follows the nucleophilic mechanism. The nucleophilic mechanism is⁵⁶ (Equation 8.9):

**8.8 Mixing of polymeric HALS**

A concentration of 0.2, 1 and 2 wt-% of conventional hindered amine light stabilizers (i.e. Tinuvin 770 and Tinuvin 144) and polymeric SMAN-g-HALS stabilizers were mixed into HIPS and PS polymers by melt blending in a minimax mixer at 200° and 250°C for 4 min, respectively, and then extruded. Thin films (~100 μ) were prepared in quench cooling with a Carver press at 200°C for 4 min.

8.9 Diffusion Measurement

Diffusion measurements were carried out using the system described by Roe et al.⁵⁷ A stack of 30 additive-free polymer films was placed between additive source. Additives (2 wt-%) were melt blended [Tinuvin 770, Tinuvin 144 and SMAN-g-1,2,2,6,6-pentamethyl-4-piperidinol (AVP-59)] in HIPS at 250°C for 2min. This air bubble free additive film was kept at the bottom of the film stack. These films were kept in a vacuum oven at constant temperature [Tinuvin 770 and Tinuvin 144, 65°C for 48 and 100 h, and SMAN-g-1,2,2,6,6-pentamethyl-4-piperidinol (AVP-59), 60°C for 120 h]. The additive concentration in the polymer film was determined directly by UV spectroscopy. The calibration was made with HIPS neat film. The additive concentration was determined in DMSO solution at 264 nm in UV absorption. To avoid error caused by the additive adsorbed on the surface contacting the additive source, concentration of the film next to the additive source was not used in the calculation.

The diffusion coefficient was determined using the principle given by Moisan.^{5,7} This method treats the process as a one-dimensional diffusion problem. It is assumed that at the start of the experiment ($t = 0$) the additive concentration ($C = 0$) at any distance from the additive source ($x > 0$) and that during the experiment ($t > 0$) concentration of the additive in the additive source ($x \leq 0$) remains constant and equals the solubility ($C = S$). The concentration at position x and time t is described by

$$C(x,t) = S [1 - \text{erf}(x/K)]$$

where K is determined by the time and the diffusion coefficient (D) and can be given by

$$K = 2(Dt)^{1/2}$$

For calculation of the parameters D and S from the concentration profile, an interactive least-squares curve-fitting programme was used. The solubility is given directly by this calculation.

8.10 RESULTS AND DISCUSSION

8.10.1 Performance evaluation of polymeric HALS stabilizers in high impact polystyrene

Diffusion of polymeric SMAN-g-1,2,2,6,6-pentamethyl-4-piperidinol

The solubility of additives is influenced by the specific volume and the physical state of the additives, the interaction between components as well as the strength of self-association of the dissolving molecules. The migration of the additive through a semi-crystalline polymer can be considered exclusively diffusive when the swelling ratio is sufficiently low and its driving force is wholly based on the concentration gradient.^{58, 59} The driving force is estimated from the chemical potential of the diffusant. The penetrant diffuses exclusively through the amorphous phase.^{60, 61}

Diffusion of a liquid in another homogeneous liquid is controlled macroscopically by the friction of the molecules.⁶² In unoriented semicrystalline polymers, a tortuosity factor also has to be taken into account, which represents the mechanical hindrance of the crystallites to the movement of the diffusant.⁵⁸ Orientation of the amorphous component is another parameter that also affects the sorption and diffusion of small molecules.

Figure 8.9 shows the concentration profile of SMAN-g-1,2,2,6,6-pentamethyl-4-piperidinol in a film stack of HIPS after at 60°C for 120 h. This additive is in amorphous nature. The solubility of additive in HIPS was determined by extrapolating method. The results show that the solubility of the additive is ~2 wt-% and the diffusion coefficient is $2.104 \times 10^{-14} \text{ mm}^2/\text{sec}$. The Tinuvin 770 and Tinuvin 144 have not shown any diffusion in HIPS at 65°C for 50 and 100 h. These additives are crystalline in nature, therefore, we did not observe the diffusion.

Dudler⁶³ had explained the high solubility of HALS (Tinuvin 770 and Chimassorb 944) compared to their HALS-NO in PP, HDPE, LDPE, LLDPE. In these stabilizers the conformations (boat, chair and twisted boat form) of the piperidine ring are known to change the polarity. Rozantsev⁶⁴ has measured the dipole moment for the 4-oxo-2,2,6,6-tetramethyl-piperidine-1-oxy (1.36 D) which agrees with a twisted form, but Aroney⁶⁵ reported the value 2.93 D for the same compound. Moreover, the

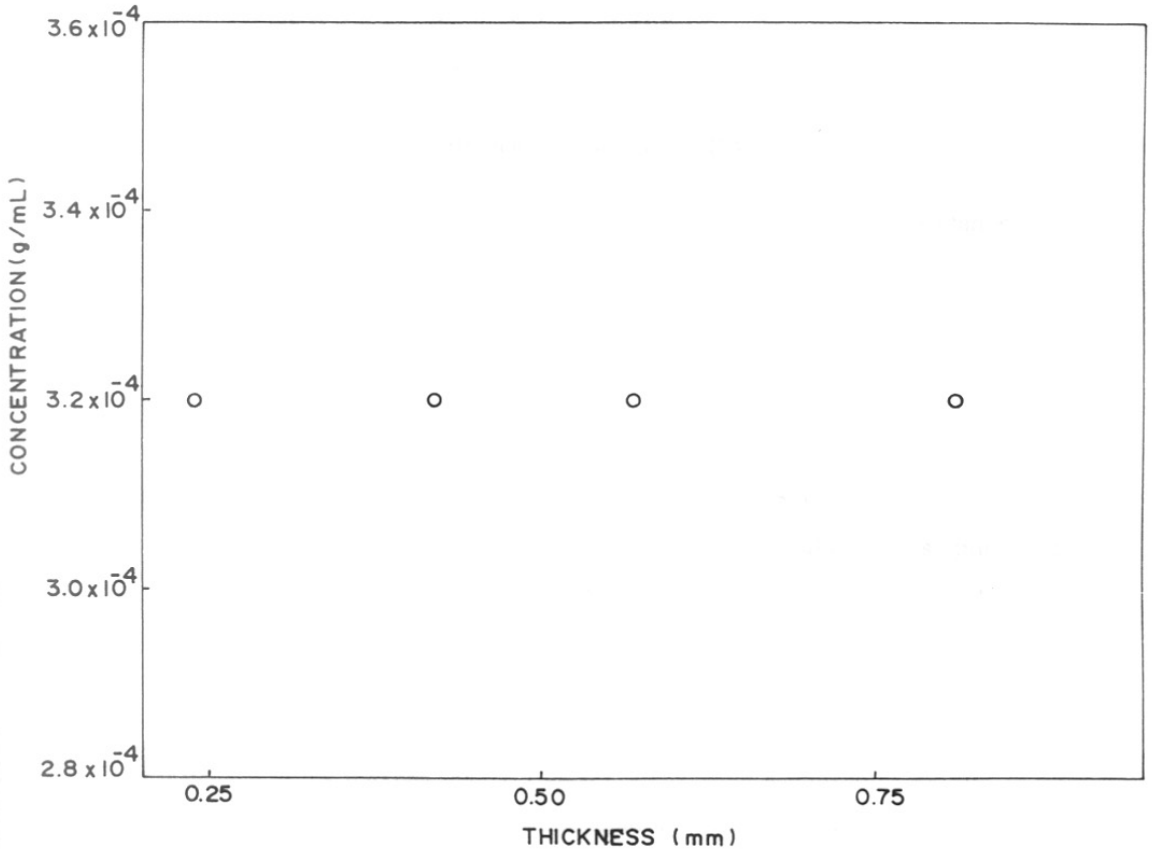


FIG.8.9: CONCENTRATION DISTRIBUTION OF POLYMERIC SMAN-g-1,2,2,6,6-PENTAMETHYL-4-PIPERIDINOL-IN HIPS 8350 COPOLYMER SAMPLES MEASURED AFTER DIFFUSION TIME 120h AT 60°C.

ester function in the para position could form an intramolecular hydrogen bond (N...H...O) with the amine when the piperidine is in a boat conformation, lowering its polarity.

The importance of additive solubility in relation to its diffusion coefficient suggests that solubility is not only the significant parameter for the physical loss of the stabilizer but this parameter is also important for the effective chemical reactions of the additive in polymer matrix.

8.10.2 Photostabilizing efficiency of polymeric HALS

Photostabilizing efficiency of polymeric SMAN-g-1,2,2,6,6-pentamethyl-4-piperidinol (AVP-59) and conventional stabilizers (i.e. Tinuvin 770 and Tinuvin 144) in HIPS were plotted in Figures. 8.10 and 8.11. The efficiency of light stabilizer measured in the form of carbonyl index (area under the peak 1630-1850 cm^{-1}) and hydroxyl index (area under the peak 3200-3700 cm^{-1}). The carbonyl absorption is maximum at 1720-1740 cm^{-1} . The hydroxyl absorption is maximum at 3420 cm^{-1} . The 1 wt-% concentration of the light stabilizer showed very better performance in HIPS. The neat HIPS film showed carbonyl absorption with exposure time and the maximum absorption was observed at 200 h UV exposure. Among these stabilizers, the carbonyl absorption is maximum with Tinuvin 144. The polymeric SMAN-g-1,2,2,6,6-pentamethyl-4-piperidinol stabilizer is amorphous in nature and highly compatible with the polymer backbone, therefore, is well dispersed in the polymer matrix. Hence it gives better stabilization and due to this reason the carbonyl absorption is comparatively less. The stabilizing efficiency of polymeric HALS is more than conventional additives only after 100 h irradiation. This is probably due to the decreased homogeneity of conventional additives active moieties throughout the polymer matrix as these are more concentrated to one place only, leaving other parts of polymer matrix unprotected.

The concentration of polymeric HALS stabilizer (AVP-59) does not contribute much to the photostabilization of HIPS. The 0.2 to 2.0 wt-% concentration also showed similar stabilization effect. The carbonyl and hydroxyl absorptions are very less at 50 h and the maximum at 200 h. (Figures. 8.12 and 8.13). The carbonyl and hydroxyl absorption of conventional HALS (Tinuvin 770 and Tinuvin 144) are

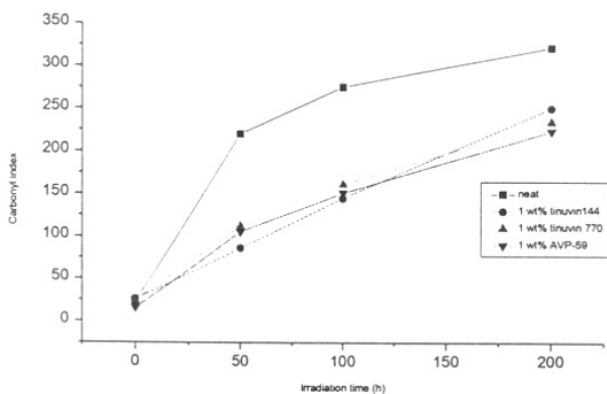


Fig. 8.10: Plot of carbonyl index vs irradiation time in HIPS films stabilized with various light stabilizers

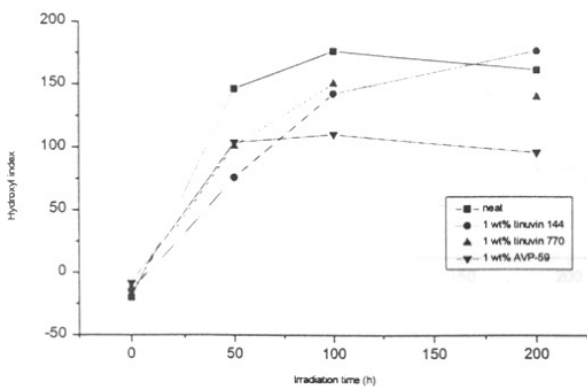


Fig. 8.11: Plot of hydroxyl index vs irradiation time in HIPS films stabilized with various light stabilizers

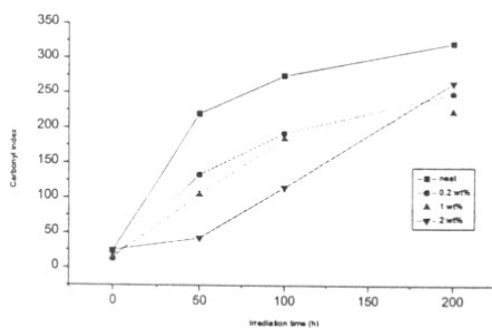


Fig. 8.12: Plot of carbonyl index vs irradiation time in HIPS films stabilized with polymeric SMAN-g-1,2,2,6,6-pentamethyl-4-piperidinol (AVP-59)

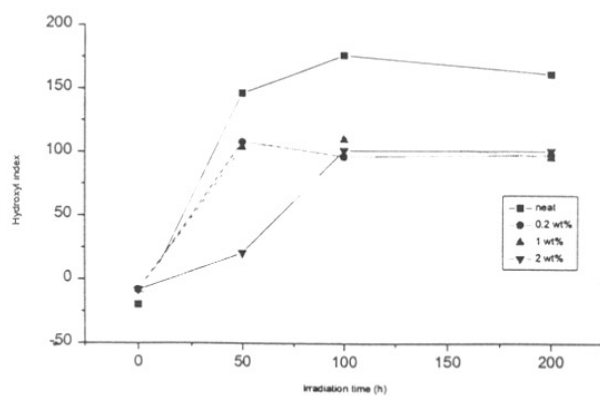
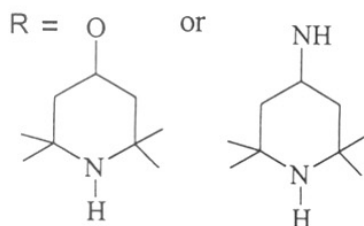
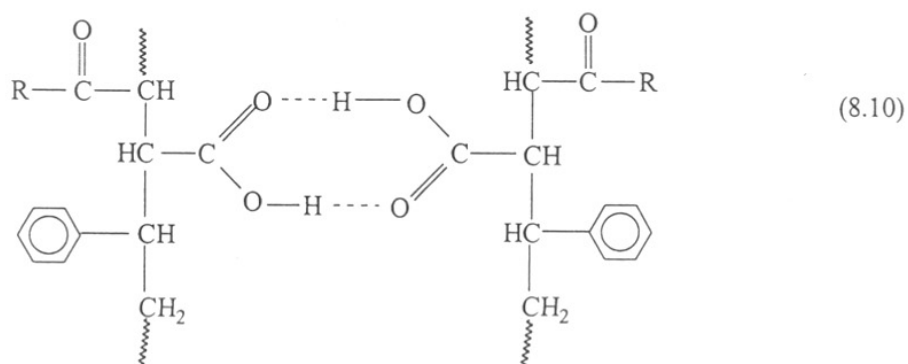


Fig. 8.13: Plot of hydroxyl index vs irradiation time in HIPS films stabilized with polymeric SMAN-g-1,2,2,6,6-pentamethyl-4-piperidinol (AVP-59)

shown in Figures. 8.14 to 8.17. Among these systems all concentrations of stabilizers showed similar stabilization performance. With these observations we can conclude that the stabilizer nature is much important than the concentration.

The polymeric low & high molecular weight. SMAN-g-4-amino-2,2,6,6-tetramethyl piperidiene and SMAN-g-2,2,6,6-tetramethyl-4-piperidinol stabilizers are not compatible with the HIPS and PS matrix. These stabilizers are forming an inter and intramolecular hydrogen bonding in the molecules. The intermolecular hydrogen bonding is (Equation 8.10):



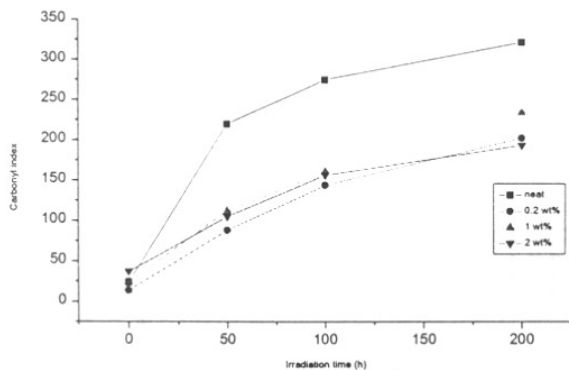


Fig. 8.14: Plot of carbonyl index vs irradiation time in HIPS films stabilized with Tinuvin 770 at different concentrations

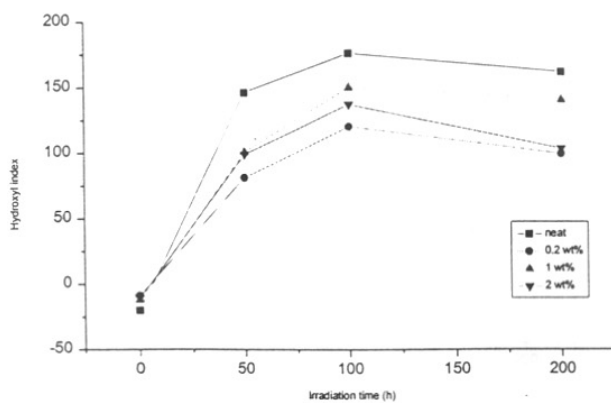


Fig. 8.15: Plot of hydroxyl index vs irradiation time in HIPS films stabilized with Tinuvin 770 at different concentrations

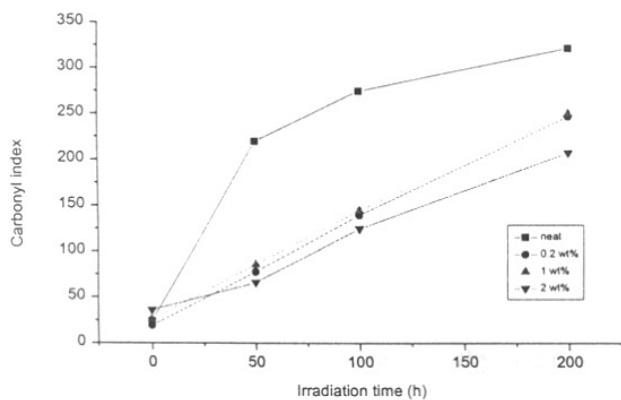


Fig. 8.16: Plot of carbonyl index vs irradiation time in HIPS films stabilized with Tinuvin 144 at different concentrations

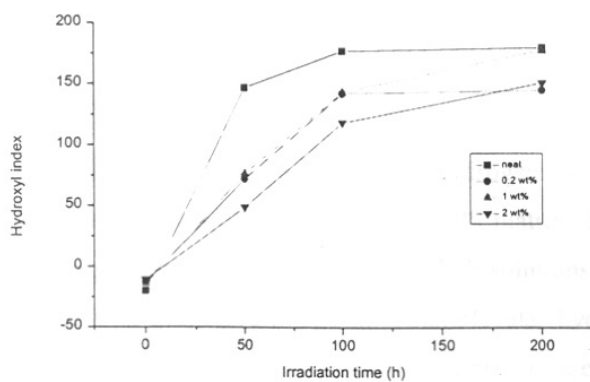
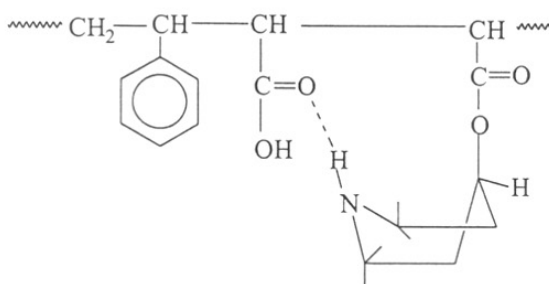
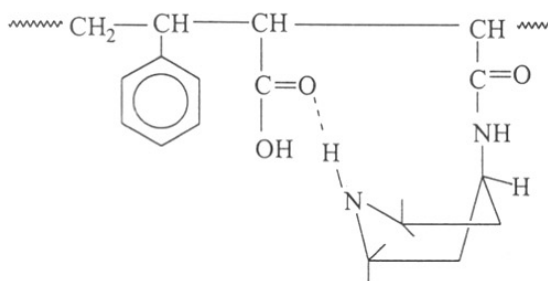


Fig. 8.17: Plot of hydroxyl index vs irradiation time in HIPS films stabilized with Tinuvin 144 at different concentrations

The intramolecular hydrogen bonding is (Equation 8.11):



Polymeric SMAN-g-2,2,6,6,-tetramethyl-4-piperidinol



(8.11)

Polymeric SMAN-g-4-amino-2,2,6,6-tetramethyl piperidine

Due to the inter and intramolecular hydrogen bonding these additives are not compatible and soluble in the HIPS and PS matrix. These additives are not soluble in any organic solvents but soluble in alkali solutions. With this observation we can conclude that they have inter and intramolecular hydrogen bonding in the system. Sedlar et al.^{21, 64} observed an intramolecular hydrogen bonding in PP with Tinuvin 770. Apart from this, these stabilizers have high T_g value (Table 8.3). Figures 8.18 and 8.19 shows TGA and DSC thermograms of these polymeric light stabilizers. The TGA curves show multiple decomposition in the thermal analysis.

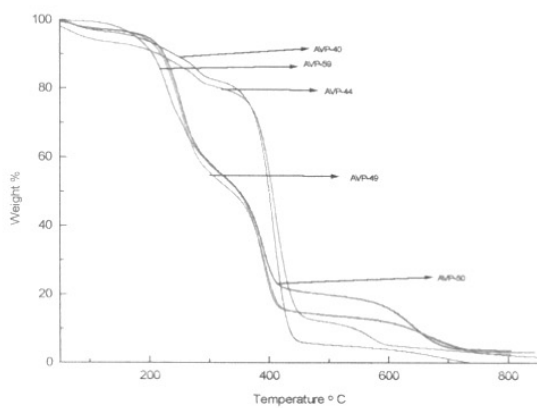


Fig. 8.18 TGA thermograms of polymeric SMAN-g-HALS stabilizers (AVP-40, 44, 49, 50 and 59)

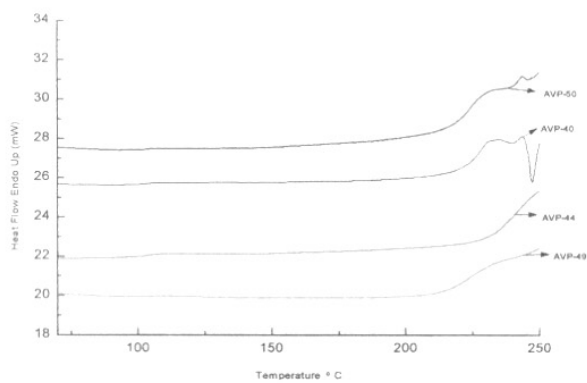
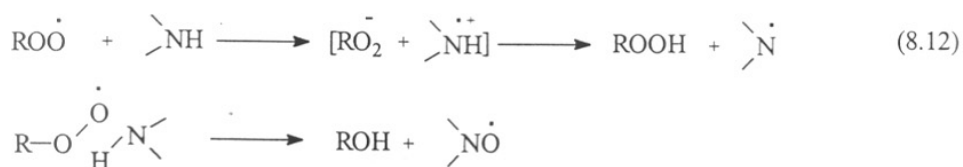


Fig. 8.19 DSC thermograms of polymeric SMAN-g-HALS stabilizers (AVP-40, 44, 49 and 50)

Table 8.3: T_g values of polymeric light stabilizers

Expt. No.	T_g ($^{\circ}\text{C}$)
AVP-40	224
AVP-44	242
AVP-49	226
AVP-50	227
AVP-59	196

Chirinos Padron^{66, 67} emphasized the role of alkyl peroxy radicals and alkyl hydroperoxides in the photo-oxidation mechanism of polymers. Hence in accordance with the classical philosophy of stabilization, the termination of the oxidation chain is explained to proceed by the deactivation of the alkyl peroxy radical formation in a synchronous mechanism as proposed by Geuskens on the basis of a steady-state kinetic study⁶⁸⁻⁷⁰ (Equation 8.12):



In the stabilization process, the H-abstraction from the >N-H group requires more energy to convert into nitroxyl radical (>NO \cdot), whereas the >N-CH $_3$ requires less energy. This nitroxyl radical will scavenge the hydroperoxides and alkyl radicals which are generated in the polymer backbone with photo-oxidation. Since these groups are in the intramolecular hydrogen bonding, therefore, the stabilization is very less. Concentrations of these polymeric stabilizers (AVP-40, 44, 49 and 50) do not have significant effect on photostabilization. These stabilizers showed very negligible stabilization as compared to polymeric SMAN-g-1,2,2,6,6-pentamethyl-4-

piperidinol and Tinuvin 770 and Tinuvin 144. These observations are shown in Figures 8.20 to 8.27. Among these stabilizers the polymeric SMAN-g-2,2,6,6-tetramethyl-4-piperidinol showed better results compared to polymeric SMAN-g-4-amino-2,2,6,6-tetramethyl piperidine. In these stabilizers the high mol.wt. SMAN-g-2,2,6,6-tetramethyl-4-piperidinol showed better stabilization effect than low.mol.wt. stabilizer.

Figures 8.28 and 8.29 show the comparison of carbonyl and hydroxyl absorptions in HIPS and PS with 1 wt-% various light stabilizers for 100 h UV exposure. HIPS showed maximum absorption as compared to PS. This is due to the PB phase in HIPS.

8.10.3 Morphological changes upon UV irradiation

Figure 8.30 showed SEM photograph of HIPS with evenly dispersed polymeric SMAN-g-1,2,2,6,6-pentamethyl-4-piperidinol (AVP-59) light stabilizer. This additive has better compatibility with HIPS matrix and is grafted on the polystyrene phase. The polybutadiene nodules are not clearly observed in this film due to the melt blending. The solution cast films showed good phase separation in the HIPS (described in chapter VI). The 75 h photo-oxidized film showed micro-cavities on the surface. The same behavior was observed in 150 h irradiated film also. The micro-cracks were not observed in these films for longer hour irradiation also whereas neat film showed micro-cracks on the surface (described in chapter VI). This indicates that polymeric HALS is protecting the surface from the photo-oxidative degradation.

Figure 8.31 showed SEM photograph of HIPS with polymeric SMAN-g-4-amino-2,2,6,6-tetramethyl piperidine (AVP-40). The phase separation is observed in the film. The stabilizer particles are dispersed throughout the film. It indicates that the additive is not compatible with the polymer matrix. The 75 h exposed film showed micro-cavities on the film surface. The 150 h exposed film showed the maximum micro-cavities formation on the surface. The same behavior was observed with polymeric SMAN-g-2,2,6,6-tetramethyl-4-piperidinol (AVP-49). (Figure 8.32)

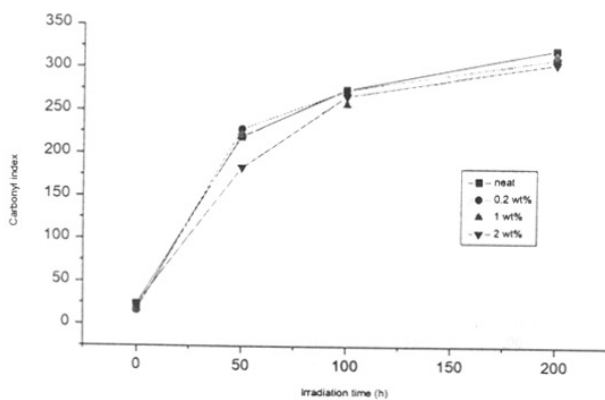


Fig. 8.20: Plot of carbonyl index vs irradiation time in HIPS films stabilized with high mol. wt polymeric SMAN-g-4-amino-2,2,6,6-tetramethyl piperidine (AVP-40)

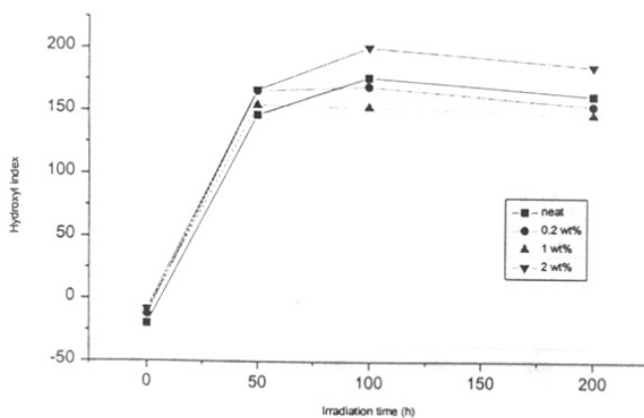


Fig. 8.21: Plot of hydroxyl index vs irradiation time in HIPS films stabilized with high mol. wt polymeric SMAN-g-4-amino-2,2,6,6-tetramethyl piperidine (AVP-40)

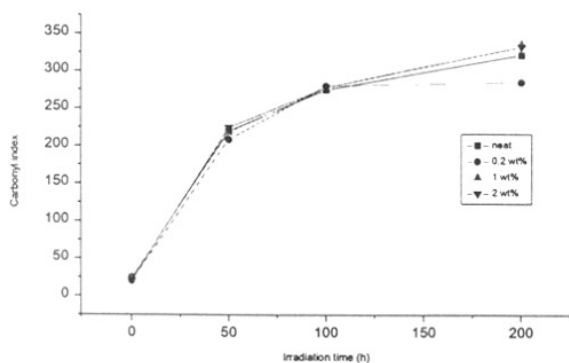


Fig. 8.22 Plot of carbonyl index vs irradiation time in HIPS films stabilized with low mol.wt polymeric SMAN-g-4-amino-2,2,6,6-tetramethyl piperidine (AVP-44)

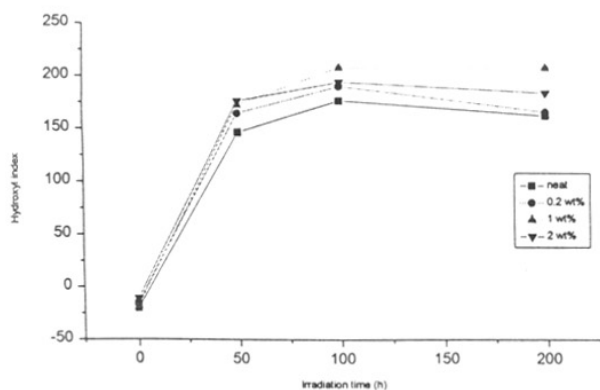


Fig. 8.23: Plot of hydroxyl index vs irradiation time in HIPS from stabilized with low mol.wt polymeric SMAN-g-4-amino-2,2,6,6-tetramethyl piperidine (AVP-44).

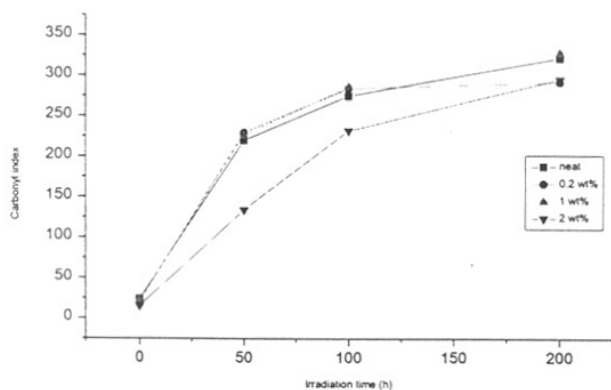


Fig. 8.24: Plot of carbonyl index vs irradiation time in HIPS films stabilized with high mol. wt polymeric SMAN-g-2,2,6,6-tetramethyl-4-piperidinol (AVP-49)

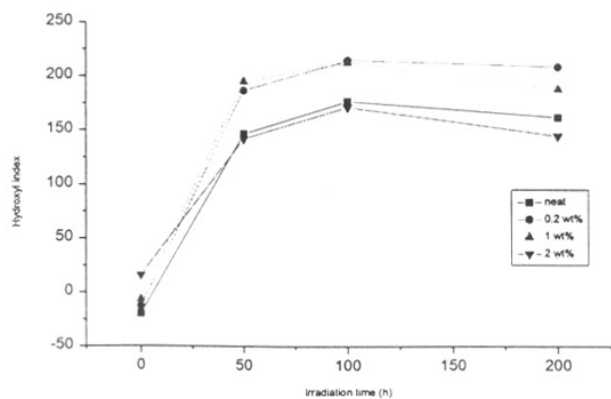


Fig. 8.25: Plot of hydroxyl index vs irradiation time in HIPS films stabilized with high mol. wt polymeric SMAN-g-2,2,6,6-tetramethyl-4-piperidinol (AVP-49)

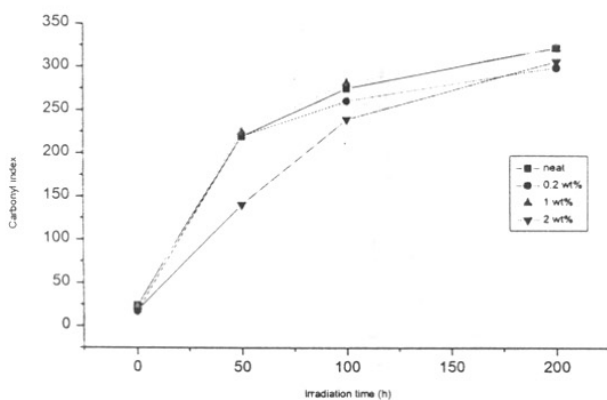


Fig. 8.26: Plot of carbonyl index vs irradiation time in HIPS films stabilized with low mol. wt polymeric SMAN-g-2,2,6,6-tetramethyl-4-piperidinol (AVP-50)

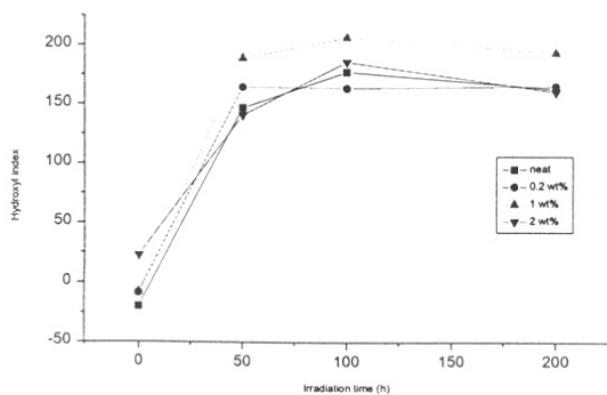


Fig. 8.27: Plot of hydroxyl index vs irradiation time in HIPS films stabilized with low mol.wt polymeric SMAN-g-2,2,6,6-tetramethyl-4-piperidinol (AVP-50)

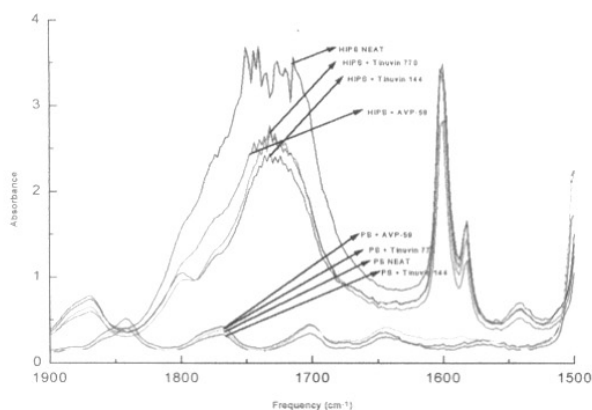


Fig. 8.28: Plot of carbonyl index vs irradiation time (100 h) in comparison between HIPS and PS films stabilized with 1 wt-% various stabilizers

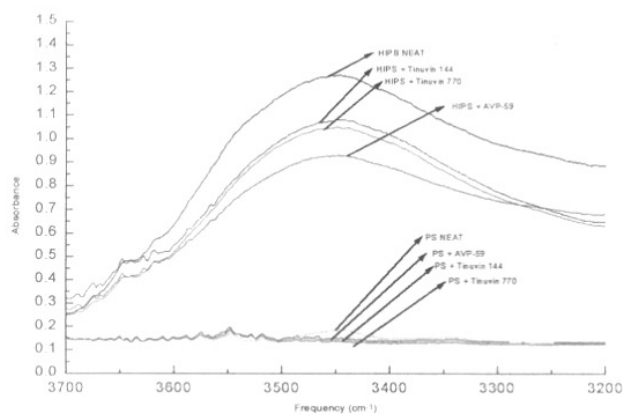


Fig. 8.29: Plot of hydroxyl index vs irradiation time (100 h) in comparison between HIPS and PS films stabilized with 1 wt-% various stabilizers

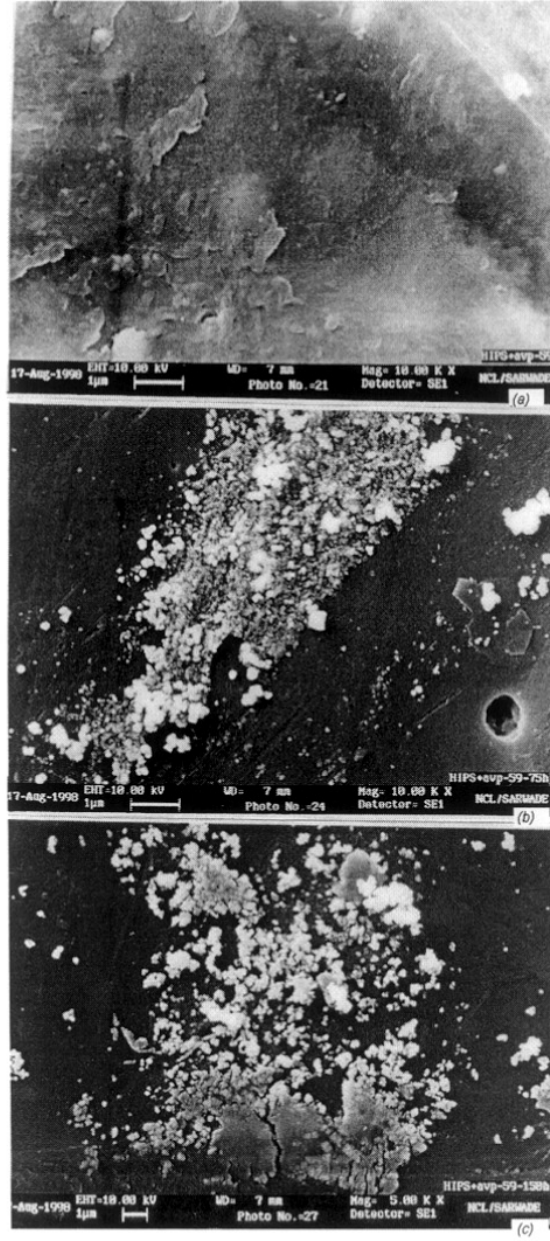


Fig. 8.30: SEM photographs of HIPS stabilized with polymeric SMAN-g-1,2,2,6,6-pentamethyl-4-piperidinol (AVP-59): (a) initial, (b) 75 h UV exposure, (c) 150 h UV exposure

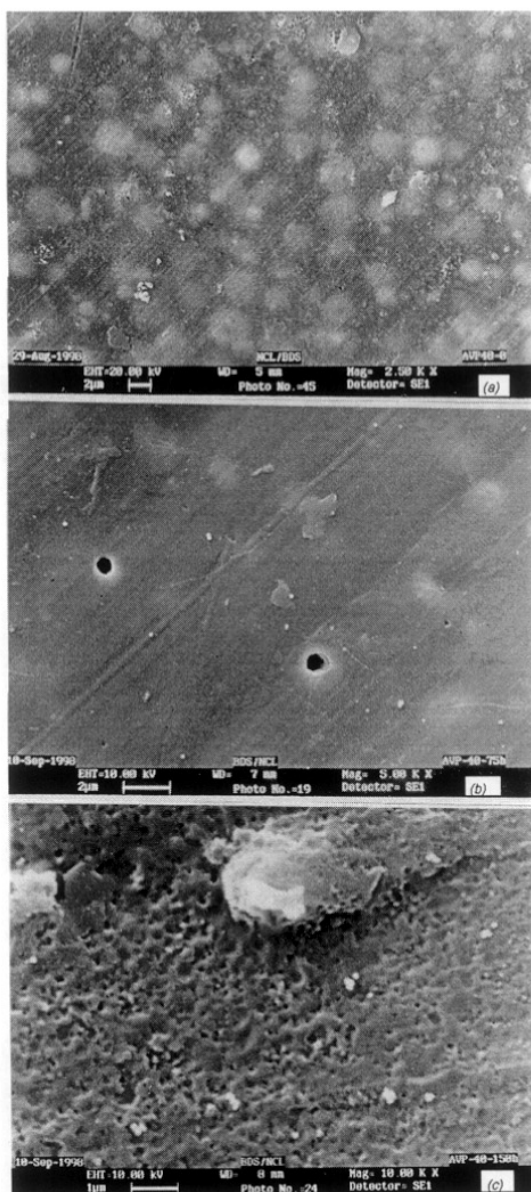


Figure 8.31: SEM photographs of HIPS stabilized with polymeric SMAN-g-4-amino-2,2,6,6-tetramethyl piperidine (AVP-40): (a) initial, (b) 75 h UV exposure, (c) 150 h UV exposure

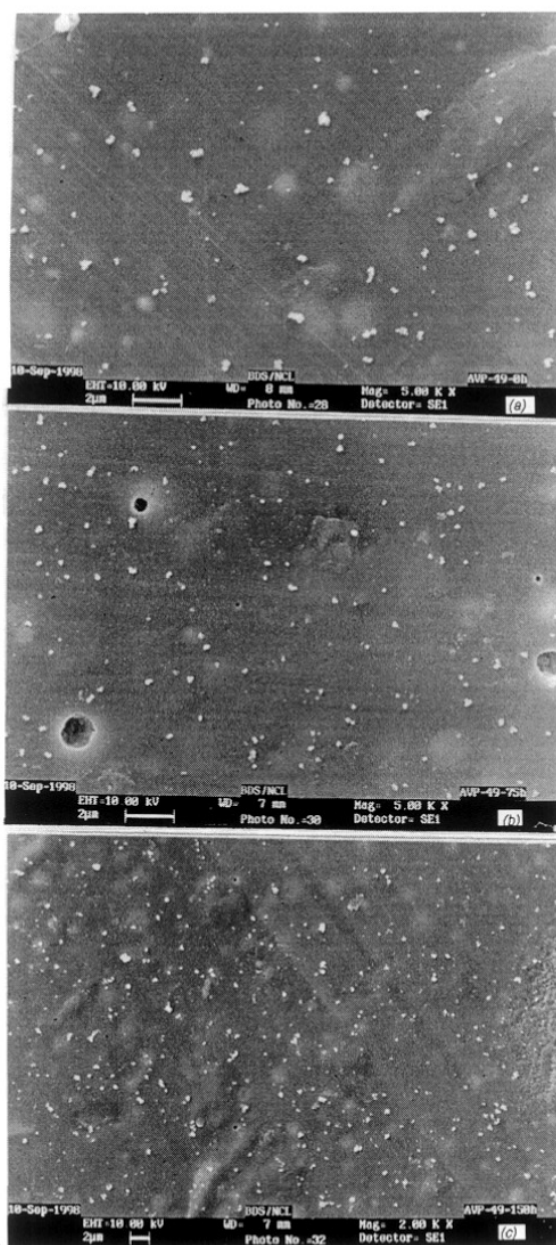


Fig. 8.32: SEM photographs of HIPS stabilized with polymeric SMAN-g-2,2,6,6-tetramethyl-4-piperidinol (AVP-49): (a) initial, (b) 75 h UV exposure, (c) 150 h UV exposure

The conventional light stabilizers are comparatively less protecting stabilizers in HIPS systems. HIPS with Tinuvin 770 (Figure 8.33) showed that the stabilizer is dispersed throughout in the polymer matrix. Phase separation was observed in this case also. The UV irradiated (75 & 150 h) film showed the micro-cavities on the surface. The same trend was observed with Tinuvin 144 also. (Figure 8.34)

8.11 CONCLUSIONS

In conclusion, the polymeric SMAN-g-1,2,2,6,6-pentamethyl-4-piperidinol showed excellent photostabilization as compared to the conventional stabilizers. The polymeric SMAN-g-4-amino-2,2,6,6-tetramethyl piperidine and SMAN-g-2,2,6,6-tetramethyl-4-piperidinol showed poor performance in photostabilization. The polymeric SMAN-g-1,2,2,6,6-pentamethyl-4-piperidinol is dispersing well in HIPS matrix.

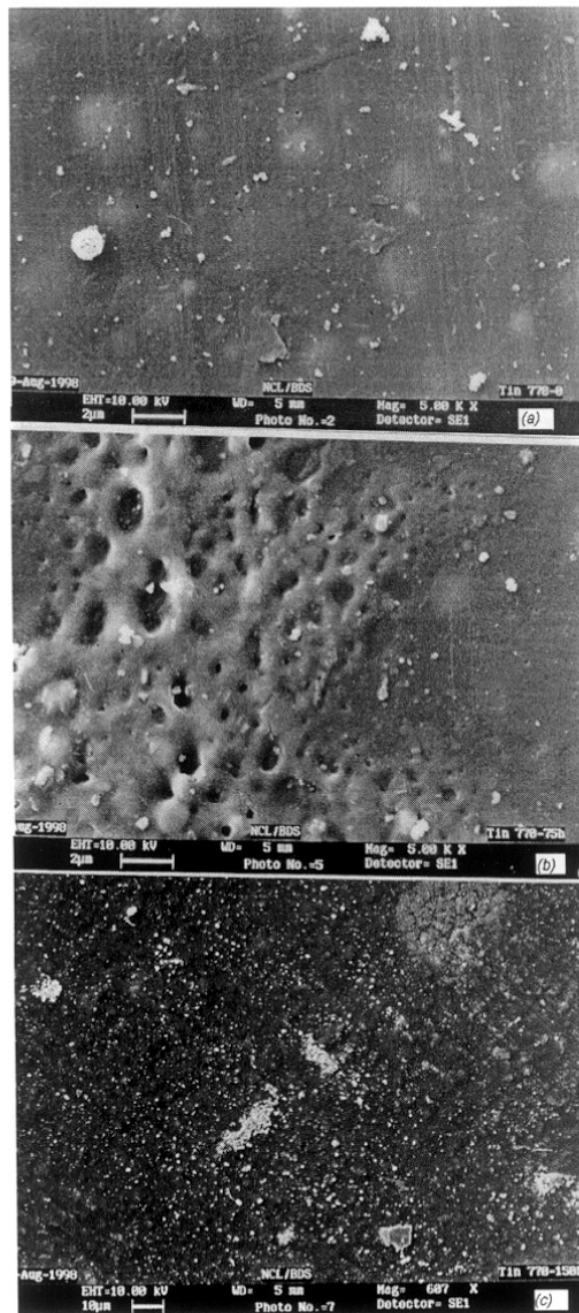


Fig. 8.33: SEM photographs of HIPS stabilized with tinuvin 770: (a) initial, (b) 75 h UV exposure, (c) 150 h UV exposure



Fig. 8.34: SEM photographs of HIPS stabilized with tinuvin 144: (a) initial, (b) 75 h UV exposure, (c) 150 h UV exposure

8.12 References

1. J. Crank, G.S. Park, in '*Diffusion in Polymers*', (J. Crank and G.S. Park, Eds.), Academic Press, London, 1968, Chap 1, p.1
2. H.E. Bair, *Polym. Eng. Sci.*, **13**, 435 (1973)
3. R.J. Roe, H.E. Bair, C. Gieniewski, *J. Appl. Polym. Sci.*, **18**, 843 (1974)
4. J. Luston, in '*Developments in Polymer Stabilization*', (G. Scott, Ed.), Applied Science, London, 1980, Vol. 3, Chapter 5, p.139
5. J.Y. Moisan, *Eur. Polym. J.*, **16**, 979 (1980)
7. J.Y. Moisan, in '*Polymer Permeability*', (J. Comyn, Ed.), Elsevier, London, 1985, Chapter 4, p. 119
8. K. Murayama, *J. Synth. Org. Chem. (Japan)* **31**, 198 (1973)
9. J.Q. Pan, Y.H. Liu, *Additives Commn.*, **3**, 1 (1981)
10. F. Gugumus, *Polym. Degrad. Stab.*, **24**, 292 (1989)
11. J.Q. Pan, *Plastics Technol.*, **11**, 16 (1991)
12. J. Shimada, K. Kabuki, M. Ando, *Rev. Electr. Commun. Lab.*, **20**, 564 (1972)
13. B.D. Gesner, *J. Appl. Polym. Sci.*, **9**, 3701 (1965)
14. P.G. Kelleher, *J. Appl. Polym. Sci.*, **10**, 843 (1966)
15. M.D. Wolkowicz, S.K. Gaggar, *Polym. Eng. Sci.*, **21**, 571 (1981)
16. *Developments in Polymer Stabilization-I*, (G. Scott Ed.), Applied Science, London, 1979, Chapt. 9.
17. M. Ghaemy, G. Scott, *Polym. Degrad. Stab.*, **3**, 233 (1981)
18. D.M. Kulich, M.D. Wokowicz, *Adv. In Chem.*, **222**, 329 (1984)
19. C.S. Lee, Wayne W.Y. Lau, S.Y. Lee, S.H. Goh, *J. Polym. Sci. Part A. Polym. Chem.*, **30**, 983 (1992)

20. E.N Step, N.J. Turro, M.E. Gande, P.P. Klemchuk, *Macromolecules*, **27**, 2529 (1994)
21. J. Sedlar, J. Marchal, J. Petruj, *Polym. Photochem.*, **2**, 175 (1982)
22. D.M. Wiles, J.P.T. Jensen, D.J. Carlsson, *Pure. Appl. Chem.*, **55**, 1651 (1983)
23. D.W. Grattan, D.J. Carlsson, D.M. Wiles, *Polym. Degrad. Stab.*, **1**, 69 (1979)
24. P.P. Klemchuk, M.E. Gande, *Makromol. Chem., Makromol. Symp.*, **28**, 117 (1989)
25. P.P. Klemchuk, M.E. Gande, *Polym. Degrad. Stab.*, **22**, 241 (1988)
26. P.P. Klemchuk, M.E. Gande, *Polym. Degrad. Stab.*, **27**, 65 (1990)
27. E.T. Denisov, *Polym. Degrad. Stab.*, **34**, 325 (1991)
28. M.V. Sudnik, M.F. Romantsev, A.B. Shapiro, E.G. Rozantsev, *Bull. Acad. Sci. USSR Div. Chem. Sci.*, **24**, 2702 (1975)
29. G.A. Kovtun, A.L. Alexandrov, V.A. Golubev, *Bull. Acad. Sci. USSR Div. Chem. Sci.*, **423**, 2115 (1974)
30. A. Faucitano, A. Buttafava, F. Martinotti, L. Greci, *Polym. Degrad. Stab.*, **35**, 211 (1992)
31. F. Gugumus, *Polym. Degrad. Stab.*, **40**, 167 (1993)
32. J. Chateaufneuf, J. Luszyk, K.U. Ingold, *J. Org. Chem.*, **53**, 1629 (1988)
33. A.L.J. Beckwith, V.W. Bowry, K.U. Ingold., *J. Am. Chem. Soc.*, **114**, 4983 (1992)
34. V.W. Bowry, K.U. Ingold, *J. Am. Chem. Soc.*, **114**, 4992 (1992)
35. E. Foldes, *J. Appl. Polym. Sci.*, **48**, 1905 (1993)
36. A. Peterlin, *J. Macromol. Sci. Phys.*, **B11**, 57 (1975)
37. J. Klein, *J. Polym. Sci. Polym. Phys. Ed.*, **15**, 2057, 2065 (1977)
38. R. Kosiyanon, R. McGregor, *J. Appl. Polym. Sci.*, **26**, 629 (1981)

39. V.M. Shah, S.A. Stern, P.J. Ludovice, *Macromolecules*, **22**, 4660 (1989)
40. J. Koszinowski, *J. Appl. Polym. Sci.*, **31**, 1805 (1986)
41. J. Durmis, M. Karvas, P. Caucik, J. Holcik, *Eur. Polym. J.*, **11**, 219 (1975)
42. J.H. Hiblebrand, R.L. Scott, in '*The solubility of Nonelectrolites*', 3rd ed., Reinhold, New York, 1950.
43. V. Stannett, H. Yasuda, in '*Crystalline olefin Polymers*', (R.A.V. Raff and K.W. Doak Eds.) Interscience, New York, 1964, Part II, Chapter 4, p. 131.
44. S.A. Pushpa, P. Goonetilleu, N.C. Billingham, *Rubber Chemistry and Technology*, **69**, 885 (1996)
45. W.B. Lutz, S. Lazams, R.I. Meltzer, *J. Org. Chem.*, **27**, 1695 (1962)
46. W.G. Barb, *J. Polym. Sci.*, **11**, 117 (1953)
47. C. Walling, '*Free radicals in solution*', Wiley, New York 1957
48. Q. Lin, M. Talukder, C.U. Pittman JR, *J. Polym. Sci. Part A. Polym. Chem.*, **33**, 2375 (1995)
49. C. Walling, E.R. Briggs, K.B. Wolfstirn, F.R. Mayo, *J. Am. Chem. Soc.*, **70**, 1537, 1544 (1948)
50. P.D. Bartlett, K. Nozaki, *J. Am. Chem. Soc.*, **68**, 1495 (1946)
51. M. Yoshimura, H. Mikawas, Y. Shirota, *Macromolecules*, **11**, 1085 (1978)
52. N.G. Gaylord, *J. Macromol. Sci. Chem.*, **A6**, 259 (9172)
53. A.S. Brown and K. Fujimori, *Macromol. Chem.*, **188**, 2177 (1987)
54. A.S. Brown, K. Fujimori, I.E. Craven, *J. Polym. Sci. Part A: Polym. Chem.*, **27**, 3315 (1989)
55. L.M. Litvinenko, A.I. Kirichenko, *Doki. Akad. Nauk. SSSR Ser. Khim.*, **176**, 97 (1967)
56. G.H. Hu, J.T. Lindt, *J. Polym. Sci. Part A. Polym. Chem.*, **31**, 691 (1993)
57. R.J. Roe, H.E. Bair, C. Gieniewski, *J. Appl. Polym. Sci.*, **18**, 843 (1974)

CHAPTER IX

SUMMARY AND CONCLUSIONS

58. A. Peterlin, *Pure Appl. Chem.*, **39**, 239 (1974)
59. E. Foldes, B. Turcsany, *J. Appl. Polym. Sci.*, **46**, 507 (1992)
60. N.C. Billingham, in '*Oxidation Inhibition in Organic Materials*', (J. Pospisil and P.P. Klemchuk, Eds.,) CRC Press, Boca Raton, FL, 1990, Vol. 2, Chapter 6, p.249.
61. P.N. Lowell, N.G. McCrum, *J. Polym. Sci. A-2.*, **9**, 1935 (1971)
62. T. Erdey – Gruz, A. Fizikai Kemia Alapjai (Basics of Physical Chemistry), Muszaki Konyvkiado, Budapest, 1963
63. V. Dudler, *Polym. Degrad. Stab.*, **42**, 205 (1993)
64. E. G. Rozantsev, in '*Free nitroxyl radicals*', Plenum Press, New York, 1970
65. M.J. Aroney, *J. Chem. Soc. B.* **98** (966)
66. A.J. Chirinos Padron, *J. Photochem. Photobiol. A: Chem.*, **49**, 1 (1989)
67. A.J. Chirinos Padron, *JMS-Rev. Macromol. Chem. Phys.*, **C30**, 107 (1990)
68. G. Geuskens, G. Nedelkos, *Polym. Degrad. Stab.*, **19**, 365 (1987)
69. G. Geuskens, M.N. Kanda, *Polym. Degrad. Stab.*, **51**, 227 (1996)
70. O. Brede, D. Beckert, C. Windolph, H.A. Gottinger, *J. Phys. Chem. A.*, **102**, 1457 (1998)

Degradation studies of high impact polystyrene (HIPS)

High impact polystyrene contains polystyrene as a continuous phase and polybutadiene as dispersed phase. The polybutadiene contents will vary from 5-20 wt-% in the copolymer. The polybutadiene phase microstructure exists in trans-1,4, cis-1,4 and vinyl-1,2 forms. The microstructure of polybutadiene in HIPS has been determined with FT-IR spectroscopy, FT Raman spectroscopy, ^1H NMR and ^{13}C NMR spectroscopy. The absorption peaks in FT-IR spectra at 967 cm^{-1} , 729 cm^{-1} and 912 cm^{-1} have been assigned trans-1,4, cis-1,4, and vinyl-1,2, respectively. FT Raman spectra of HIPS also confirmed the microstructure of polybutadiene by the absorption signals at 1666 cm^{-1} (trans-1,4), 1654 cm^{-1} (cis-1,4) and 1641 cm^{-1} (vinyl-1,2). The vinyl, cis and trans protons are very difficult to analyze by proton NMR due to poor resolution. The ^{13}C NMR spectroscopy is more suitable than ^1H NMR. The cis and trans polybutadiene microstructure was identified by both, the aliphatic (27.4 and 32.8 ppm, respectively) and the olefinic region (129.2 and 129.3 ppm) but vinyl microstructure is not detected.

The vinyl-1,2 structure are well characterized by FT-IR because relatively higher values for the absorption coefficient, but Raman and ^1H NMR confirmed the low content and no detection was possible by ^{13}C NMR.

The main method employed for studying the extent of photo-and thermal-oxidative degradation in HIPS was FT-IR spectroscopy. The photo-oxidation of three different grades of HIPS at longer wavelength ($\geq 300\text{ nm}$, 60°C) resulted in the formation of carbonyl and hydroxyl groups. The polybutadiene phase is the main oxidation site for degradation as it is very susceptible to oxidation. The degree of photo-oxidation will depend on the content of polybutadiene. The photo-oxidative products were separated and identified by reactive gases such as sulfur tetrafluoride and ammonia. The acyl fluoride showed absorption at 1840 cm^{-1} and ammonium salt at 1565 cm^{-1} . The kinetic curves for photo-oxidized HIPS (three different grades) showed very fast photo-oxidation up to 50 h irradiation. These curves showed that the formation of photoproducts and disappearance of unsaturation are accelerated with exposure. The photoproduct distribution was measured by using micro-FT-IR technique. The

thermal oxidation of HIPS resulted in the formation of α , β -unsaturated ketones. The rate of product formation depends on the temperature.

Intrinsic viscosity $[\eta]$, tensile impact strength and change in color (yellowness index) were studied in the photo-oxidized HIPS (different grades). The intrinsic viscosity $[\eta]$ of HIPS solution showed rapid decrease initially which slows down and then tend to increase at 45 h, after this period the intrinsic viscosity rapidly decreased. It indicates that the polybutadiene phase is oxidizing initially and crosslinking develops later on (~ 45 h). After 45 h, a random chain-scissions occurred in the polymer chain. The intrinsic viscosity of HIPS was compared with that of pure polystyrene. The tensile impact strength also showed the same behavior. All the samples showed the yellowness upon the photo-oxidation.

The photo-oxidized HIPS solution was analyzed by ^{13}C NMR spectroscopy. The photoproducts were not detected by ^{13}C NMR in HIPS, whereas in the SBS solution the cis/trans epoxides and alcohols were detected. This is because of low content of polybutadiene in HIPS. The morphology of photo-oxidized HIPS and SBS films were studied by scanning electron microscope. The morphology showed the micro-cavities on the surface at the initial stages of oxidation. This is because chain-scissions are occurring in the polybutadiene phase. The micro-cavities are regular and spherical in nature and internal surface is rough.

The natural weathering and photo-oxidation of three different grades of HIPS showed the carbonyl and hydroxyl absorptions in FT-IR spectra. The rate of formation of these products depends on the climatic conditions. The rate of formation of photoproducts in accelerated weathering is more than in natural weathering.

Photostabilization of HIPS with Polymeric HALS

Styrene-maleic anhydride copolymer (different mol.wt.) was synthesized by free-radical copolymerization. 1,2,2,6,6-pentamethyl-4-piperidinol, 2,2,6,6-tetramethyl-4-piperidinol and 4-amino-2,2,6,6-tetramethyl piperidine were grafted on styrene-maleic anhydride copolymer. These additives are incorporated with melt mixing. The solubility and diffusibility has been measured (in HIPS) with polymeric SMAN-

g-1,2,2,6,6-pentamethyl-4-piperidinol, Tinuvin 770 and Tinuvin 144. The polymeric SMAN-g-1,2,2,6,6-pentamethyl-4-piperidinol is highly compatible with the HIPS substrate. The low and high mol.wt. of 2,2,6,6-tetramethyl-4-piperidinol and 4-amino-2,2,6,6-tetramethyl piperidine were not compatible with the polymer matrix. These additives are forming intra and inter molecular hydrogen bonding *in situ*. The photostabilization efficiency of polymeric HALS was compared with conventional stabilizers like Tinuvin 770 and Tinuvin 144.

In conclusion, the results presented in this thesis clearly suggest that the photo-oxidation of heterophasic high impact polystyrene at 55° C in air changes both, the chain molecular structure and the morphology. Based on these results it can be concluded that the polybutadiene phase of HIPS is the main site of oxidation. The oxidation increases with the exposure time and content of polybutadiene present in HIPS. Polymeric SMAN-g-1,2,2,6,6-pentamethyl-4-piperidinol, SMAN-g-2,2,6,6-tetramethyl-4-piperidinol, SMAN-g-4-amino-2,2,6,6-tetramethyl piperidine were synthesized during this study. Polymeric SMAN-g-1,2,2,6,6-pentamethyl-4-piperidinol showed a better photostabilizing efficiency compared to conventional HALS due to its superior diffusion and solubility character.

Future scope of the work

Heterophase thermoplastic elastomers have technologically useful properties such as high impact and tensile properties. Study of thermal and photo-oxidative degradation of such heterophase copolymers is a fertile area of development. There is an urgent need to understand the relationship between morphology and the aging reaction rate and the distribution of additives between the two phases. New stabilizer molecules may have to be designed that provide effective protection to such multiphase polymers.

With better understanding of the mechanisms of degradation and stabilization, there undoubtedly will be an increased effort to produce polymers with greater photo-, thermal/ radiation resistance and also more effective stabilizers to achieve this end. Thus, the study of degradation and stabilization aspects of HIPS appears to be both intellectually stimulating and of practical importance.

SYNOPSIS

The thesis entitled **Physico-Chemical studies on degradation and stabilization of styrenic polymers** is divided into nine chapters.

Photo-oxidation mechanism in polymers is classified into two main types depending on the mode of light absorption. The first mechanism is based upon the absorption of light through impurity chromophores and the second mechanism is a direct absorption of light by groups which form part of the chemical constitution of the polymer. Polymeric materials are exposed to sunlight, wind, rain and temperature in daily use. The ultra violet light in the sunlight is the most effective factor for polymer degradation. During the degradation, polymer loses its molecular weight, mechanical properties, embrittlement, changes in morphology and changes in color until ultimately it becomes useless. These changes are mainly due to chain scissions in the polymer. The increase in the molecular weight is also observed sometimes in few cases, which is due to crosslinking of free-radicals generated on the backbone of polymers. Therefore, it is necessary to understand the mechanism of photo-oxidative degradation of polymers in order to improve their photostability.

Styrenic polymers have valuable properties and are continuously finding new applications in the daily life. When these polymers are exposed to sunlight in the presence and absence of oxygen, it shows adverse effect on the lifetime of a polymer product in both outdoor and indoor applications. Apart from sunlight, temperature, humidity, ozone, atmospheric pollutants, contact with corrosive chemicals and attack of microorganisms also effect the polymer degradation. These factors lead to gradual deterioration of the critical properties of the polymer which can cause premature failure of the product or unsuitability for a particular purpose.

The photo-oxidation of polystyrene has been studied since several decades¹⁻³. The polystyrene is quite resistant to photodegradation initiated by solar radiations, as it does not contain any chromophoric groups that could absorb radiation with a wavelength of over 290 nm. But the maximum absorption of polystyrene lies below 260 nm.

High impact polystyrene [HIPS] is a heterophasic copolymer. The polystyrene is a continuous phase and polybutadiene is a dispersed phase. HIPS absorb UV light in the region of 295 to 360 nm^{4, 5}. In the photo-oxidation of HIPS, mainly chain

scissions are occurring in the polymer backbone. In HIPS, the photo-oxidative products were observed as aldehydes, ketones, along with free acids and their esters. The photo-oxidation is mainly occurring in the polybutadiene phase^{6,7}. Apart from these products crosslinking is also occurring in the polybutadiene phase^{8,9}. Upon irradiation, HIPS leads to a deterioration in molecular weight, loss in the mechanical properties, dielectrical properties, changes in morphology and in color (yellowness).

The photostabilization of light-sensitive polymers involves the retardation or elimination of the various photophysical and photochemical processes that occur during the photo-oxidation and may be achieved in many ways, depending on the type of stabilizer and type of mechanism that is operative in the polymer. The oxidative degradation can be prevented with incorporating the antioxidants, UV stabilizers, UV absorbers and excited state quenchers in the polymer. Generally, these additives are incorporated in the polymer during processing. In the stabilization process, the low molecular weight stabilizers will leach out from the polymer. But the compatible additives will give the best protection. In the photo-stabilizers, hindered amine light stabilizers (HALS) are most effective stabilizers. They are considered as multifunctional stabilizers and their action is not limited to a single step in the photo-oxidation process, their transformation products also acts as a stabilizers and undergo multiple regeneration¹⁰⁻¹².

Objective of the present investigation

The objectives of the present investigations are:

1. To determine the polybutadiene content and its microstructure determination in heterophasic elastomeric high impact polystyrene.
2. To examine the thermal and photo-oxidative degradation in the heterophasic HIPS (different grades) and comparison of the results with the glassy polystyrene homopolymer.
3. Evaluation of chain scission, changes in mechanical properties and color (yellowness) and surface morphology upon UV irradiation in HIPS.

4. To study the natural weathering of heterophasic elastomeric HIPS and the comparison of photoproducts formation under natural and accelerated exposure condition.
5. To design, synthesis and property evaluation of specific polymeric stabilizers in HIPS.

Outline of the thesis

Chapter I

This introductory chapter explores with a discussion of various types of degradation reaction pathways for photo and thermal degradation, general mechanisms and degradation kinetics of styrenic copolymers. A general background on the mechanisms of photostabilization, structural classes of light stabilizers, particularly hindered amine light stabilizers (HALS) and their photostabilization mechanisms and kinetics are also discussed.

Chapter II

The objective and scope of the present investigations are described in this chapter.

Chapter III

This chapter deals with the polybutadiene content and its microstructure in the different grades of high impact polystyrene with various spectroscopic methods. Polybutadiene is characterized by deformation bands in FT- IR spectroscopy at 994, 967, 912 and 729 cm^{-1} . FT- Raman spectroscopy was used for higher constant resolution over the range of wave numbers. It provides reasonable signal to noise ratios in near IR excited Raman. The polybutadiene content and microstructure of HIPS determined with proton and ^{13}C -NMR spectroscopy.

Chapter IV

This chapter deals with the thermal and photo-oxidative degradation of different grades of high impact polystyrene in the solid phase. These results are compared

degradation of HIPS and PS were compared by FT-IR spectroscopy. The photo-oxidized films were treated with NH_3 and SF_4 for the rapid identification and resolution of the various carbonyl species. The heterogeneity in the film was also determined by micro FT-IR spectroscopy.

Chapter V

This chapter deals with the photo-oxidation of different grades of HIPS and degradation is compared with polystyrene. HIPS and PS films were photo-irradiated at 55°C with the light wavelength at $\geq 300\text{nm}$. The changes in intrinsic viscosity, tensile impact tests and yellowness were studied. These films underwent extensive reduction in the viscosity and tensile impact strength. In photo-oxidation, mainly chain scissions are occurring in the polybutadiene phase. Tristimulus values were calculated for unirradiated and irradiated samples. The rate of oxidative degradation was maximum in the sample possessing higher unsaturation content.

Chapter VI

This chapter deals with the HIPS and styrene-butadiene-styrene (SBS) block copolymer photo-oxidation. The photo-irradiation was carried out at 55°C with the polychromatic light for different intervals. The photo-oxidized films were analyzed by ^{13}C -NMR spectroscopy in the liquid state. Epoxides and alcohols were observed as photoproducts in SBS block copolymer. In HIPS, epoxides were not detected. The morphological changes of the solution casted HIPS and SBS films caused by irradiation were studied by scanning electron microscopy. The property deterioration was explained in terms of scission reactions in HIPS and SBS matrix. The micrographs indicate that both the materials are of two phasic systems.

Chapter VII

Natural weathering of HIPS samples is studied in this chapter. The natural weathering of HIPS and PS has also been compared with artificial weathering. The natural weathering and artificial weathering products are monitored by FT-IR spectroscopy.

Chapter VIII

In this chapter the stabilizer synthesis and their performance evolution has been studied. Styrene-Maleic anhydride copolymer was synthesized by free-radical polymerization method. Styrene maleic anhydride copolymer synthesized in different molecular weights. Poly(styrene maleic anhydride-g-HALS) additives synthesized using basic catalyst and clay catalyst. The photostabilization of polymeric styrene maleic anhydride-g-HALS are compared with conventional stabilizers like Tinuvin 770 and Tinuvin 144 with various concentrations. The effect of concentration is also discussed.

Styrene maleic anhydride-g-HALS are mainly poly(styrene maleic anhydride-g-4-amino,2,2,6,6-tetramethyl piperidine), poly(styrene maleic anhydride-g-2,2,6,6-tetramethyl-4-piperidinol) and poly(styrene maleic anhydride-g-1,2,2,6,6-pentamethyl-4-piperidinol).

Chapter IX

This chapter summarizes the results and describes the salient conclusions of the study. Additional thoughts for further research are also indicated.

In HIPS, the polybutadiene content and microstructure has been determined with various spectroscopic methods. Photo-oxidation and thermal oxidation in the HIPS performed by FT-IR spectroscopy. The polybutadiene phase is mainly defective site in HIPS. The photo-oxidation is mainly occurring in this phase. The photoproducts were identified by derivatization techniques. Upon photo-oxidation the intrinsic viscosity was decreased with irradiation time. Initially, a small crosslinking was observed in HIPS due to polybutadiene phase. Upon photo-oxidation tensile impact strength decreased while yellowness increased as a function of time. The surface damage also observed with photo-oxidation.

The performance of synthesized polymeric HALS and conventional HALS was studied. The comparative performance was also evaluated.

References

1. B.G. Achhammer, M.J. Reiney and F.W. Reinhart, *J. Res. Nat. Bur. Stand.*, **47**, 116 (1951)
2. N.A. Weir, P. Kutok and K. Whiting, *Polym. Degd. Stab.*, **24**, 247 (1989)
3. B. Ranby and J.F. Rabek, *Photodegradation, Photooxidation and Photostabilization of Polymers: Principles and Applications*, Wiley Publishers, London, (1975)
4. L. Rosik and J. Sedlacek, *Plasto* **70**, Marinske Lazne, (1970)
5. L. Rosik and J. Sedlacek, *Synt. Kauc*, **21**, 1 (1970)
6. J. Sedlacek and J. Rosik, *Chem. Zvesti*, **26**, 412 (1972)
7. Y. Israeli, J. Lacoste, J. Lemaire, R.P. Singh and S. Sivaram, *J. Polym. Sci. Part A Polym.Chem.*, **32**, 485 (1994).
8. G. Scott, *Developments in polymer stabilization Vol. I*, p309, Applied Publishers, London, 1979.
9. A. Ghaffar, A. Scott and G. Scott, *Eur. Polym.J.* **13**, 89 (1977).
10. P.D. Gabriele, J.R.Geib, R.M. Iannulc and W.J. Reid, *ACS Symp. Ser.* **229**, 317 (1983)
11. R. Tsunoda and T. Yamauch, *Jpn. Kokai Tokkyo Koho JP* 04, 15, 248 (1992)
12. A. Yamazalev, Y. Tsubakera and Y. Suetsugu, *Jpn. Kokai Tokkyo Koho JP* 03, 220, 256 (1992).

LIST OF PUBLICATIONS

1. R.P. Singh, R.A. Raj, **A. Vishwa Prasad**, S. Sivaram, J. Lacoste and J. Lemaire, Chain-scission and Yellowing of HIPS, *Polymer International* **36**, 309 (1995).
2. **A. Vishwa Prasad** and R.P. Singh
Thermal decomposition kinetics of a commercial Fluoropolymer
Materials Res. Bull., **30**, 1407 (1995).
3. **A. Vishwa Prasad** and R.P. Singh
Studies on radiation effects of Fluoropolymers: Radiation-induced structural and crystallinity changes of Tefzel
J. Macromol. Sci. Pure & Appl. Chem., **A33**, 91 (1996).
4. J. Lacoste, F. Delor, J.F. Pilichowski, R.P. Singh, **A. Vishwa Prasad** and S. Sivaram
Polybutadiene content and Microstructure in High Impact Polystyrene
J. Appl. Polym. Sci., **59**, 953 (1996).
5. **A. Vishwa Prasad**, P.N. Thanki and R.P. Singh
Photo and thermo-oxidative degradation of ethylene - propylene blends: Comparison of oxidation products
J. Macromol. Sci., Pure & Appl. Chem., **A34**, 349 (1997)
6. **A. Vishwa Prasad** and R. P. Singh
Photo-oxidative Degradation of styrenic polymers: ^{13}C -NMR and morphological changes upon irradiation.
J. Appl. Polym. Sci., (in press 1998)
7. R.P. Singh and **A. Vishwa Prasad**
Photodegradation studies on polyurethane coating: Effect of additives on yellowing of polyurethane
Die Angew. Makromol. Chemie., (communicated 1998)
8. **A. Vishwa Prasad** and R.P. Singh
The oxidative degradation of styrenic copolymers: A comparison of photoproducts formation under natural and accelerated conditions
Macromolecular Chemistry and Physics, (to be communicated)
9. **A. Vishwa Prasad** and R.P. Singh
Synthesis, characterization and performance evaluation of polymeric HALS in styrenic copolymers
Macromolecules, (to be communicated)

Chapters in Books

1. **A. Vishwa Prasad**, R.P. Singh, S. Sivaram, J. Lacoste and J. Lemaire
Effect of U.V. Irradiation on Discolouration of HIPS, in '*Macromolecules Current Trends*' ed. S. Venkatachalam, V.S. Joseph, R. Ramaswamy and V.N. Krishnamurthy, Allied Publishers Ltd., New Delhi, Vol. I, 463 (1995).
2. R.P. Singh, **A. Vishwa Prasad** and S. Sivaram
Photodegradation studies on polyurethane coating: Effect of additives on yellowing of polyurethane, in '*Proceedings of the International Conference on Rubbers*' ed. Prajna P. De, Anil K. Bhowmick and S.K. De, Vol III, 120 (1997).

Scientific Reviews

1. **A. Vishwa Prasad** and R.P. Singh
Recent developments in degradation and stabilization of High Impact Polystyrene
J. Macromol. Sci.-Rev. Macromol. Chem. & Phys., **C 37(4)** 581 (1997).